PHYTOALEXINS AND OTHER ANTIFUNGAL METABOLITES FROM CRUCIFERS: ISOLATION, SYNTHESIS AND BIOSYNTHESIS

A thesis submitted to the
College of Graduate Studies and Research
in partial fulfillment of the requirements
for the degree of
Doctor of Philosophy
in the
Department of Chemistry
University of Saskatchewan
Saskatoon

By

Estifanos Ele Yaya

PERMISSION TO USE

In presenting this thesis in partial fulfillment of the requirements for a Postgraduate degree from the University of Saskatchewan, I agree that the Libraries of this University may make it freely available for inspection. I further agree that permission for copying of this thesis in any manner, in whole or in part, for scholarly purposes may be granted by the professor who supervised this thesis work, or in her absence, by the Head of the Department of Chemistry, or the Dean of the College of Graduate Studies and Research. It is understood that any copying, publication, or use of this thesis or parts thereof for financial gain shall not be allowed without my written permission. It is also understood that due recognition shall be given to me and to the University of Saskatchewan in any scholarly use which may be made of any material in my thesis.

Requests for permission to copy or to make other use of material in this thesis in whole or part should be addressed to:

The Head
Department of Chemistry
University of Saskatchewan
Saskatoon, Saskatchewan,
S7N 5C9, CANADA.

ABSTRACT

Phytoalexins and phytoanticipins are antimicrobial natural products involved in plant defence pathways against plant pathogens and other stresses. Most cruciferous phytoalexins are indole containing compounds with various side chains (dithiocarbamates, isothiocyanate, isonitrile, acetonitriles etc.). Many phytoanticipins of crucifers are glucosinolates and their metabolites, which have diverse structures and precursors, including aliphatic, phenyl or indolyl containing amino acids. Indole glucosinolates are derived from tryptophan (**66**), which is also a biosynthetic precursor to cruciferous phytoalexins, however the biosynthetic relationship between cruciferous phytoalexins and indole glucosinolates has not been clarified. In this work, investigation of antifungal metabolites from wild crucifers, synthesis of antifungal metabolites and potential perdeuterated biosynthetic precursors, biosynthesis of metabolites of salt cress and that of rutabaga will be described.

Investigation of the wild crucifers *Brassica tournefortii*, *Crambe abyssinica*, *Diplotaxis tenuifolia* and *Diplotaxis tenuisiliqua* for production of elicited antifungal metabolites, resulted in the discovery of a new phytoalexin, 1',4'-dimethoxyindolyl-3'-acetonitrile (**148**), from *D. tenuisiliqua*. 1',4'-Dimethoxyindolyl-3'-acetonitrile (**148**) is the first dimethoxy substituted phytoalexin with strong antifungal activity against plant fungal pathogens. The remaining plant species produced known phytoalexins which were initially discovered in wild and cultivated species; all of them produced arvelexin (**135**). A novel phytoalexin, isocyalexin A (**104**) was isolated from rutabaga roots irradiated with UV-light; this is the first isocyanide of plant origin.

The second part of the thesis deals with the biosynthesis of metabolites of salt cress (*T. salsuginea*) and their biosynthetic relationships with indole glucosinolates. In that regard, non-isotopically labeled compounds and perdeuterated biosynthetic intermediates such as [2,2,4',5',6',7'-$^{2}H_6$]glucobrassicin (**57b**), [$^{2}H_3$CS;4',5',6',7'-$^{2}H_4$]-1'-methoxybrassinin (**105a**), *L*-[2',4',5',6',7'-$^{2}H_5$]tryptophan (**66a**), [$^{2}H_3$CO]-1'-methoxyindolyl-3'-acetaldoxime (**74a**), *L*-[$^{2}H_3$CS]methionine (**97a**), [4',5',6',7'-$^{2}H_4$]brassinin (**45a**) and 1'-methoxy-2'-methylbrassinin (**160**) were administered to salt

cress leaves. For the first time, the biosynthetic relationship between indole glucosinolates and cruciferous phytoalexins was established. Intact incorporations of hexadeuterated glucobrassicin ([2,2,4',5',6',7'-$^{2}H_6$]glucobrassicin (**57b**)) into wasalexins A (**43**), B (**109**) and biswasalexin A1 (**131**) and A2 (**132**) were observed. Based on the feeding experiment results, for the first time a biosynthetic route that includes both indole glucosinolates (glucobrassicin (**57**) and 1'-methoxyglucobrassicin (**69**)) and 1'-methoxybrassinin was proposed.

The third part of the thesis is about biosynthesis of metabolites of rutabaga (*Brassica napus*). Rutabaga produces phytoalexins that differ on their side chains. Biosynthetic origin of their side chains was investigated by administering fully labeled tryptophan (*L*-[U-$^{13}C_{11}$,U-$^{15}N_2$]Trp) (**66b**) and other perdeuterated precursors to rutabaga roots which revealed that the carbon and nitrogen atoms of cyclobrassinin (**78**), rapalexin A (**103**), isocyalexin A (**104**) and spirobrassinin (**101**) are fully derived from tryptophan (**66**), and also both rapalexin A (**103**) and isocyalexin A (**104**) incorporated deuterium from glucobrassicin (**57**). [4',5',6',7'-$^{2}H_4$]-4'-Methoxybrassinin (**108a**) was incorporated into 4'-methoxycyclobrassinin (**110**) and 4'-methoxydehydrocyclobrassinin (**113**) but not into rapalexin A (**103**), isocyalexin A (**104**) and isalexin (**102**). The biosynthetic pathway that leads to isalexin (**102**), rapalexin A (**103**) and isocyalexin A (**104**) was further investigated using perdeuterated biosynthetic precursors such as (*R*,*S*)-[$^{2}H_3$CO,5',6',7'-$^{2}H_3$]-4'-methoxyindolyl-3'-glycine (**107b**), [$^{2}H_3$CO,5',6',7'-$^{2}H_3$]-4'-methoxyindole-3'-carboxaldehyde oxime (**171b**), [$^{2}H_3$CO,5',6',7'-$^{2}H_3$]desulfoglucorapassicin (**172b**) and etc. It has been confirmed that the pathway involves series of rearrangements that allow transformation of side chain of tryptophan (**66**) into the side chains of rapalexin A (**103**) and isocyalexin A (**104**) without any degradations.

In conclusion, cruciferous phytoalexins are derived from glucobrassicin (**57**), which is a precursor for 1'- and 4'-methoxyglucobrassicins (**69** and **70**). 1-Methoxylated phytoalexins are biosynthesized through 1'-methoxyglucobrassicin (**69**) via 1'-methoxybrassinin (**105**). Similarly, 4-methoxy phytoalexins are derived from 4'-methoxyglucobrassicin (**70**) through two distinct pathways: via 4'-methoxybrassinin

(**108**) and 4'-methoxyindolyl-3'-glycine (**107**), a novel pathway discovered during work reported in this thesis.

ACKNOWLEDGEMENTS

I would like to express my sincere gratitude to my supervisor, Prof M. S. C. Pedras, Thorvaldson Professor, Department of Chemistry, University of Saskatchewan, for giving me a chance to work under her excellent supervision to complete my thesis work. Her professional guidance, encouragement, supports and deep knowledge in natural products biosynthesis has significantly contributed to the successful completion of the present thesis work.

I am also grateful to the members of my Advisory Committee: Prof. D. E. Ward, Dr. S. Reid and Dr. D. R. J. Palmer Department of Chemistry, University of Saskatchewan; and Dr. P. Covello National Research Council, Saskatoon Saskatchewan. Their valuable advice and help during my PhD. work is greatly acknowledged. I also thank my external examiner, Dr. B. M. Lange, Institute of Biological Chemistry, Washington State University, for his review of my thesis, suggestions and advice.

I would like to acknowledge the support and encouragement from all past and present members of Prof. Pedras group: Dr. P. B. Chumala, Dr. D. P. O. Okinyo, Dr. Z. Minic, Dr. Q-A. Zheng, Dr. Y. Yu, Dr. A. Vogt, Dr. S. Hossain, Dr. V. K. Sarma-Mamillapalle, Dr. I. Khallaf, R. B. Snitynsky, G. Hussain, S. Islam, M. Y. Park, A. Abdoli, M. Alavi, C. Thapa, H. To and I also wish to extend my warmest thanks to K. Thoms, Dr. K. Brown, and Dr. G. Schatte for their technical assistance.

I express my heart felt gratitude to my wife Saron Bizuneh, my son Eleazar (Ele) Estifanos and my father, mother, brothers, sisters and their family members for their loving support and encouragement.

Finally I wish to acknowledge the Department of Chemistry and the College of Graduate Studies and Research, University of Saskatchewan for financial support and prestigious awards.

Dedication

to

My parents

Lae Giro and Ele Yaya

My Family

Saron Bizuneh and Eleazar (Ele) Estifanos

And

In memory of my Brother

Samuel (Giro) Ele Yaya (1962-1981)

TABLE OF CONTENTS

LIST OF FIGURES

LIST OF SCHEMES

LIST OF TABLES

LIST OF ABBREVIATIONS

A. brassicicola	*Alternaria brassicicola*
A. repens	*Acroptilon repens*
A. thaliana	*Arabidopsis thaliana*
AC	Aconitase
Ac_2O	Acetic anhydride
ACN	Acetonitrile
AcOH	Acetic acid
BCAT	Branched chain amino-acid transaminase
B. tournefortii	*Brassica tournefortii*
br	Broad
C. abyssinica	*Crambe abyssinica*
ca.	Approximately
calcd.	Calculated
CNGs	Cyanogenic glucosides
^{13}C-NMR	Carbon-13- nuclear magnetic resonance
d	Doublet
β-D-Glc	β-D-Glucose
D. tenuifolia	*Diplotaxis tenuifolia*
D. tenuisiliqua	*Diplotaxis tenuisiliqua*
DAD	Diode Array Detector
dd	Doublet of doublets
DMAP	4-Dimethylaminopyridine
DME	1,2-Dimethoxyether
DMF	Dimethylformamide
DMSO	Dimethylsulfoxide
Et_3N	Triethylamine
EtOAc	Ethyl acetate
EtOH	Ethanol
FCC	Flash column chromatography

FMO	Flavin monooxygenase
FTIR	Fourier transformed infrared
G. graminis	*Gaeumannomyces graminis*
GGP	γ-Glutamyl peptidases
GSH	Glutathione
GST	Glutathione S-transferase
h	Hour
^{1}H-NMR	Proton- nuclear magnetic resonance
HPLC	High performance liquid chromatography
HPLC-ESI-MS	High performance liquid chromatography-electrospray ionization-mass spectrometry
HR-EI-MS	High resolution-electron ionization-mass spectrometry
Hz	Hertz
IAN	Indolyl-3-acetonitrile
IGM1	Indole glucosinolate modifier1
% inh.	Percentage of inhibition
IPM	Isopropyl malate dehydrogenase
J	Coupling constant
L. japonicus	*Lotus japonicus*
L. maculans	*Leptosphaeria maculans*
liq.	Liquid
m	Multiplet
MAM	Methylthioalkylmalate synthase
m/z	Mass to charge ratio
MeOH	Methanol
Met	Methionine
MHz	Megahertz
min	Minutes
NADP	Nicotinamide adenine dinucleotide phosphate
NCS	*N*-Chlorosuccinimide

P. nemorum	*Phyllotreta nemorum*
PDA	Potato dextrose agar
Phe	Phenylalanine
ppm	Parts per million
PTLC	Preparative thin layer chromatography
Quant.	Quantitative
R. solani	*Rhizoctonia solani*
r.t.	Room temperature
s	Singlet
S. bicolor	*Sorghum bicolor*
S. sclerotiorum	*Sclerotinia sclerotiorum*
S. virgate	*Sesbania virgate*
STD	Standard deviation
SUR1	SUPERROOT1
T. majus	*Tropaeolum majus*
T. salsuginea	*Thellungiella salsuginea*
T80	Tween 80
t-Boc	*tert*-Butoxycarbonyl
(t-Boc)$_2$O	Di-*tert*-butyl dicarbonate
TFA	Trifluoroacetic acid
THF	Tetrahydrofuran
TGG	Thioglucoside glucohydrolase
TLC	Thin layer chromatography
t_R	Retention time
Trp	Tryptophan
TTFA	Thallium (III) trifluoroacetate
UDPG	Uridine diphosphoglucose
UGT	Uridine 5'- diphospho-glucuronosyl transferase
UV	Ultraviolet
W. japonica	*Wasabia japonica*

1 INTRODUCTION

1.1 General objectives

Plants are subjected to biotic and abiotic stresses that can result in yield losses and poor quality products. They use their own chemical and physiological defense mechanisms to protect themselves. Chemical defenses include secondary metabolites of which some are constitutive (phytoanticipins) and others are inducible (phytoalexins) (Pedras, Yaya et al., 2011; Vanetten, Mansfield et al., 1994). Brassicaceae is a plant family that comprises economically important crops including oilseeds, vegetables and condiments (Schranz, Lysak et al., 2006). Many of them are susceptible to fungal pathogens such as black spot, blackleg, clubroot, stem rot and root rot fungi, while some wild and cultivated species are reported to be resistant (Chen and Séguin-Swartz, 1999; Conn, Tewari et al., 1988; Pedras, Chumala et al., 2003). Some resistant wild and cultivated crucifers produce strong antifungal phytoalexins with diverse structures (Pedras, Yaya et al., 2011). Biosynthetically they are derived from *L*-tryptophan (**66**) and reported to share some biosynthetic intermediates with indole glucosinolates (Pedras and Okinyo, 2008; Pedras, Zheng et al., 2007b). Establishment of biosynthetic intermediates will facilitate isolation of biosynthetic enzymes and eventual transfer of related pathways into susceptible species.

Objectives of my research project:

1. Investigation of the wild crucifers *Brassica tournefortii*, *Crambe abyssinica*, *Diplotaxis tenuifolia* and *Diplotaxis tenuisiliqua* for production of antifungal metabolites;
2. Isolation, characterization and synthesis of new metabolites;

3. Investigation of biosynthetic pathways of phytoalexins of salt cress and 4-methoxyphytoalexins of rutabaga, which involves:
    a. Synthesis and complete chemical characterization of deuterium labeled biosynthetic precursors,
    b. Feeding of labeled precursors to each species and determination of levels of incorporation using HPLC-DAD-ESI-MS analysis,
    c. Use incorporation results to propose complete biosynthetic pathways.

1.2 Plant secondary metabolites

Plants produce both primary and secondary metabolites. Primary metabolites are the one that are important for basic growth and development. Secondary metabolites include low molecular weight compounds that may not be necessary for basic growth and development. However, they are involved in environmental adaptation and defense from both biotic and abiotic stresses and are important for the fitness of the producer (Bennett and Wallsgrove, 1994; Dewick, 2006). Secondary metabolites mediate interactions that plants make with microbes, other plants, insects, parasites and predators in indirect as well as direct defence processes (Hartmann, 2007). Some secondary metabolites are produced only under specific conditions (for example by elicitation); however, all of them play an important role for plants that produced them (Bennett and Wallsgrove, 1994). In addition, many of these secondary metabolites are used in pharmaceutical and agricultural industries.

The origin of the major biosynthetic intermediates (precursors) of secondary metabolites are from acetyl coenzyme A, shikimic acid, mevalonic acid and/or 1-deoxyxylulose-5-phosphate and different amino acids, which are used in the acetate pathway (e.g. fatty acids and polyketides), shikimate pathway (e.g. phenylpropanoids), mevalonate and deoxyxylulose phosphate pathway (e.g. terpenoids and steroids), and in the synthesis of alkaloids (e.g. pyrrolizidine, piperidine, indole), respectively (Dewick, 2006). Secondary metabolites formed from the acetate pathway include phenols,

macrolide antibiotics and etc. while the shikimate pathway is responsible for the biosynthesis of phenols, cinnamic acid derivatives, lignans, and alkaloids. Terpenoids and steroids are biosynthesized via the mevalonate and deoxyxylulose phosphate pathways. The amino acids ornithine, lysine, tryptophan etc. are precursors for various types of alkaloid metabolites (Dewick, 2006).

1.2.1 Non-crucifers

1.2.1.1 Phytoanticipins and allelochemicals

Plants produce constitutive (phytoanticipins) as well as inducible (phytoalexins) secondary metabolites. Phytoanticipins as defined by Vanetten et al., are "low molecular weight antimicrobial secondary metabolites that are present in plants before challenge by microorganisms or are produced after infection solely from pre-existing constituents" (Vanetten, Mansfield et al., 1994). Constitutive secondary metabolites include saponins, cyanogenic glucosides and glucosinolates among others (Osbourn, 1996). As most of the glucosinolates that have been isolated and reported are from the family Brassicaceae, it will be discussed in detail in the next section (under cruciferous secondary metabolites). Plants interact with each other or other organisms using their chemical compounds. Allelopathy is a chemically mediated interaction between the same or different species of organisms (Bais, Weir et al., 2006). The term allelopathy is derived from the Latin words allelon 'of each other' and pathos 'to suffer' (Weir, Park et al., 2004). Allelochemicals (chemicals that mediate interactions) can be present in almost all plant tissues and emitted to the environment in different forms (Bais, Weir et al., 2006; Weir, Park et al., 2004; Weir and Vivanco, 2008). For example methyl jasmonate (**1**) and α-pinene (**2**) are released as volatile components while *p*-hydroxybenzoic acid (**3**) and *p*-coumaric acid (**4**) are carried to the surrounding environment through leaching and decomposing residue. Sorgoleone (**9**) and (-)-catechin (**8**) are root exudates while quercetin (**5**), DIBOA (2,4-dihydroxy-1,4-benzoxazin-3-one) (**6**) and juglone (**7**) are released as leaf, bark and root exudates (Weir, Park et al., 2004) (**Figure 1.1**).

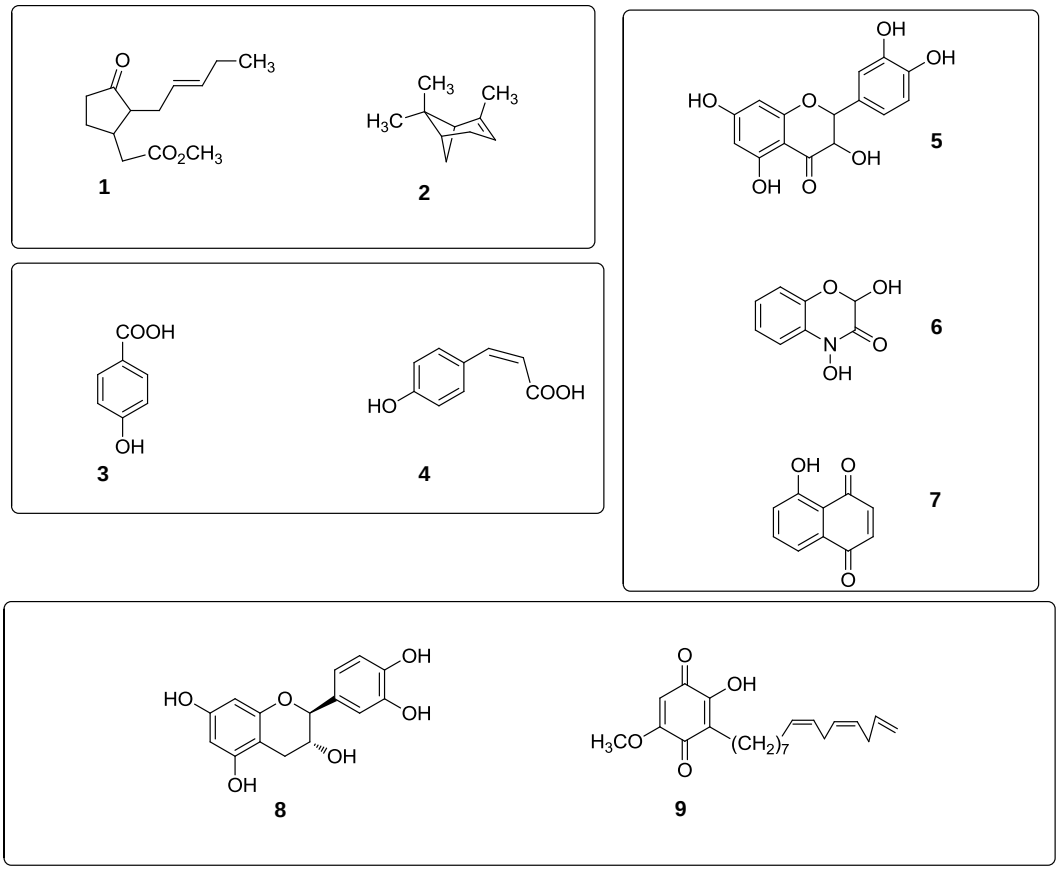

Figure 1.1 Examples of allelochemicals (Weir, Park et al., 2004).

Plants interact with their neighbouring plants or other organisms in two different ways. Positive interactions include those in support of one another for their survival. On the other hand, situations such as competition for survival, parasitism, etc. that threat others existence result in negative interactions (Bais, Weir et al., 2006). The mediators of these interactions (plant phytotoxins) have different chemical structures and functions (Bais, Weir et al., 2006; Weir, Park et al., 2004). The term phytotoxins used in this context refers to toxic secondary metabolites that are produced by plants. *Acroptilon repens* (L.) DC. (Asteraceae) produce phytotoxic compounds found to affect the normal growth of *Arabidopsis thaliana* L. seedlings (**Figure 1.2**) (Quintana, Weir et al., 2008). In these experiments isolated compounds were dissolved in methanol and given to the

plants through roots and significant changes were observed. For example, 1-Chloro-4-(5-(penta-1,3-diyn-1-yl)thiophen-2-yl)but-3-yn-2-ol (**10**) (12.5 µg/mL) was found to reduce *A. thaliana* fresh weight by 64%. 4-(5-(Penta-1,3-diyn-1-yl)thiophen-2-yl)but-3-yne-1,2-diol (**13**) decreased the fresh weight by 37% at 50 µg/mL. The polyacetylene, 2-methoxy-6-(5-(prop-1-yn-1-yl)thiophen-2-yl)hexa-3,5-diyn-1-ylacetate (**11**) (25 µg/mL) decreased the plant fresh weight by 54.5%. Treatment of *A. thaliana* seedlings with 2-((5-(penta-1,3-diyn-1-yl)thiophen-2-yl)ethynyl)oxirane (**12**) reduced *A. thaliana* growth by 45% at 250 µg/mL (Quintana, Weir et al., 2008).

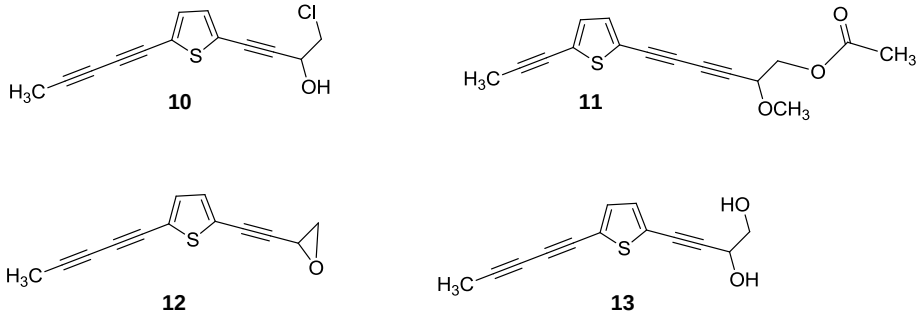

Figure 1.2 Allelochemicals produced by *Acroptilon repens*

On the other hand, other metabolites such as Catechin (**8**) produced by *Centaurea maculosa* Lam. and *Sesbania virgata* (Cav.) Pers. found to affect neighbouring plants (Simões, Du et al., 2008). Aqueous extracts of wheat (*Triticum aestivum* L.) affected the germination and growth of some plant species (Steinsiek, Oliver et al., 1982; Wu, Haig et al., 2000; Wu, Haig et al., 2002). Potential allelochemicals such as *p*-hydroxybenzoic acid (**3**), *cis*-*p*-coumaric acid (**4**), vanillic acid (**14**), syringic acid (**15**), *trans*-*p*-coumaric acid (**16**), naphthoic acid (**17**), *trans*-ferulic acid (**18**), *cis*-ferulic acid (**19**) and DIMBOA (2,4-dihydroxy-7-methoxy-1,4-benzoxazin-3-one) (**20**) were detected in wheat extracts (Wu, Haig et al., 2002; Wu, Pratley et al., 2001) (**Figure 1.3**).

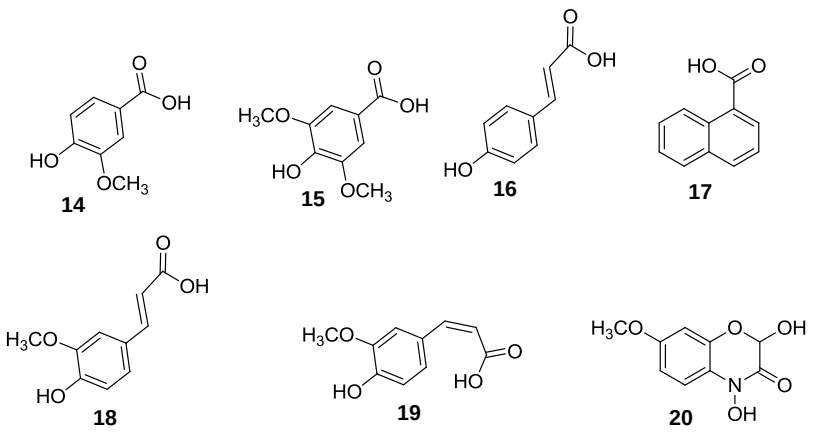

Figure 1.3 Allelochemicals produced by wheat (*Triticum aestivum*)

Plant-plant interactions can also be considered positive if they can defend themselves because of the effect of neighbouring plants. Volatile organic compounds (VOC) or root exudates from a plant may trigger the nearby plants to prepare their defenses for immediate use when threatened by insects. For example *Elytrigia repens* (L.) Desv. ex Nevski (couch-grass) produces phytotoxic compounds including 6-hydroxy-1,2,3,4-tetrahydro-β-carboline-3-carboxylic acid (carboline) (**21**) (Glinwood, Pettersson et al., 2003) (**Figure 1.4**) that reduced aphid interest towards the neighbouring plants (Bais, Weir et al., 2006; Glinwood, Pettersson et al., 2003).

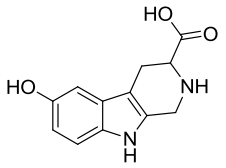

Figure 1.4 An allelochemical involved in positive plant-plant interactions

Pyrrolizidine alkaloids (PAs) produced by plants of the family Boraginaceae, Leguminosae, Asteraceae, and Apocynaceae are part of constitutive defence secondary metabolites that protect plants from plant pathogens (Hartmann, 2004). The two major forms of PAs are the pro-toxic free base and the non-toxic *N*-oxide which have different effects based on their oxidation state (Hartmann, 2004) (**Figure 1.5**). Generalist insects

are mostly affected by the toxicity of PA free bases. On the other hand, all adapted (specialist) insects can control unnecessary accumulations of the free bases in their tissues (Hartmann and Ober, 2000; Hartmann, Theuring et al., 2005). According to Marcel et al., the effects of PAs on generalist insects and free leaving nematode may depend on (i) variations in their chemical structures and oxidation state of the PA molecules (ii) the insect and nematode species (iii) the exposure period (Macel, Bruinsma et al., 2005). For example seneciphylline *N*-oxide (**23**) was found to be toxic to generalist insects that cannot stop conversion of the *N*-oxide into the free base (Narberhaus, Zintgraf et al., 2005).

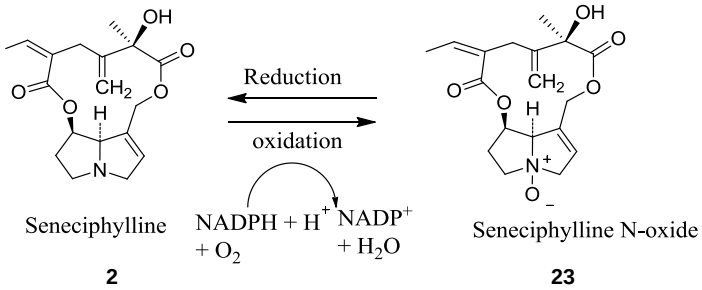

Figure 1.5 Detoxification of seneciphylline via *N*-oxidation

Saponins are constitutive secondary metabolites that protect plants from plant pathogens. They contain a steroidal or triterpene core structures (Szakiel, Pączkowski et al., 2011) that have carbohydrate moieties attached to them. Saponins are abundant among plant families and have shown various biological activities (Francis, Kerem et al., 2002; Szakiel, Pączkowski et al., 2011), including insecticidal (Chaieb, 2010; De Geyter, Lambert et al., 2007) and antifungal effects (e.g. steroidal saponins **24-27**) (Barile, Bonanomi et al., 2007; Tsuzuki, Svidzinski et al., 2007; Yang, Zhang et al., 2006). Saponins' role in protecting plants from fungal attack was demonstrated (Osbourn, Clarke et al., 1994). Oats species that produce avenacin (**28-31**) (**Figure 1.6**) were resistant to *Gaeumannomyces graminis* (var. *tritici*) while *Auena longiglumis* that does not produce metabolites **28-31** was susceptible to *G. graminis* (Osbourn, Clarke et al., 1994). Likewise, saponin-deficient (*sad*) mutants showed susceptibly to fungal pathogens (Papadopoulou, Melton et al., 1999). On the other hand, host oats were not infected by

fungal mutants lacking gene encoding a saponin detoxifying enzyme (Bowyer, Clarke et al., 1995).

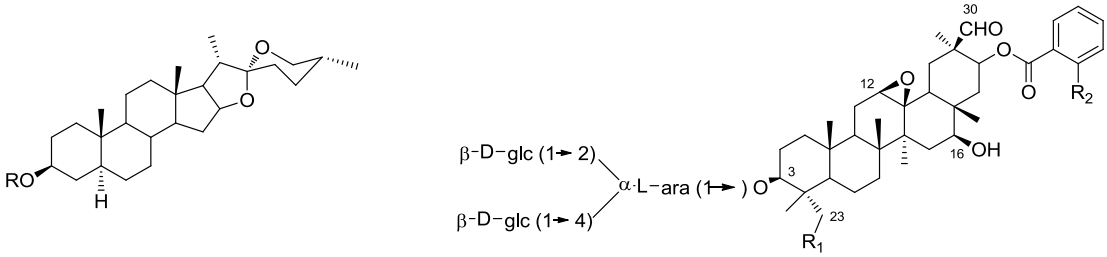

24 gal(4-1)glc(3-1)xyl(2-1)glc(3-1)rha
25 gal(4-1)glc(3-1)glc(2-1)glc(3-1)rha
26 gal (4-1)glc(3-1)xyl(2-1)glc
27 gal(4-1)glc(3-1)xyl(2-1)glc(3-1)xyl

(**28**) avenacin A-1: R_1= OH, R_2 = $NHCH_3$
(**29**) avenacin A-2: R_1 = OH, R_2 = H
(**30**) avenacin B-1: R_1 = H, R_2 = $NHCH_3$
(**31**) avenacin B-2: R_1 = H, R_2 = H

Figure 1.6 Examples of antifungal saponins

Saponins are divided into three major groups, triterpenoid, steroid or steroidal glycoalkaloids (Iriti and Faoro, 2009; Osbourn, 1996). Steroidal saponins (such as avenacoside A (**32**)) are biosynthetically derived from cholesterol via side chain modifications, while steroidal alkaloids (such as α-tomatine (**33**)) are nitrogen analogues of steroidal saponins (**Figure 1.7**) (Dewick, 2006).

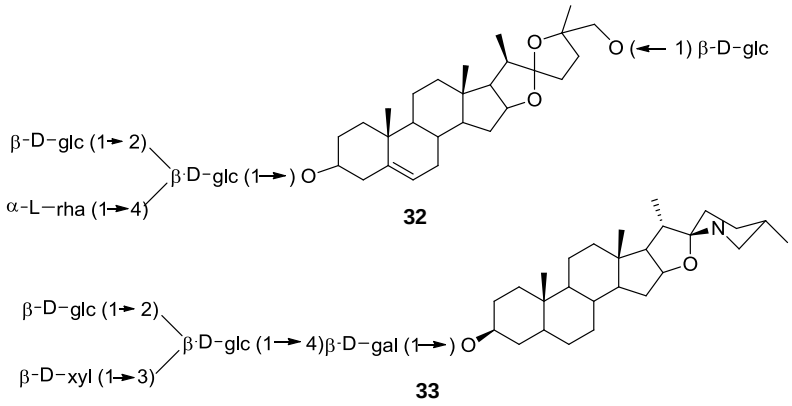

Figure 1.7 Structures of avenacoside A (**32**) and α-tomatine (**33**)

Another group of phytoanticipins are the cyanogenic glucosides (CNGs) that are ecologically important and produced by different plant species (Osbourn, 1996; Zagrobelny, Bak et al., 2004). For example, these group of metabolites are feeding

deterrents and phagostimulants (Zagrobelny, Bak et al., 2004). One of the metabolic products of CNGs is hydrogen cyanide (HCN) which is toxic to plant pathogens (Osbourn, 1996; Zagrobelny, Bak et al., 2004). Specialist insect herbivores can take advantage of them (CNGs) by sequestering and also synthesizing them *de novo* (Zagrobelny and Møller, 2011).

Biosyntheses of CNGs involve four major steps. The first two steps are catalyzed by cytochromes P450 (Bak, Paquette et al., 2006; Jørgensen, Morant et al., 2011; Zagrobelny, Bak et al., 2004). The first P450 catalyzes *N*-hydroxylation of the parent amino acid (**34**) which is followed by decarboxylation (Jørgensen, Morant et al., 2011; Sibbesen, Koch et al., 1994). The second cytochrome P450 converts aldoxime (**35**) into α-hydroxynitrile (**36**), a step involving dehydration and α-hydroxylation (Bak, Paquette et al., 2006). Finally, glucosylation of α-hydroxynitrile (**36**) is catalyzed by a UDPG-glycosyltransferase (**Scheme 1.1**) (Bak, Paquette et al., 2006; Jørgensen, Morant et al., 2011) to afford **37**.

One of the directions considered in order to enhance the self-defending ability of susceptible plant species was the introduction of new biosynthetic pathways. For that reason, introduction of the cyanogenic glucoside biosynthetic pathways into transgenic plants was viewed as a useful and remarkable step in understanding the role of secondary metabolites in plant defense (Tattersall, Bak et al., 2001). *Sorghum bicolor* (L.) Moench produces a CNG, dhurrin (**37**), which is not synthesized in *A. thaliana* and *Lotus japonicus* (Morant, Jørgensen et al., 2007). The expression of *S. bicolor* CYP79A1, CYP71E1 and UGT85B1 in *L. japonicus* and *A. thaliana* allowed them to produce dhurrin (**37**) (Morant, Jørgensen et al., 2007; Tattersall, Bak et al., 2001; Verpoorte and Memelink, 2002). As a result, larvae of *Phyllotreta nemorum* L. refused to eat leaves from transgenic *Arabidopsis* (Tattersall, Bak et al., 2001; Verpoorte and Memelink, 2002). The production of metabolite **37** was also demonstrated in transgenic *Nicotiana tabacum* cv Xanthi (tobacco) (Bak, Olsen et al., 2000; Morant, Jørgensen et al., 2007). Expression of CYP450 (CYP79A1 and CYP71E1) alone resulted in accumulation of intermediates and decomposition products (Bak, Olsen et al., 2000); however, **37** was

detected only when UGT85B1 was expressed along with CYP450s (Morant, Jørgensen et al., 2007) (**Scheme 1.1**).

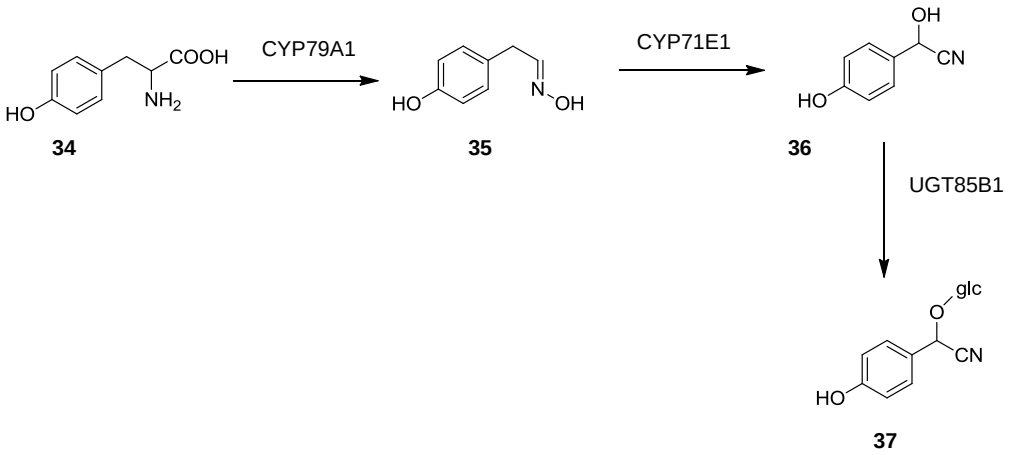

Scheme 1.1 Biosynthesis of dhurrin (**37)** (cyanogenic glucosides)

1.2.1.2 Phytoalexins

Phytoalexins are "low molecular weight antimicrobial secondary metabolites that are produced when plants are under stress" (Bailey and Mansfield, 1982; Smith, 1996). The term phytoalexin was coined from Greek words meaning, "warding-off agents in plants" (Bailey and Mansfield, 1982). The first phytoalexin (pisatin (**51**)) structure was reported 20 years after the first proposal of the concept of phytoalexin by Muller and Borger (Muller and Borger, 1941). Structurally, phytoalexins may differ from one plant family to another. Plants from the same family may produce structurally related phytoalexins (Grayer and Harborne, 1994; Hammerschmidt, 1999; Pedras, Yaya et al., 2011). There are cases in which a single compound (e.g. resveratrol (**50**)) was detected in different plant families (Grayer and Harborne, 1994).

The role of phytoalexins as defense metabolites was demonstrated using transgenic tobacco (*N. tabacum*). The gene for biosynthesis of stilbene phytoalexins was transferred from *Vitis vinifera* L. (grapevine) to tobacco (*N. tabacum*). After inoculation with *Botrytis cinerea*, the transgenic plants accumulated a phytoalexin resveratrol (**50**) with enhanced resistance to pathogens (Hain, Reif et al., 1993).

Phytoalexin precursors can be derived from shikimic acid, acetate-malonate, mevalonate and/or deoxyxylulose and alkaloids, or their combinations (Brooks and Watson, 1985; Kuc, 1995). There are quite a few phytoalexins biosynthesized in rice and maize plants via mevalonate pathways (Otomo, Kanno et al., 2004; Peters, 2006). Rishitin (**38**) isolated from potato tuber (Lyon, 1972), capsidiol (**39**) isolated from several plant species including tobacco and pepper and phytoalexin **40** are biosynthesized via mevalonate pathway (Literakova, Lochman et al., 2010) (**Figure 1.8**). 6-Methoxymellein (**41**), a phytoalexin isolated from carrot root infected by different fungal species, is biosynthesized via acetate-malonate pathway (Kurosaki and Nishi, 1983) (**Figure 1.9**). Scopoletin (**42**), a major phytoalexin of tobacco plants, is biosynthesized via the shikimic acid pathway (Ahuja, Kissen et al., 2012; Kai, Mizutani et al., 2008) (**Figure 1.10**). Benzophenanthridine alkaloids, sanguinarine (**46**) and macarpine (**47**) are phytoalexins biosynthesized from *L*-tyrosine (Angelova, Buchheim et al., 2010; Schumacher, Gundlach et al., 1987). Indole alkaloids (**43**, **44**, **45**) are biosynthesized from *L*-tryptophan (**Figure 1.11**) (Pedras, Yaya et al., 2011).

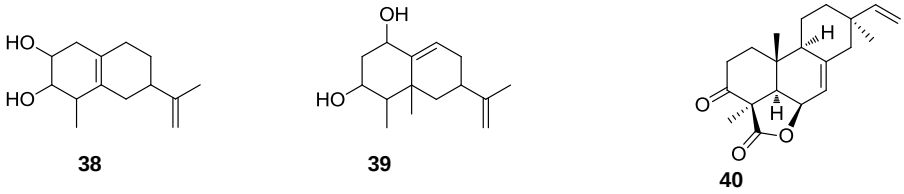

Figure 1.8 Phytoalexins biosynthesized through the mevalonate and/or deoxyxylulose pathway

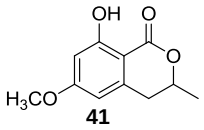

Figure 1.9 A phytoalexins biosynthesized through acetate-malonate pathway

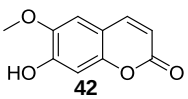

Figure 1.10 A phytoalexin biosynthesized through the shikimate (phenyl-propionate) pathway

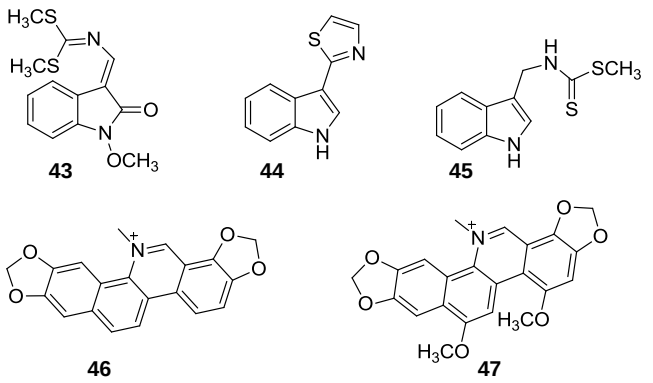

Figure 1.11 Indole (**43**, **44**, **45**) and benzophenanthridine (**46**, **47**) phytoalexins (alkaloids)

Plants can biosynthesize phytoalexins through mixed biosynthetic pathways. Xanthotoxin (**48**) was shown to be biosynthesized via the combination of shikimate and mevalonate and/or deoxyxylulose pathways (Stanjek, Piel et al., 1999) (**Figure 1.12**). Phytoalexins biosynthesized through the combination of shikimate and acetate-malonate pathways are common in plant families such as Fabaceae, Vitaceae and Poaceae (Ahuja, Kissen et al., 2012). For example, pisatin (**51**) which is the main phytoalexin in pea (Arman, 2011), is of mixed biosynthetic origin, the shikimate and acetate-malonate pathway. Resveratrol (**50**) is a building block for the biosynthesis of stilbenoids such as ε-viniferin (**49**) in peanut, also biosynthesized through shikimate and acetate-malonate pathways (**Figure 1.13**) (Ahuja, Kissen et al., 2012).

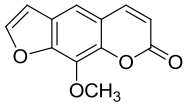

48

Figure 1.12 A phytoalexin biosynthesized through combination of shikimate and mevalonate and/or deoxyxylulose pathways

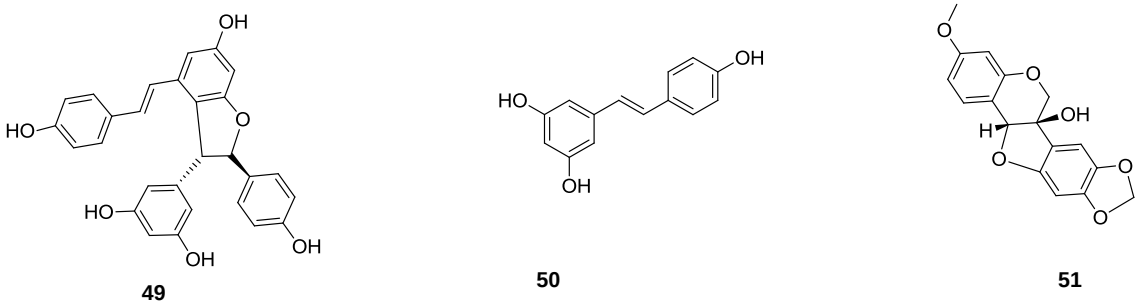

Figure 1.13 Phytoalexins biosynthesized through the combination of shikimate and acetate-malonate pathways

Plants produce phytoalexins biosynthesized through shikimate, acetate-malonate and mevalonate and/or deoxyxylulose. These compounds are produced mostly in the Fabaceae (Ahuja, Kissen et al., 2012). Arachidin 1-3 (**52**-**54**), stilbenoids of peanut seeds, glyceollin I (**55**) and wighteone (**56**) have mixed biosynthetic origin (Sobolev, Neff et al., 2008) (**Figure 1.14**).

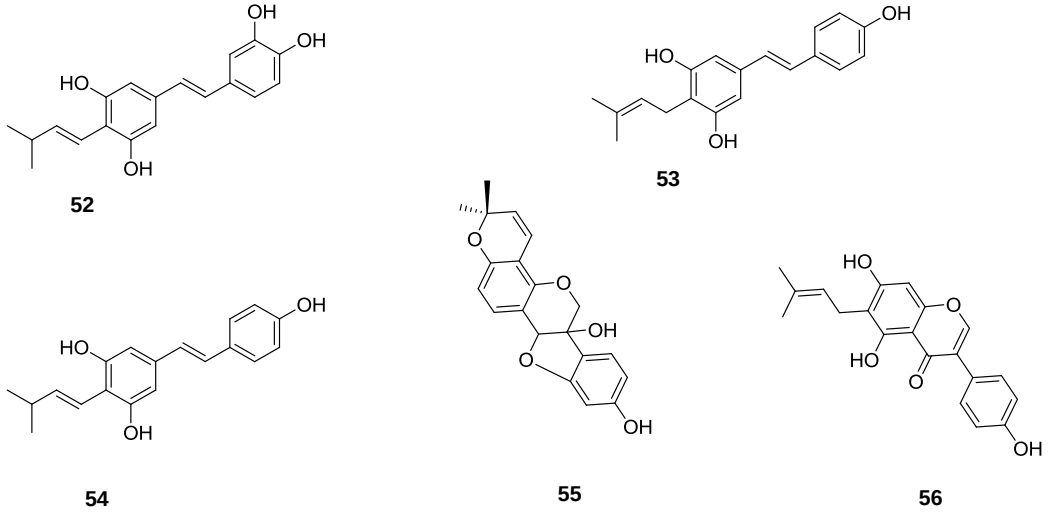

Figure 1.14 Phytoalexins biosynthesized through the combination of shikimate, mevalonate/deoxyxylulose and acetate-malonate pathways

1.2.2 Crucifers

1.2.2.1 Phytoanticipins

Glucosinolates are well studied, constitutive secondary metabolites containing nitrogen and sulphur in their functional group. They are widespread in the order Brassicales, mainly in members of the family Brassicaceae, including the genus *Brassica* and wild species such as *A. thaliana*. In this part of the thesis, the importance of glucosinolates in crucifers and their biosynthesis will be reviewed.

So far, about 132 glucosinolates have been isolated and characterized (Agerbirk and Olsen, 2012). Research on glucosinolates has been advanced since the discovery of importance of their metabolic products as a remedy for human health as well as crop-protection (Halkier and Gershenzon, 2006). Based on the parent amino acid structures, glucosinolates can be subdivided into three major classes: i) aliphatic glucosinolates, derived from aliphatic amino acids such as Ala, Leu, Ile, Val, and Met; ii) aromatic (phenyl) glucosinolates, derived from Phe or Tyr; and iii) indolic glucosinolates, derived from Trp (Halkier and Gershenzon, 2006; Iriti and Faoro, 2009; Sønderby, Geu-Flores et al., 2010). The final structures can be modified through oxidation, methoxylation, acetylation or hydroxylation of the side chain (Hopkins, van Dam et al., 2009) (**Figure 1.15**).

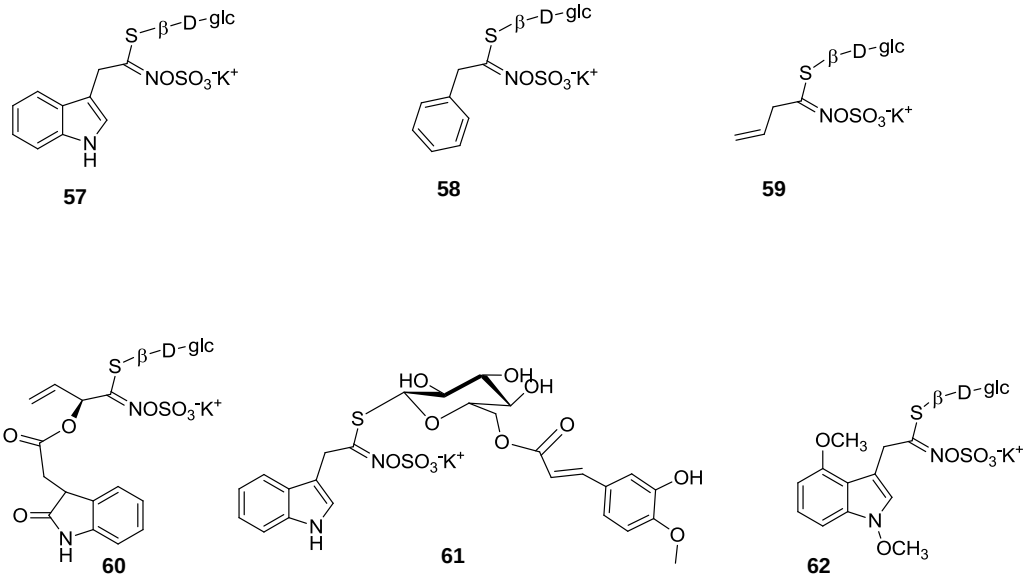

Figure 1.15 Structures of representative glucosinolates (Agerbirk and Olsen, 2012)

Very recently, the formation of unnatural selenoglucosinolates such as 3-(methylseleno)propylglucosinolate (glucoselenoiberverin) (**63**), 4-(methylseleno)butylglucosinolate (glucoselenoerucin) (**64**), and 5-(methylseleno)pentylglucosinolate (glucoselenoberteroin) (**65**) was reported (**Figure 1.15**) (Matich, McKenzie et al., 2012). They were obtained by fertilizing *Brassica* species with sodium selenite (Matich, McKenzie et al., 2012). Selenium was incorporated into the side chain via selenomethionine (which is equivalent to an amino acid methionine).

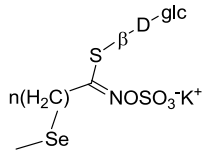

63 n=3
64 n=4
65 n=5

Figure 1.16 Structures of selenoglucosinolates (Matich, McKenzie et al., 2012)

Glucosinolates have great agricultural significance due to the increasing commercial importance of oilseed crops (mostly brassica species) (Cartea and Velasco,

2008; Griffiths, Birch et al., 1998; Halkier and Gershenzon, 2006). Some of them are harmful for animal feeding (Cartea and Velasco, 2008). For example, 2-hydroxy-3-butenylglucosinolate (**94**) causes goiter and other damaging effects on animals (Cartea and Velasco, 2008; Griffiths, Birch et al., 1998). As a result, reducing the levels of seed glucosinolates was required (Halkier and Gershenzon, 2006). Apart from their toxic nature to domestic animals, these compounds also function as defence chemicals against plant pathogens (Halkier and Gershenzon, 2006).

In order to resist damage by insects, plants accumulate glucosinolates in higher concentrations (Halkier and Gershenzon, 2006). On the contrary, specialized insects use them as signals for various stimulations (Halkier and Gershenzon, 2006). Specialized insects may overcome the toxicity of glucosinolates and their metabolic products through quick excretion from their body, detoxification (metabolizing into less toxic structures), metabolizing into intermediates that will not give rise to toxic hydrolysis products or remain dormant to the toxic compounds (Halkier and Gershenzon, 2006). For example, the diamond back moth converts glucosinolates into their desulfo form using a sulfatase enzyme (Ratzka, Vogel et al., 2002). The cabbage white butterfly was able to convert glucosinolate hydrolysis products into nitriles and excrete them out (Wittstock, Agerbirk et al., 2004). Specialized herbivores can also sequester glucosinolates and use them to fight predators (Müller, Boevé et al., 2002; Vlieger, Brakefield et al., 2004). The aphid *Brevicoryn brassicae* L. has its own myrosinase(s) used to hydrolyze the glucosinolates (Bridges, Jones et al., 2002; Halkier and Gershenzon, 2006).

Biosynthetically, glucosinolates are derived from amino acid precursors. There are three biosynthetic stages: (i) chain elongation (ii) formation of the functional group, and (iii) side chain modifications of the parent amino acid (Sønderby, Geu-Flores et al., 2010).

Early *in vivo* studies laid the foundation for studying the biosynthesis of metabolites through feeding experiments using radiolabeled amino acids and acetates. The incorporation of labeled [^{14}C[acetate and [^{14}C]methionine into allyl isothiocyanate of horseradish was reported in 1964 (Chisholm and Wetter, 1964). Incorporations of [2-^{14}C]methionine and [2-^{14}C]acetate into the thioglucoside progoitrin (**94**) were also

demonstrated using rutabaga leaves (Serif and Schmotzer, 1968). Later a more comprehensive study regarding chain elongation reactions was carried out (Graser, Schneider et al., 2000). Using leaves of *Eruca sativa* (Miller), it was demonstrated that the carbon atoms of 4-methylthiobutylglucosinolate (**99**) were derived from methionine (**97**). Feeding of [U-^{13}C]methionine (**97a**) to leaves of *E. sativa* resulted in the incorporation of the entire carbon atoms except for the carboxylic acid carbon suggesting decarboxylation of the first acetate residue (Graser, Schneider et al., 2000). Administration of [^{13}C] and [^{14}C]acetate have confirmed steps in the chain elongation cycle (Graser, Schneider et al., 2000).

1.2.2.1.1 Functional group biosynthesis

Well before the discovery of biosynthetic genes, the biosynthesis of the glucosinolate functional group was studied through feeding experiments using labeled biosynthetic precursors. Those early findings laid the ground work essential to the current discoveries. Labeled precursors with radioisotopes ^{14}C and ^{3}H and cold isotopes ^{2}H, ^{13}C and ^{15}N were used for feeding experiments. Biosynthetic studies of glucosinolates through feeding experiments started as early as 1960, as follows.

Incorporation of isotopically labelled precursors

The use of ^{14}C, ^{3}H and ^{15}N was a common practice in early biosynthetic studies. In the biosynthetic study of indole glucosinolates functional group, one of the first labeled precursors used was ^{14}C labeled tryptophan (**66**) (Kutacek, Prochazka et al., 1960). Kutacek and coworkers investigated the biosynthetic origin of indole derived metabolites using (*D,L)*-[3-^{14}C]tryptophan (**66a**). Tryptophan (**66**) was reported as the biosynthetic precursor of indolyl-3'-acetonitrile (**67**), indole-3-acetic acid and ascorbigen (**68**) (Kutacek, Prochazka et al., 1960). Years later, Kutacek and coworkers administered (*D,L)*-[3-^{14}C]tryptophan (**66a**) to cabbage leaves and confirmed the incorporation of radioactive component in glucobrassicin (**57**) (Kutacek and Kefeli, 1970; Kutacek,

Prochazka et al., 1962). No incorporation of ^{14}C labeled indole-3'-acetonitrile (**67a**) or ascorbigen (**68**) was detected in to glucobrassicin (**57**), suggesting the irreversibility of glucobrassicin (**57**) metabolism (Kutacek, Prochazka et al., 1962) **Figure 1.17**.

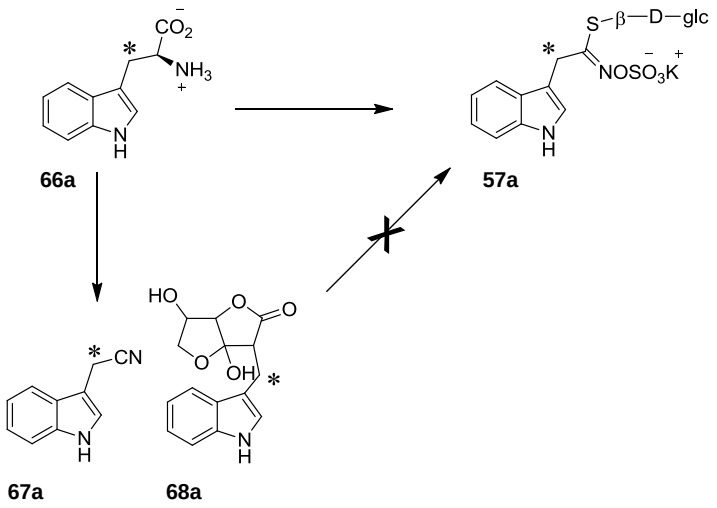

*C = ^{14}C

Figure 1.17 Biosynthetic relationship between tryptophan (**66a**), indolyl-3'-acetonitrile (**67a**), ascorbigen (**68**) and glucobrassicin (**57a**) (Kutacek, Prochazka et al., 1962).

Schraudolf and Bergmann investigated the biosynthetic origin of indole glucosinolates using ring-labeled (*D,L*)-[^{14}C]tryptophan (**66a**) and [^{35}S]sulphate which revealed incorporation of ^{14}C and ^{35}S into glucobrassicin (**57**) and 1'-methoxyglucobrassicin (**69**) (Schraudolf and Bergmann, 1965). Indole (**120**) was shown to be a biosynthetic precursor of tryptophan (**66**), glucobrassicin (**57**) and 1'-methoxy glucobrassicin (**69**) (Schraudolf, 1966). Administration of mixture of *L*-[3-^{14}C]tryptophan (**66a**) and *L*-[$^{15}NH_2$]tryptophan (**66a**) to winter rape resulted in the incorporation of nitrogen into indole glucosinolates and derivatives (Kutacek and Kralova, 1972) (**Figure 1.18**). Absence of incorporation of *L*-[1-^{14}C]tryptophan (**66a**) suggested decarboxylation of tryptophan during the metabolism (Kutacek and Kralova, 1972).

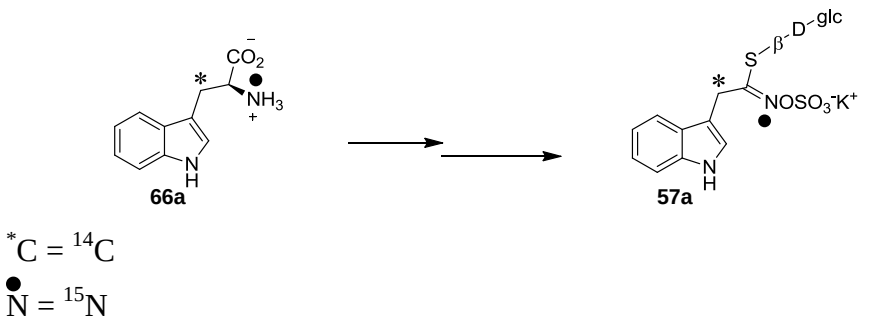

Figure 1.18 Incorporation of *L*-[3-^{14}C] and *L*-[$^{15}NH_2$]tryptophan (**66a**) into glucobrassicin (**57a**) (Kutacek and Kralova, 1972).

B. napus roots infected by *Plasmodiophora brassicae* metabolized *L*-[^{14}C]tryptophan (**66a**) into glucobrassicin (**57**) and indolyl-3'-acetonitrile (**67**) (Rausch, Butcher et al., 1983). The incorporation of radioactive elements into **57** and **67** was higher in infected tissue. Administration of *L*-[2',4',5',6',7'-^{2}H]tryptophan (**66a**) to UV-elicited rutabaga roots and salt cress (*T. salsuginea*) leaves showed incorporation of deuterium into glucobrassicin (**57**), 1'-methoxyglucobrassicin (**69**), 4'-methoxyglucobrassicin (**70**) and cruciferous phytoalexins (**Figure 1.19**) (Pedras, Okinyo et al., 2009; Pedras, Yaya et al., 2010).

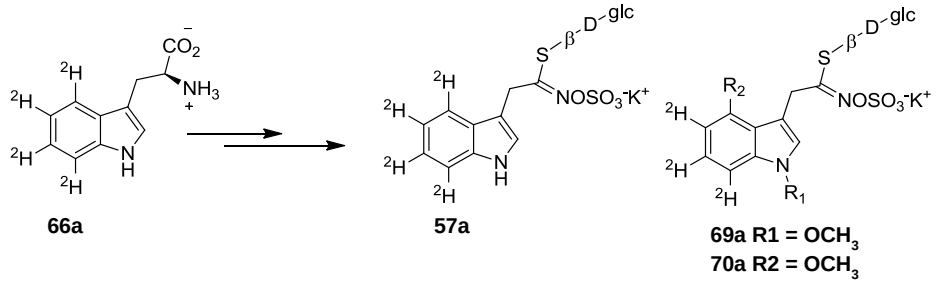

Figure 1.19 Incorporation of *L*-[2',4',5',6',7'-^{2}H]tryptophan (**66a**) into indole glucosinolates (Pedras, Okinyo et al., 2009; Pedras, Yaya et al., 2010)

Oximes were proposed and tested by Underhill as biosynthetic intermediates in the biosynthesis of glucosinolates (Underhil, 1967). Administration of [1-^{14}C]phenylacetaldoxime (**71a**) to *Tropaeolum majus* L. shoot showed incorporation of ^{14}C into glucotropaeolin (benzylglucosinolate) (**58**). Likewise, 3-phenyl[1-

^{14}C]propionaldoxime (**72a**) administered to *Nasturtium officinale* (R. Br.) was incorporated into gluconasturtiin (**73**) (**Figure 1.20**) (Underhil, 1967).

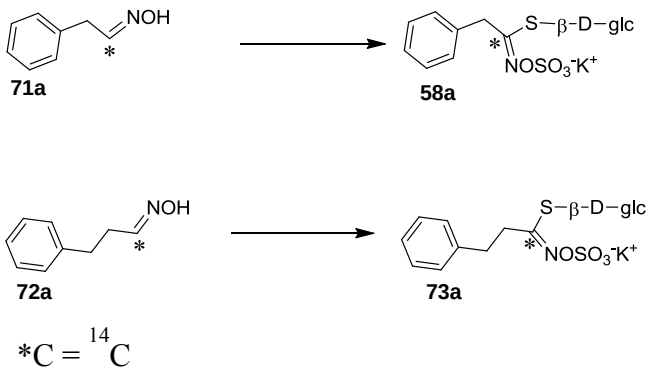

Figure 1.20 Incorporation of [1-^{14}C]phenylacetaldoxime (**71a**) and 3-phenyl[1-^{14}C]propionaldoxime (**72a**) into the corresponding glucosinolates (**58a** and **73a**) (Underhil, 1967).

Indolyl-3'-acetaldoxime (**122**) was shown to be a biosynthetic precursor of glucobrassicin (**57**). Administration of tritiated indolyl-3-acetaldoxime (**122**) to leaves of woad (*Isatis tinctoria* L.) showed incorporation into glucobrassicin (**57**) (Mahadevan and Stowe, 1972). Cysteine was proposed to be a sulfur donor (Mahadevan and Stowe, 1972). Metabolism of indolyl-3'-acetaldoxime (**122**) by Chinese cabbage hypocotyls was investigated using [^{14}C]indolyl-3'-acetaldoxime (**122a**). Incorporation of the precursor into indolyl-3'-acetonitrile (**67**), glucobrassicin (**57**) and desulfoglucobrassicin (**80**) was detected (Helmlinger, Rausch et al., 1985). [$^{2}H_3$O,4',5',6',7']-1'-Methoxyindolyl-3'-acetaldoxime (**74a**) was shown to be a biosynthetic precursor of 1'-methoxyglucobrassicin (**69**) (Pedras, Okinyo et al., 2009). Similarly, [$^{2}H_3$C]-1'-methylindolyl-3'-acetaldoxime (**75a**) was metabolized to 1'-methylglucobrassicin (**76**) (**Figure 1.21**) (Pedras, Okinyo et al., 2009), suggesting the non-selective nature of the post-aldoxime enzymes in the biosynthetic pathway of indole glucosinolates (Halkier and Gershenzon, 2006; Pedras, Okinyo et al., 2009)

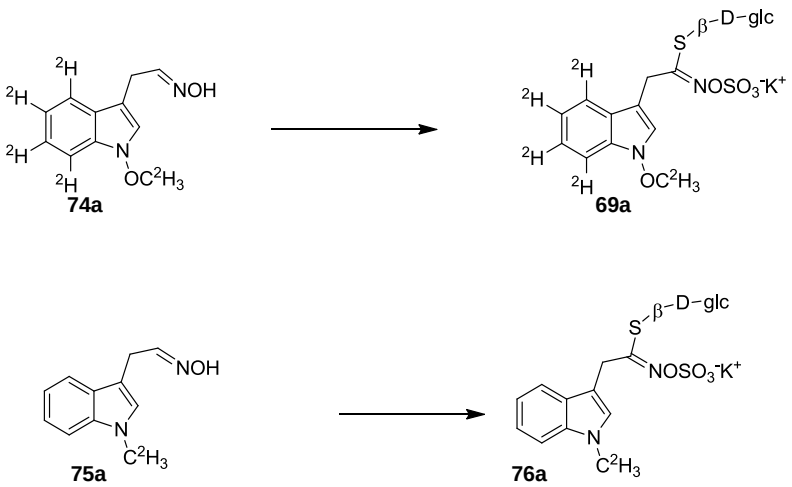

Figure 1.21 Incorporation of substituted indolyl-3'-acetaldoximes (**74a** and **75a**) into 1-substituted glucobrassicins (**69a** and **76a**) (Pedras, Okinyo et al., 2009)

Administration of a mixture of [1-^{14}C]sodium phenylacetothiohydroximate (**77a**) and [^{35}S]sodium phenylacetothiohydroximate (**77a**) to *T. majus* shoot resulted in incorporation of the precursor into benzylglucosinolate (**58**). The stage at which glucosylation occurred was investigated using [G-^{14}C]-1-thioglucose and [G-^{14}C]-D-glucose (Underhil and Wetter, 1969). In the study of biosynthetic intermediates of indole glucosinolates, ^{2}H and ^{34}S labeled indolyl-3'-acetothiohydroxamic acid (**79**) was prepared and administered to UV-irradiated roots of rutabaga (Pedras and Okinyo, 2008), and the intact incorporation of [4',5',6',7'-$^{2}H_4$]indolyl-3'-[^{34}S]acetothiohydroxamic acid (**79a**) into glucobrassicin (**57**) and cruciferous phytoalexins was demonstrated (**Figure 1.22**).

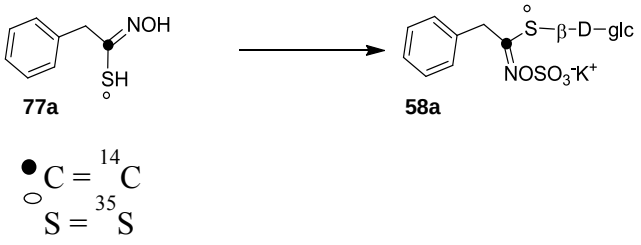

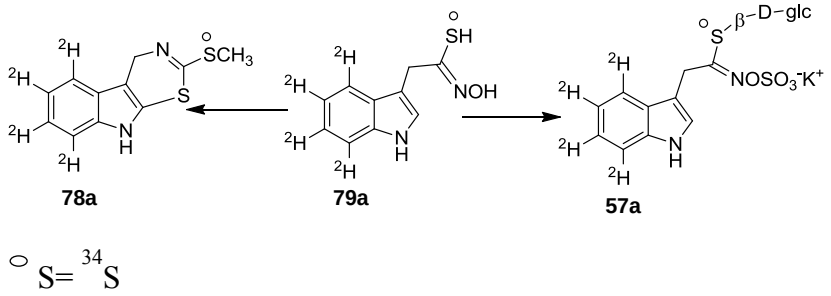

Figure 1.22 Incorporation of [4',5',6',7'-$^{2}H_4$]indolyl-3'-[^{34}S]acetothiohydroxamic acid (**79a**) into glucobrassicin (**57a**) and cyclobrassinin (**78a**) (Pedras and Okinyo, 2008); and [1-^{14}C]sodium phenylacetothiohydroximate (**77a**) and [^{35}S]sodium phenylacetothiohydroximate (**77b**) into the corresponding benzylglucosinolate (**58a**) (Underhil and Wetter, 1969)

Recently, desulfoglucobrassicin (**80a**) was shown to be a biosynthetic precursor of glucobrassicin (**57**), 1'-methoxyglucobrassicin (**69**) and 4'-methoxyglucobrassicin (**70**). Feeding of perdeuterated **80a** showed incorporation into indole glucosinolates (Pedras and Yaya, 2013). It is worthy to mention that glucobrassicin (**57**) is a biosynthetic precursor of 1'-methoxyglucobrassicin (**69**) and 4'-methoxyglucobrassicin (**70**). Administration of hexadeuterated glucobrassicin (**57b**) to leaves of salt cress (*T. salsuginea*) and rutabaga roots showed intact incorporations into 1'-methoxyglucobrassicin (**69**) and 4'-methoxyglucobrassicin (**70**) (**Figure 1.23**) (Pedras and Yaya, 2013; Pedras, Yaya et al., 2010).

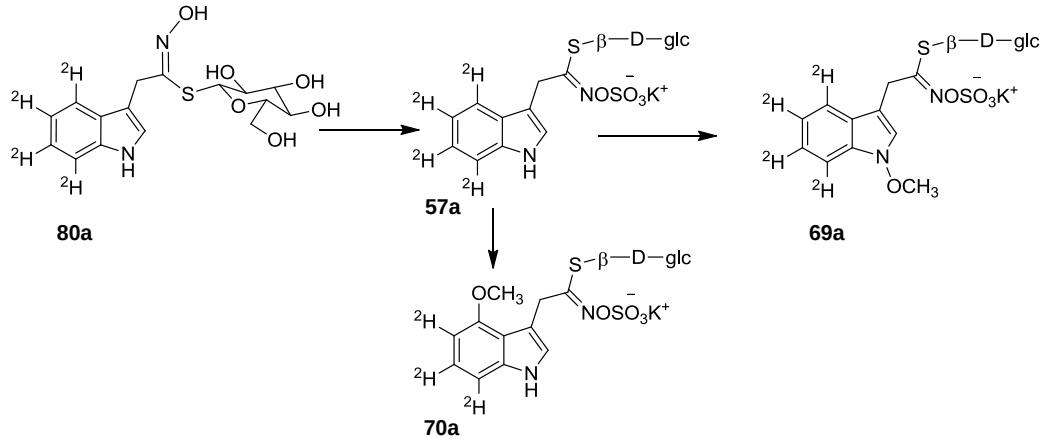

Figure 1.23 Incorporation of [4',5',6',7'-$^{2}H_4$]desulfoglucobrassicin (**80a**) into indole glucosinolates (Pedras and Yaya, 2013; Pedras, Yaya et al., 2010)

Molecular genetics

It has been noted that the transformation of an amino acid to the final glucosinolate includes intermediates such as *N*-hydroxy amino acids, aldoximes, *aci*-nitro or nitrile oxides, *S*-alkyl thiohydroximates, thiohydroximic acids, and desulfoglucosinolates (Halkier and Gershenzon, 2006). The first two steps are catalyzed by cytochrome P450 enzymes (CYP79 and CYP83). Conversion of amino acid (**81**) into the corresponding aldoxime (**82**) is catalyzed by CYP79 (Mikkelsen, Hansen et al., 2000). Tryptophan (**66**) was found to be metabolized by both CYP79B2 and CYP79B3 (Sønderby, Geu-Flores et al., 2010), while CYP79A2 converts Phe into benzyl glucosinolates (Wittstock and Halkier, 2000). CYP79F1 and CYP79F2 use Met derived aliphatic amino acids as their substrates (Chen, Glawischnig et al., 2003; Sønderby, Geu-Flores et al., 2010).

The second step in the biosynthesis of the glucosinolate functional group involves the oxidation of aldoxime (**82**) into nitrile oxide (**83**) by CYP83. The CYP83A1 and CYP83B1 were demonstrated to transform several aldoximes: aliphatic, aromatic and indolic (Bak and Feyereisen, 2001; Halkier and Gershenzon, 2006; Hansen, Du et al., 2001; Naur, Petersen et al., 2003; Sønderby, Geu-Flores et al., 2010).

The mechanism by which nitrile oxide (**83**) can be conjugated to glutathione (GSH) is not yet clear. However, there are two hypotheses that the reaction can either be happening spontaneously or through a reaction catalyzed by enzymes of the family GST (GSTF9, GSTF10) (Geu-Flores, Møldrup et al., 2011; Sønderby, Geu-Flores et al., 2010). The metabolism of the GSH conjugate (**84**) to the Cys-Gly conjugate (**85**) is catalyzed by γ-glutamyl peptidases (GGP1 and GGP3), and the Cys-Gly conjugate is further converted by a carboxypeptidase to yield a Cys-conjugate (**86**) (Geu-Flores, Møldrup et al., 2011). The C–S lyase called SUR1 was identified as an enzyme that catalyzes the conversion of alkylthiohydroximate (**86**) to thiohydroximic acid (**87**) (Sønderby, Geu-Flores et al., 2010). The formation of desulfoglucosinolate (**88**) is catalyzed by glucosyltransferases (UGT74) (Grubb, Zipp et al., 2004; Sønderby, Geu-Flores et al., 2010) (**Scheme 1.2**). The final step in the biosynthesis of the glucosinolate functional group, the *O*-sulfation of

desulfoglucosinolate (**88**), is catalyzed by AtST5a, AtST5b and AtST5c (Piotrowski, Schemenewitz et al., 2004) (**Scheme 1.2**).

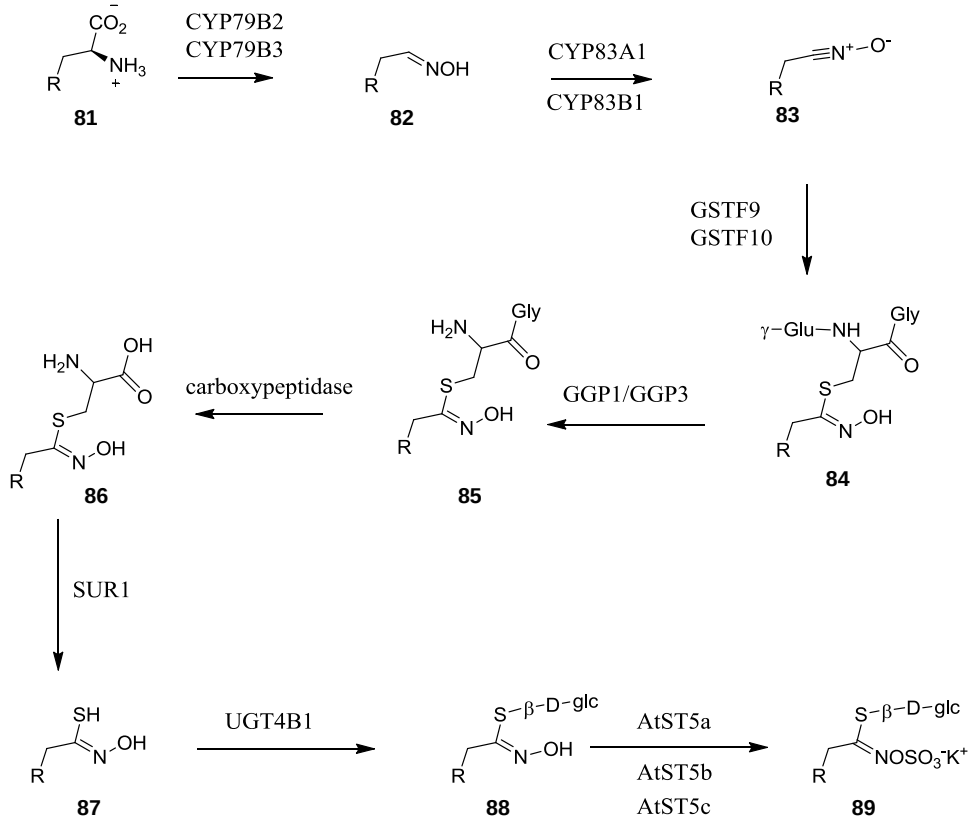

Scheme 1.2 Biosynthesis of the glucosinolate functional group (Geu-Flores, Møldrup et al., 2011; Sønderby, Geu-Flores et al., 2010)

1.2.2.1.2 Side chain modifications

The major differences among glucosinolates arise from their side chain appearances (derived from amino acid precursors) that determine their biological activities (Hopkins, van Dam et al., 2009; Sønderby, Geu-Flores et al., 2010). Changes on the side chains may affect their activity as well as the activity of the hydrolysis products (Halkier and Gershenzon, 2006; Pedras and Hossain, 2011). Some of these changes comprise oxidations, hydroxylations, alkenylations, methoxylations and benzoylations. In *Arabidopsis*, *GS-ELONG*, *GS-OX*, *GS-AOP* and *GS-OH* genes play major roles in

modifying structures of aliphatic glucosinolates (Kliebenstein, Kroymann et al., 2001; Sønderby, Geu-Flores et al., 2010). The conversion of methylthioalkyls (**90**) into methylsulfinylalkyl glucosinolates (**91**) is catalyzed by flavin monooxygenase FMOGS-OX1. This was confirmed by either knocking out the gene or overexpressing it (Sønderby, Geu-Flores et al., 2010). Substrate specificity of the FMOGS-OXs was also determined (Hansen, Kliebenstein et al., 2007; Li, Hansen et al., 2008). AOP2 and AOP3 catalyze the formation of two distinct products from a single substrate (Sønderby, Geu-Flores et al., 2010). AOP2 catalyzes the cleavage of methylsulfoxide moiety to form alkenyl glucosinolates (**92**) (**Scheme 1.3**), whereas, AOP3 catalyzes the cleavage of methylsulfoxide moiety and then hydroxylation of the side chain to form hydroxyalkyl glucosinolates (**93**). Knocking out the genes resulted in the accumulation of the precursor methylsulfinylalkyl glucosinolates (**91**) (Kliebenstein, Lambrix et al., 2001). The GS-OH catalyzes a hydroxylation reaction, which was confirmed by *in vivo* feeding experiments (Sønderby, Geu-Flores et al., 2010) (**Scheme 1.3**).

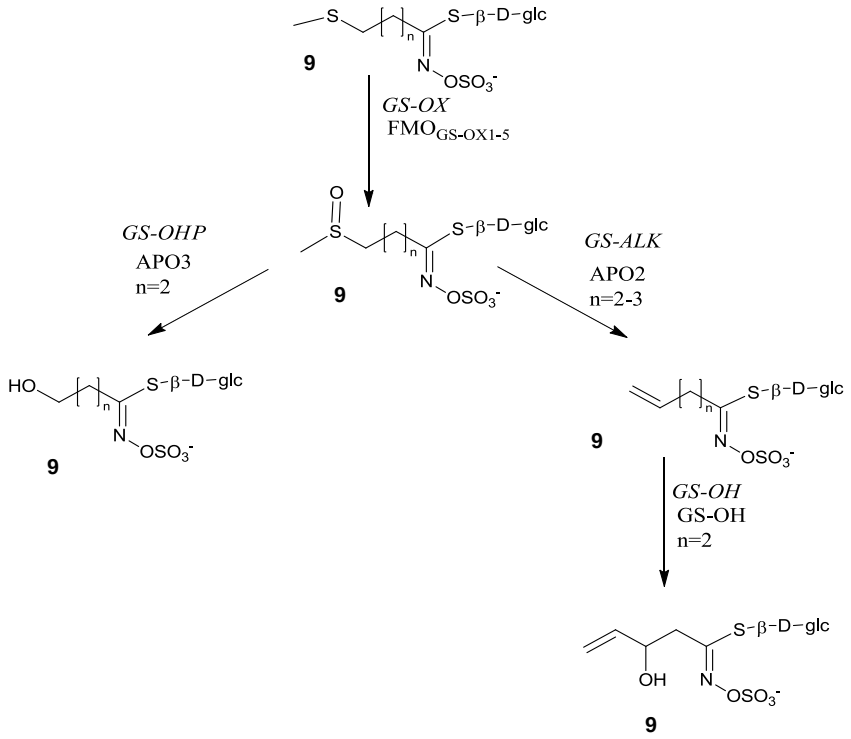

Scheme 1.3 Side chain modification of aliphatic glucosinolates (Sønderby, Geu-Flores et al., 2010).

The four common indolic glucosinolates are glucobrassicin (**57**), 1'-methoxyglucobrassicin (**69**), 4'-hydroxyglucobrassicin (**96**) and 4'-methoxyglucobrassicin (**70**). Biosynthetically, metabolites **69**, **70** and **96** are likely derived from **57** via side chain modifications (Pedras and Yaya, 2013; Pedras, Yaya et al., 2010). So far, the only identified gene encodes an enzyme catalyzing the 4'-hydroxylation of glucobrassicin (**57**) (Sønderby, Geu-Flores et al., 2010). A transgenic plant devoid of the gene *CYP81F2* resulted in a decreased accumulation of 4'-hydroxyglucobrassicin (**96**) and 4'-methoxyglucobrassicin (**70**) when compared to the wild type (**Scheme 1.4**) (Sønderby, Geu-Flores et al., 2010). The essential role of 4'-methoxyglucobrassicin (**70**) in the defense against powdery mildew was proposed based on the susceptibility of the plant in which the gene responsible for the production of 4'-methoxyglucobrassicin (**70**) was knocked out (Sønderby, Geu-Flores et al., 2010). However, it has been shown that indole glucosinolates do not have anti-fungal effects but, hydrolysis products of indole glucosinolates (indolyl-3'-acetonitriles **135**, **67**, **136**) inhibited fungal mycelial growth of plant pathogens (Pedras and Hossain, 2011).

Recently, the biosynthetic relationship between indole glucosinolates and cruciferous phytoalexins was demonstrated (Pedras and Yaya, 2013; Pedras, Yaya et al., 2010). Cruciferous phytoalexins were shown to be derived from indole glucosinolates; 4-methoxy phytoalexins were proposed to derive from glucobrassicin (**57**) via 4'-methoxyglucobrassicin (**70**) (Pedras and Yaya, 2013). 4-Methoxylated phytoalexins were shown to be potent against different fungal pathogens (Pedras and Sarma-Mamillapalle, 2012; Pedras and Yaya, 2012). This suggests that the activity of 4'-methoxyglucobrassicin against powdery mildew may be attributed to the involvement of 4-methoxylated metabolic products of 4'-methoxyglucobrassicin (**70**), including 4-methoxylated phytoalexins.

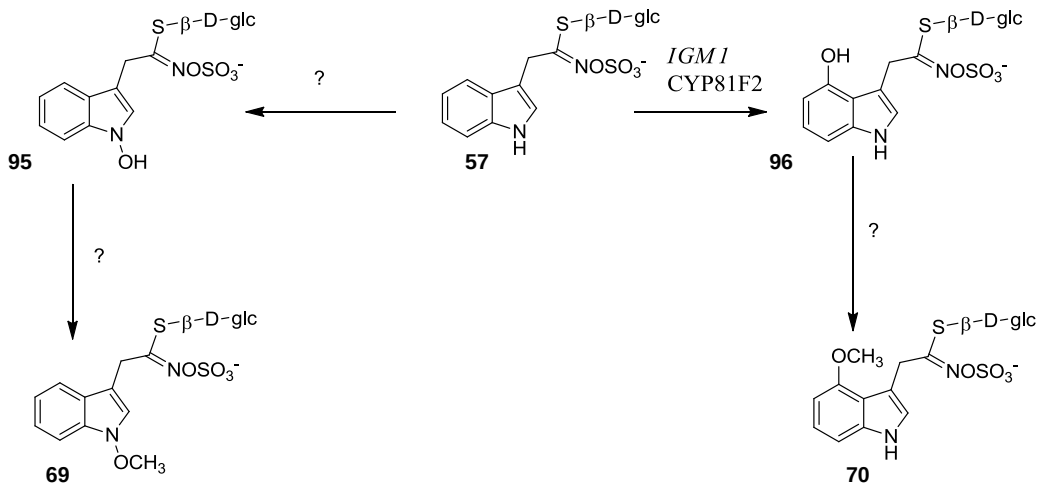

Scheme 1.4 Side chain modification of indole glucosinolates (Sønderby, Geu-Flores et al., 2010)

1.2.2.1.3 Pathway engineering

The dietary importance of crucifers is partly due to metabolic (hydrolysis) products of glucosinolates, as some of them have the potential of reducing the risk of developing cancer. Recent advances in engineering the glucosinolate pathway in non-cruciferous plant was viewed as a major success in the field (Mikkelsen, Olsen et al., 2010). The glucoraphanin (**100**) pathway was expressed in *N. benthamiana* (tobacco): the side chain elongation of the parent amino acid, methionine (**97**), to get the corresponding elongated intermediate, dihomo-methionine (**98**), was the first step in a series of reactions catalyzed by five enzymes (**i-v**) (BCAT4, MAM1, AC, IPM and BCAT3) of the chain-elongation pathway (Mikkelsen, Olsen et al., 2010). After transferring genes into *N. benthamiana*, plants were incubated for 7 days, extracted and analyzed for the detection of dihomo-methionine (**98**) (Mikkelsen, Olsen et al., 2010). In the second stage of the biosynthetic pathway (functional group formation), the conversion of dihomo-methionine (**98**) to 4-methylthiobutylglucosinolate (**99**) was facilitated by the involvement of seven enzymes (**vi-xi**) (CYP79F1, CYP83A1, GSTF11, SUR1/GGP1, UGT74C1 and AtST5b). The final step, the secondary modification of the side chain, was catalyzed by (**xii**) FMO

to yield metabolite **100** (Mikkelsen, Olsen et al., 2010) (**Scheme 1.5**). In different experiment, the conversion of phenylacetothiohydroxamate (**77**) to benzylglucosinolate (**58**) was also demonstrated using transgenic tobacco in which the last three steps of benzylglucosinolate (**58**) biosynthetic pathway were transferred to (Geu-Flores, Olsen et al., 2009).

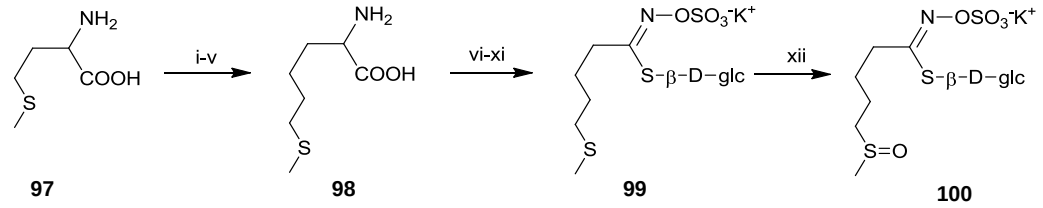

97 **98** **99** **100**

Scheme 1.5 Biosynthetic pathway of glucoraphanin (**100**), engineered in tobacco (Mikkelsen, Olsen et al., 2010)

1.2.2.2 Phytoalexins

Of the vast number of cruciferous plants species, only a limited number of (ca. 30) have been investigated for phytoalexin production. The majority cruciferous phytoalexins have been isolated from *Brassica* species (Pedras, Yaya et al., 2011). Since the first isolation of the cruciferous phytoalexins brassinin (**45**), cyclobrassinin (**78**) and 1'-methoxybrassinin (**105**) from Chinese cabbage inoculated with the bacterium *Pseudomonas cichorii* (Swingle) (Takasugi, Katsui et al., 1986), 45 cruciferous phytoalexins have been isolated and characterised (Pedras and Yaya, 2012; Pedras, Yaya et al., 2011). This group of metabolites are antimicrobial secondary metabolites which do not exist in healthy plant tissue. They are produced when plants are under stress either due to abiotic stress, such as metal salts ($CuCl_2$, AgCl, Cu_2SO_4) and UV-radiation, or biotic stress inflicted by microbes (Pedras, Yaya et al., 2011; Smith, 1996). Recently, a comprehensive review on their chemical synthesis, biosynthesis, metabolism by plant fungal pathogens and biological activities, has been published (Pedras, Yaya et al., 2011). Biosynthesis of cruciferous phytoalexins, pertinent to this thesis work, will be reviewed.

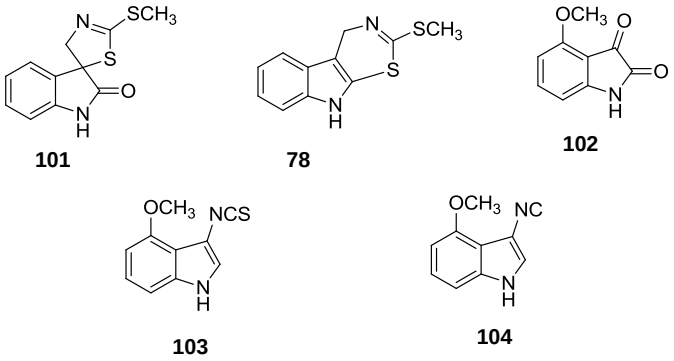

Figure 1.24 Examples of cruciferous phytoalexins

1.2.2.2.1 Biosynthesis

Most cruciferous phytoalexins are derived from the amino acid *L*-tryptophan (**66**) (Pedras, Yaya et al., 2011), which in turn is biosynthesized from anthranilic acid through the shikimate pathway (Dewick, 1998). The phytoalexins can be classified into four groups: non-methoxylated, 1-methoxylated, 4-methoxylated and a newly identified 1,4-dimethoxylated. The first biosynthetic study of cruciferous phytoalexins was conducted 5 years after the first isolation, revealing *L*-tryptophan (**66**) as the biosynthetic building block (Monde and Takasugi, 1991). The origin of the indole group was confirmed through feeding experiments using *L*-[4'-^{2}H]tryptophan (**66a**) (Monde and Takasugi, 1991), in which 18% deuterium incorporation was measured into spirobrassinin (**101**). The biosynthetic relationship between brassinin (**45**), cyclobrassinin (**78**) and 1'-methoxybrassinin (**105**) was investigated using Japanese radish roots incubated with [$^{2}H_3$CS]brassinin (**45a**) and [$^{2}H_3$CS]-1'-methoxybrassinin (**105a**). Brassinin (**45**) was not incorporated into 1'-methoxybrassinin (**105**), which in turn was not incorporated into cyclobrassinin (**78**). Therefore, it was suggested that cyclobrassinin (**78**) was not biosynthesized from 1'-methoxybrassinin (**105)** and that **105** was not derived from brassinin (**45**) (Monde, Tamura et al., 1995). Absence of incorporation of brassinin (**45**) into 1'-methoxybrassinin (**105**) suggested that they are likely derived from different biosynthetic precursors/intermediates, indolyl-3'-acetaldoxime (**122)** and 1'-methoxyindolyl-3'-acetaldoxime (**74),** respectively (Pedras, Zheng et al., 2007b).

[$^{2}H_3CS$]Brassinin (**45a**) was shown to be a biosynthetic precursor of spirobrassinin (**101**) and cyclobrassinin (**78**) (Monde and Takasugi, 1991) (**Scheme 1.6**). Brassilexin (**117**) was shown to be derived from Brassinin (**45**) and cyclobrassinin (**78**) (Pedras, Loukaci et al., 1998; Pedras, Yaya et al., 2011). Similarly, in rutabaga roots, cyclobrassinin (**78**) was shown to be a biosynthetic precursor of rutalexin (**116**) (Pedras, Montaut et al., 2004; Pedras, Yaya et al., 2011) (**Scheme 1.6**).

Recently, indole glucosinolates were identified as biosynthetic intermediates between tryptophan (**66**) and cruciferous phytoalexins (Pedras and Yaya, 2013; Pedras, Yaya et al., 2010). Glucobrassicin (**57**) as a common biosynthetic precursor for other indole glucosinolates and most of cruciferous phytoalexins was discovered, for the first time, in UV elicited leaves of salt cress (*T. salsuginea*) (Pedras, Yaya et al., 2010). The consistency of this discovery was further proven in rutabaga roots irradiated with UV, in which phytoalexins and indole glucosinolates incorporated glucobrassicin (**57**) (Pedras and Yaya, 2013). This suggests that indole glucosinolates and cruciferous phytoalexins may have some biosynthetic connections. Prior to the above discovery, a major breakthrough was achieved when indolyl-3'-thiohydroxamic acid (**79**) was incorporated into indole glucosinolates and cruciferous phytoalexins (Pedras and Okinyo, 2008). Desulfoglucobrassicin (**80**) was also incorporated into rutabaga phytoalexins (Pedras and Yaya, 2013), consistent with the incorporation of glucobrassicin (**57**) into the phytoalexins (Pedras and Yaya, 2013). The biosynthetic intermediate between glucobrassicin (**57**) and *T. salsuginea* phytoalexins (wasalexins A (**43**) and B (**109**) and biswasalexins A1 (**131**) and A2 (**132**)) was examined using heptadeuterated 1'-methoxybrassinin (**105a**) that was incorporated into *T. salsuginea* phytoalexins (Pedras, Yaya et al., 2010), suggesting **105** is a biosynthetic precursor of the phytoalexins **43**, **109**, **131** and **132**. However, administration of brassinin (**45**) to *T. salsuginea* leaves did not show incorporation (Pedras, Yaya et al., 2010), suggesting 1-methoxylated phytoalexins are derived from glucobrassicin (**57**) through 1'-methoxyglucobrassicin (**69**) (**Scheme 1.6**), which is consistent with lack of incorporation of brassinin (**45**) into 1'-methoxybrassinin (**105**) (Monde, Tamura et al., 1995). In agreement with the above

findings, 1'-methoxyindolyl-3'-acetaldoxime (**74)** was incorporated into **105** and **69** (**Scheme 1.6**) (Pedras and Montaut, 2004; Pedras, Okinyo et al., 2009).

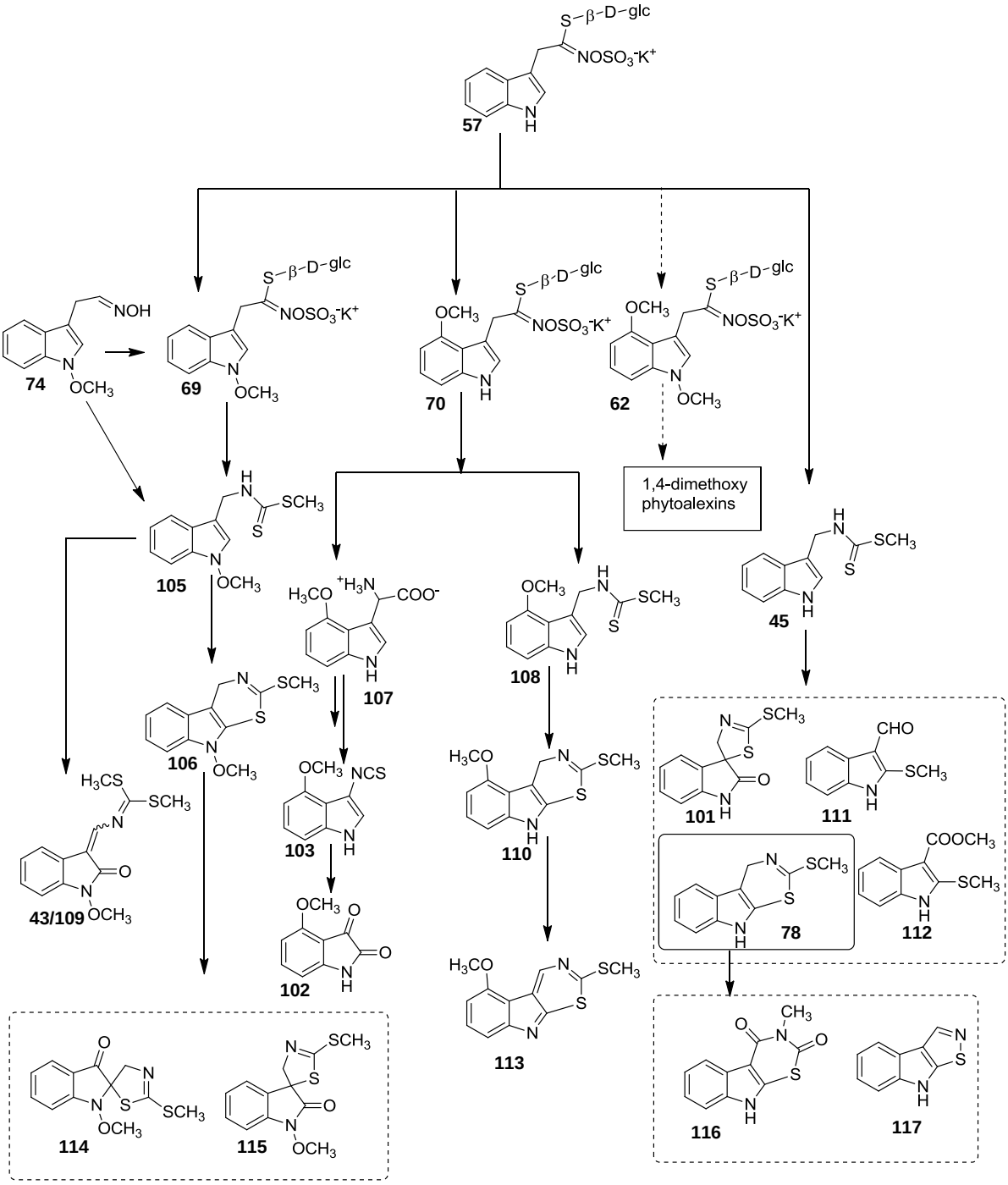

Scheme 1.6 Biosynthetic map of cruciferous phytoalexins (Pedras, Okinyo et al., 2009; Pedras and Yaya, 2013; Pedras, Yaya et al., 2011; Pedras, Yaya et al., 2010).

The incorporation of 1'-methoxybrassinin (**105**) and sinalbin B (**106**) into 1-methoxylated phytoalexins in *E. gallicum* showed that erucalexin (**114**) and 1'-methoxyspirobrassinin (**115**) are derived from 1'-methoxybrassinin **105** via sinalbin B (**106**) (Pedras and Okinyo, 2006a). Feeding experiments carried out with rutabaga roots revealed an incorporation of brassinin (**45**) into brassicanal A (**111**) and brassicanate A (**112**). The lack of incorporation of compound **78** into **111** and **112** suggested that **111**, **112** and **78** are likely share the same biosynthetic precursor (brassinin (**45**)) (Pedras, Montaut et al., 2004; Pedras, Yaya et al., 2011) (**Scheme 1.6**).

The biosynthetic pathway of 4-methoxy phytoalexins was investigated using rutabaga roots (Pedras and Yaya, 2013). The incorporation of glucobrassicin (**57**) into 4-methoxy phytoalexins including rapalexin A (**103**) suggested the involvement of 4'-methoxyglucobrassicin (**70**) as an intermediate. 4'-Methoxybrassinin (**108**), a proposed biosynthetic intermediate between metabolite **70** and 4-methoxy phytoalexins, was incorporated into 4'-methoxycyclobrassinin (**110**) and 4'-methoxydehydrocyclobrassinin (**113**), but not into rapalexin A (**103**) and isocyalexin A (**104**) (Pedras and Yaya, 2013).

Rapalexin A (**103)**, the first aromatic isothiocyanate, was isolated from canola leaves infected by *Albugo candida* (Pedras, Zheng et al., 2007a). It was later detected in rutabaga, turnip and *A. thaliana* (Pedras and Adio, 2008; Pedras, Okinyo et al., 2009); biosynthetically it is derived from tryptophan (**66**) (Pedras, Okinyo et al., 2009). Both *L* and *D*-tryptophan were incorporated into rapalexin A (**103)** suggesting isomerization of *D*- to *L*-tryptophan before the metabolism. By analogy to other phytoalexins, glucosinolate (**118**) was proposed to be a biosynthetic intermediate (Pedras, Zheng et al., 2007a) (**Scheme 1.7**).

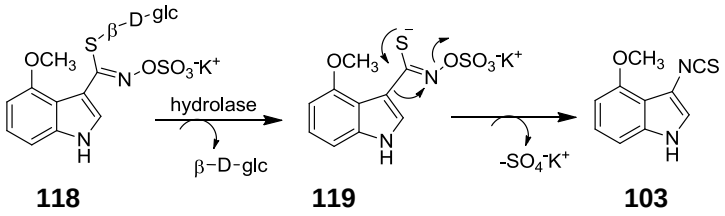

Scheme 1.7 Proposed biosynthetic precursor of rapalexin A (**103)** (Pedras, Zheng et al., 2007a)

Most recently, isocyalexin A (**104**), the first isocyanide of plant origin, was isolated from rutabaga roots irradiated by UV (Pedras and Yaya, 2012). The biosynthetic intermediate was proposed based on the isocyanide functional group that likely derived from **118** or an activated 4'-methoxyindole-3'-carboxaldehyde oxime (**121**) (Pedras and Yaya, 2012) (**Scheme 1.8**). The biosynthetic intermediates of rapalexin A (**103**) and isocyalexin A (**104**) are the main subject of this thesis. It is described in detail in the results and discussion and experimental sections of this thesis.

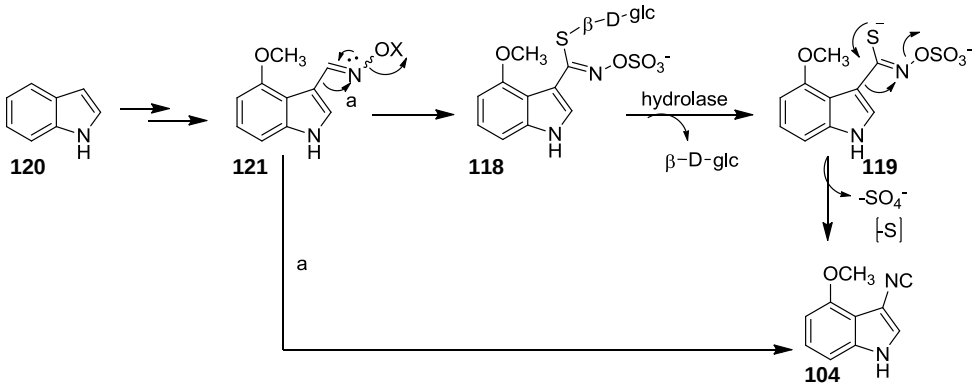

Scheme 1.8 Proposed biosynthetic intermediates of isocyalexin A (**104**) (Pedras and Yaya, 2012)

Camalexin (**44**) is a phytoalexin produced by the model plant *A. thaliana* whose biosynthetic pathway has been investigated more widely than that of cultivated plants. Most of its biosynthetic genes have been cloned (Geu-Flores, Møldrup et al., 2011; Pedras, Yaya et al., 2011). The initial step in the biosynthesis of camalexin (**44)** is common to indole glucosinolates and other cruciferous phytoalexins. The transformation of *L*-tryptophan (**66)** to indolyl-3'-acetaldoxime (**122)** is catalyzed by cytochrome P450 enzymes of the family CYP79 (CYP79B2 and CYP79B3) (Mikkelsen, Hansen et al., 2000). It was confirmed using a double knockout mutant (*cyp79b2/cyp79b3)* which was unable to synthesize camalexin (**44)** (Glawischnig, Hansen et al., 2004). The transformation of indolyl-3'-acetaldoxime (**122)** to indolyl-3'-acetonitrile (**67)** is catalyzed by CYP71A13. The ability of the knockout mutant *cyp71a13* to produce camalexin was reduced (Nafisi, Goregaoker et al., 2007; Pedras, Yaya et al., 2011). Further confirmation was made by expressing CYP71A13 in *Escherichia coli.* Transformation of tryptophan

(**66**) into indolyl-3'-acetonitrile (**67**) was achieved when CYP79B2 along with CYP71A13 were expressed in *N. benthamiana* (Nafisi, Goregaoker et al., 2007). The GSTF6 enzyme catalyzes the coupling of activated indolyl-3'-acetonitrile (**67**) to GSH to yield a GS-IAN (**123**) conjugate (Su, Xu et al., 2011). This transformation was confirmed by overexpressing *GSTF6*, using transgenic plants, as well as expressing the enzyme in yeast cells (Su, Xu et al., 2011). Xu and co-workers proposed that the hydrolysis of GS-IAN (**123)** to Cys-IAN (**125)** might be carried out by γ-glutamyl transpeptidases GGT1 and GGT2 and the phytochelatin synthase PCS1. Later GGPs involvement in camalexin biosynthesis was demonstrated by Geu-Flores and co-workers that GGP1 and GGP3 hydrolyze GS-IAN (**123)** to Cys-Gly-IAN (**124)** conjugate (Geu-Flores, Møldrup et al., 2011). Mutants lacking these genes accumulated lower amounts of camalexin (**44),** while the concentration of the intermediate (GS-IAN) was increased compared to the wild type. The hydrolysis of Cys-Gly-IAN (**124)** to Cys-IAN (**125)** was proposed to be catalyzed by carboxypeptidase (Geu-Flores, Møldrup et al., 2011). Lastly, the multifunctional CYP71B15 catalyzes the cyclization as well as oxidative decarboxylation steps **(Scheme 1.9)** (Geu-Flores, Møldrup et al., 2011; Pedras, Yaya et al., 2011).

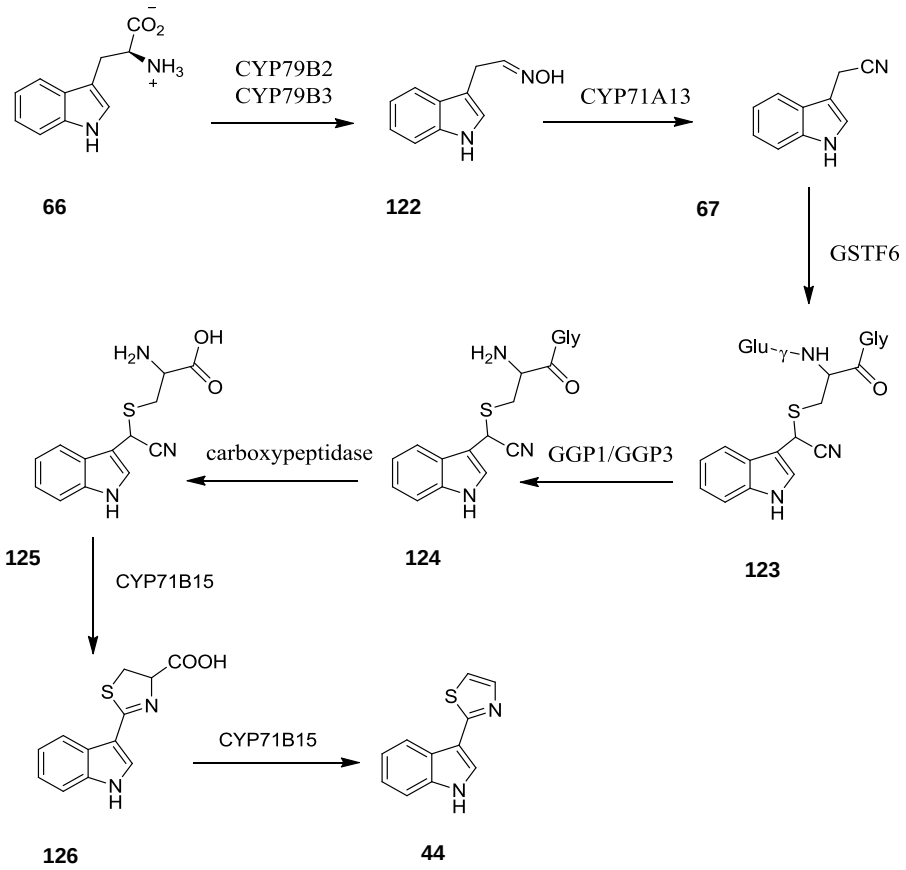

Scheme 1.9 Biosynthetic pathway of camalexin (**44**) (Geu-Flores, Møldrup et al., 2011; Pedras, Yaya et al., 2011).

1.2.3 Wild crucifers

The plant family Brassicaceae (Cruciferae) comprises a large number of agriculturally important crops including oilseeds, vegetables and condiments (Pedras, 2008; Schranz, Lysak et al., 2006). Brassicas are cultivated and consumed on all over the world. Oilseed crucifers (mainly *Brassica* species) are sources of edible vegetable oils. Apart from this, some wild species are good sources of industrial oils (Cromack, 1998; Warwick and Gugel, 2003). *Crambe abyssinica* (R.E.Fr) is a wild crucifer endemic to East Africa and the Red Sea region with high industrial potential (Gupta, 2009; Warwick and Gugel, 2003). *C. abyssinica* is resistant to drought and colder weather (Gupta, 2009), tolerant to heavy metals (Paulose, Kandasamy et al., 2010), contains high erucic acid and

glucosinolate levels (Mustakas, Kirk et al., 1976; Vaughn and Berhow, 1998), and has insecticidal activity (Peterson, Cossé et al., 2000). Epiprogoitrin (**94**) is one of the major glucosinolates detected in *C. abyssinica* that hydrolyzes to give toxic 2-hydroxy-3-butenenitrile (**127**) (Bellostas, Bjergegaard et al., 2007; Gupta, 2009; Mustakas, Kirk et al., 1976).

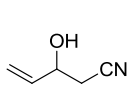

12

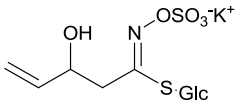

94

The genus *Diplotaxis* from the tribe Brassicaceae comprises about 34 species (Pignone and Martínez-Laborde, 2011), of which some are important sources of food (vegetable and salad) (Pignone and Martínez-Laborde, 2011; Scherrer, Motti et al., 2005) and forage for animals (Gupta, 2009). They are also known for their chemo-preventive (e.g. *D. tenuifolia*) (Melchini and Traka, 2010) and anti-inflammatory properties (Scherrer, Motti et al., 2005). *D. tenuifolia* showed strong resistance to a plant pathogen *Leptosphaeria maculans* (Chen and Séguin-Swartz, 1999).

The genus *Brassica* consists of economically important and commercially valuable species. Cultivated *Brassica* species are good sources of industrial and edible oils, vegetables and condiments. *B. tournefortii* (Gouan.) (a wild crucifer) native to northern Africa, the Middle East, eastern Pakistan, and the Mediterranean region (Gupta, 2009) is well adapted to the dry environments (Prakash, 1974) and has allelopathic properties (Gupta, 2009). It is resistant to acetolactate synthase (ALS)-inhibiting herbicides (Boutsalis, Karotam et al., 1999).

Different studies have indicated that some cultivated crucifers show resistance to destructive fungal pathogens (Pedras, Yaya et al., 2011; Pedras, Yaya et al., 2010). Similarly, a number of wild crucifers have been reported to show resistance to a variety of crucifer pathogens (Chen and Séguin-Swartz, 1999; Conn, Tewari et al., 1988; Pedras, Chumala et al., 2003). Their ability to resist disease can be attributed to complex metabolic processes involving the participation of secondary metabolites, including phytoanticipins and phytoalexins. When compared to cultivated species, the number of wild species investigated for the production of phytoalexins is much lower. Those

investigated have demonstrated the ability to produce phytoalexins in some cases unique to wild crucifers (e.g. camalexin (**44**) and wasalexins (**43, 109, 131 and 132**)) (**Table 1.1**). Most of these metabolites have been isolated characterised and reported. However, the chemical structure of 1',4'-dimethoxyindolyl-3'-acetonitrile from *D. muralis* was proposed based on ^{1}H-NMR data only, no other data (^{13}C, HRMS, UV, IR) were available (Sarwar, 2007). As this group of metabolites have a major role to play in defending plants from plant pathogens, investigations of wild crucifers for additional metabolites with diverse chemical structure are important. Wild crucifers that have been reported to produce phytoalexins are summarised in the table below (**Table 1.1**).

Table 1.1 Phytoalexins from wild crucifers reported to date.

Species (common name)	Phytoalexins	References
Arabidopsis thaliana (mouse-ear cress)	Camalexin (**44**)	(Tsuji, Jackson et al., 1992)
Arabis lyrata (lyrata rock cress)	Camalexin (**44**)	(Zook, Leege et al., 1998)
Brassica adpressa	Brassinin (**45**), cyclobrassinin (**78**), cyclobrassinin sulfoxide (**128**), 1'-methoxybrassinin (**105**)	(Rouxel, Kollmann et al., 1991)
B. atlantica	Brassinin (**45**), cyclobrassinin (**78**), 1'-methoxybrassinin (**105**)	(Rouxel, Kollmann et al., 1991)
B. carinata (Abyssinian cabbage)	Brassilexin (**117**), cyclobrassinin (**78**), cyclobrassinin sulfoxide (**128**), 1'-methoxybrassinin (**105**), spirobrassinin (**101**)	(Rouxel, Kollmann et al., 1991; Storck and Sacristan, 1995)
B. montana	Brassilexin (**117**), cyclobrassinin (**78**), 1'-methoxybrassinin (**105**),	(Rouxel, Kollmann et al., 1991)
Camelina sativa (false flax)	Camalexin (**44**), 6-methoxycamalexin(**130**)	(Browne, Conn et al., 1991)
Capsella bursa-pastoris (shepherde's purse)	Camalexin (**44**), 6-methoxycamalexin (**130**), 1-methylcamalexin (**129**)	(Jimenez, Ayer et al., 1997)
C. abyssinica (Abyssinian mustard)	Rapalexin B (**134**), arvelexin (**135**)	(Sarwar, 2007)
D. muralis (wall rocket)	Arvelexin (**135**), rapalexin A (**103**)	(Sarwar, 2007)
Erucastrum gallicum (dog mustard)	Arvelexin (**135**), indolyl-3'-acetonitrile (**67**), erucalexin (**114**), 1-methoxyspirobrassinin (**115**)	(Pedras, Suchy et al., 2006)
Sysimbrium officinale (hedge mustard)	Indolyl-3'-acetonitrile (**67**), methyl-1'-methoxyindolyl-3'-carboxylate (**133**)	(Sarwar, 2007)
Thlaspi arvense (stinkweed)	Arvelexin (**135**), wasalexin A (**43**)	(Pedras, Chumala et al., 2003; Pedras, Sorensen et al., 1999)
Thellungiella salsuginea (salt cress)	Wasalexin A (**43**), B (**109**), biswasalexin A1(**131**), A2 (**132**), methoxybrassenin B (**137**), rapalexin A (**103**)	(Pedras and Adio, 2008; Pedras, Zheng et al., 2009)

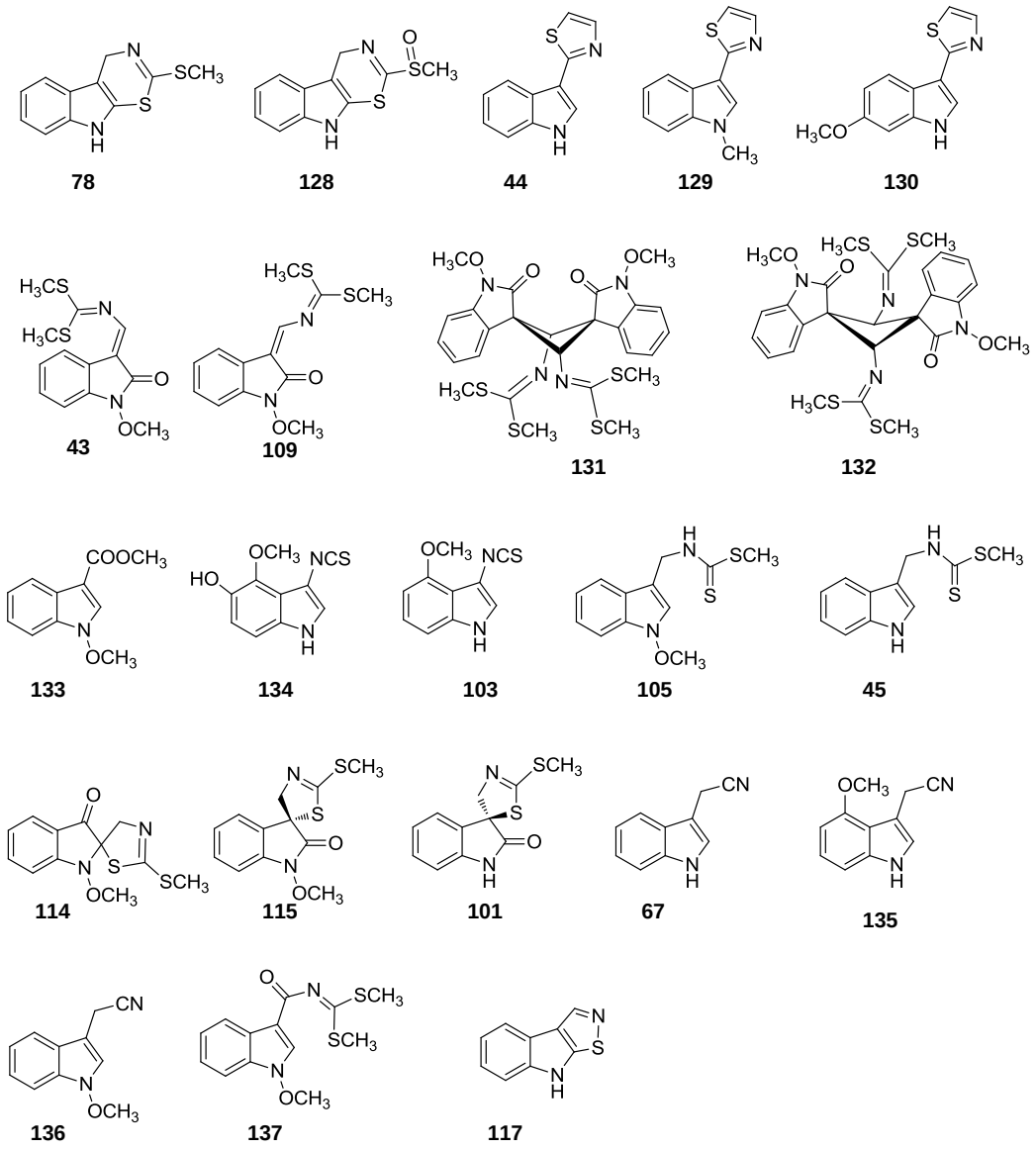

Figure 1.25 Phytoalexins isolated from wild crucifers: cyclobrassinin (**78**), cyclobrassinin sulfoxide (**128**), camalexin (**44**), 1-methylcamalexin (**129),** 6-methoxycamalexin (**130**), wasalexin A (**43**), wasalexin B (**109**), biswasalexin A1 (**131**), biswasalexin A2 (**132**), methyl 1'-methoxyindole-3'-carboxylate (**133**), rapalexin B (**134**), rapalexin A (**103**), 1'-methoxybrassinin (**105**), brassinin (**45**), erucalexin (**114**), (*R*)-1'-methoxyspirobrassinin (**115**), (*S*)-spirobrassinin (**101**), indolyl-3'-acetonitrile (**67**), arvelexin (**135**), caulilexin C (**136**), 1'-methoxybrassenin B (**137**), brassilexin (**117**) (Pedras, Yaya et al., 2011).

1.3 Myrosinases

Hydrolysis of glucosinolates is facilitated by a group of enzymes called myrosinases (thioglucosidases, EC 3.2.1.147) (Bor, Ozkur et al., 2009; Zhang, Pontoppidan et al., 2002).

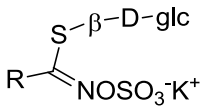

glucosinolate

Myrosinase isoenzymes present in the Brassicaceae family are proteins containing oligosaccharide chains. Their degrees of glycosylation and isoelectric points are different depending on the species and the organs in which they are produced (Bellostas, Petersen et al., 2008; Bones, 1990; Zhou, Tokuhisa et al., 2012). Myrosinases are abundant in all plant species producing glucosinolates (Bones and Rossiter, 1996) and have been purified and characterized from various organs of Brassicaceae species: seeds of S*inapis alba* L. (Bjorkman and Janson, 1972), roots of *Rapahnus sativa* L., *B. campestris* L. and *W. japonica* (Matsum.) (Hara, Eto et al., 2001), *B. napus* L. (Härtel and Brandt, 2002), seeds of *B. carinata* (A. Braun) and *B. oleracea* var. *capitata* L. (Bellostas, Petersen et al., 2008) (**Table 1.2)**. Myrosinases are disulfide-linked dimers of 75 kDa subunits coordinated by a zinc atom (Bones and Slupphaug, 1989; Eriksson, Andreasson et al., 2002; Lonnerda and Janson, 1973) that can further link with myrosinase binding proteins and form complexes of higher molecular weights (Eriksson, Andreasson et al., 2002; Geshi, Andreasson et al., 1998) ranging from 140-600 kDa (Bellostas, Petersen et al., 2008). Plant myrosinases are encoded by the "thioglucoside glucohydrolase (TGG)" (Bor, Ozkur et al., 2009) of which six (TGG1-TGG6) have been identified in *A. thaliana* (Andersson, Chakrabarty et al., 2009). Some of them share up to 73% amino acid identity with distinct physicochemical properties (Zhou, Tokuhisa et al., 2012). The myrosinases characterised and reported to date from Brassicaceae are listed in **Table 1.2**.

Table 1.2 Myrosinases from Brassicaceae

Plant species	Thioglucosidases (isolated, characterised, cloned)	References
A. thaliana	TGG1-TGG5 isolated, characterized; TGG1,3,4,5 cloned	(Andersson, Chakrabarty et al., 2009; Zhang, Pontoppidan et al., 2002; Zhou, Tokuhisa et al., 2012)
Armoracia rusticana	Isolated, characterized	(Li and Kushad, 2005)
B. carinata	Isolated, characterized	(Bellostas, Petersen et al., 2008; Bellostas, Sørensen et al., 2006)
B. napus	MA, MB, MC isolated, characterized; MA, MB cloned	(Borgen, Thangstad et al., 2010; Härtel and Brandt, 2002; Lonnerda and Janson, 1973; Thangstad, Winge et al., 1993)
B. oleracea var. *capitata*	Isolated, characterized	(Bellostas, Petersen et al., 2008; Peñas, Frias et al., 2011)
C. abyssinica	Isolated, characterized	(Bernardi, Finiguerra et al., 2003)
Lepidium sativum	Isolated, characterized	(Durham and Poulton, 1989; Iversen and Baggerud, 1980)
R. sativa	Isolated, characterized	(Shikita, Fahey et al., 1999)
Sinapis alba	SA, SB, SC isolated, characterized	(Bjorkman and Janson, 1972; Björkman and Lönnerdal, 1973; Eriksson, Ek et al., 2001; Iversen and Baggerud, 1980)
T. halophila	TGG1, TGG2 detected	(Pang, Chen et al., 2009)

Myrosinases and glucosinolates are stored in separate compartments called myrosin cells and vacuole respectively (Bones and Iversen, 1985; Bones and Rossiter, 2006; Kissen, Rossiter et al., 2009). They come in contact when tissue damage occurs that gives rise to hydrolysis of glucosinolates to form glucose and an unstable aglycone (**138**). Intermediate **138** rearranges itself spontaneously to release sulfate and other products such as isothiocyanates (**139**), thiocyanates (**140**), nitriles (**141**), oxazolidinethiones (**142**), 1-cyano-2,3-epithiopropane (**143**) and other more (**Scheme 1.10**) (Bones and Rossiter, 2006; Halkier and Gershenzon, 2006; Yang, Wang et al., 2012) Their formation mainly depends on the chemical structure of the parent amino acid

and other factors (Bones and Rossiter, 1996; Hopkins, van Dam et al., 2009). For example, isothiocyanates (**139**) are formed at neutral pH, while nitrile (**141**) formation requires low pH conditions. In the presence of epithiospecifier proteins, epithionitriles are more favoured products (Bones and Rossiter, 1996; Hopkins, van Dam et al., 2009). In the case of indole glucosinolates (e.g. glucobrassicin (**57)**) the enzymatic hydrolysis products include unstable indolyl-3'-isothiocyanate (**144**), indolyl-3'-methanol (**145**), indolyl-3'-acetonitrile (**67**) and 3,3'-diindolylmethane (**146**) (Bones and Rossiter, 1996; Bones and Rossiter, 2006) (**Figure 1.26**).

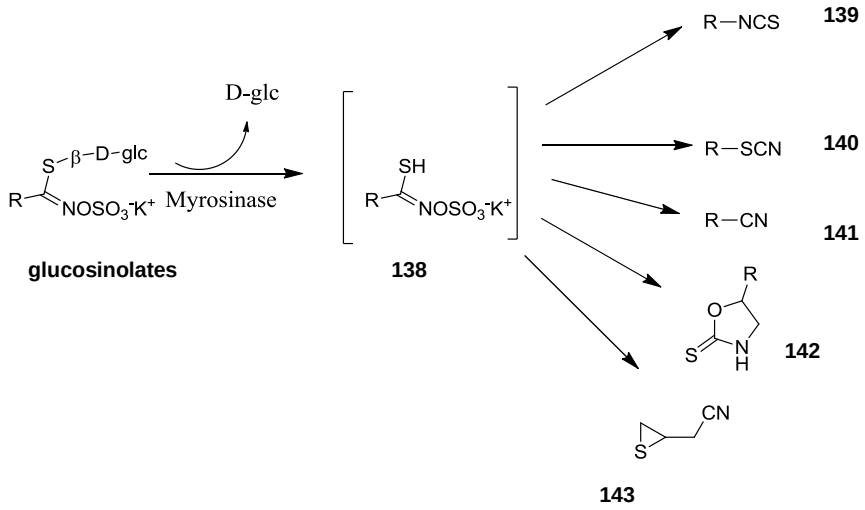

Scheme 1.10 Hydrolysis products of glucosinolates (Bones and Rossiter, 2006)

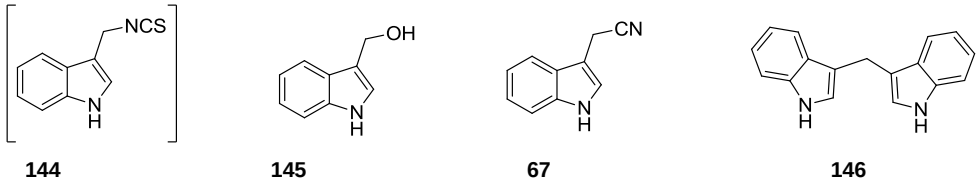

Figure 1.26 Glucobrassicin hydrolysis products: **144** is unstable and has never been isolated (Bones and Rossiter, 2006)

Certain hydrolysis products of glucosinolates such as sulforaphane 4-(methylsulfinyl)butylisothiocyanate (**147**), have cancer chemo-preventive activities (Abbaoui, Riedl et al., 2012; Li, Karagöz et al., 2012) and neuro-protective effects

(Benedict, Mountney et al., 2012). In plant-pathogen interactions, hydrolysis products of glucosinolates play a great role in protecting plants from plant pathogens. For example, long chain aliphatic isothiocyanates are toxic to plant pathogens (Kurt, Güneş et al., 2011; Stotz, Sawada et al., 2011). Indolyl-3'-acetonitriles (**67**), a hydrolysis product of glucobrassicin (**57**), deters oviposition by insects (De Vos, Kriksunov et al., 2008). Indole glucosinolates are also biosynthetic precursors for cruciferous phytoalexins, which are plant defence antimicrobial secondary metabolites (Pedras, Yaya et al., 2011; Pedras, Yaya et al., 2010). Therefore, the glucosinolate-myrosinase system can be regarded as a plant defence mechanism against different stresses.

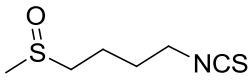

147

1.4 Conclusion

Crucifers, one of the agro-economically important plant species, are sources of vegetables, condiment and oils (edible and industrial) (Schranz, Lysak et al., 2006). Worldwide yield loss is mainly caused by biotic and abiotic stresses. Crucifers produce a variety of defense metabolites including indole glucosinolates (Agerbirk and Olsen, 2012; Pedras, Yaya et al., 2011). Their concentration increases when plants are under stress or attacked by pathogen which shows their role in plant defences. The three major indole glucosinolates are glucobrassicin (**57**), 1'-methoxyglucobrassicin (**69**) and 4'-methoxyglucobrassicin (**70**). Their metabolic products are found to be active against different microbes (Pedras and Hossain, 2011).

Indole glucosinolates are biosynthesized from tryptophan (**66**) and are intermediates in the biosynthesis of cruciferous phytoalexins (Pedras and Yaya, 2013). Most biosynthetic intermediates and biosynthetic genes involved in the biosynthesis of indole glucosinolates have been identified (Halkier and Gershenzon, 2006; Sønderby, Geu-Flores et al., 2010). Of 45 cruciferous phytoalexins that have been isolated, most are

from cultivated species (Pedras, Yaya et al., 2011). Because of the availability of *A. thaliana* mutants, only the genes of camalexin (**44**) biosynthesis have been isolated and cloned (Geu-Flores, Møldrup et al., 2011; Pedras, Yaya et al., 2011). No gene has been isolated or cloned for the rest of the 44 cruciferous phytoalexins. The structural diversity of cruciferous phytoalexins is an indication of complex biosynthetic pathways, where unique enzymes are yet to be discovered.

A tremendous amount of work has been done in understanding biosynthetic intermediates of cruciferous phytoalexins through feeding experiments. Different ^{2}H, ^{13}C and ^{15}N labeled intermediates have been used to elucidate the biosynthetic map (Pedras and Yaya, 2010; Pedras, Yaya et al., 2011; Pedras, Zheng et al., 2007b). Most biosynthetic intermediates linking tryptophan (**66**) to cruciferous phytoalexins have been proposed (Pedras, Yaya et al., 2011). Brassinin (**45**) is a biosynthetic precursor for most non methoxylated phytoalexins. 1'- and 4'-methoxybrassinins (**105** and **108**) are proposed to be biosynthetic precursors for most of 1- and 4-methoxylated phytoalexins, respectively (Pedras and Yaya, 2013; Pedras, Yaya et al., 2011). Unlike other 4-methoxylated phytoalexins, rapalexin A (**103**), isocyalexin A (**104**) and isalexin (**102**) follow a different biosynthetic route (Pedras and Yaya, 2013). The recent discovery of 4'-methoxyindolyl-3'-glycine (**107**), as an intermediate in the biosynthesis of **103**, **104** and **102** is regarded as a great achievement in mapping cruciferous phytoalexin biosynthetic pathways. Determination of such biosynthetic intermediates will facilitate the isolation of biosynthetic enzymes, and the cloning of biosynthetic genes, which is important for genetic manipulations of the susceptible species (Pedras and Yaya, 2013).

2 RESULTS AND DISCUSSION

2.1. Investigation of elicited metabolites of wild crucifers

Elicitation of plant secondary metabolites can be carried using either biotic (e.g. pathogens) or abiotic (e.g. UV radiation, salt solutions) stresses (Pedras, Yaya et al., 2011). The type and amounts of elicited metabolites depend on the type of elicitor used and the environmental conditions. Elicitation can cause leaf necrosis to mild leaf damage and even no macroscopic symptoms. To investigate the production of elicited metabolites by the wild crucifers *Brassica tournefortii*, *Crambe abyssinica*, *Diplotaxis tenuifolia* and *Diplotaxis tenuisiliqua*, solutions of $CuCl_2$ were sprayed on potted plants. Plants were sprayed with 2, 5, 10, 15 and 20 mM $CuCl_2$ solutions to determine the concentration that induced macroscopic damage. *B. tournefortii*, *C. abyssinica* and *D. tenuifolia* showed severe damage on the leaves when sprayed with 5 mM or higher; $CuCl_2$ concentrations lower than 10 mM did not cause substantial damage on leaves of *D. tenuisiliqua*. Therefore, *B. tournefortii*, *C. abyssinica* and *D. tenuifolia* were sprayed with 2 mM solutions while *D. tenuisiliqua* was sprayed with 10 mM solution of $CuCl_2$. Prior to this work, *C. abyssinica* was investigated and found to produce elicited indole derived metabolites: arvelexin (**135**) and rapalexin B (**134**) (Sarwar, 2007); however, no elicited metabolites were reported from *B. tournefortii*, *D. tenuifolia* and *D. tenuisiliqua*. Therefore, further investigations were carried out using $CuCl_2$ solutions as described above.

2.1.1 *Diplotaxis tenuisiliqua*

2.1.1.1 Time-course analysis, isolation and structural elucidation

Phytoalexin production in *D. tenuisiliqua* was elicited by spraying 4-week-old plants with $CuCl_2$ (10 mM) solution to the point of run-off. Control leaves were sprayed with water in a similar way. After 24 h of incubation, leaves were excised and the excised leaves were frozen in liquid nitrogen, ground and extracted with methanol as summarised in **Figure 2.1**. The plant tissue was filtered off and the solvent evaporated; the residue (extract) was washed with CH_2Cl_2 to yield the CH_2Cl_2 extract and the MeOH residue. The CH_2Cl_2 was evaporated and the residue dissolved in CH_3CN and subjected to HPLC-DAD analyses. The methanolic extract was dissolved in water-methanol (1:1) and analyzed by HPLC-DAD. Additional leaves, harvested from elicited and control plants at 72, 120 and 168 hours, were also extracted and analyzed by HPLC-DAD as described above.

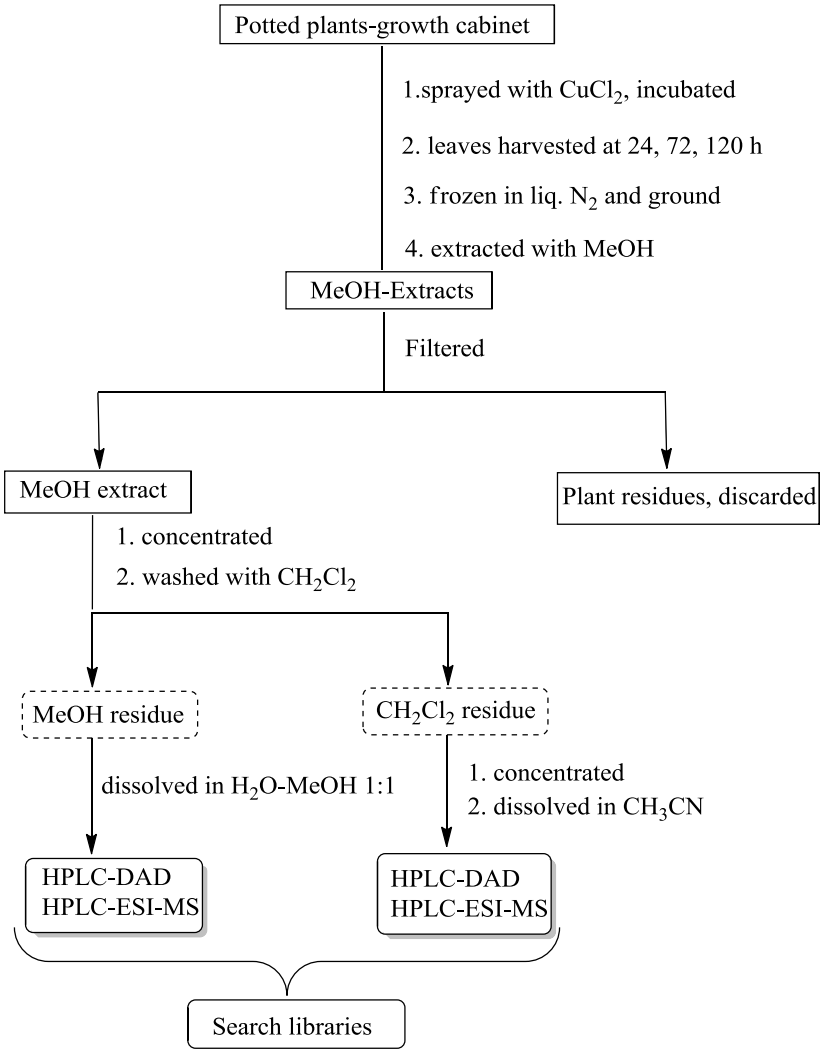

Figure 2.1 Flow chart for time-course analysis of elicited plants

Metabolite profiles of elicited leaf extracts were compared against control leaf extracts. The extracts of elicited leaves showed peaks at t_R = 13.8 and 19.7 min that were absent in extracts of control leaves. Comparison of retention times and UV spectra of elicited metabolite peaks with the phytoalexin database available in Dr. Pedras' group revealed that the peak at t_R = 13.8 min was arvelexin (**135**). However, no UV spectrum match was found for the peak at t_R = 19.7 min. The methanolic extracts were also analyzed by HPLC-DAD for the detection of indole glucosinolates (glucobrassicin (**57**), 1'-methoxyglucobrassicin (**69**) and 4'-methoxyglucobrassicin (**70**)). No indole glucosinolates were detected in either control or elicited leaf extracts (**Table 2.1**).

To isolate the new metabolite present in CH_2Cl_2 extracts, elicited leaves (300 g) were cut and frozen in liquid nitrogen, crushed and extracted with CH_3OH (1 L). The mixture was filtered, the leaf pieces were discarded and the solvent was evaporated. The crude extract was washed with CH_2Cl_2 and the solvent was evaporated. The CH_2Cl_2 extract was subjected to flush column chromatography (FCC) (Hex-EtOAc; 80:20-0:100), fractions were analyzed by thin layer chromatography (TLC) and those fractions containing identical components were combined. The combined fractions were analyzed by HPLC-DAD and the fraction containing elicited compounds (fraction-1) (**Figure 2.2**) was further purified by FCC (Hex-EtOAc; 90:10-70:30) to yield six fractions; fractions were analyzed by HPLC-DAD and fraction-2 was found to contain the elicited compound at t_R = 19.7 min. This fraction (fraction-2) was subjected to PTLC (Hex-EtOAc; 85:15) to afford six bands that were eluted and analyzed by HPLC-DAD and the least polar (R_f = 0.5) band contained the desire compound **X** (0.8 mg) with t_R = 19.7 min (**Figure 2.2**). Compound **X** was characterized by ^{1}H-NMR and HR-EI-MS.

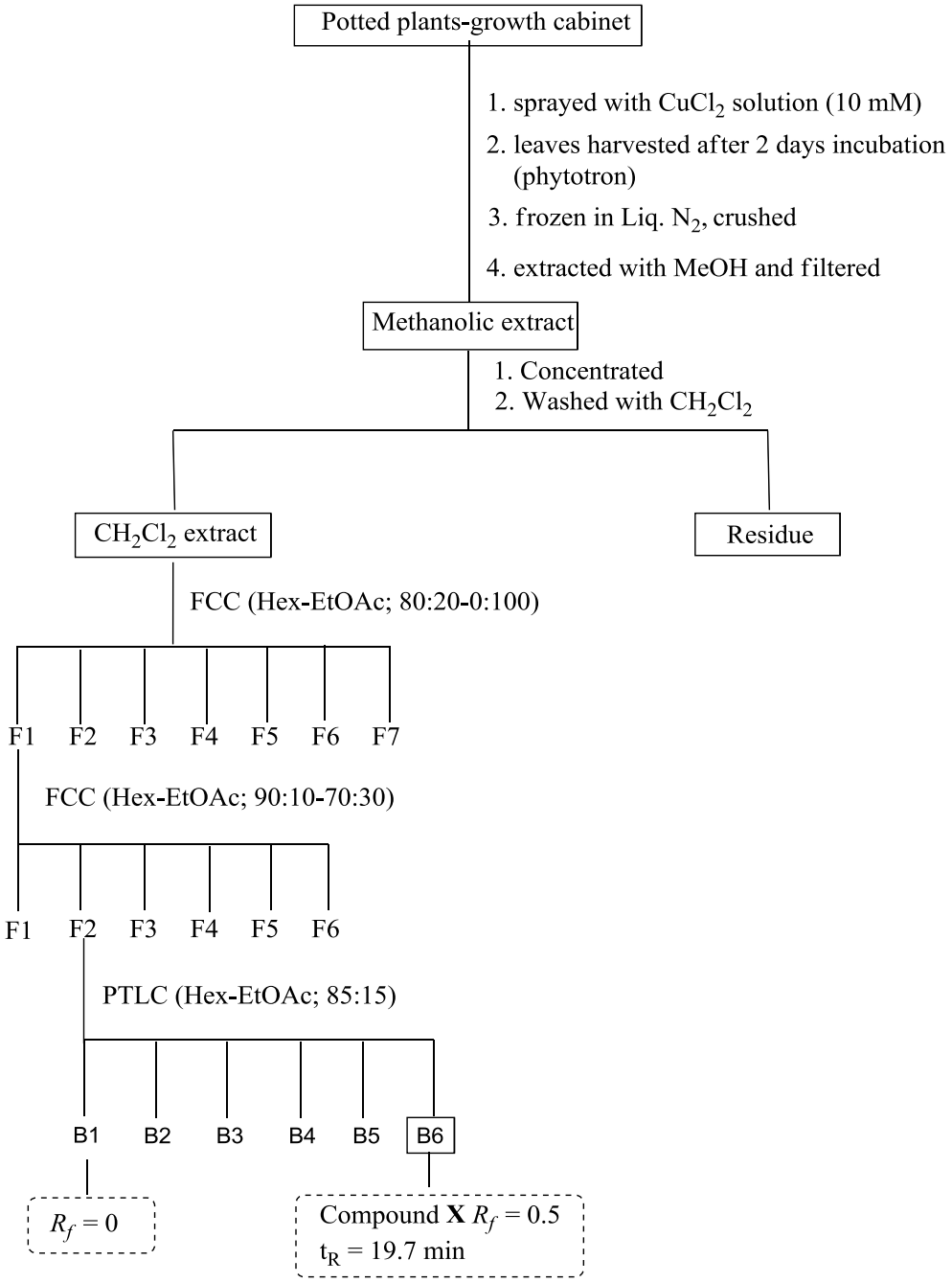

Figure 2.2 Isolation of UV-elicited metabolites from leaves of *Diplotaxis tenuisiliqua*

The HR-EI-MS of compound **X** showed a molecular ion at *m/z* $[M]^+$ 216.0897 consistent with the molecular formula $C_{12}H_{12}N_2O_2$ (calcd. 216.0899). Consistent with the HR-EI-MS data, the ^{1}H-NMR spectrum showed 12 protons: a singlet at δ_H 7.19 (1H), a

doublet of doublets at δ_H 7.17 (1H), two doublets at δ_H 7.02 (1H) and δ_H 6.50 (1H), two methyl singlets at δ_H 4.06 and 3.92 and a singlet at δ_H 4.02 (2H). The presence of four protons in the aromatic region (δ 7.19-6.50) suggested the presence of an indole ring substituted at N-1, C-3 and either C-4 or C-7. The two methyl singlets (δ 4.06 and 3.92) were most likely due to methoxy groups attached to the indole ring at C-4 and N-1, by analogy to other indolic structures. The remaining substituent CH_2-CN was likely located at C-3. Based on these data, the structure of the compound **X** (t_R = 19.7 min) was assigned as 1',4'-dimethoxyindolyl-3'-acetonitrile (**148**) (**Figure 2.3**). This structure was confirmed by synthesis.

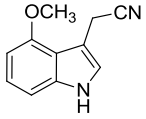

135

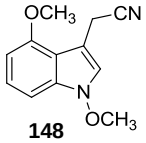

148

Figure 2.3 Elicited metabolites of *Diplotaxis tenuisiliqua.*

Table 2.1 Time-course HPLC analysis (using method A) of metabolites of *Diplotaxis tenuisiliqua.*

Metabolites- t_R (min)	Incubation period (h)	Total amount of metabolites (nmol/ g of fresh tissue ± STD)[a]
arvelexin (**135**): 13.8	24	0.3 ± 0.0
	72	1.3 ± 0.2
	120	1.2 ± 0.6
	168	0.4 ± 0.1
1',4'-dimethoxyindolyl-3'-acetonitrile (**148**): 19.7	24	0.1 ± 0.0
	72	0.2 ± 0.0
	120	0.1 ± 0.0
	168	0

[a]Amounts of arvelexin (**135**) and 1',4'-dimethoxyindolyl-3'-acetonitrile (**148**) determined by HPLC-DAD using calibration curves. Values are the averages of one experiment conducted in triplicate ± standard deviation (STD).

2.1.1.2 Synthesis of 1',4'-dimethoxyindolyl-3'-acetonitrile (148)

1',4'-Dimethoxyindolyl-3'-acetonitrile (**148**) was prepared from commercially available 4-methoxyindole (**149**). 4-Methoxyindole (**149**) was reduced to the corresponding 4-methoxyindoline (**150**) with $NaCNBH_3$ in AcOH (Wang, Gao et al., 2009), which was then oxidized with $Na_2WO_4.2H_2O/H_2O_2$ and methylated with $(CH_3O)_2SO_2$ (Somei and Kawasaki, 1989) to yield 1,4-dimethoxyindole (**151**) in 41% yield. Formylation of **151** was accomplished via a Vilsmeier-Haak reaction that yielded 1',4'-dimethoxyindole-3'-carboxaldehyde (**152**) in 81% yield. Condensation of 1',4'-dimethoxyindole-3'-carboxaldehyde (**152**) with excess nitromethane in the presence of ammonium acetate under reflux (Canoira, Rodriguez et al., 1989; Somei, Sato et al., 1985) yielded 1,4-dimethoxy-3-nitrovinyl indole (**153**), which was used without further purification. Compound **153** was reduced with sodium borohydride in THF in the presence of methanol to yield 1,4-dimethoxy-3-(2'-nitroethyl)indole (**154**) in moderate yield (Robertson and Botting, 1999). The final step, the transformation of 1,4-dimethoxy-3-(2'-nitroethyl)indole (**154**) into 1',4'-dimethoxyindolyl-3'-acetonitrile (**148**), was accomplished in 77% yield by treating **154** with carbon disulfide in the presence of triethylamine in a sealed reaction vial at 40 ºC (**Scheme 2.1**).

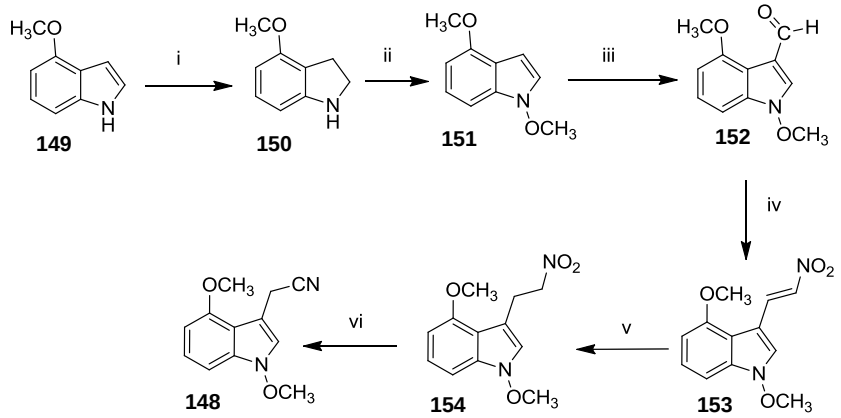

Scheme 2.1 Synthesis of **148**. Reagents and conditions: i) $NaCNBH_3$, AcOH; ii) Na_2WO_4, H_2O_2, K_2CO_3, $(CH_3)_2SO_4$ 41%; iii) $POCl_3$, DMF; iv) CH_3NO_2, NH_4OAc, 105 ºC; v) $NaBH_4$, THF, MeOH; vi) CS_2, Et_3N , 40 ºC 77%.

Compound **148** was assayed against the plant pathogenic fungi *A. brassicicola*, *L. maculans*, *R. solani* and *S. sclerotiorum.* At the highest concentration, 0.5 mM, the mycelial growth of *A. brassicicola*, *R. solani* and *S. sclerotiorum* were completely inhibited (**Table 2.2**). Therefore, considering that **148** is an elicited metabolite and displays antifungal activity, it is a phytoalexin for which the name tenualexin is proposed.

Table 2.2 Inhibitory activity of 1',4'-dimethoxyindolyl-3'-acetonitrile (**148**) against mycelia[a] of plant pathogenic fungi *Alternaria brassicicola*, *Leptosphaeria maculans*, *Rhizoctonia solani* and *Sclerotinia sclerotiorum.*

1',4'-dimethoxyindolyl-3'-acetonitrile (**148**)[b]	*A. brassicicola* (% inh.)	*L. maculans* (% inh.)	*R. solani* (% inh.)	*S. sclerotiorum* (% inh.)
5.0×10^{-4} M	100 ± 0	69 ± 4	100 ± 0	100 ± 0
2.0×10^{-4} M	47 ± 4	31 ± 4	86 ± 0	57 ± 2
1.0×10^{-4} M	31 ± 4	18 ± 4	67 ± 4	23 ± 2

[a] Percentage of inhibition = 100 – [{(growth on medium containing compound-plug[c])/growth on control medium-plug[c])} × 100)] ± standard deviation. Results are the averages ± standard deviations of independent experiments conducted in triplicate.
[b]Compound was dissolved in DMSO and added to potato dextrose agar medium.
[c]Plug diameter = 4 mm

2.1.2 *Brassica tournefortii*

2.1.2.1 Time-course analysis

An investigation of the production of elicited metabolites in *B. tournefortii* was carried out after spraying 3-week-old plants with $CuCl_2$ (2 mM) solution as described in **Figure 2.1**. The metabolite profiles of elicited leaf extracts were compared against those of control leaves. Extracts of elicited leaves showed five peaks that were absent in extracts of control leaves at t_R 12.0, 13.8, 14.5, 19.9 and 25.2 min. A comparison of HPLC-DAD and HPLC-ESI-MS data with those of compounds available in Dr. Pedras' group revealed that the peaks at t_R = 12.0 min corresponded to spirobrassinin (**101**), t_R =

13.8 min to arvelexin (**135**), t_R = 14.5 min to rutalexin (**116**), t_R = 19.9 min to 4'-methoxybrassinin (**108**) and t_R = 25.2 min to cyclobrassinin (**78**). The amount of each metabolite was determined using calibration curves built with synthetic samples (**Table 2.3**). Production of these metabolites from cultivated *Brassica* species has been reported (Pedras, Yaya et al., 2011).

The methanolic extracts were also analyzed by HPLC-DAD for the detection of indole glucosinolates (glucobrassicin (**57**), 1'-methoxyglucobrassicin (**69**) and 4'-methoxyglucobrassicin (**70**)). The HPLC-DAD and HPLC-ESI-MS data indicated that glucobrassicin (**57**) and 4'-methoxyglucobrassicin (**70**) were produced by the plant. However, 1'-methoxyglucobrassicin (**69**) was not detected in the polar extract (**Table 2.3**). These results suggest that both wild and cultivated species of *Brassica* share pathways that are responsible for phytoalexin biosynthesis.

Table 2.3 Time-course HPLC analysis (using method A for phytoalexins and method B for indole glucosinolates) of metabolites of *Brassica tournefortii.*

Metabolites; t_R (min)	Incubation period (h)	Total amount of metabolites (nmol/ g of fresh tissue ± STD)[a]
spirobrassinin (**101**); 12.0	24	5.6 ± 0.9
	72	4.6 ± 0.3
	120	4.6 ± 0.2
arvelexin (**135**); 13.8	24	0.5 ± 0.1
	72	1.2 ± 0.5
	120	0.7 ± 0.3
rutalexin (**116**); 14.5	24	1.0 ± 0.1
	72	1.0 ± 0.1
	120	1.1 ± 0.0
4'-methoxybrassinin (**108**); 19.9	24	1.0 ± 0.1
	72	0.1 ± 0.0
	120	0
cyclobrassinin (**78**); 25.2	24	3.2 ± 0.4
	72	0.6 ± 0.0
	120	0.4 ± 0.0
glucobrassicin (**57**); 19.6	24	18.5 ± 4.4
	72	9.0 ± 5.0
	120	5.8 ± 1.0
4'-methoxyglucobrassicin (**70**); 26.2	24	3.4 ± 1.0
	72	2.0 ± 1.1
	120	1.0 ± 0.3

[a]Amounts of spirobrassinin (**101**), arvelexin (**135**), rutalexin (**116**), 4'-methoxybrassinin (**108**), cyclobrassinin (**78**), glucobrassicin (**57**) and 4'-methoxyglucobrassicin (**70**) determined by HPLC-DAD using calibration curves. Values are the averages of one experiment conducted in triplicate ± standard deviation (STD).

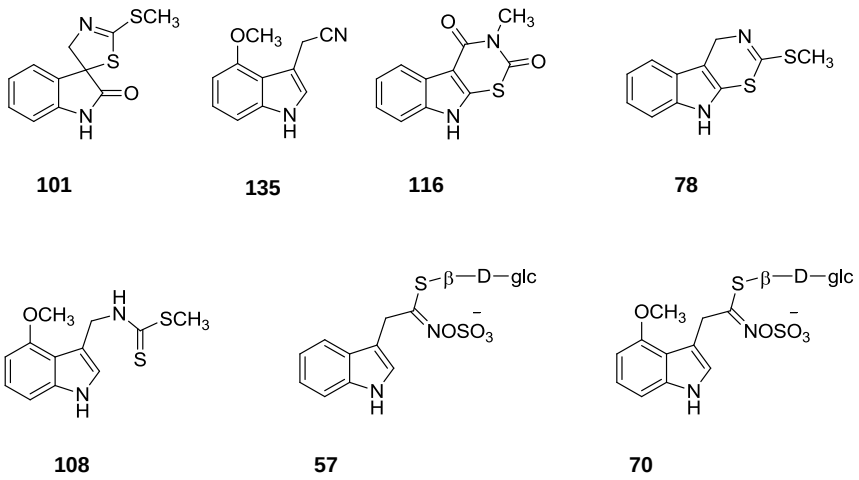

Figure 2.4 Elicited and constitutive metabolites of *Brassica tournefortii.*

2.1.3 *Crambe abyssinica*

2.1.3.1 Time-course analysis

C. abyssinica (17-days-old) was sprayed with $CuCl_2$ (2 mM) solution and incubated. Control leaves were sprayed with water in a similar fashion and analyzed as described in **Figure 2.1**. The metabolite profiles of elicited leaf extracts were compared against control leaves. Extracts of elicited leaves showed three peaks at t_R 11.7, 13.6 and 24.7 min which were absent from extracts of control leaves. The HPLC-DAD, HPLC-ESI-MS data and comparison with UV and MS libraries of compounds available in Dr. Pedras' group revealed that the peaks at t_R = 11.7 min corresponded to spirobrassinin (**101**), t_R = 13.8 min to arvelexin (**135**) and t_R = 24.7 min to cyclobrassinin (**78**). The amounts of induced metabolites were determined using calibration curves (**Table 2.4**). Analysis of the polar extracts showed absence of 4'-methoxyglucobrassicin (**70**) and 1'-methoxyglucobrassicin (**69**), while glucobrassicin (**57**) was detected in the polar extract (**Table 2.4**).

Table 2.4 Time-course HPLC analysis (using method A for phytoalexins and method B for indole glucosinolates) of metabolites of *Crambe abyssinica.*

Metabolites; t_R (min)	Incubation period (h)	Total amount of metabolites (nmol/ g of fresh tissue ± STD)[a]
spirobrassinin (**101**); 11.7	24	4.1 ± 0.1
	72	3.3 ± 0.5
	120	2.9 ± 0.9
arvelexin (**135**); 13.6	24	0.6 ± 0.0
	72	7.3 ± 2.9
	120	9.5 ± 4.7
cyclobrassinin (**78**); 24.7	24	1.9 ± 0.3
	72	0.7 ± 0.1
	120	0
glucobrassicin (**57**); 19.6	24	3.8 ± 1.6
	72	6.1 ± 3.0
	120	2.5 ± 0.4

[a]Amounts of spirobrassinin (**101**), arvelexin (**135**), cyclobrassinin (**78**) and glucobrassicin (**57**) determined by HPLC-DAD using calibration curves. Values are the averages of one experiment conducted in triplicate ± standard deviation (STD).

2.1.4 *Diplotaxis tenuifolia*

2.1.4.1 Time-course analysis

D. tenuifolia (24-days-old) was sprayed with $CuCl_2$ (2 mM) solution and analyzed as described in **Figure 2.1**. The metabolite profiles of elicited leaves extracts were compared against control leaves. Extracts of elicited leaves showed a peak at t_R = 13.6 min which was absent from extracts of control leaves. The HPLC-DAD, HPLC-ESI-MS data and comparison with compounds in Dr. Pedras' group UV and MS libraries revealed that the peak at t_R = 13.6 min corresponded to arvelexin (**135**). The

amount of arvelexin produced was determined using a HPLC-DAD calibration curve (**Table 2.5**). The methanolic extracts were analyzed by HPLC-DAD for the detection of indole glucosinolates: glucobrassicin (**57**), 1'-methoxyglucobrassicin (**69**) and 4'-methoxyglucobrassicin (**70**). The polar extracts showed metabolite peaks corresponded to glucobrassicin (**57**) and 4'-methoxyglucobrassicin (**70**). No 1'-methoxyglucobrassicin was detected (**Table 2.5**).

Table 2.5 Time-course HPLC analysis (using method A for phytoalexins and method B for indole glucosinolates) of metabolites of *Diplotaxis tenuifolia.*

Metabolites; t_R (min)	Incubation period (h)	Total amount of metabolites (nmol/ g of fresh tissue ± STD)[a]
arvelexin (**135**); 13.6	24	1.6 ± 0.3
	72	6.8 ± 3.9
	120	11.1 ± 6.1
	168	9.3 ± 1.2
glucobrassicin (**57**); 19.6	24	0.7 ± 0.5
	72	2.6 ± 0.9
	120	1.2 ± 0.7
	168	1.5 ± 0.3
4'-methoxyglucobrassicin (**70**); 26.2	24	0.5 ± 0.2
	72	1.0 ± 0.7
	120	0.3 ±0.1
	168	0.3 ± 0.1

[a]Amounts of arvelexin (**135**), glucobrassicin (**57**) and 4'-methoxyglucobrassicin (**70**) determined by HPLC-DAD using calibration curves. Values are the averages of one experiment conducted in triplicate ± standard deviation (STD).

2.1.5 Conclusion

The number of cruciferous species is estimated to be around 3700; however, only a limited number of species (ca. 30) have been investigated for production of phytoalexins, the majority of which are *Brassica* spp. Most cruciferous phytoalexins have been isolated from *Brassica* species, mostly from cultivated species (Pedras, Yaya et al., 2011). In this thesis, the wild crucifers *B. tournefortii, C. abyssinica, D. tenuifolia* and *D. tenuisiliqua* were investigated for the production of elicited metabolites after treatment with $CuCl_2$ solution. All species produced arvelexin (**135**) (Pedras, Chumala et al., 2003). Arvelexin (**135**) was the only phytoalexin detected in *D. tenuifolia*, while in *D. tenuisiliqua*, arvelexin (**135**) was produced together with another elicited metabolite, 1',4'-dimethoxyindolyl-3'-acetonitrile (**148**). Compound **148** was detected in *D. muralis* treated with $CuCl_2$ solution, and its structure had been proposed based on ^{1}H-NMR data only (Sarwar, 2007). In this work, the same compound was isolated from *D. tenuisiliqua*, fully characterized and its structure was confirmed by chemical synthesis. It is the first cruciferous phytoalexin ever reported with dimethoxy substitution for which the name tenualexin is proposed. Its antifungal activity was determined against the plant pathogens *A. brassicicola*, *L. maculans*, *R. solani* and *S. sclerotiorum*. At the highest concentration (0.5 mM), 1',4'-dimethoxyindolyl-3'-acetonitrile (**148**) completely inhibited mycelial growth of *A. brassicicola, R. solani* and *S. sclerotiorum.* Previously it was reported that, at the highest concentration, 1'-methoxyindolyl-3'-acetonitrile (**136**) inhibited mycelial growth of *A. brassicicola* and *S. sclerotiorum* by 43 and 54% respectively while 4'-methoxyindolyl-3'-acetonitrile (**67**) inhibited mycelial growth of *A. brassicicola* and *S. sclerotiorum* by 59 and 77% respectively (Pedras and Hossain, 2011).

In crucifers, indolyl-3'-acetonitriles are derived from indole glucosinolates through enzymatic processes that involve myrosinase and nitrile-specifier proteins (Kissen and Bones, 2009; Williams, Critchley et al., 2009). Glucobrassicin (**57**) is a precursor of indolyl-3'-acetonitrile (**67**), while 4'-methoxyglucobrassicin (**70**) is a precursor of 4'-methoxyindolyl-3'-acetonitrile (**135**). In the case of 1',4'-dimethoxyindolyl-3'-acetonitrile (**148**), 1',4'-dimethoxyglucobrassicin (**62**), isolated for the first time from roots of

Barbarea vulgaris ssp. arcuata (Agerbirk, Petersen et al., 2001), is likely to be its biosynthetic precursor. *C. abyssinica* produced the phytoalexins spirobrassinin (**101**), cyclobrassinin (**78**) and arvelexin (**135**), which were initially isolated from cultivated species (Pedras, Yaya et al., 2011; Takasugi, Kawashima et al., 1987). The metabolic profile of *B. tournefortii* resembles that of cultivated *Brassica* species. It produced the phytoalexins spirobrassinin (**101**), arvelexin (**135**), rutalexin (**116**), 4'-methoxybrassinin (**108**) and cyclobrassinin (**78**). This shows overlap of the biosynthetic pathways of cruciferous phytoalexins in cultivated and some wild species. As crucifers produce a mixture of phytoalexins, whose composition and amounts depend on the type of stress (Pedras and Yaya, 2010; Pedras, Yaya et al., 2011; Pedras, Zheng et al., 2007b), it is worthy to investigate different plant tissues using different elicitation techniques. The absence of additional phytoalexins in, for example, elicited leaves of *D. tenuifolia* suggests the need to try different elicitation strategies, including UV-light and other heavy metal salt solutions. Especially wild crucifers are likely to produce biologically active new metabolites, as most of them are not yet investigated

2.2 Biosynthesis of cruciferous phytoalexins

The biosynthesis of secondary metabolites occurs either under normal growth conditions or when plants are stressed by external factors such as pathogens, salinity, UV light, drought, etc. A number of cruciferous plants have been reported to show resistance to a variety of crucifer pathogens. For example, *Camelina sativa* L. (false flax), *Capsella bursa-pastoris* L. (Shepherd's purse) and *Eruca sativa* Mill. (rocker) were reported to display resistance against *A. brassicae* (Conn, Tewari et al., 1988). Their ability to defend themselves may be partly due to the production of secondary metabolites including phytoalexins and phytoanticipins. Unlike phytoanticipins, phytoalexins are biosynthesized when plants are under stress (Bailey and Mansfield, 1982; Pedras, Yaya et al., 2011; Vanetten, Mansfield et al., 1994). Knowledge of the biosynthetic pathways of phytoalexins and phytoanticipins will facilitate the identification of plant defense genes

and the potential breeding of plants producing more potent antifungal metabolites. Biosynthetic studies require a proposal of biosynthetic intermediates, their retro-biosynthetic analysis, chemical syntheses and administration of isotopically labeled precursors to different plant tissues. Finally, the level of incorporation is determined using spectroscopic techniques such as NMR and MS.

2.2.1 *Thellungiella salsuginea* (salt cress)

T. salsuginea is a wild crucifer extremophile resistant to a variety of abiotic stresses, such as high salinity, low humidity and frost (Gong, Li et al., 2005; Inan, Zhang et al., 2004). It is a model plant whose genome is being sequenced (Wu, Zhang et al., 2012). When under stress, it produces phytoalexins that are structurally unique, the wasalexins A (**43**) and B (**109**) and biswasalexins A1 (**131**) and A2 (**132**) (Pedras, Sorensen et al., 1999; Pedras and Zheng, 2010; Pedras, Zheng et al., 2009). The methoxy substituent at *N*-1 of the indole ring and their side chains suggest that they have a relationship with 1'-methoxybrassinin (**105**), a phytoalexin of *Brassica* species (**Scheme 2.2**) (Pedras, Yaya et al., 2010). Thus, a biosynthetic study of the phytoalexins of *T. salsuginea* was carried out using perdeuterated biosynthetic intermediates: [2,2,4',5',6',7'-$^{2}H_6$]glucobrassicin (**57b**), [$^{2}H_3$CS,4',5',6',7'-$^{2}H_4$]-1'-methoxybrassinin (**105a**), *L*-[2',4',5',6',7'-$^{2}H_5$]tryptophan (**66a**), [$^{2}H_3$CO]-1'-methoxyindolyl-3'-acetaldoxime (**74a**), *L*-[$^{2}H_3$CS]methionine (**97a**), [4',5',6',7'-$^{2}H_4$]brassinin (**45a**), 1'-methoxy-2'-methylbrassinin (**160**) and 1'-methylindolyl-3'-acetaldoxime (**75**) (**Table 2.6**). Labeled compounds, except tryptophan and methionine, used in this section were synthesized in Dr. Pedras' lab according to references shown in **Table 2.6**.

Table 2.6 Perdeuterated compounds used in precursor administration experiments.

Deuterated compound (#)[a]	Origin
[$^2H_3$CS, 4',5',6',7'-$^2H_4$]-1'-methoxybrassinin (**105a**)	synthetic (Pedras and Okinyo, 2006c)
[4',5',6',7'-$^2H_4$]brassinin (**45a**)	synthetic (Pedras and Okinyo, 2006c)
[2,2,4',5',6',7'-$^2H_6$]glucobrassicin (**57b**)	synthetic (Pedras, Yaya et al., 2010)
[$^2H_3$CO]-1'-methoxyindolyl-3'-acetaldoxime (**74a**)	synthetic (Pedras and Okinyo, 2006c)
L-[2',4',5',6',7'-$^2H_5$]tryptophan (**66a**)	commercial (Cambridge Isotope Laboratories)
L-[$^2H_3$CS]methionine (**97**)	Commercial (*C/D/N* Isotopes)
1'-methoxy-2'-methylbrassinin (**160**)	synthetic (Pedras, Okinyo et al., 2009)
1'-methylindolyl-3'-acetaldoxime (**75**)	synthetic (Pedras, Okinyo et al., 2009)

[a] Deuterated compounds are referred to by a number followed by the letter a or b.

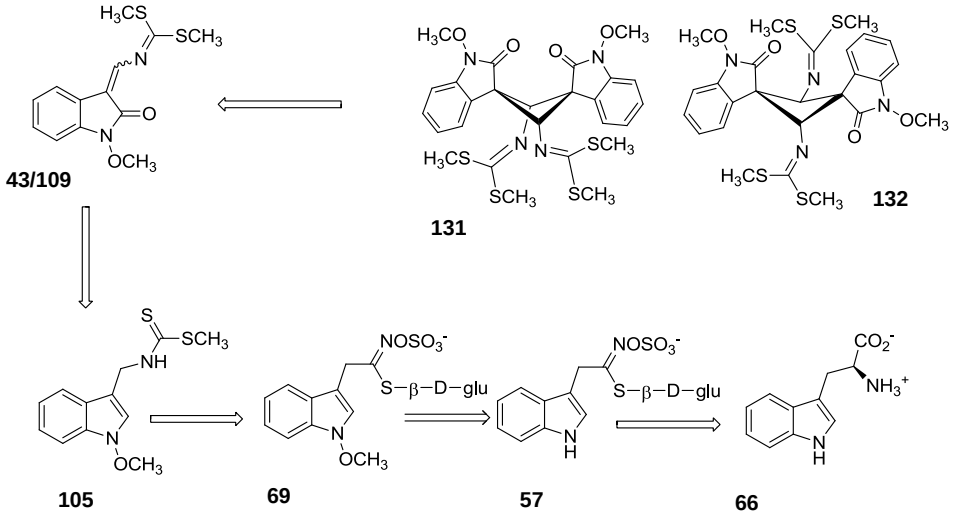

Scheme 2.2 Retro-biosynthetic analysis of wasalexin A (**43**), B (**109**) and biswasalexin A1 (**131**) and A2 (**132**) (Pedras, Yaya et al., 2010)

2.2.1.1 Incorporation experiments using synthetic and commercially available compounds

In order to investigate the biosynthetic pathway of wasalexin A (**43**), wasalexin B (**109**), biswasalexin A1 (**131**) and biswasalexin A2 (**132**), previously reported growth and analysis conditions were used (Pedras and Zheng, 2010; Pedras, Zheng et al., 2009). For feeding experiments, 4-week-old potted plants were irradiated with UV for 60 min. After UV-elicitation, plants were allowed to stand in a laminar flow cabinet under fluorescent light for 3 h, and then were uprooted, the leaves were cut at the base of the petioles and were immediately immersed in tubes containing an aqueous solution of the precursor (4 mL, 5×10^{-4} M). Following the uptake of each precursor solution (ca. 12 h), the tubes were filled with H_2O and leaves were further incubated for 48 h under continuous fluorescent light. After the incubation period was over, leaves were frozen in liq. nitrogen, extracted with methanol; the methanol extract was filtered and was concentrated to dryness. The methanolic residue was rinsed with CH_2Cl_2, the CH_2Cl_2 fraction was concentrated under reduced pressure, and the residue was dissolved in acetonitrile to yield the non-polar fraction containing mostly phytoalexins for HPLC-ESI-MS analysis as summarized in **Figure 2.5**. The insoluble residue was dissolved in MeOH–H_2O (1:1) and was filtered to yield the polar fraction for HPLC-ESI-MS analysis (Pedras, Yaya et al., 2010).

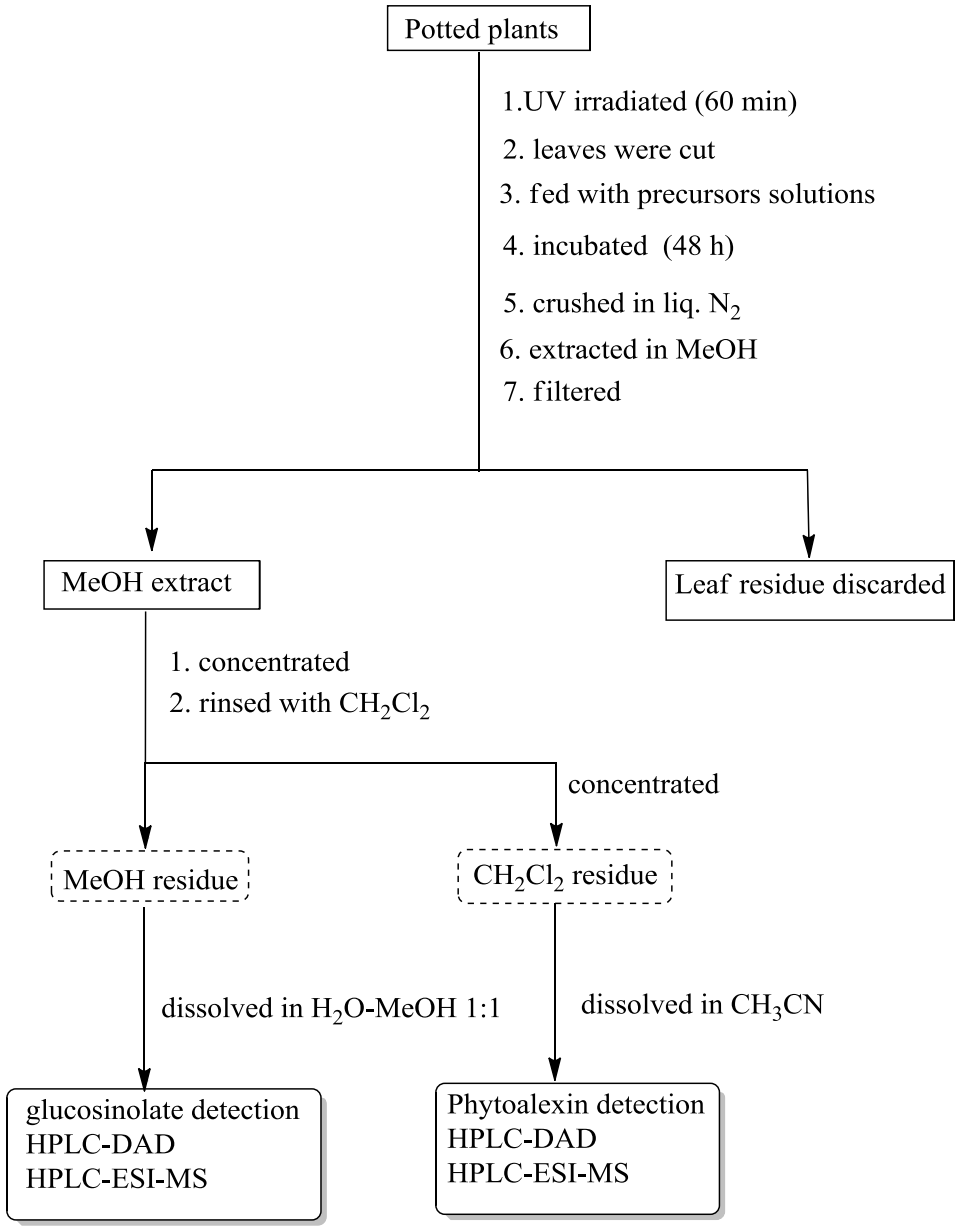

Figure 2.5 Summary of elicitation, extraction and analysis of phytoalexins and indole glucosinolates produced in *Thellungiella salsuginea*

The percentage of deuterium (^2H) incorporation was established using intensity of peaks obtained in ESI-MS positive or negative modes, according to the equation: % of incorporation = $[M \pm 1 + n]^{\pm}/([M \pm 1]^{\pm} + [M \pm 1 + n]^{\pm}) \times 100$ ($n = 3, \ldots$), n is the number of deuteria and M is the peak intensity of each ion $[M - 1]^-$ or $[M + 1]^+$.

2.2.1.1.1 Incorporation of *L*-[2',4',5',6',7'-$^2H_5$]tryptophan (66a)

Leaves of 4-weeks-old plants of *T. salsuginea* were prepared for the feeding experiment as described above (**Figure 2.5**). Commercially available *L*-[2',4',5',6',7'-$^2H_5$]tryptophan (**66a**) dissolved in water (4 mL, 5×10^{-4} M) was administered to UV-elicited petiolated leaves of *T. salsuginea* and worked up followed as shown in **Figure 2.5**. Control leaves fed with naturally occurring *L*-tryptophan (**66**) or carrier solution were treated in a similar way. HPLC-ESI-MS (positive mode) of the CH_2Cl_2 fractions that contained phytoalexins showed the wasalexin A (**43**) peak at t_R = 21.6 min containing two ions: $[M + 1]^+$ at *m/z* 295 and the corresponding $[M + 1 + 4]^+$ at *m/z* 299, the latter resulting from incorporation of *L*-[2',4',5',6',7'-$^2H_5$]tryptophan (**66a**). The ion with *m/z* 299 was not detected in the control sample that was fed with non-labeled *L*-tryptophan (**66**). Peak intensities of the natural abundance and of the deuterated ions were used to determine the percentage of deuterium incorporation as indicated above (% of ^2H incorporation = $\{[M + 1 + 4]^+/([M + 1]^+ + [M + 1 + 4]^+)\} \times 100 \pm$ standard deviation (Pedras, Yaya et al., 2010). Accordingly, the percentage of deuterium incorporation was determined to be 4.6 ± 0.8% (**Table 2.7**). Similarly, the wasalexin B (**109**) peak at t_R = 19.3 min showed two ions: $[M + 1]^+$ at *m/z* 295 and the corresponding $[M + 1 + 4]^+$ at *m/z* 299. The percentage of deuterium incorporation into wasalexin B (**109**) was calculated to be 2.8 ± 0.3% (**Table 2.7; Figure 2.6**).

Table 2.7 Metabolites of *L*-[2',4',5',6',7'-$^2H_5$]tryptophan (**66a**) in UV-irradiated leaves of *Thellungiella salsuginea*.

Metabolites isolated (nmoles / g of fresh tissue)[a]	% Incorporation of deuterium ± Std
[4',5',6',7'-$^2H_4$]wasalexin A (**43a**) (280 ± 14)	4.6 ± 0.8[b]
[4',5',6',7'-$^2H_4$]wasalexin B (**109a**) (16 ± 3)	2.8 ± 0.3[b]
[4',5',6',7'-$^2H_4$]biswasalexin A1 (**131a**) (60 ± 4)	2.5 ± 1.9[b]
[4',5',6',7'-$^2H_4$]biswasalexin A2 (**132a**) (≤0.5)	NI[d]
[2',4',5',6',7'-$^2H_5$]glucobrassicin (**57a**) (≤1)	11.1 ± 2.7[c]
[2',4',5',6',7'-$^2H_5$]-1'-methoxyglucobrassicin (**69a**) (118 ± 6)	22.8 ± 2.6[c]
[2',5',6',7'-$^2H_4$]-4'-methoxyglucobrassicin (**70a**) (412 ± 24)	11.9 ± 2.5[c]

[a] Deuterated compounds are referred to by a number followed by the letter a; nmoles = total amount of deuterated plus non-deuterated compound..
[b] Positive ion mode. Incorporations calculated from HPLC-ESI-MS (peak intensities); % of ^2H incorporation = $\{[M + 1 + n]^+/([M + 1]^+ + [M + 1 + n]^+)\} \times 100$ (n = 4) ± Std (standard deviation), where n = number of deuterium atoms.
[c] Negative ion mode. % of ^2H incorporation = $\{[M-1 + n]^-/([M-1]^- + [M - 1 + n]^-)\} \times 100$ (n = 4 or 5) ± Std (standard deviation), where n = number of deuterium atoms.
[d] NI=no incorporation implies ≤0.1% deuterium

The biswasalexin A1 (**131**) peak at t_R = 29.7 min showed two ions: $[M + 1]^+$ at *m/z* 589 and the corresponding $[M + 1 + 4]^+$ at *m/z* 593, that resulted from the incorporation of *L*-[2',4',5',6',7'-$^2H_5$]tryptophan (**66a**). The percentage of deuterium incorporation into biswasalexin A1 (**131**) was calculated as indicated above to be 2.5 ± 1.9% (**Table 2.7**). In the case of biswasalexin A2 (**132**) peak at t_R = 32.7 min, only one ion with *m/z* 589 due to $[M + 1]^+$ was detected (**Table 2.7; Figure 2.6**).

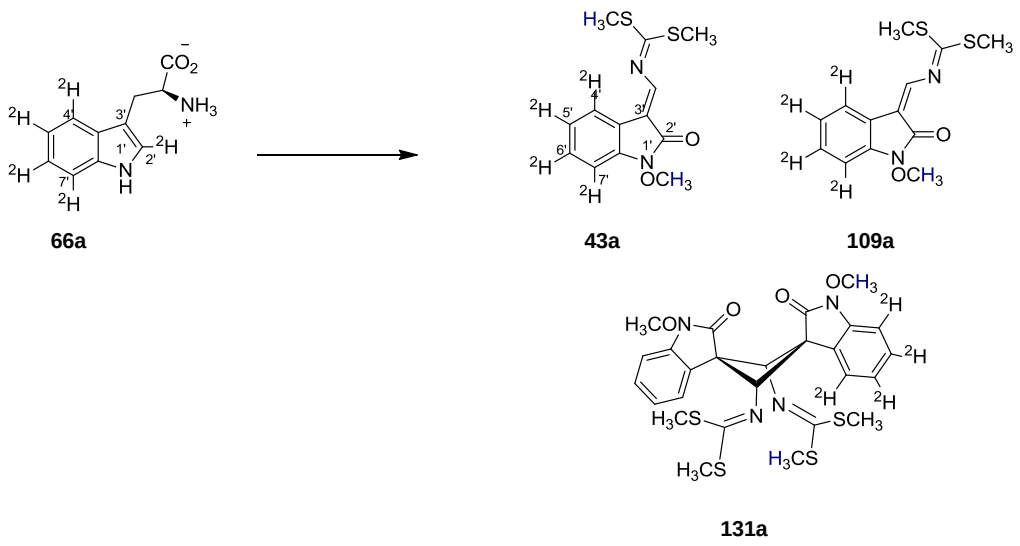

Figure 2.6 Deuterated phytoalexins obtained from feeding of *L*-[2',4',5',6',7'-$^2H_5$]tryptophan (**66a**) to UV-irradiated leaves of *Thellungiella salsuginea*: [4',5',6',7'-$^2H_4$]wasalexin A (**43a**) (4.6 ± 0.8%), [4',5',6',7'-$^2H_4$]wasalexin B (**109a**) (2.8 ± 0.3%) and [4',5',6',7'-$^2H_4$]biswasalexin A1 (**131a**) (2.5 ± 1.9%).

Incorporation of *L*-[2',4',5',6',7'-$^2H_5$]tryptophan (**66a**) into indole glucosinolates (glucobrassicin (**57**), 4'-methoxyglucobrassicin (**70**) and 1'-methoxyglucobrassicin (**69**)) produced in *T. salsuginea* was also determined. Methanolic extracts of leaves were dissolved in water-methanol (50:50) and analyzed by HPLC-DAD and HPLC-ESI-MS. The HPLC-ESI-MS analysis of the polar extracts showed the glucobrassicin (**57**) peak at t_R = 5.3 min containing two ions (negative mode): $[M]^-$ at *m/z* 447 and the corresponding ion $[M + 5]^-$ at *m/z* 452, that resulted from incorporation of *L*-[2',4',5',6',7'-$^2H_5$]tryptophan (**66a**). The percentage of incorporation of deuterium into glucobrassicin (**57**) was calculated to be 11.1 ± 2.7% (**Table 2.7**). From analysis of the HPLC-ESI-MS of the 4'-methoxyglucobrassicin (**70**) peak at t_R = 6.9 min two ions were observed in the negative mode: $[M]^-$ at *m/z* 477 and the corresponding $[M + 4]^-$ at *m/z* 481. The percentage of deuterium incorporation was calculated to be 11.9 ± 2.5% (**Table 2.7**). In a similar fashion, HPLC-ESI-MS analysis of the polar extract showed the 1'-methoxy glucobrassicin (**69**) peak at t_R = 9.4 min containing two ions in the negative mode: $[M]^-$ at

m/z 477 and the corresponding $[M + 5]^-$ at *m/z* 482. The percentage of deuterium incorporation was measured to be 22.8 ± 2.6% (**Table 2.7, Figure 2.7**).

Incorporation of *L*-tryptophan (**66**) into wasalexin A (**43**), wasalexin B (**109**) biswasalexin A1 (**131**), glucobrassicin (**57**), 4'-methoxyglucobrassicin (**70**) and 1'-methoxyglucobrassicin (**69**) shows that they are biosynthesized from *L*-tryptophan (**66**) (**Figures 2.6** and **2.7**). This result is consistent with previously reported data, demonstrating the incorporation of *L*-tryptophan **66** into cruciferous phytoalexins (Pedras, Yaya et al., 2011; Pedras, Zheng et al., 2007b) and indole glucosinolates (Kutacek and Kralova, 1972; Kutacek, Prochazka et al., 1962; Pedras, Okinyo et al., 2009).

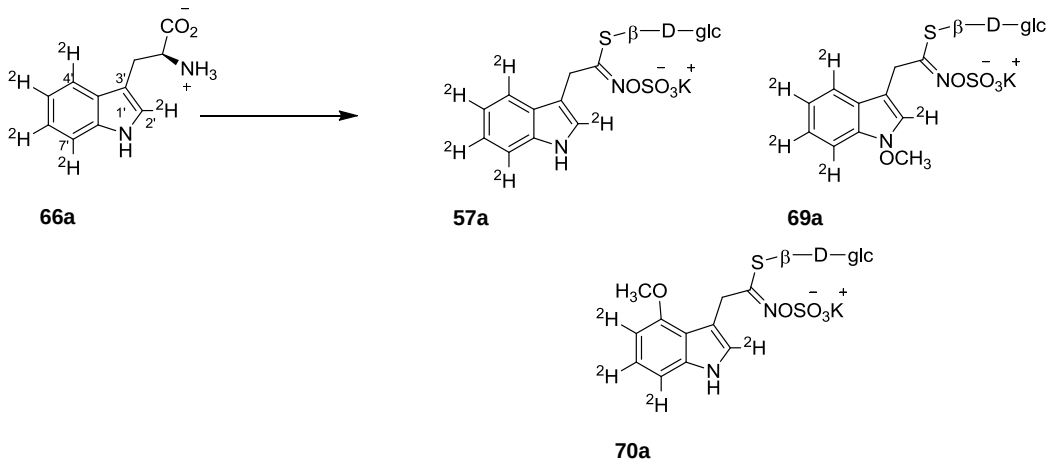

66a **57a** **69a** **70a**

Figure 2.7 Deuterated indole glucosinolates obtained from feeding of *L*-[2',4',5',6',7'-$^2H_5$]tryptophan (**66a**) to UV-irradiated leaves of *Thellungiella salsuginea*: [2',4',5',6',7'-$^2H_5$]glucobrassicin (**57a**) (11.1 ± 2.7%), [2',5',6',7'-$^2H_4$]-4'-methoxyglucobrassicin (**70a**) (11.9 ± 2.5%) and [2',4',5',6',7'-$^2H_5$]-1'-methoxyglucobrassicin (**69a**) (22.8 ± 2.6%).

2.2.1.1.2 Incorporation of [2,2,4',5',6',7'-$^2H_6$]glucobrassicin (57b)

Biosynthetic relationships among indole glucosinolates and cruciferous phytoalexins were investigated by using hexadeuterated [2,2,4',5',6',7'-$^2H_6$]glucobrassicin (**57b**). Feeding experiments were conducted using 4-week-old plants of *T. salsuginea.* A [2,2,4',5',6',7'-$^2H_6$]glucobrassicin (**57b**) solution (4 mL, 5×10^{-4} M) was administered to UV-elicited petiolated leaves and analyzed as described in **Figure 2.5**. HPLC-ESI-MS

(positive mode) of the nonpolar fractions that contained phytoalexins showed a wasalexin A (**43**) peak at t_R = 21.6 min containing two ions: $[M + 1]^+$ at *m/z* 295 and the corresponding $[M + 1 + 5]^+$ at *m/z* 300, that resulted from the incorporation of [2,2,4',5',6',7'-$^2H_6$]glucobrassicin (**57b**). The ion with *m/z* 300 was not detected in the control sample that was fed with non-labeled glucobrassicin (**57**). Peak intensities of the natural abundance and of the deuterated ions were used to determine the percentage of deuterium incorporation as indicated in **Table 2.8**. Accordingly, the percentage of deuterium incorporation was determined to be 3.7 ± 1.0%. Similarly, the wasalexin B (**109**) peak at t_R = 19.3 min showed two ions: $[M + 1]^+$ at *m/z* 295 and the corresponding $[M + 1 + 5]^+$ at *m/z* 300 that resulted from incorporation of [2,2,4',5',6',7'-$^2H_6$]glucobrassicin (**57b**). The percentage of deuterium incorporation into wasalexin B (**109**) was determined to be 2.4 ± 0.6% (**Table 2.8**).

Table 2.8 Metabolites of [2,2,4',5',6',7'-$^2H_6$]glucobrassicin (**57b**) in UV-irradiated leaves of *Thellungiella salsuginea*.

Metabolites isolated (nmoles / g of fresh tissue)[a]	% Incorporation of deuterium ± Std
[1,4',5',6',7'-$^2H_5$]wasalexin A (**43a**) (550 ± 36)	3.7 ± 1.0%[b]
[1,4',5',6',7'-$^2H_5$]wasalexin B (**109a**) (54 ± 6)	2.4 ± 0.6%[b]
[1,4',5',6',7'-$^2H_5$]biswasalexin A1 (**131a**) (128 ± 18)	2.0 ± 0.6%[b]
[1,4',5',6',7'-$^2H_5$]biswasalexin A2 (**132a**) (≤0.5)	NI[d]
[2,2,4',5',6',7'-$^2H_6$]glucobrassicin (**57b**) (≤1)	77.5 ± 13.8%[c]
[2,2,4',5',6',7'-$^2H_6$]-1'-methoxyglucobrassicin (**69a**) (154 ± 10)	4.7 ± 1.6%[c]
[2,2,5',6',7'-$^2H_5$]-4'-methoxyglucobrassicin (**70a**) (366 ± 21)	13.9 ± 2.6%[c]

[a] All deuterated compounds are referred to by a number followed by the letter a or b; conc. = total concentration of deuterated plus non-deuterated compound.
[b] Positive ion mode. Incorporations calculated from HPLC-ESI -MS (peak intensities); % of ^2H incorporation = $\{[M + 1 + n]^+/([M + 1]^+ + [M + 1 + n]^+)\} \times 100$ (n = 5) ± Std (standard deviation), where n = number of deuterium atoms.
[c] Negative ion mode. Incorporations calculated from HPLC-ESI -MS; % of ^2H incorporation = $\{[M + n]^-/([M-1]^- + [M-1 + n]^-)\} \times 100$ (n = 5 or 6) ± Std (standard deviation), where n = number of deuterium atoms.
[d] NI=no incorporation implies ≤0.1% deuterium

The biswasalexin A1 (**131**) peak at t_R = 29.7 min showed two ions: $[M + 1]^+$ at *m/z* 589 and the corresponding $[M + 1 + 5]^+$ at *m/z* 594, that resulted from the incorporation of deuterium of [2,2,4',5',6',7'-$^2H_6$]glucobrassicin (**57b**). The percentage of deuterium incorporation into biswasalexin A1 (**131**) was calculated to be 2.0 ± 0.6%. In the case of biswasalexin A2 (**132**) peak at t_R = 32.7 min, only one ion with *m/z* 589 due to $[M + 1]^+$ was detected (**Table 2.8; Figure 2.8**).

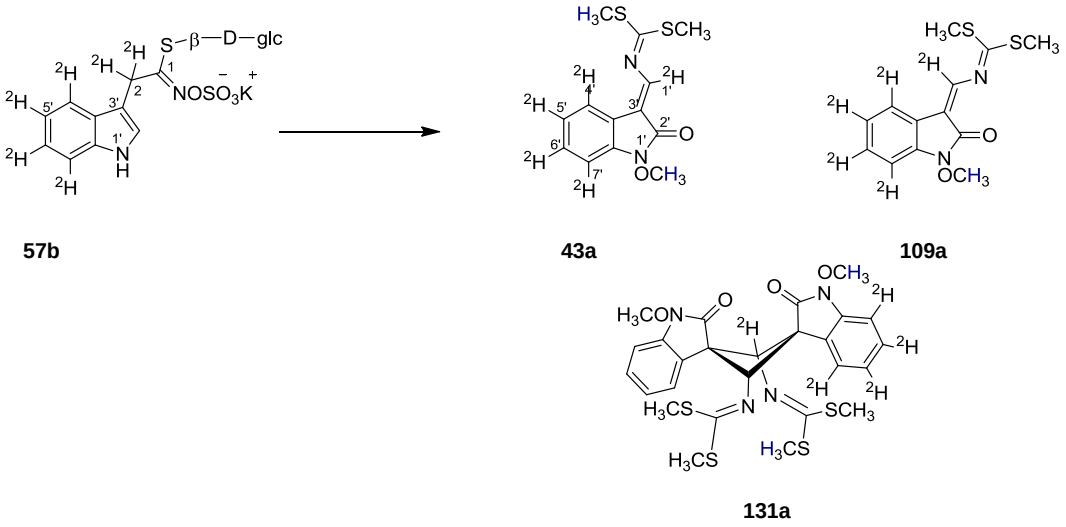

Figure 2.8 Deuterated phytoalexins obtained from feeding of [2,2,4',5',6',7'-$^2H_6$]glucobrassicin (**57b**) to UV-irradiated leaves of *Thellungiella salsuginea*: [1,4',5',6',7'-$^2H_5$]wasalexin A (**43a**) (3.7 ± 1%), [1,4',5',6',7'-$^2H_5$]wasalexin B (**109a**) (2.4 ± 0.6%) and [1,4',5',6',7'-$^2H_5$]biswasalexin A1 (**131a**) (2.0 ± 0.6%).

The incorporation of [2,2,4',5',6',7'-$^2H_6$]glucobrassicin (**57b**) into the indole glucosinolates (4'-methoxyglucobrassicin (**70**) and 1'-methoxyglucobrassicin (**69**)) produced in *T. salsuginea* was investigated. Methanolic extracts of leaves were dissolved in water-methanol (50:50) and analyzed by HPLC-DAD and HPLC-ESI-MS. The HPLC-ESI-MS analysis of the polar extracts showed the 4'-methoxyglucobrassicin (**70**) peak at t_R = 6.9 min containing two ions (negative mode): $[M]^-$ at *m/z* 477 and the corresponding $[M + 5]^-$ at *m/z* 482, that resulted from incorporation of [2,2,4',5',6',7'-$^2H_6$]glucobrassicin (**57b)**. The percentage of deuterium incorporation was calculated as indicated above to be 13.9 ± 2.6% **Table 2.8**. In a similar fashion, the HPLC-ESI-MS analysis of the polar extracts showed the 1'-methoxyglucobrassicin (**69**) peak at t_R = 9.4 min containing two

ions: $[M]^-$ at *m/z* 477 and the corresponding $[M + 6]^-$ at *m/z* 483. Thus, the percentage of deuterium incorporation was determined to be 4.7 ± 1.6% (**Table 2.8; Figure 2.9**).

This is the first report showing a biosynthetic relationship between indole glucosinolates and cruciferous phytoalexins. It suggested that cruciferous phytoalexins are derived from indole glucosinolates. Incorporation of glucobrassicin into wasalexins A (**43**) and B (**109**) and biswasalexin A1 (**131**) was proposed (retro-biosynthetic analysis) to pass through 1'-methoxyglucobrassicin (**69**) (**Scheme 2.2**). *N*-oxidation and then methylation occur during the transformation of **57** to **69** (**Scheme 2.2**).

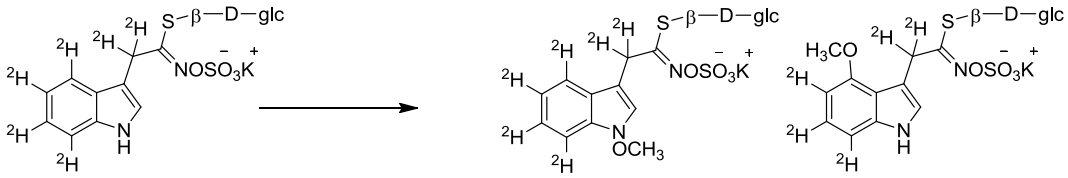

57b **69a** **70a**

Figure 2.9 Deuterated indole glucosinolates obtained from feeding of [2,2,4',5',6',7'-$^2H_6$]glucobrassicin (**57b**) to UV-irradiated leaves of *Thellungiella salsuginea*: [2,2,5',6',7'-$^2H_5$]-4'-methoxyglucobrassicin (**70a**) (13.9 ± 2.6%) and [2,2,4',5',6',7'-$^2H_6$]-1'-methoxyglucobrassicin (**69a**) (4.7 ± 1.6%).

2.2.1.1.3 Incorporation of [$^2H_3$CS,4',5',6',7'-$^2H_4$]-1'-methoxybrassinin (105a)

The incorporation of deuterated 1'-methoxybrassinin (**105a**), a likely precursor of wasalexins, was investigated. Feeding experiments were carried out using UV-elicited leaves of *T. salsuginea* as described in **Figure 2.5**. The HPLC-ESI-MS (positive mode) analysis of the nonpolar fractions that contained phytoalexins showed the wasalexin A (**43**) peak at t_R = 21.6 min containing two ions: $[M + 1]^+$ at *m/z* 295 and the corresponding $[M + 1 + 7]^+$ at *m/z* 302, that resulted from incorporation of [$^2H_3$CS,4',5',6',7'-$^2H_4$]-1'-methoxybrassinin (**105a**). The ion *m/z* 302 was not detected in control sample that was fed with non-labeled 1-methoxybrassinin (**105**). Peak intensities of the natural abundance and of the deuterated ions were used to determine the percentage of deuterium incorporation as indicated in **Table 2.9**. Thus, the percentage of deuterium incorporation was determined to be 19.2 ± 3.9%. The wasalexin B (**109**) peak at t_R = 19.3 min showed

two ions as well: $[M + 1]^+$ at *m/z* 295 and the corresponding $[M + 1 + 7]^+$ at *m/z* 302, that resulted from incorporation of [$^2H_3$CS,4',5',6',7'-$^2H_4$]-1'-methoxybrassinin (**105a**). The percentage of deuterium incorporation into wasalexin B (**109**) was calculated to be 16.7 ± 4.3% (**Table 2.9; Figure 2.10**).

Table 2.9 Metabolites of [$^2H_3$CS,4',5',6',7'-$^2H_4$]-1'-methoxybrassinin (**105a**) in UV-irradiated leaves of *Thellungiella salsuginea*.

Metabolites isolated (nmoles ± Std / g of fresh tissue)[a]	% Incorporation of deuterium ±Std
[$^2H_3$CS,4',5',6',7'-$^2H_4$]wasalexin A (**43a**) (794 ± 54)	19.2 ± 3.9%[b]
[$^2H_3$CS,4',5',6',7'-$^2H_4$]wasalexin B (**109a**) (103 ± 16)	16.7 ± 4.3%[b]
[$^2H_3$CS,4',5',6',7'-$^2H_4$]biswasalexin A1 (**131a**) (129 ± 38)	10.7 ± 1.6%[b]
[$^2H_3$CS,4',5',6',7'-$^2H_4$]biswasalexin A2 (**132a**) (<0.5)	8.1 ± 0.4%[b]
glucobrassicin (**57a**)	NI (≤0.1%)[d]
1'-methoxyglucobrassicin (**69a**)	NI (≤0.1%)[d]
4'-methoxyglucobrassicin (**70a**)	NI (≤0.1%)[d]

[a] Deuterated compounds are referred to by a number followed by the letter **a**; nmoles = total amount of deuterated plus non-deuterated compound; n.d.=not determined.
[b] Positive ion mode. Incorporations calculated from HPLC-ESI-MS (peak intensities); % of ^2H incorporation = $\{[M + 1+ n]^+ /([M + 1]^+ + [M +1 + n]^+)\} \times 100$ ($n = 7$) ± Std (standard deviation), where n = number of deuterium atoms.
[d] NI=no incorporation implies ≤0.1% deuterium

Similarly, the biswasalexin A1 (**131**) peak at t_R = 29.7 min showed two ions: $[M + 1]^+$ at *m/z* 589 and the corresponding $[M + 1 + 7]^+$ at *m/z* 596, that resulted from the incorporation of [$^2H_3$CS,4',5',6',7'-$^2H_4$]-1'-methoxybrassinin (**105a**). The percentage of deuterium incorporation into biswasalexin A1 was determined as described above to be 10.7 ± 1.6% **Table 2.9**. The biswasalexin A2 (**132**) peak at t_R = 32.7 min showed two ions as well: $[M + 1]^+$ at m/z 589 and the corresponding $[M + 1 + 7]^+$ at m/z 596. The percentage of deuterium incorporation into biswasalexin A2 (**132**) was determined to be 8.1 ± 0.4% (**Table 2.9; Figure 2.10**).

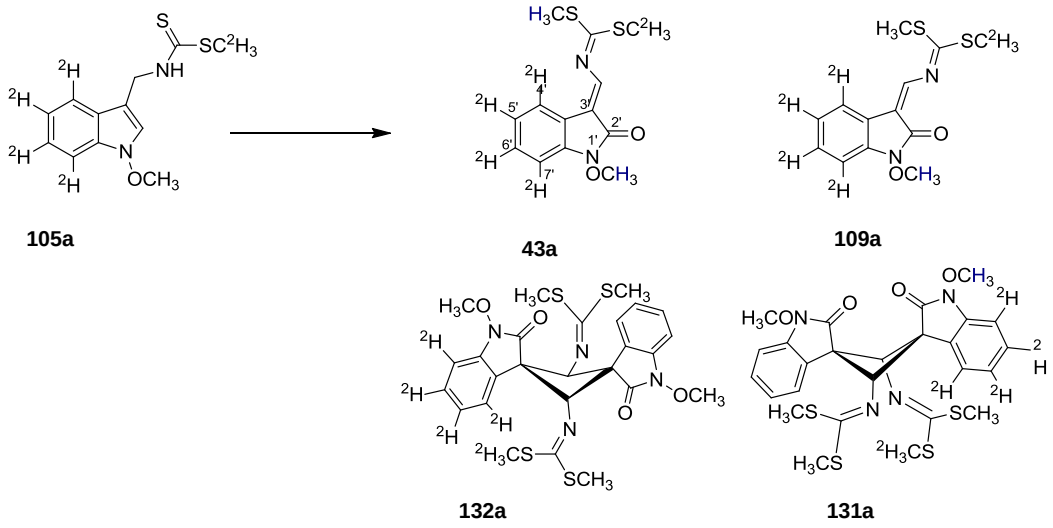

Figure 2.10 Deuterated phytoalexins obtained from feeding of [^2H_3CS,4',5',6',7'-$^2H_4$]-1'-methoxybrassinin (**105a**) to UV-irradiated leaves of *Thellungiella salsuginea*: [^2H_3CS,4',5',6',7'-$^2H_4$]wasalexin A (**43a**) (19.2 ± 3.9%), [^2H_3CS,4',5',6',7'-$^2H_4$]wasalexin B (**109a**) (16.7 ± 4.3%), [^2H_3CS,4',5',6',7'-$^2H_4$]biswasalexin A1 (**131a**) (10.7 ± 1.6%), [^2H_3CS,4',5',6',7'-$^2H_4$]biswasalexin A2 (**132a**) (8.1 ± 0.4%).

To determine the rate of incorporation of deuterium from feeding of [^2H_3CS,4',5',6',7'-$^2H_4$]-1'-methoxybrassinin (**105a**) into indole glucosinolates, polar fractions containing indole glucosinolates were analyzed as described above. The HPLC-ESI-MS analysis (negative mode) showed the glucobrassicin (**57**) peak at t_R = 5.3 min containing an ion at *m/z* 447, the 4'-methoxyglucobrassicin (**70**) peak at t_R = 6.9 min containing an ion at *m/z* 477 and the 1'-methoxyglucobrassicin (**69**) peak at t_R = 9.4 min containing an ion at *m/z* 477. From comparisons of HPLC-ESI-MS data of the experimental and control samples, it was concluded that there was no incorporation of deuterium of [^2H_3CS,4',5',6',7'-$^2H_4$]-1'-methoxybrassinin (**105a**) (**Table 2.9**).

As it was proposed (**Scheme 2.2**), 1'-methoxybrassinin (**105**) was incorporated into **43**, **109**, **131** and **132** suggesting that phytoalexins produced by the wild crucifer, *T. salsuginea,* share biosynthetic intermediates with cultivated species (Pedras, Yaya et al., 2011; Pedras, Zheng et al., 2007b). High level of incorporation and structural similarity

suggested that **105** is a close biosynthetic precursor of **43**, **109**, **131** and **132.** Hence**, 105** is a likely biosynthetic intermediated located between 1'-methoxyglucobrassicin (**69**) and 1-methoxylated phytoalexins (Pedras, Yaya et al., 2010).

2.2.1.1.4 Incorporation of [^2H_3CO]-1'-methoxyindolyl-3'-acetaldoxime (74a)

The incorporation of deuterated 1'-methoxyindolyl-3'-acetaldoxime (**74a**), a likely precursor of wasalexins and 1'-methoxyglucobrassicin (**69**), was investigated. Feeding experiments were carried out using UV-elicited leaves of *T. salsuginea* as described in **Figure 2.5**. The HPLC-ESI-MS (positive mode) analysis of the nonpolar fractions showed the wasalexin A (**43**) peak at t_R = 21.6 min, wasalexin B (**109**) peak at t_R = 19.3 min, biswasalexins A1 peak at t_R = 29.7 (**131**) and A2 (**132**) peak at 32.7 min, but no incorporation of deuterium was detected.

Incorporation of [^2H_3CO]-1'-methoxyindolyl-3'-acetaldoxime (**74a**) into 1'-methoxyglucobrassicin (**69**) produced in leaves of *T. salsuginea* was investigated. Methanolic extracts of leaves were dissolved in water-methanol (50:50) and analyzed as described above. The HPLC-ESI-MS analysis of the polar extracts showed the 1'-methoxy glucobrassicin peak at t_R = 9.4 min containing two ions: $[M]^-$ at *m/z* 477 and the corresponding $[M + 3]^-$ at *m/z* 480, that resulted from incorporation of [^2H_3CO]-1'-methoxyindolyl-3'-acetaldoxime (**74a**). The percentage of deuterium incorporation into 1'-methoxyglucobrassicin (**69**) was calculated to be 3.4 ± 0.9% (**Table 2.10**; **Figure 2.11**).

Table 2.10 Metabolites of [^2H_3CO]-1'-methoxyindolyl-3'-acetaldoxime (**74a**) in UV-irradiated leaves of *Thellungiella salsuginea*.

Metabolites isolated (nmoles/g of fresh tissue)[a]	% Incorporation of deuterium ± Std
wasalexin A (**43**) (501 ± 32)	NI[d]
wasalexin B (**109**) (56 ± 2)	NI[d]
biswasalexin A1 (**131**) (152 ± 39)	NI[d]
biswasalexin A2 (**132**) (<0.5)	NI[d]
glucobrassicin (**57**) (≤1 nmoles)	NI[d]
[^2H_3CO]-1'-methoxyglucobrassicin (**69a**) (49 ± 6)	3.4 ± 0.9[c]
4-methoxyglucobrassicin (**70**) (423 ± 52)	NI[d]

[a] Deuterated compounds are referred to by a number followed by the letter **a**; nmoles = total amount of deuterated plus non-deuterated compound.
[c] Negative ion mode. Incorporations calculated from HPLC-ESI-MS (peak intensities); % of ^2H incorporation = $\{[M + n]^-/([M-1]^- + [M-1 + n]^-)\} \times 100$ ($n = 3$) ± Std (standard deviation), where n = number of deuterium atoms.
[d] NI=no incorporation implies ≤0.1% deuterium

Previously, 1'-methoxyindolyl-3'-acetaldoxime (**74**) was reported as a biosynthetic precursor for 1'-methoxybrassinin (**105**) and 1'-methoxyglucobrassicin (**69**) (Pedras, Okinyo et al., 2009). However, **74** was not incorporated into wasalexins A (**43**), B (**109**) and biswasalexins A1 (**131**) and A2 (**132**), perhaps due to low level incorporation. Compound **74** is likely used in another biosynthetic route apart from transformation into **69**. At this point, the relationship between **74** and **105** was not confirmed, as *T. salsuginea* does not produce detectable amounts of **105**.

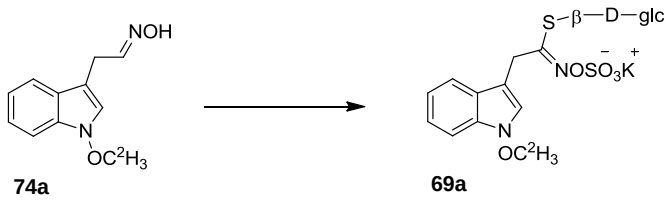

Figure 2.11 Deuterated indole glucosinolate obtained from feeding of [^2H_3CO]-1'-methoxyindolyl-3'-acetaldoxime (**74a**) to UV-irradiated leaves of *Thellungiella salsuginea*: [^2H_3CO]-1'-methoxy glucobrassicin (**69a**) (3.4 ± 0.9%).

2.2.1.1.5 Incorporation of *L*-[^2H_3CS]methionine (97a)

The biosynthetic origin of the methyl groups of wasalexins and methoxyglucobrassicins was investigated using *L*-[^2H_3CS]methionine (**97a**) as described in **Figure 2.5**. The HPLC-ESI-MS (positive mode) analysis of the nonpolar fractions that contained phytoalexins showed the wasalexin A (**43**) peak at t_R = 21.6 min containing four ions: $[M + 1]^+$ at *m/z* 295, $[M + 1 + 3]^+$ at *m/z* 298, $[M + 1 + 6]^+$ at *m/z* 301 and $[M + 1 + 9]^+$ at *m/z* 304. The ions with *m/z* 298, 301 and 304 were not detected in the control sample that was fed with non-labeled *L*-methionine (**97**). Peak intensities of the natural abundance and of the deuterated ions were used to determining the level of deuterium incorporation. Accordingly, the percentage of deuterium incorporation was calculated to be 7.6 ± 2.3% for n=3, 3.7 ± 1.2% for n=6 and 1.6 ± 0.4% for n=9. Similarly, the wasalexin B (**109**) peak at t_R = 19.3 min showed four ions as well: $[M + 1]^+$ at *m/z* 295, $[M + 1 + 3]^+$ at *m/z* 298, $[M + 1 + 6]^+$ at *m/z* 301 and $[M + 1 + 9]^+$ at *m/z* 304. The ions *m/z* 298, 301 and 304 were not detected in the control sample that was fed with non-labeled *L*-methionine (**97**). The percentage of deuterium incorporation was calculated to be 5.6 ± 1.8% for n=3, 2.7 ± 0.9% for n=6 and 1.3 ± 0.3% for n=9 **(Table 2.11; Figure 2.12)**.

Table 2.11 Metabolites of *L*-[$^2H_3$CS]methionine (**97a**) in UV-irradiated leaves of *Thellungiella salsuginea*.

Metabolites isolated (nmoles / g of fresh tissue)[a]	% Incorporation of deuterium ± Std
[x $^2H_3$C]wasalexin A (**43a**) (612 ± 38)	x=1 => $^2H_3$ 7.6 ± 2.3[b] x=2 => $^2H_6$ 3.7 ± 1.2[b] x=3 => $^2H_9$ 1.6 ± 0.4[b]
[x $^2H_3$C]wasalexin B (**109a**) (91 ± 4)	x=1 => $^2H_3$ 5.6 ± 1.8[b] x=2 => $^2H_6$ 2.7 ± 0.9[b] x=3 => $^2H_9$ 1.3 ± 0.3[b]
[x $^2H_3$C]biswasalexin A1 (**131a**) (223 ± 10)	x=1 => $^2H_3$ 4.6 ± 1.8[b] x=2 => $^2H_6$ 1.6 ± 0.6[b]
[x $^2H_3$C]biswasalexin A2 (**132a**) (<0.5)	x=1 => $^2H_3$ 2.3 ± 0.6[b]
Glucobrassicin (**57**) (≤1)	NI[d]
[$^2H_3$CO]-1'-methoxyglucobrassicin (**69a**) (129 ± 30)	8.1 ± 1.6%[c]
[$^2H_3$CO]-4'-methoxyglucobrassicin (**70a**) (321 ± 53)	12.5 ± 1.6%[c]

[a] Deuterated compounds are referred to by a number followed by the letter **a**; nmoles = total amount of deuterated plus non-deuterated compound.
[b] Positive ion mode. Incorporations calculated from HPLC-ESI-MS (peak intensities); % of ^2H incorporation = $\{[M + 1 + n]^+/([M + 1]^+ + [M + 1 + n]^+)\} \times 100$ (n = 3, 6 or 9) ± Std (standard deviation), where n = number of deuterium atoms.
[c] Negative ion mode. Incorporations calculated from HPLC-ESI-MS; % of ^2H incorporation = $\{[M-1+ n]^-/([M-1]^- + [M-1 + n]^-)\} \times 100$ (n = 3) ± Std (standard deviation).
[d] NI= no incorporation implies ≤0.1% deuterium
X= number of deuterium labeled methyl groups

The HPLC-ESI-MS (positive mode) analysis of the nonpolar fractions that contained phytoalexins showed the biswasalexin A1 (**131**) peak at t_R = 29.7 min containing three ions: $[M + 1]^+$ at *m/z* 589, $[M + 1 + 3]^+$ at *m/z* 592 and $[M + 1 + 6]^+$ at *m/z* 595. The ions at *m/z* 592 and 595 were not detected in the control sample that was fed with non-labeled *L*-methionine (**97**). Accordingly, the percentage of deuterium incorporations were calculated to be 4.6 ± 1.8% for n=3 and 1.6 ± 0.6% for n=6. The

biswasalexin A2 (**132**) peak at t_R = 32.7 min showed two ions: $[M + 1]^+$ at *m/z* 589 and $[M + 1 + 3]^+$ at *m/z* 592. The ion at *m/z* 592 was not detected in the control sample that was fed with non-labeled *L*-methionine (**97**). The percentage of deuterium incorporation was calculated to be 2.3 ± 0.6% (**Table 2.11**; **Figure 2.12**).

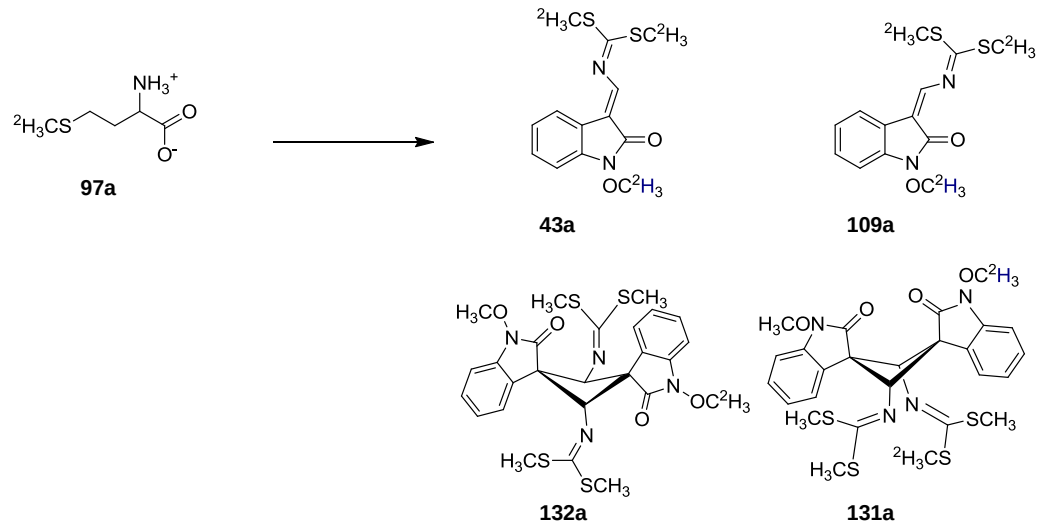

Figure 2.12 Deuterated phytoalexins obtained from feeding of *L*-[$^2H_3$CS]methionine (**97a**) to UV-irradiated leaves of *Thellungiella salsuginea*: [3×$^2H_3$]wasalexin A (**43a**),[3×$^2H_3$]wasalexin B (**109a**), [2×$^2H_3$]biswasalexin A1 (**131a**), [$^2H_3$]biswasalexin A2 (**132a**).

In order to determine the rate of the incorporation of deuterium from feeding of *L*-[$^2H_3$CS]methionine (**97a**), polar fractions containing indole glucosinolates were analyzed. The HPLC-ESI-MS analysis of the polar extract (negative mode) showed 4'-methoxyglucobrassicin peak (**70**) at t_R = 6.9 min containing two ions: $[M]^-$ at *m/z* 477 and the corresponding $[M + 3]^-$ at *m/z* 480, that resulted from incorporation of *L*-[$^2H_3$CS]methionine (**97a**). The percentage of deuterium incorporation was calculated to be 12.5 ± 1.6%. Similarly, the HPLC-ESI-MS analysis of the polar extract showed the 1'-methoxyglucobrassicin (**69**) peak at t_R = 9.4 min containing two ions: $[M]^-$ at *m/z* 477 and the corresponding $[M + 3]^-$ *m/z* 480. The percentage of deuterium incorporation was measured to be 8.1 ± 1.6% (**Scheme 2.10**; **Figure 2.13**).

As expected, all methyl groups of cruciferous phytoalexins (**43**, **109**, **131** and **132**) and indole glucosinolates (**70** and **69**) are derived from *L*-methionine (**97**) via methyl donor (*S*-adenosyl methionine) (Pedras, Yaya et al., 2010)

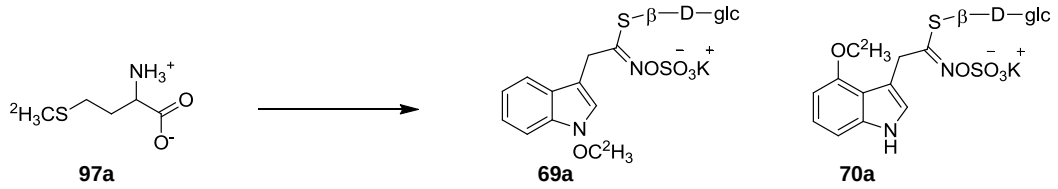

97a **69a** **70a**

Figure 2.13 Deuterated indole glucosinolates obtained from feeding of *L*-[$^2H_3$CS]methionine (**97a**) to UV-irradiated leaves of *Thellungiella salsuginea*:: [$^2H_3$OC]-1'-methoxyglucobrassicin (**69a**) (8.1 ± 1.6%) and [$^2H_3$OC]-4'-methoxyglucobrassicin (**70a**) (12.5 ± 1.6%)

2.2.1.1.6 Incorporation of [4',5',6',7'-$^2H_4$]brassinin (45a)

The metabolism of [4',5',6',7'-$^2H_4$]brassinin (**45a**) in *T. salsuginea* leaves was investigated. A solution of [4',5',6',7'-$^2H_4$]brassinin (**45a**) was administered to UV elicited petiolated leaves of *T. salsuginea* and leaves were extracted as described in **Figure 2.5**. The HPLC-ESI-MS (positive mode) analysis of the nonpolar fractions showed the wasalexin A (**43**) peak at t_R = 21.6 min containing $[M + 1]^+$ at *m/z* 295, the wasalexin B (**109**) peak at t_R = 19.3 min containing $[M + 1]^+$ at *m/z* 295, the biswasalexin A1 (**131**) peak at t_R = 29.7 min containing $[M + 1]^+$ at *m/z* 589 and the biswasalexin A2 (**132**) peak at t_R = 32.7 min containing $[M + 1]^+$ at *m/z* 589. No corresponding ions due to deuterium incorporation were detected. These results suggest that brassinin is not a biosynthetic precursor of wasalexins and biswasalexins.

On the other hand, analysis of HPLC chromatograms of samples fed with deuterated brassinin and control (fed with carrier solution) revealed the presence of additional peaks in the samples treated with deuterated brassinin. To identify the peaks, mass spectra of deuterated samples (fed with deuterated brassinin (**45a**)) were compared against those of nondeuterated samples (fed with nondeuterated brassinin (**45**)). The peaks detected in deuterated samples showed masses four units higher than those detected in samples treated with nondeuterated brassinin (**45**). Comparison of the retention times

and the mass spectra of these products with UV and MS libraries (Dr. Pedras group) revealed that three of the six compounds were known metabolites: spirobrassinin (**101**), brassitin (**155**) and indolyl-3-carboxylic acid (**156**) (Pedras, Yaya et al., 2010). The remaining three metabolites at 14.8, 16.0, and 17.0 minutes were deduced by comparing their mass fragments with mass fragments of wasalexins A (**43**) and B (**109**). Two of the three compounds showed identical masses: $[M + 1]^+$ at *m/z* 265 which was 30 units lower than that of wasalexins A (**43**) and B (**109**), while the third peak showed $[M + 1]^+$ at *m/z* 267. Based on these mass fragments, the hypothetical compounds were synthesized (for details see 2.2.1.2) and their masses and retention times were compared against the metabolic products of brassinin (**45**) and were confirmed to be demethoxywasalexins A (**157**), B (**158**) and demethoxydihydrowasalexin (**159**) respectively (**Figure 2.14**).

A lack of incorporation of brassinin (**45**) into **43**, **109**, **131** and **132** indicates that there is no biosynthetic relationship between brassinin (**45**) and 1'-methoxybrassinin (**105**) (Monde, Tamura et al., 1995). On the other hand, deuterium incorporations into metabolites **157**, **158**, **159**, **101**, **155** and **156** were $\geq$ 99%, suggesting these metabolites are derived solely from brassinin (**45**) (Pedras, Yaya et al., 2010). Metabolites **157**, **158**, **159**, **101**, **155** and **156** were not detected in non-fed plants, which might be due to the presence of non-selective enzymes that can take and metabolize brassinin (**45**).

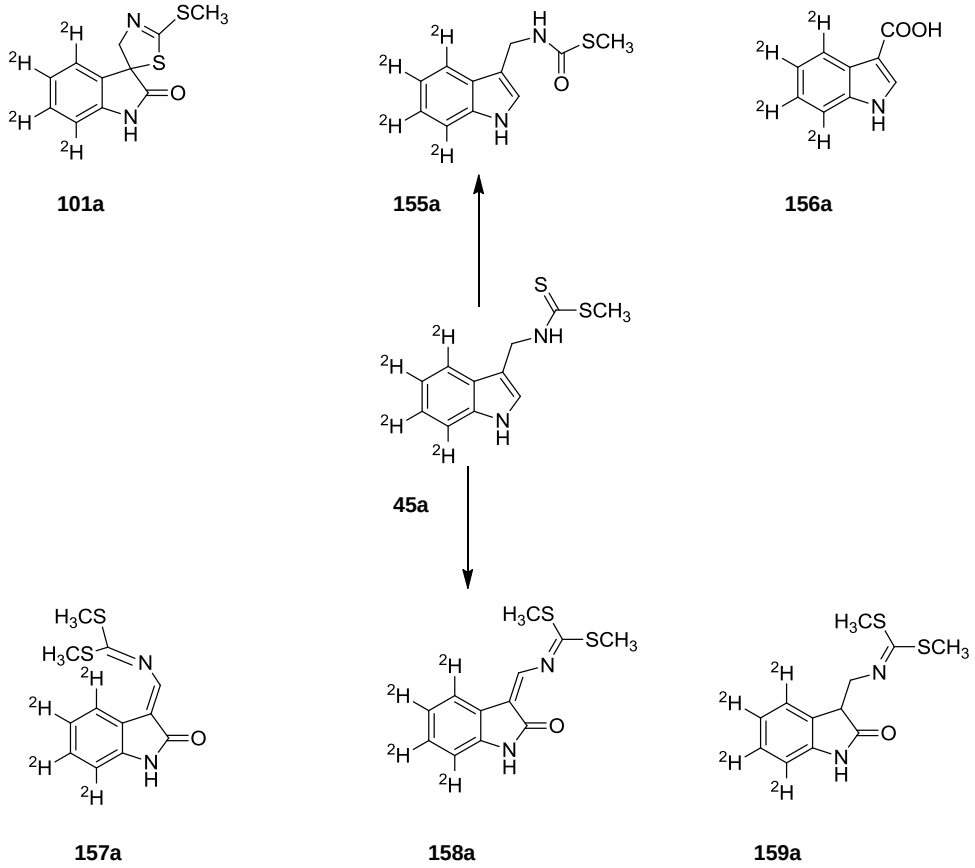

Figure 2.14 Deuterated metabolites and metabolic products from feeding of [4',5',6',7'-$^2H_4$]brassinin (**45a**) to elicited leaves of *Thellungiella salsuginea*: [4',5',6',7'-$^2H_4$]spirobrassinin (**101a**), [4',5',6',7'-$^2H_4$]brassitin (**155a**), [4',5',6',7'-$^2H_4$]indolyl-3'-carboxylic acid (**156a**), [4',5',6',7'-$^2H_4$]demethoxywasalexins A (**157a**), B (**158a**), [4',5',6',7'-$^2H_4$]demethoxydihydrowasalexin (**159a**).

2.2.1.1.7 Metabolism of 1'-methoxy-2'-methyl brassinin (160)

The potential metabolism of 1'-methoxy-2'-methylbrassinin (**160**) was investigated as described above in **Figure 2.5**. Comparison of the HPLC-DAD and HPLC-ESI-MS data of fed samples against the controls (fed with carrier solution) revealed a similar profile. These results suggest that *T. salsuginea* was not able to metabolize compound **160**, indicating the importance of H-2 of the indole ring in formation of wasalexins from 1'-methoxybrassinin (**105**).

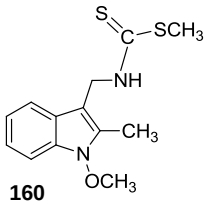

160

2.2.1.2 Synthesis of new compounds

Demethoxywasalexin A (**157**) and B (**158**) were prepared from 2-oxindole (**161**). A solution of **161** in DMF was added to a solution of $POCl_3$ in DMF and stirred at 45 ºC for 30 min, after which NH_4OH (28%) at 0 ºC was added; the reaction mixture was stirred at rt for 1 h (Pedras and Jha, 2005; Pedras and Suchy, 2006; Pedras and Zaharia, 2001) to yield 3-aminomethylene-2-oxindole (**162**) in 67%. A solution of **162** was treated with CS_2 in the presence of NaH to generate a dithiocarbamate salt which was treated with methyl iodide to yield crude (*E*,*Z*)-methyl((2-oxoindolin-3-ylidene)methyl)carbamodithioate (**163**). The crude solution of **163** was further treated with methyl iodide in the presence of pyridine and Et_3N and stirred for 14 h at rt to yield demethoxywasalexins A (**157**) and B (**158**) (yellow solid, mixture of *E* and *Z* isomers 4:1) in 53% yield (Pedras, Yaya et al., 2010) (**Scheme 2.3**).

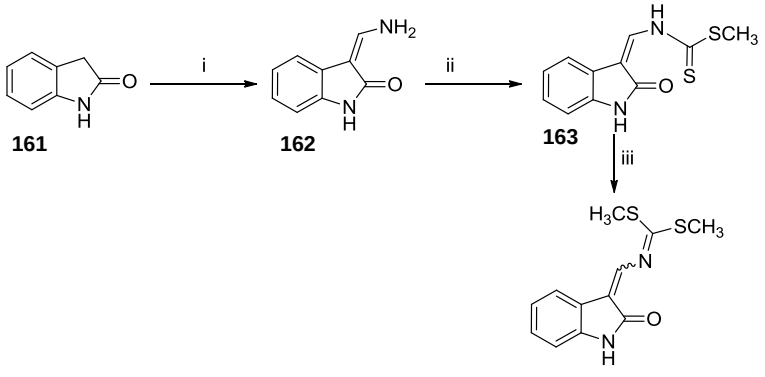

161 **162** **163** **157, 158**

Scheme 2.3 Synthesis of **157** and **158**. Reagents and conditions: i) DMF, $POCl_3$, 45 ºC, (aq. NH_3, 28%) 67%; ii) NaH, CS_2, MeI, THF, 0 ºC; iii) pyridine, Et_3N, MeI, CH_2Cl_2 53%.

Demethoxydihydrowasalexin was synthesized from methyl((2-oxoindolin-3-ylidene)methyl)carbamodithioate (**163**), which was treated with $NaBH_3CN$ in the presence of AcOH to yield methyl ((2-oxoindolin-3-yl)methyl)carbamodithioate (**164**) in 55%. Methylation of compound **164** was achieved using dimethylsulfate in the presence of K_2CO_3 to yield the final product, demethoxydihydrowasalexin (**159**) in moderate yield (Pedras, Yaya et al., 2010) (**Scheme 2.4**).

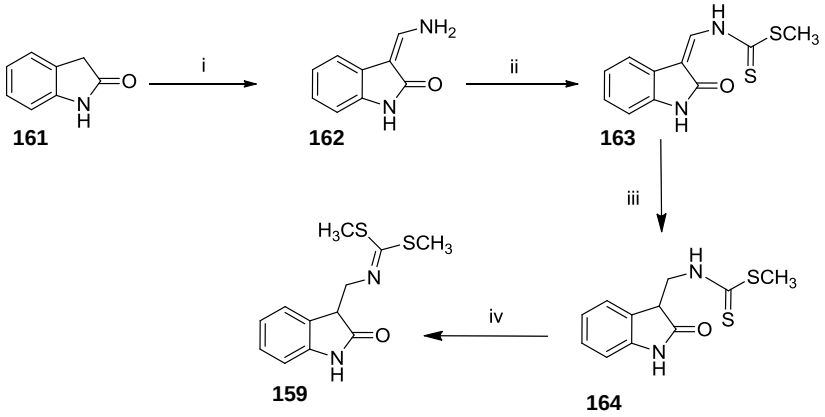

Scheme 2.4 Synthesis of **159**. Reagents and conditions: i) DMF, $POCl_3$, 45 ºC, (aq. NH_3, 28%); ii) NaH, CS_2, MeI, THF, 0 ºC; iii) $NaCNBH_3$, AcOH, 60 ºC, 55%; (iv) K_2CO_3, $(CH_3O)_2SO_2$, acetone, 30 ºC, 58%.

2.2.1.3 Conclusion

T. salsuginea, an extremophile resistant to salinity, drought and frost (Williams, Critchley et al., 2009), produces a group of phytoalexins with unique structural features (Pedras and Zheng, 2010; Pedras, Zheng et al., 2009) not produced in the other *Brassica* species. For this reason, the biosynthetic pathway of the phytoalexins was investigated using perdeuterated compounds. The biosynthetic origin of wasalexins A (**43)**, B (**109**) and biswasalexins A1 (**131**) and A2 (**132**) was confirmed by administering *L*-[2',4',5',6',7'-$^2H_5$]tryptophan (**66a**) to leaves of *T. salsuginea*, which showed incorporation of deuterium of *L*-[2',4',5',6',7'-$^2H_5$]tryptophan (**66a**) into the phytoalexins (Pedras, Yaya et al., 2010). They share the same biosynthetic building block (*L*-tryptophan (**66**)) as

other cruciferous phytoalexins (Pedras and Yaya, 2010; Pedras, Yaya et al., 2011; Pedras, Zheng et al., 2007b) and indole glucosinolates (Kutacek and Kralova, 1972; Kutacek, Prochazka et al., 1962). Incorporation of [$^{2}H_{3}$CS,4',5',6',7'-$^{2}H_{4}$]-1'-methoxybrassinin (**105a**) into wasalexins A (**43)**, B (**109**) and biswasalexins A1 (**131**) and A2 (**132**) suggests that **105** is a close biosynthetic precursor that upon successive oxidations of the indole ring (C-2) and the side chain and thiomethylation can give **43** and **109** (**Scheme 2.5**). A major breakthrough was achieved when [2,2,4',5',6',7'-$^{2}H_{6}$]glucobrassicin (**57b**) showed unprecedented incorporation into the cruciferous phytoalexins **43, 109, 131** and **132**. It suggested that the biosynthetic pathway of wasalexins requires indole glucosinolates as intermediates. This was the first report showing the biosynthetic relationship between cruciferous phytoalexins and indole glucosinolates (Pedras, Yaya et al., 2010). The first step in the metabolism of 1'-methoxyglucobrassicin (**69**) into 1'-methoxybrassinin (**105**) could be deglucosylation of the glucosinolate by a hydrolase enzyme. The resulting aglycone (**138**), which is unstable, could spontaneously rearrange into the corresponding 1'-methoxyindolyl-3'-methylisothiocyanate (**165**) (Pedras, Yaya et al., 2010) which, in the presence of thiomethyl donor (*S*-adenosylmethionine), could give rise to 1'-methoxybrassinin (**105**) (**Scheme 2.5**).

The observed absence of incorporation of [4',5',6',7'-$^{2}H_{4}$]brassinin (**45a**) into **43, 109, 131** and **132** was consistent with a methoxylation of glucobrassicin (**57**) before functional group modifications. Nevertheless, the detection of metabolites **157, 158, 159** and metabolic products **101, 155, 156** deriving from [4',5',6',7'-$^{2}H_{4}$]brassinin (**45a**) suggests that the enzymes can metabolize brassinin similarly to 1'-methoxybrassinin. Stages at which oxidations could occur were probed by administering 1'-methoxy-2'-methyl brassinin (**160**). Interestingly, no metabolic products were detected, which suggested the importance of H-2 of indole for the oxidation of the ring and side chain. *L*-methionine was found to be a methyl source for the phytoalexins as well as indole glucosinolates (Pedras, Yaya et al., 2010).

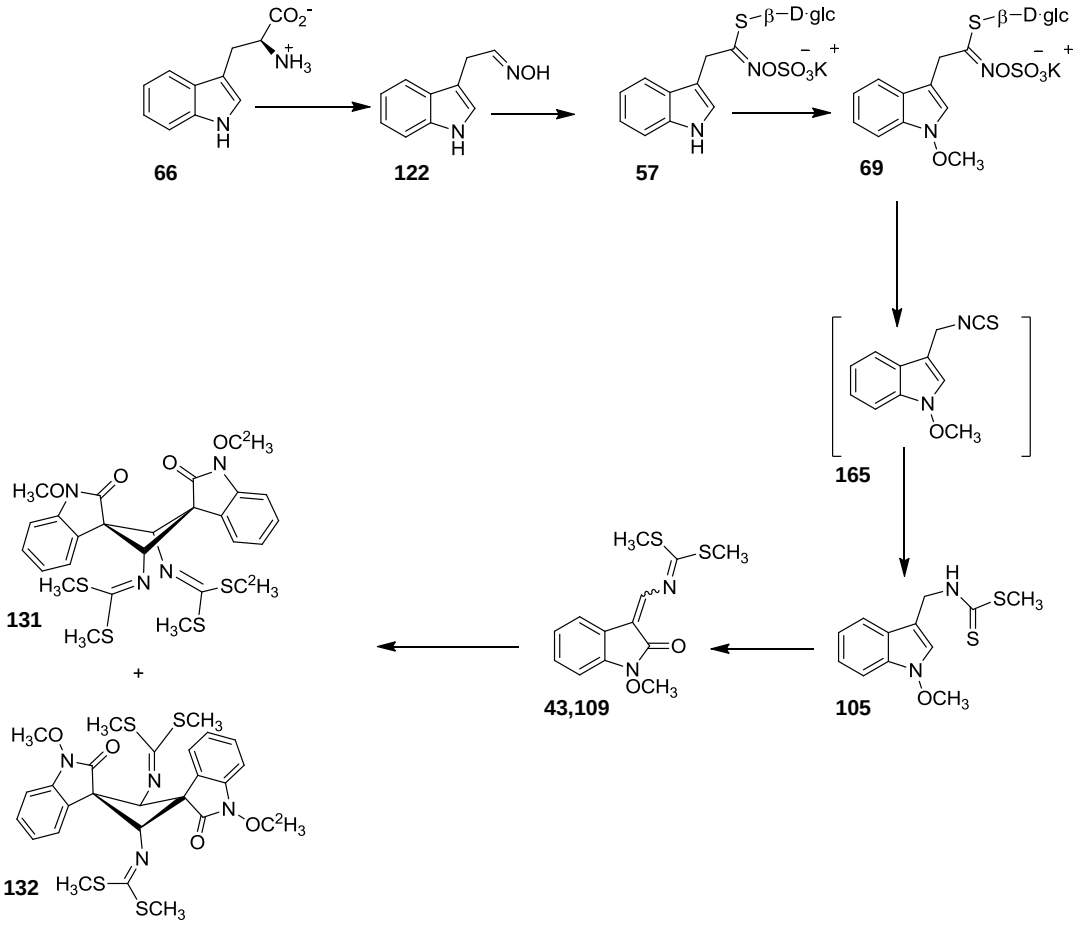

Scheme 2.5 Proposed biosynthetic pathway of wasalexins (Pedras, Yaya et al., 2010)

2.2.2 *Brassica napus* (rutabaga)

Rutabaga roots were used to investigate biosynthetic pathway(s) of crucifer phytoalexins, indole glucosinolates and their biosynthetic relationships (roots are available in fresh produce markets year-round). The roots of rutabaga after elicitation using UV radiation produce a variety of indole phytoalexins and indole glucosinolates (Pedras and Montaut, 2004; Pedras, Montaut et al., 2004; Pedras and Yaya, 2012). Biosynthetic intermediates of 1-methoxylated and non-methoxylated cruciferous phytoalexins were elucidated using rutabaga roots (Pedras, Montaut et al., 2004; Pedras and Okinyo, 2008; Pedras, Okinyo et al., 2009). Production of the 4-methoxylated

phytoalexins, 4'-methoxybrassinin (**108**), rapalexin A (**103**), isocyalexin A (**104**) 4'-methoxycyclobrassinin (**110**), 4'-methoxydehydrocyclobrassinin (**113**) and isalexin (**102**) by rutabaga roots suggested the need for further biosynthetic studies.

2.2.2.1 Isolation of new elicited metabolites

During biosynthetic studies of phytoalexins and indole glucosinolates produced in UV-irradiated rutabaga roots, two potentially new metabolites with t_R 7.2 and 13.0 min were detected. Comparison of their UV spectra, HPLC retention times and HPLC-ESI-MS data with those available in Dr. Pedras' libraries showed no matches. After testing different elicitation times, an increase from 60 min to 90 min led to the production of the two metabolites in reasonable amounts (Pedras and Yaya, 2012). Next, a large scale experiment was conducted to isolate both metabolites using ca. 4 kg of rutabaga roots. The roots were sliced (10-15 mm disc), holes were made on the upper surface of the slices using a cork-borer and slices were incubated for 1 day, UV-irradiated (90 min), and kept in the dark for 1 day. Water was added to the wells, followed by incubation for 2 additional days. Next, the water from each well was collected, freeze-dried to reduce the volume, and extracted with EtOAc. The organic extracts were combined, dried over Na_2SO_4 and concentrated to dryness. The crude extract was separated by FCC (CH_2Cl_2-EtOAc 100:0 to 80:20). After HPLC-DAD analysis of each fraction, fractions containing elicited new metabolites were combined and fractionated by preparative TLC (silica gel developing twice with CH_2Cl_2, 100%). The metabolite at t_R = 13.0 min was isolated from fractions and characterized. The HREI-MS showed a M^+ at *m/z* 172.0633 (calcd. for $C_{10}H_8N_2O$ 172.0632 (100%)) indicating eight degrees of unsaturation. Consistent with the HRMS, the ^{1}H-NMR revealed a total of eight protons of which five were in the aromatic region and one of them was D_2O exchangeable. The remaining three protons were assigned to a methoxy group. Based on the spectral data, the structure was proposed as 4-methoxyindole with a substitution at position C-3'; however, it was not clear if this substituent was a nitrile or an isonitrile. 4-Methoxyindole-3-carbonitrile was synthesized

and the data was compared with those of the isolated compound, but it did not match. Next, 4'-methoxyindole-3'-isonitrile (**104**) was synthesized (**Scheme 2.6**) and comparison of its data with that of the natural product confirmed its identity. The second metabolite was also isolated, purified and characterized as 4'-methoxyindolyl-3'-formamide (**168**). The structure was confirmed by chemical synthesis (Pedras and Yaya, 2012) (**Scheme 2.6**).

2.2.2.2 Synthesis of new metabolites and analogues

4'-Methoxyindolyl-3'-isonitrile (104) and 4'-methoxyindolyl-3'-formamide (168)

3-Nitroindole (**166**) was prepared, as previously reported, by nitration of indole in the presence of $AgNO_3$ and PhCOCl (Bahekar, Jain et al., 2007). Methoxylation of 3-nitroindole (**166**) was initiated by reacting **166** in TFA with thallium (III) trifluoroacetate, followed by treatment with iodine in the presence of CuI and $NaOCH_3$ to yield 4-methoxy-3-nitroindole (**167**). 4-Methoxy-3-nitroindole (**167**) was reduced with Pd/C-H_2 in ethanol. The reaction mixture was treated with a mixture of formic acid and acetic anhydride along with Et_3N at -10 °C to yield 4'-methoxyindole-3'-formamide (**168**) in moderate yield. Another approach to prepare this compound was through reduction of 4-methoxy-3-nitroindole (**167**) in the presence of a mixture of formic acid/acetic anhydride and ethanol at -10 °C. Finally, a one pot, one step reaction yielded 4'-methoxyindolyl-3'-formamide (**168**) and 4'-methoxyindolyl-3'-acetamide (**206**) in a 10:1 ratio, respectively. This procedure was shorter and more efficient than the first approach (66% **168** and 7% **207**). 4'-Methoxyindolyl-3'-isonitrile (**104**) was synthesized from 4'-methoxyindolyl-3'-formamide (**168**) after treatment with Et_3N and $POCl_3$ at 0 °C under inert atmosphere in 41% yield (**Scheme 2.6**).

Indolyl-3'-isonitrile (170) and indolyl-3'-formamide (169)

3-Nitroindole (**166**) was reduced with Pd/C-H_2 in ethanol. The reaction mixture was treated with a mixture of formic acid and acetic anhydride along with Et_3N at -10 °C to give indolyl-3'-formamide (**169**) in moderate yield. Alternatively, the reduction of

3-nitroindole (**166**) in the presence of a mixture of formic acid/acetic anhydride and ethanol at -10 °C yielded indole-3'-formamide (**169**) and indolyl-3'-acetamide (**207**) in a 3:1 ratio, respectively. This procedure was shorter and more efficient than the first approach (64% **169** and 18% **207**). Indolyl-3'-isonitrile (**170**) was synthesized from indolyl-3'-formamide (**169**) after treatment with Et_3N and $POCl_3$ at 0 °C under inert atmosphere in 54% yield (**Scheme 2.6**).

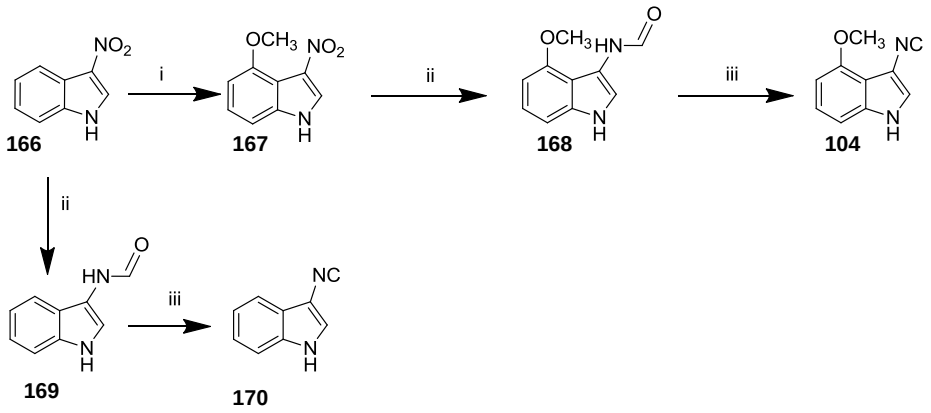

Scheme 2.6 Synthesis of **168**, **104**, **169** and **170**. Reagents and conditions: i) TTFA/TFA, I_2/CuI, $NaOCH_3$, 64%; ii) Pd/C-H_2, acetic-formic anhydride, -10 °C, (64%, **169**), (66%, **168**); iii) $POCl_3$, THF, EtN_3, 0 °C, (54%, **170**, 41%, **104**).

Compounds **168** and **104** and their analogues (**169** and **170**) were assayed against the plant pathogenic fungi: *A. brassicicola, L. maculans, R. solani* and *S. sclerotiorum.* Compound **104** strongly inhibited the fungal mycelial growth of *R. solani* and *S. sclerotiorum* at the concentration of $5x10^{-4}$ M, while 4'-methoxyindolyl-3'-formamide (**168**) inhibitory effect was much lower (Pedras and Yaya, 2012). Non methoxylated analogs **169** and **170** were also synthesised and assayed; **170** showed higher inhibitory effect than **169.** Therefore, it was suggested that the isonitrile side chain is contributing towards the inhibition of the fungal mycelial growth (**Table 2.12)** (Pedras and Yaya, 2012). Metabolite **104** was identified as the first isonitrile isolated from plant origin (Pedras and Yaya, 2012). Since it is an elicited metabolite and antifungal, it is categorized under cruciferous phytoalexin and given the name

isocyalexin A. Plants produce biologically active compounds that can protect them from pathogen attacks. The effect of rapalexin A (**103**) on *L. maculans* is a remarkable example (Pedras and Sarma-Mamillapalle, 2012).

Table 2.12 Antifungal activity of isocyalexin A (**104**), 4'-methoxyindolyl-3'-formamide (**168**), indolyl-3'-isonitrile (**170**) and indolyl-3'-formamide (**169**) against mycelia[a] of *Alternaria brassicicola*, *Leptosphaeria maculans*, *Rhizoctonia solani* and *Sclerotinia sclerotiorum.*

Compounds[b]	*A. brassicicola* (% inh.)	*L. maculans* (% inh.)	*R. solani* (% inh.)	*S. sclerotiorum* (% inh.)
isocyalexin A (**104**)				
5.0×10^{-4} M	47 ± 0	29 ± 2	100	65 ± 2
2.0×10^{-4} M	14 ± 2	9 ± 0	51 ± 4	40 ± 2
1.0×10^{-4} M	0	8 ± 2	32 ± 2	31 ± 5
indolyl-3'-isonitrile (**170**)				
5.0×10^{-4} M	42 ± 4	5 ± 0	100	60 ± 2
2.0×10^{-4} M	27 ± 4	0	51 ± 4	31 ± 2
1.0×10^{-4} M	17 ± 4	0	31 ± 4	17 ± 0
4'-methoxyindolyl-3'-formamide (**168**)				
5.0×10^{-4} M	21 ± 2	27 ± 0	29 ± 4	32 ± 2
2.0×10^{-4} M	9 ± 4	7 ± 0	12 ± 2	25 ± 4
1.0×10^{-4} M	0	2 ± 2	6 ± 2	17 ± 0
indolyl-3'-formamide (**169**)				
5.0×10^{-4} M	42 ± 4	31 ± 3	15 ± 4	25 ± 0
2.0×10^{-4} M	27 ± 4	16 ± 2	0	19 ± 2
1.0×10^{-4} M	17 ± 4	5 ± 2	0	15 ± 2

[a]Percentage of inhibition = 100 – [(growth on medium containing compound-plug/growth on control medium-plug) × 100)] ± standard deviation. Results are the averages ± standard deviations of two independent experiments conducted in triplicate. [b]Compounds were dissolved in DMSO and added to potato dextrose agar medium.

2.2.2.3 Retro-biosynthetic analysis

Biosynthetic studies involve proposing possible biosynthetic intermediates, their synthesis (labeled), and feeding of labeled compounds to appropriate plant tissues/organs, extraction and analysis (HPLC-DAD, HPLC-ESI-MS, NMR etc.). Using this approach, the biosynthesis of cruciferous phytoalexins has been studied in different plant species (e.g. rutabaga, turnip, kohlrabi, dog mustard, salt cress, etc.) using different tissues (roots, leaves, tubers etc.) (Pedras, Yaya et al., 2011). The biosynthetic intermediates of 1-methoxylated phytoalexins were investigated in dog mustard, salt cress and rutabaga (Pedras and Okinyo, 2006b; Pedras, Okinyo et al., 2009; Pedras, Yaya et al., 2010). However, the biosynthesis of 4-methoxy cruciferous phytoalexins has not been studied, even though they are detected in quite a few species (Pedras and Yaya, 2010). The discovery of new 4-methoxylated cruciferous phytoalexins, rapalexin A (**103**) and isocyalexin A (**104**), has triggered investigation of their biosynthetic intermediates, as they contain unusual side chains (isothiocyanate and isocyanide respectively). Because of significant differences in their side chain, when compared to other phytoalexins of the brassinin series (with a carbon linker connecting indole ring with the side chain nitrogen), different biosynthetic routes and intermediates were proposed as shown in the retro-biosynthetic analysis (**Scheme 2.7**) (Pedras and Yaya, 2012; 2013; Pedras, Zheng et al., 2007a; Pedras, Zheng et al., 2007b). For the biosynthetic studies, different labeled biosynthetic intermediates were proposed, synthesized and used (**Table 2.13**).

Table 2.13 Perdeuterated compounds used in biosynthetic studies.

Deuterated compound (#)[a]	Origin
L-[2',4',5',6',7'-$^{2}H_5$]tryptophan (**66a**)	commercial (Cambridge Isotopes)
L-[U-$^{13}C_{11}$,U-$^{15}N_2$]tryptophan (**66b**)	commercial (Cambridge Isotopes)
[4',5',6',7'-$^{2}H_4$]desulfoglucobrassicin (**80a**)	synthetic (Pedras and Yaya, 2013)
[2,2,4',5',6',7'-$^{2}H_6$]glucobrassicin (**57b**)	synthetic (Pedras, Yaya et al., 2010)
(D,L)-[$^{2}H_3$CO,5',6',7'-$^{2}H_3$]-4'-methoxyindolyl-3'-glycine (**107b**)	synthetic (Pedras and Yaya, 2013)
(D,L)-[$^{2}H_3$CO]-4'-methoxyindolyl-3'-glycine (**107a**)	synthetic (Pedras and Yaya, 2013)
(D,L)-[4',5',6',7'-$^{2}H_4$]indolyl-3'-glycine (**185a**)	synthetic (Pedras and Yaya, 2013)
[$^{2}H_3$CO,5',6',7'-$^{2}H_3$]-4'-methoxyindole-3'-carboxaldehyde oxime (**171b**)	synthetic (Pedras and Yaya, 2013)
[4',5',6',7'-$^{2}H_4$]indole-3'-carboxaldehyde oxime (**176a**)	synthetic (Pedras and Yaya, 2013)
[$^{2}H_3$CO]-4'-methoxyindole-3'-carboxaldehyde (**190a**)	synthetic (Pedras and Yaya, 2013)
[$^{2}H_3$CO,5',6',7'-$^{2}H_3$]desulfoglucorapacissin (**172b**)	synthetic (Pedras and Yaya, 2013)
[$^{2}H_3$CO]desulfoglucorapassicin (**172a**)	synthetic (Pedras and Yaya, 2013)
[4',5',6',7'-$^{2}H_4$]indole desulfoglucosinolate (**186a**)	synthetic (Pedras and Yaya, 2013)
[5,6,7-$^{2}H_3$]-4-methoxyindole (**149a**)	synthetic (Pedras and Yaya, 2013)
[$^{2}H_3$CO]-4'-methoxyindolyl-3'-acetonitrile (**135a**)	synthetic (Pedras and Yaya, 2013)
[$^{2}H_3$CO]rapalexin A (**103a**)	synthetic (Pedras and Yaya, 2013)
[$^{2}H_3$CO]-4'-methoxybrassinin (**108a**)	synthetic (Pedras and Yaya, 2013)
[4',5',6',7'-$^{2}H_4$]indole (**120a**)	synthetic (Pedras and Yaya, 2013)

[a] Deuterated compounds are referred to by a number followed by the letter a or b.

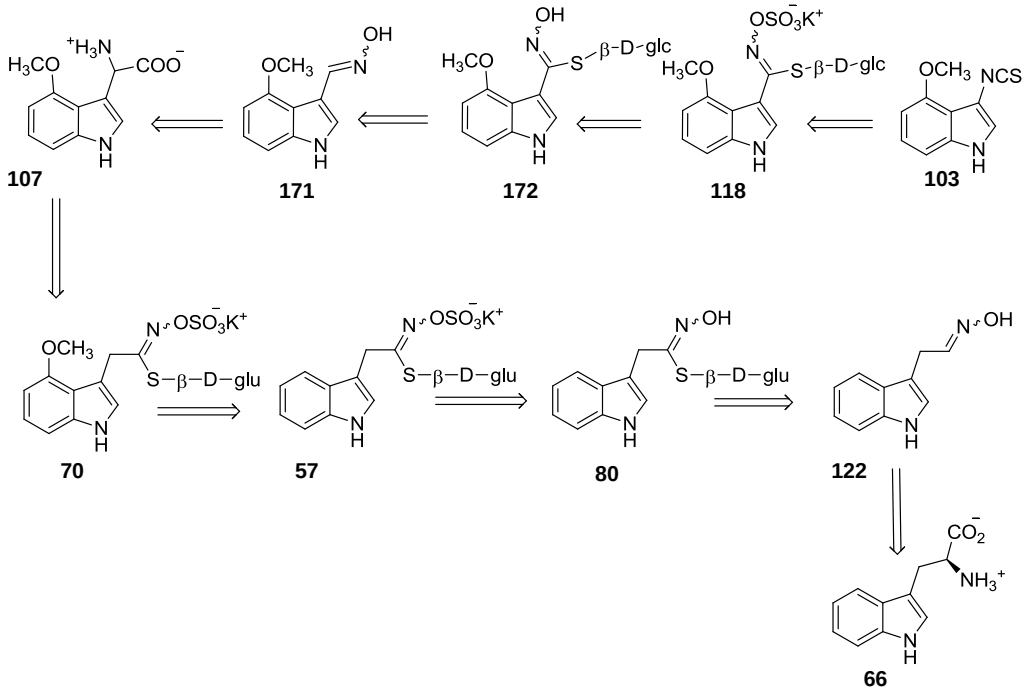

Scheme 2.7 Retro-biosynthetic analysis of rapalexin A (**103**) biosynthesis.

2.2.2.4 Synthesis of deuterated compounds

[4,5,6,7-$^2H_4$]Indole (120a), [4',5',6',7'-$^2H_4$]indole-3'-carboxaldehyde (175a), [4',5',6',7'-$^2H_4$]indole-3'-carboxaldehyde oxime (176a)

[4,5,6,7-$^2H_4$]Indole (**120a**) was synthesized with a slight modification of a previously published procedure (Pedras and Okinyo, 2006c), from [3,4,5,6-$^2H_4$]-2-nitrophenyl acetonitrile (**174a**) via reductive cyclization with 10% palladium on activated carbon in the presence of a catalytic amount of AcOH in 69% yield. [3,4,5,6-$^2H_4$]-2-Nitrophenylacetonitrile (**174**) was prepared from [2,3,4,5,6-$^2H_5$]nitrobenzene (**173**) as previously published (Makosza and Winiarski, 1984). Indole was converted to [4',5',6',7'-$^2H_4$]indole-3'-carboxaldehyde (**175a**) via a Vilsmeier-Haack reaction in 95% yield, which on treatment with $NH_2OH.HCl$ and Na_2CO_3 yielded the corresponding oxime (**176a**) in quantitative yield (**Scheme 2.8**).

[4',5',6',7'-$^2H_4$]Indole desulfoglucosinolate (186a)

[4',5',6',7'-$^2H_4$]Indole desulfoglucosinolate (**186a**) was synthesized as previously published for the nondeuterated compound (**186**) (Brochard, Joseph et al., 1994). In a one pot reaction, the chlorination of [4',5',6',7'-$^2H_4$]indolyl-3'-carboxaldehyde oxime (**176a**) with NCS was followed by coupling with 1-thio-β-D-glucopyranose-2,3,4,6-tetraacetate to afford [4',5',6',7'-$^2H_4$]indolyl-3'-tetraacetyl glucocarboxythiohydroxamate (**183a**) in 22% yield which was hydrolyzed in $KOCH_3$ to afford [4',5',6',7'-$^2H_4$]indole desulfoglucosinolate (**186a**) in quantitative yield (**Scheme 2.8)**.

[4',5',6',7'-$^2H_4$]indolyl-3'-glycine (185a)

[4',5',6',7'-$^2H_4$]indolyl-3'-glycine (**185a**) was prepared from [4,5,6,7-$^2H_4$]indole (**120a**) analogous to a previously published for the non-deuterated compound (**185**) (Droste and Wileland, 1987). Indole **120a** was allowed to react with oxalylchloride in anhydrous diethyl ether at 0 °C to yield [4',5',6',7'-$^2H_4$]indolyl-3'-oxalylchloride (**177a**), which was hydrolyzed by NaOH to yield [4',5',6',7'-$^2H_4$]indolyl-3'-oxo acid (**181a**) quantitatively. Oximation of **181a** was accomplished following a standard procedure using $NH_2OH.HCl$ and Na_2CO_3. [4',5',6',7'-$^2H_4$]Indolyl-3'-oximino acid (**184a**) was reduced with $NaBH_4$ and $NiCl_2.6H_2O$ to yield the amino acid [4',5',6',7'-$^2H_4$]-4'-methoxyindolyl-3'-glycine (**185a**) (**Scheme 2.8**).

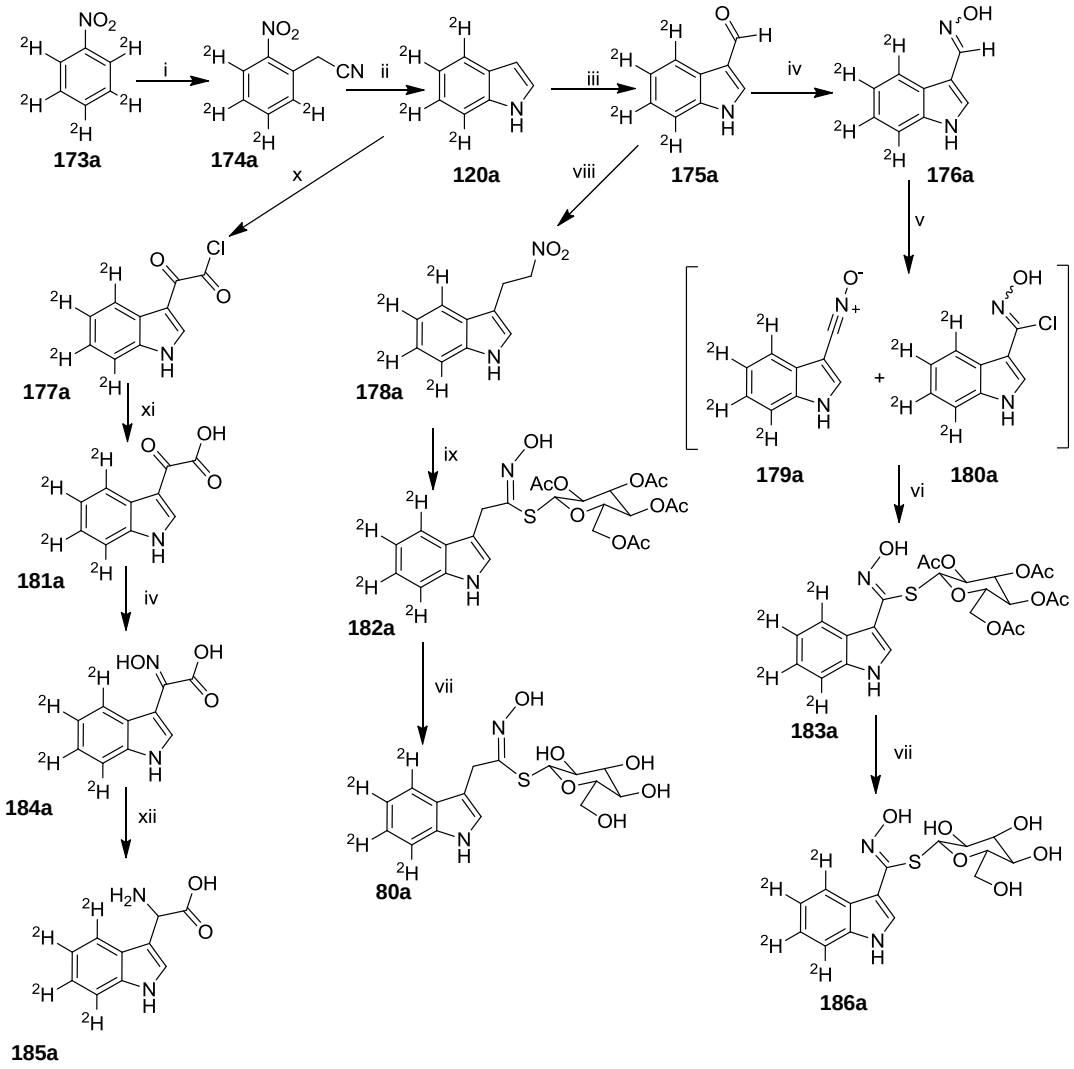

Scheme 2.8 Syntheses of **120a, 175a, 176a, 186a, 80a and 185a.** Reagents and conditions: i) $ClCH_2CN$, NaOH, 49%; ii) Pd/C, EtOAc, AcOH, 68%; iii) $POCl_3$, DMF, 95%; iv) Na_2CO_3, $NH_2OH.HCl$, 70 °C; v) pyridine, NCS, CH_2Cl_2; vi) 1-thio-β-D-glucopyranose-2,3,4,6-tetraacetate, Et_3N, 22%; vii) $KOCH_3$, MeOH; viii) CH_3NO_2, NaOAc; $NaBH_4$, THF, MeOH; ix) $NaOCH_3$, MeOH; $SOCl_2$, DME,-40 °C, 38%; 1-thio-β-D-glucopyranose-2,3,4,6-tetraacetate, Et_3N, CH_2Cl_2, Et_2O, 33%; x) $C_2O_2Cl_2$, Et_2O; xi) NaOH; xii) $NaBH_4$, $NiCl_2.6H_2O$.

[4',5',6',7'-$^2H_4$]Desulfoglucobrassicin (80a)

Synthesis of [4',5',6',7'-$^2H_4$]desulfoglucobrassicin (**80a**) was achieved as previously published for the nondeuterated compound (**80**) (Viaud and Rollin, 1990). [4,5,6,7-$^2H_4$]indole (**120a**) was subjected to a Vilsmeier-Haack formylation reaction to afford [4',5',6',7'-$^2H_4$]indole-3'-carboxaldehyde (**175a**), which was condensed with nitromethane to afford [4,5,6,7-$^2H_4$]-3-nitrovinylindole (**208a**) that led to the formation of [4,5,6,7-$^2H_4$]-3-(2'-nitroethyl)indole (**178a**) after reduction with $NaBH_4$ in 38% yield. [4,5,6,7-$^2H_4$]-3-(2'-Nitroethyl)indole (**178a**) was reacted with $NaOCH_3$ and thionylchloride to afford an oximoyl chloride that coupled with thioglucosetetraacetate and led to the formation of [4',5',6',7'-$^2H_4$]tetraacetyl desulfoglucobrassicin (**182a**) in 33% yield. Finally, methanolysis of **182a** afforded [4',5',6',7'-$^2H_4$]desulfoglucobrassicin (**80a**) in quantitative yield (**Scheme 2.8**).

[$^2H_3$CO]-4-Methoxyindole (149a)

[$^2H_3$CO]-4-Methoxyindole (**149a)** was synthesized from 3-nitrophenol (**187**) as previously published (Mąkosza, Danikiewicz et al., 1988; Robertson and Botting, 1999). A solution of 3-nitrophenol (**187)** was treated with ^2H_3CI in the presence of NaH at 65 ºC to yield crude [$^2H_3$CO]-3-methoxy nitrobenzene (**188a)** in quantitative yield, which on treatment with 4-chlorophenoxyacetonitrile and *t*-BuOK at -20 ºC yielded ([$^2H_3$CO]-6-methoxy-2-nitrophenyl)acetonitrile (**189a)** in 26%. Reductive cyclization of **189a** was catalyzed by palladium on activated carbon to yield [$^2H_3$CO]-4-methoxyindole (**149a)** in 81% (**Scheme 2.9**).

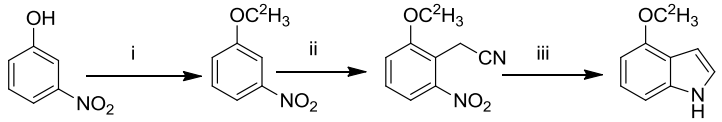

187a **188a** **189a** **149a**

Scheme 2.9 Synthesis of 4-methoxyindole (**149a)**. Reagents and conditions: i) NaH, ^2H_3CI, THF, 65°C; ii) 4-chlorophenoxyacetonitrile, *t*-BuOK, DMF,-20°C, 26%; (iii) 10% Pd/C, H_2, MeOH, AcOH 81%.

[^2H_3CO]-4'-Methoxyindole-3'-carboxaldehyde (190a)

[^2H_3CO]-4'-Methoxyindole-3'-carboxaldehyde (**190a**) was prepared via two different routes: the first route that involved formylation of 4-methoxyindole (**149a**) afforded **190a** in very good yield. However, the step involving vicarious nucleophilic substitution reaction (**188a** to **189a, Scheme 2.9**) gave poor yield (overall yield ca. 25%). The second route involved methoxylation of indole-3'-carboxaldehyde (**175**) that on successive treatment with TTFA, I_2/CuI and $NaOCD_3$ afforded **190a** in 78% yield (Somei, Yamada et al., 1984) (**Scheme 2.10**). Therefore, the second route was followed for the synthesis of deuterated **190** as it is relatively short and provides good yield.

[^2H_3CO]-4'-Methoxyindolyl-3'-acetonitrile (135a)

[^2H_3CO]-4'-Methoxyindolyl-3'-acetonitrile (**135a**) was prepared from [^2H_3CO]-4-methoxy-3-(2'-nitroethyl)indole (**195a),** synthesized from condensation of **190a** with nitromethane in the presence of NH_4OAc, followed by $NaBH_4$ reduction of the intermediate [^2H_3CO]-4-methoxy-3-nitrovinylindole (**192a**) (Robertson and Botting, 1999). Finally, treatment of **195a** with CS_2 and Et_3N yielded [^2H_3CO]-4'-methoxyindolyl-3'-acetonitrile (**135a**) in 62% yield (**Scheme 2.10**). Another reported route for the synthesis of 4'-methoxyindolyl-3'-acetonitrile (**135**) involves the reaction between Grignard reagent (prepared from 4-methoxyindole) and bromo acetonitrile (Pedras, Chumala et al., 2003).

[^2H_3CO]-4'-Methoxybrassinin (108a)

[^2H_3CO]-4'-Methoxybrassinin (**108a**) was prepared as previously published (Yamada, Kobayashi et al., 1993). Compound **190a** was transformed to the corresponding oxime **171a** using $NH_2OH.HCl$ and Na_2CO_3 in very good yield. Compound **171a** was reduced with $NaBH_4$ in the presence of $NiCl_2.6H_2O$ to yield the corresponding amine, ([^2H_3CO]-4'-methoxy-3'-indolyl)methanamine (**193a**) in 54% yield

that reacted with CS_2 and Et_3N at 0 ºC to yield a dithiocarbamate salt intermediate that afforded [^2H_3CO]-4'-methoxybrassinin (**108a**) on treatment with MeI in 77% yield (**Scheme 2.10**).

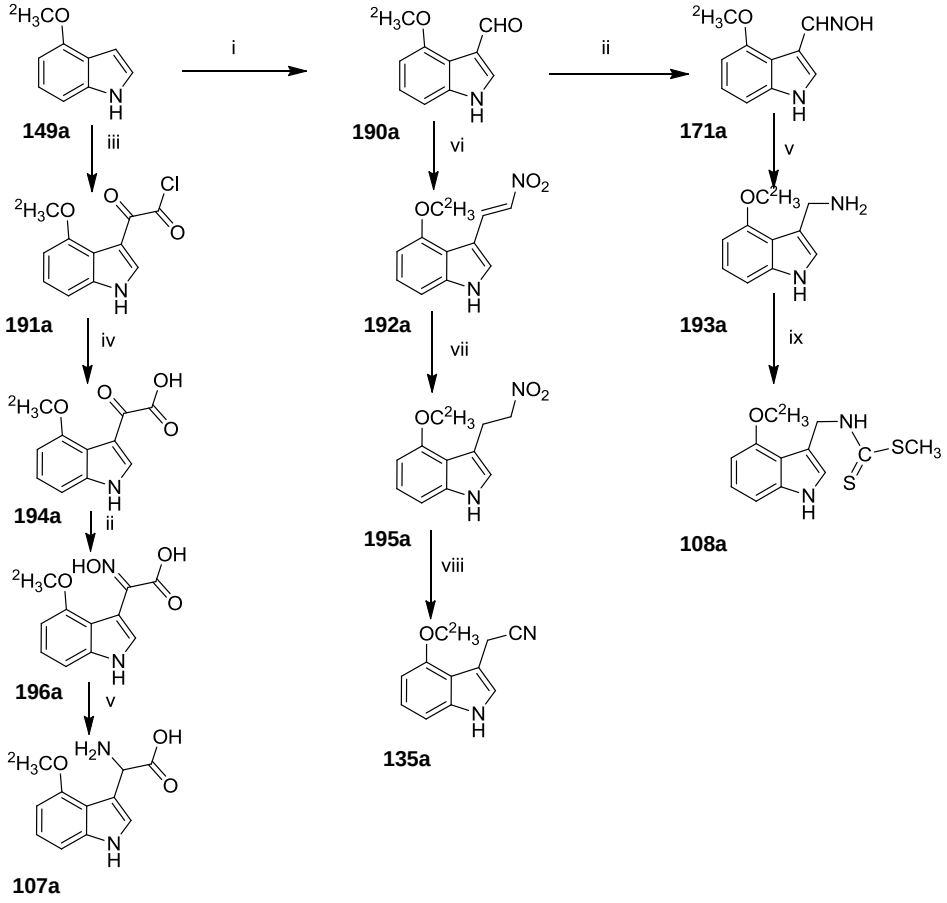

Scheme 2.10 Syntheses of **108a**, **190a**, **107a** and **135a**. Reagents and conditions: i) $POCl_3$, DMF, 95%; ii) $NH_2OH.HCl$, Na_2CO_3, 70 ºC; iii) $C_2O_2Cl_2$, Et_2O; iv) aq. NaOH; aq. HCl quantitative; v) $NaBH_4$, $NiCl_2.6H_2O$, 47%; vi) CH_3NO_2, NH_4OAc; vii) $NaBH_4$, THF, 38%; viii) CS_2, Et_3N, 62%; ix) CS_2, Et_3N, MeI, 77%.

[^2H_3CO]-4'-Methoxyindolyl-3'-glycine (107a)

[^2H_3CO]-4'-Methoxyindolyl-3'-glycine (**107a**) was prepared from [^2H_3CO]-4-methoxyindole (**149a)**. Compound **149a** was allowed to react with oxalylchloride in anhydrous diethyl ether at 0 °C to yield [^2H_3CO]-4'-methoxyindolyl-3'-oxalylchloride (**191a**) which hydrolyzed with NaOH solution and worked up with aq. HCl to yield the

corresponding oxo acid (**194a**). Oximation of **194a** was accomplished using $NH_2OH.HCl$ and Na_2CO_3 to yield [^2H_3CO]-4'-methoxyindolyl-3'-oximino acid (**196a**) in 84% that was reduced with $NaBH_4$ in the presence of $NiCl_2.6H_2O$ to yield [^2H_3CO]-4'-methoxyindolyl-3'-glycine (**107a**) in 47% (**Scheme 2.10**). Attempts to reduce **196** with Pd/C or PtO_2 under hydrogen balloon pressure resulted in mixtures of products which were inseparable.

[$^2H_3$CO 5',6',7'-$^2H_3$]-4'-methoxyindole-3'-carboxaldehyde oxime (171b)

[$^2H_3$CO,5',6',7'-$^2H_3$]-4'-Methoxyindole-3'-carboxaldehyde oxime (**171b**) was prepared as previously published for the non-deuterated compound (Yamada, Kobayashi et al., 1993). [4',5',6',7'-$^2H_4$]Indole-3'-carboxaldehyde (**175a**) in TFA was successively treated with TTFA, I_2/CuI and $NaOCD_3$ to afford [$^2H_3$CO,5',6',7'-$^2H_3$]-4'-methoxyindole-3'-carboxaldehyde (**190b**) in 45% yield. Then, [$^2H_3$CO,5',6',7'-$^2H_3$]-4'-methoxyindole-3'-carboxaldehyde (**190b**) was treated with $NH_2OH.HCl$ and Na_2CO_3 to afford **171b** in 82% (**Scheme 2.11**).

[$^2H_3$CO, 5',6',7'-$^2H_3$]Desulfoglucorapacissin (172b)

[$^2H_3$CO,5',6',7'-$^2H_3$]Desulfoglucorapacissin (**172b**) was prepared from *N*-protected [$^2H_3$CO,5',6',7'-$^2H_3$]-4'-methoxyindole-3'-carboxaldehyde (**190b**). *N*-*t*-Boc[$^2H_3$CO,5',6',7'-$^2H_3$]-4'-methoxyindole-3'-carboxaldehyde, *N*-*t*-Boc(**190b**), was treated with $NH_2OH.HCl$ and Na_2CO_3 to yield the corresponding oxime (**198b**), which on treatment with NCS yielded an oximoyl chloride intermediate that was coupled with 1-thio-β-D-glucopyranose-2,3,4,6-tetraacetate to yield *N*-*t*-Boc[$^2H_3$CO,5',6',7'-$^2H_3$]desulfoglucorapassicin tetraacetate (**199b**) in 52%. The *t*-Boc group was hydrolyzed with deuterated TFA 20% in CH_2Cl_2 to yield deprotected intermediate in 92% that hydrolyzed in KOMe to afford [$^2H_3$CO,5',6',7'-$^2H_3$]desulfoglucorapassicin (**172b**) (**Scheme 2.11**). The *t*-Boc deprotection step was carried out using deuterated TFA because, 4'-methoxy group caused exchange of indole deuterons ^{2}H-5' and ^{2}H-7' with

protons of TFA. The two affected positions were ortho and para to the methoxy group, suggesting the methoxy group has facilitated the exchange.

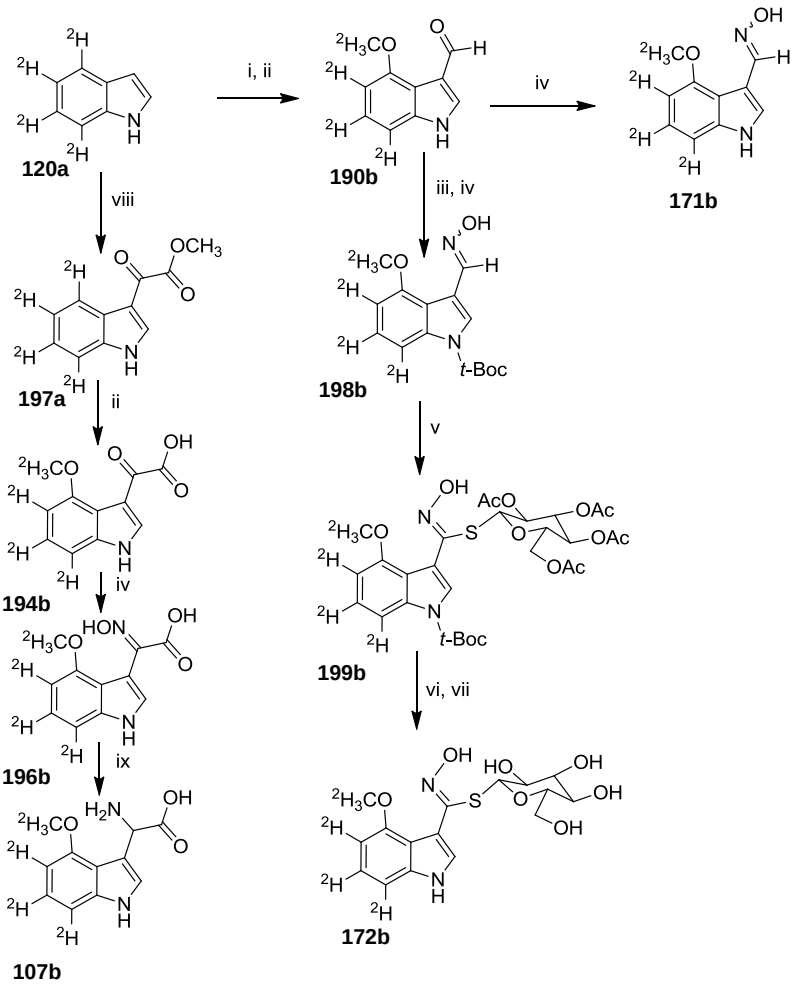

Scheme 2.11 Synthesis of **171b**, **172b** and **107b**. Reagents and conditions: i) $POCl_3$, DMF, 95%; ii) TTFA, TFA; I_2, CuI; $NaOCD_3$, 45%; iii) $(t\text{-Boc})_2O$, DMAP, THF; iv) $NH_2OH.HCl$, Na_2CO_3, 70 ºC; v) pyridine, NCS, CH_2Cl_2, 1-thio-β-D-glucopyranose tetraacetate, Et_3N, 52%; vi) D-TFA, CH_2Cl_2, 92%; vii) $KOCH_3$, MeOH, quant; viii) $C_2O_2Cl_2$, Et_2O; MeOH; ix) $NaBH_4$, $NiCl_2.6H_2O$, 47%.

(D,L)-[^{2}H$_3$CO,5',6',7'-^{2}H$_3$]-4'-Methoxyindolyl-3'-glycine (107b)

(*D,L*)-[^{2}H$_3$CO,5',6',7'-^{2}H$_3$]-4'-Methoxyindolyl-3'-glycine (**107b**) was prepared from [4',5',6',7'-^{2}H$_4$]indole (**120a**), which on treatment with oxalylchloride yielded [4',5',6',7'-^{2}H$_4$]indole-3'-oxalylchloride (**177a**). [4',5',6',7'-^{2}H$_4$]Indole-3'-oxalylchloride

(**177a**) was treated with methanol to afford the corresponding oxoacetate (**197a**), which on successive treatment with TTFA, I_2/CuI, and $NaOCD_3$ afforded [^2H_3CO,5',6',7'-$^2H_3$]-4'-methoxyindolyl-3'-oxo acid (**194b**). Compound **194b** was treated with $NH_2OH.HCl$ and Na_2CO_3 to afford the corresponding oximino acid (**196b**), which reduced with $NaBH_4$ in the presence of $NiCl_2.6H_2O$ afforded the desired product (*D,L*)-[^2H_3CO,5',6',7'-$^2H_3$]-4'-methoxyindolyl-3'-glycine (**107b**) in 37% over all yield (**Scheme 2.11**). Surprisingly when oxoacid (**181**) was used instead of the oxoacetate (**197**) the methoxylation reaction did not go to completion which could be due to involvement of carbonyl oxygen in intra-molecular hydrogen bonding that lowers the possibility of chelating and then directing the metal to C-4 position.

[^2H_3CO]Rapalexin A (103a)

[^2H_3CO]Rapalexin A (**103a**) was prepared from nitroindole (**166**) by a slight modification of previously a published procedure (Pedras, Zheng et al., 2007a). Considering nitrophenol as a staring material this route is found to be lengthy as well as low yielded. Therefore, methoxylation of nitrobenzene was proposed as an alternative and tested for the synthesis of **167** (Pedras and Yaya, 2012)**.** Methoxylation at position four of nitroindole was successfully accomplished using the nitro group as a director. First, [^2H_3O]-4-methoxy-3-nitroindole (**167a**) was prepared from nitroindole (**166**) following a standard procedure for methoxylation of indole-3'-carboxaldehyde (**175**) (Somei, Yamada et al., 1984). Reduction of **167a** with palladium on activated carbon was followed by treatment with Et_3N and $CSCl_2$ at -10 °C to yield [^2H_3CO]rapalexin A (**103a**) in 28% overall yield (Pedras and Yaya, 2012) (**Scheme 2.12**).

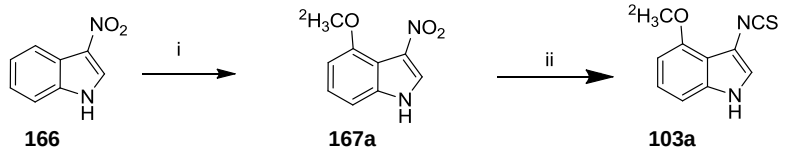

Scheme 2.12 Synthesis of [^2H_3CO]rapalexin A (**103a).** Reagents and conditions: i) TTFA, TFA; I_2, CuI; $NaOCD_3$, 54%; ii) Pd/C, H_2, THF, EtOH; $CSCl_2$, Et_3N, -10 °C, 51% over two steps.

Synthesis of *N*-*t*-Bocindole-3-glucosinolate (204)

N-*t*-Bocindolyl-3-carboxaldehyde (**200**) was treated with $NH_2OH.HCl$ and Na_2CO_3 to give the corresponding oxime (**201**) in a good yield. Chlorination of **201** was followed by coupling with 1-thio-β-D-glucopyranose tetraacetate to yield compound **202**. Sulfonation of compound **202** with HSO_3Cl yielded compound **203,** which on treatment with $KOCH_3$ yielded the target product *N*-*t*-Bocindole-3-glucosinolate (**204**) (**Scheme 2.13**). The compound was found to be unstable in both water and organic solvents, decomposes over a period of 12-24 hours.

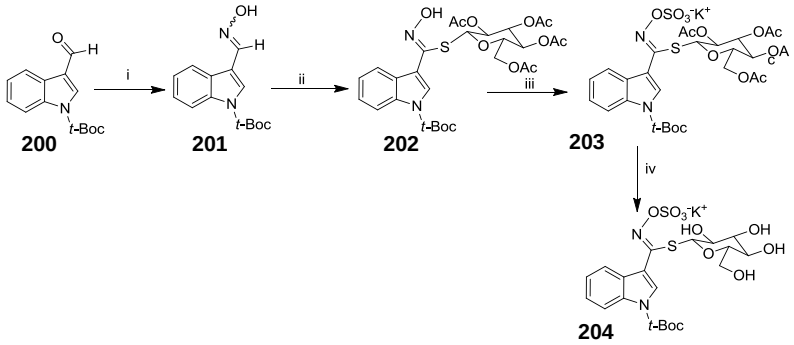

Scheme 2.13 Synthesis of **204**. Reagents and conditions: i) Na_2CO_3, $NH_2OH.HCl$, EtOH, 60 °C, quant; ii) pyridine, NCS, CH_2Cl_2; 1-thio-β-D-glucopyranose tetraacetate, NEt_3, 37%; iii) $ClSO_3H$, pyridine, CH_2Cl_2/ether, 66%; iv) $KOCH_3$, MeOH, quantitative.

2.2.2.5 Incorporation experiments using perdeuterated compounds

For biosynthetic studies rutabaga roots were cut horizontally in 10-15 mm thick discs and cylindrical holes (16 mm in diameter) were made on one surface of the discs with a cork-borer (Pedras, Montaut et al., 2004). The discs were kept in tightly sealed plastic boxes and kept at 21 °C in darkness. After 24 h, the discs were UV-irradiated on the surface with holes for 1.5 h, and were kept in dark further for 24 h. Labeled compound solution (5×10^{-4} M) dissolved in H_2O, H_2O-CH_3OH (90/10 v/v) or H_2O-CH_3OH-T80 (90/10/0.1 v/v) was pipetted into each hole (500 μL per hole) and the discs were further incubated at 21 °C in dark. Following adsorption of precursor solution, holes were filled with water (**Figure 2.15**). The aqueous solution in the holes was withdrawn after 48 h and was extracted (EtOAc 20 ml × 2). The combined organic extract was dried over Na_2SO_4 and solvent was removed under reduced pressure. The residue obtained was dissolved in CH_3CN (200 μl) and was analyzed by HPLC-DAD and HPLC-ESI-MS to determine the level of incorporation into phytoalexins. Control experiments were similarly prepared by incubating rutabaga root slices with non-labeled precursors or with carrier solution only. Tissue around the holes was cut, was ground (pestle and mortar) and extracted with CH_3OH, filtered and the filtrate was concentrated under reduced pressure. The residue was dissolved in H_2O-CH_3OH (50:50) and was analyzed by HPLC-DAD and HPLC-ESI-MS to determine the level of incorporation of labeled precursors into indole glucosinolates (Pedras, Montaut et al., 2004) (**Figure 2.15**).

The percentage of ^{2}H, ^{13}C and ^{15}N incorporation was established using peak intensities in positive or negative modes ESI-MS according to the equation: % of incorporation = $[M \pm 1 + n]^{\pm}/([M \pm 1]^{\pm} + [M \pm 1 + n]^{\pm}) \times 100$ ($n = 3, \ldots$) n is the number of isotopic elements and M is the peak intensity of each ion $[M - 1]^{-}$ or $[M + 1]^{+}$. The biosynthesis of the phytoalexin rapalexin (**103**), isocyalexin (**104**) and isalexin (**102**) was investigated using the labeled biosynthesis precursors/intermediates shown in **Table 2.13**.

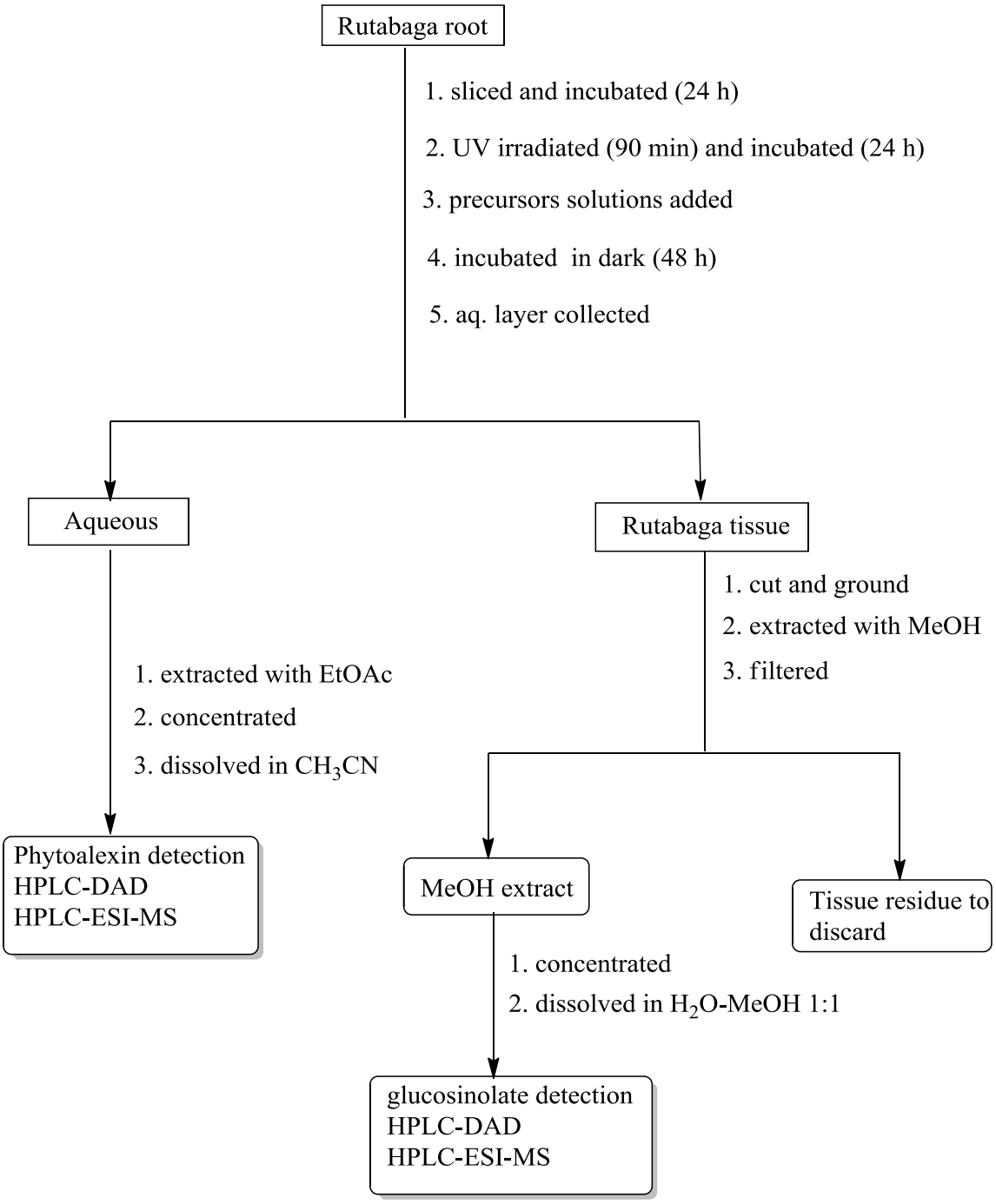

Figure 2.15 Flow-chart of elicitation, extraction and analysis of phytoalexins and indole glucosinolates produced in rutabaga root

2.2.2.5.1 Incorporation of *L*-[2',4',5',6',7'-$^2H_5$]tryptophan (66a)

Biosynthetic origin of the phytoalexins rapalexin A (**103**), isocyalexin A (**104**) and isalexin (**102**) were investigated using commercially available *L*-[2',4',5',6',7'-$^2H_5$]tryptophan (**66a**). Rutabaga tissue was prepared and an aqueous solution of *L*-[2',4',5',6',7'-$^2H_5$]tryptophan (**66a**) (500µL/hole, 5×10^{-4} M) was added as described in **Figure 2.15**. Control experiments were similarly prepared by incubating rutabaga roots with natural abundance *L*-tryptophan (**66**) or with carrier solution only. Nonpolar fractions that contained phytoalexins (rapalexin A (**103**), isalexin (**102**), isocyalexin A (**104**), spirobrassinin (**101**), rutalexin (**116**), cyclobrassinin (**78**) etc.), were analyzed by HPLC-DAD and HPLC-ESI-MS. The HPLC-ESI-MS analysis of deuterated and control samples revealed that the peak corresponding to rapalexin A (**103**) (t_R = 22.3 min) contained two ions: $[M - 1]^-$ at *m/z* 203 (natural abundance) and $[M - 1 + 4]^-$ at *m/z* 207 that resulted from incorporation of *L*-[2',4',5',6',7'-$^2H_5$]tryptophan (**66a**). The ion with *m/z* 207 was not detected in the control sample that was fed with natural abundance *L*-tryptophan (**66**). Peak intensities of the natural abundance $[M - 1]^-$ ion (*m/z* 203) and that of deuterated ions (*m/z* 207) were used to determine the deuterium incorporation (% of ^2H incorporation = $\{[M - 1 + 4]^-/([M - 1]^- + [M - 1 + 4]^-)\} \times 100 \pm$ standard deviation). Accordingly, the percentage of deuterium incorporation was calculated to be 26.8 ± 1.2% (**Table 2.14**). The percentage of deuterium incorporation into isocyalexin A (**104**) was calculated similarly (13.6 ± 0.1) (**Table 2.14)**. The HPLC-ESI-MS analysis of isalexin (**102**) peak at t_R = 2.0 min showed two ions: $[M + 1]^+$ at *m/z* 178 and $[M + 1 + 3]^+$ at *m/z* 181 that resulted from incorporation of *L*-[2',4',5',6',7'-$^2H_5$]tryptophan (**66a**) (not detected in the control samples). Using the same equation, the percentage of deuterium incorporation was calculated to be 11.2 ± 1.7%. Similarly, the rutalexin (**116**) peak at t_R = 13.5 min (negative mode) indicated two ions: $[M - 1]^-$ at *m/z* 231 and $[M - 1 + 4]^-$ at *m/z* 235 (the latter not detected in the control samples). The percentage of deuterium incorporation was determined to be 26.3 ± 3.8%. The HPLC-ESI-MS analysis of spirobrassinin (**101**) peak at t_R = 11.8 min showed two ions as well: $[M + 1]^+$ at *m/z* 251 and $[M + 1 + 4]^+$ at *m/z* 255, not detected in the control samples. Using the equation

shown above, the percentage of deuterium incorporation was calculated to be 29.9 ± 7.9%. Similarly, the percentage of deuterium incorporation into cyclobrassinin (**78**) and 4'-methoxycyclobrassinin (**110**) were calculated to be 20.1 ± 7.9% and 13.0 ± 5.4% respectively (**Table 2.14**; **Figure 2.16**).

The number of deuteria detected in **102** and **110** were three, which is consistent with structure. In compound **102,** C-2 was oxidized to carbonyl, while in **110** C-4 was oxidized to methoxy group. Variation in the standard deviation is due to variation in the production of each phytoalexin. The incorporation of *L*-tryptophan (**66**) into phytoalexins was reported by Pedras and coworkers (Pedras, Okinyo et al., 2009), and the same trend was also observed in this work. However, from the previous or current data, it was not possible to establish whether the deuterium resulted from tryptophan (**66**) incorporations intact or degradation to indole (**120**) and reincorporation of **120** back into the phytoalexins. To answer this question, use of tryptophan (**66**) labeled on both the indole ring and the side chain was necessary.

Table 2.14 Metabolites of *L*-[2',4',5',6',7'-$^{2}H_5$]tryptophan (**66a**) in UV-irradiated rutabaga roots.

Metabolites isolated [a]	% Incorporation of deuterium ± Std
[2',5',6',7'-$^{2}H_4$]rapalexin A (**103a**)	26.8 ± 1.2%[c]
[2',5',6',7'-$^{2}H_4$]isocyalexin A (**104a**)	13.6 ± 0.1%[c]
[5,6,7-$^{2}H_3$]isalexin (**102a**)	11.2 ± 1.7%[b]
[4',5',6',7'-$^{2}H_4$]rutalexin (**116a**)	26.3 ± 3.8%[c]
[4',5',6',7'-$^{2}H_4$]spirobrassinin (**101a**)	29.9 ± 7.9%[b]
[4',5',6',7'-$^{2}H_4$]cyclobrassinin (**78a**)	20.1 ± 7.9%[b]
[5',6',7'-$^{2}H_3$]-4'-methoxycyclobrassinin (**110a**)	13.0 ± 5.4%[b]
[2',4',5',6',7'-$^{2}H_5$]glucobrassicin (**57a**)	22.8 ± 2.6%[c]
[2',4',5',6',7'-$^{2}H_5$]-1'-methoxyglucobrassicin (**69a**)	2.7 ± 1.4%[c]
[2',5',6',7'-$^{2}H_4$]-4'-methoxyglucobrassicin (**70a**)	9.5 ± 1.6%[c]

[a] Deuterated compounds are referred to by a number followed by the letter a;

[b] Positive ion mode. Incorporations calculated from HPLC-ESI-MS (peak intensities); % of ^2H incorporation = $\{[M + 1 + n]^+/([M + 1]^+ + [M + 1 + n]^+)\} \times 100$ (n =3-5) ± Std (standard deviation), where n = number of deuterium atoms.
[c] Negative ion mode. % of ^2H incorporation = $\{[M-1 + n]^-/([M-1]^- + [M-1 + n]^-)\} \times 100$ (n = 3-5) ± Std (standard deviation), where n = number of deuterium atoms.

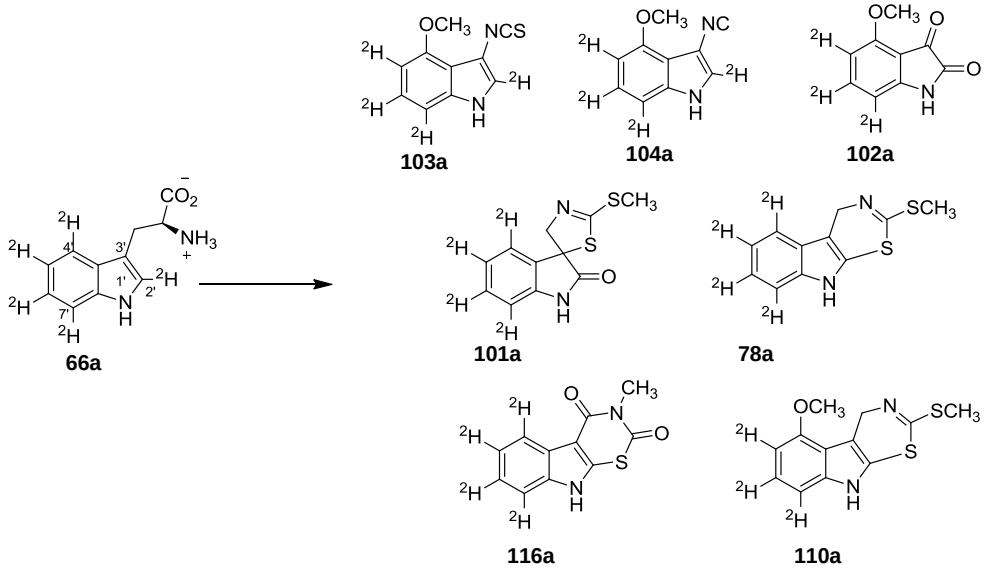

Figure 2.16 Deuterated phytoalexins obtained from feeding of *L*-[2',4',5',6',7'-$^2H_5$]tryptophan (**66a**) to UV-irradiated rutabaga root: [2',5',6',7'-$^2H_4$]rapalexin A (**103a**) (26.8 ± 1.2%), [2',5',6',7'-$^2H_4$]isocyalexin A (**104a**) (13.6 ± 0.1%), [4',5',6',7'-$^2H_4$]rutalexin (**116a**) (26.3 ± 3.8%), [5,6,7-$^2H_3$]isalexin (**102a**) (11.2 ± 1.7%), [4',5',6',7'-$^2H_4$]spirobrassinin (**101a**) (29.9 ± 7.9%), [4',5',6',7'-$^2H_4$]cyclobrassinin (**78a**) (20.1 ± 7.9%), [5',6',7'-$^2H_3$]-4'-methoxycyclobrassinin (**110a**) (13.0 ± 5.4%).

The incorporation of *L*-[2',4',5',6',7'-$^2H_5$]tryptophan (**66a**) into indole glucosinolates (glucobrassicin (**57**), 4'-methoxyglucobrassicin (**70**) and 1'-methoxyglucobrassicin (**69**)) was determined as well. Methanolic extracts of tissues were dissolved in water-methanol (50:50) and analyzed by HPLC-DAD and HPLC-ESI-MS as described above (**Figure 2.15**). The HPLC-ESI-MS analyses of the polar extracts showed the glucobrassicin (**57**) peak at t_R = 5.3 min containing two ions (negative mode): $[M]^-$ at *m/z* 447 and $[M + 5]^-$ at *m/z* 452 that was not detected in the control samples. The percentage of deuterium incorporation was calculated to be 22.8 ± 2.6% (**Table 2.14**). In

a similar fashion, the percentages of deuterium incorporation into **70** and **69** were calculated to be 9.5 ± 1.6% and 2.7 ± 1.4% respectively (**Table 2.14**; **Figure 2.17**).

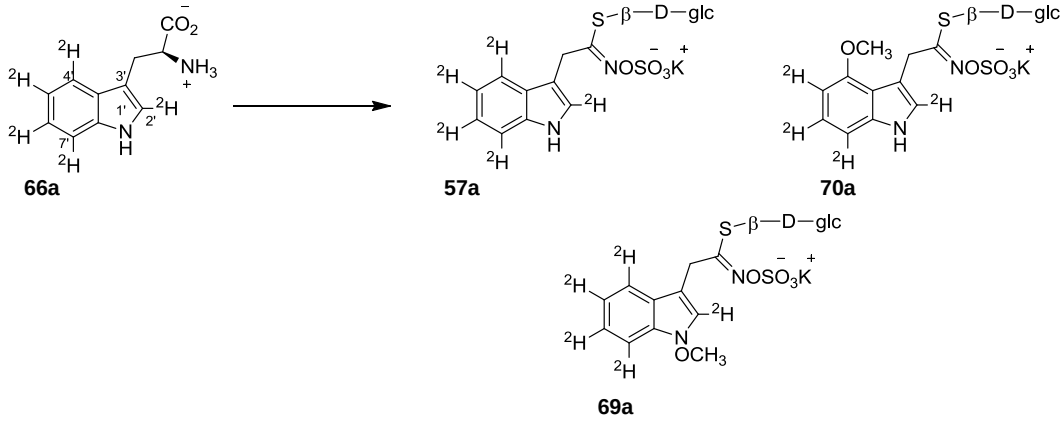

Figure 2.17 Deuterated indole glucosinolates obtained from feeding of *L*-[2',4',5',6',7'-$^2H_5$]tryptophan (**66a**) to UV-irradiated rutabaga root: [2',4',5',6',7'-$^2H_5$]glucobrassicin (**57a**) (22.8 ± 2.6%), [2',5',6',7'-$^2H_4$]-4'-methoxyglucobrassicin (**70a**) (9.5 ± 1.6%), [2',4',5',6',7'-$^2H_5$]-1'-methoxyglucobrassicin (**69a**) (2.7 ± 1.4%).

2.2.2.5.2 Incorporation of [4,5,6,7-$^2H_4$]indole (120a)

An aqueous solution of [4,5,6,7-$^2H_4$]Indole (**120a**) (500µL/hole, 5×10^{-4} M) was added to UV-irradiated slices of rutabaga roots and analyzed as described in **Figure 2.15**. The HPLC-ESI-MS analysis showed the rapalexin A (**103**) peak at t_R = 22.2 min containing two ions (negative mode): $[M - 1]^-$ at *m/z* 203 and $[M - 1 + 3]^-$ at *m/z* 206 (resulting from incorporation of [4,5,6,7-$^2H_4$] indole (**120a**)) that was not detected in the control samples. Peak intensities of the natural abundance and those of deuterated ions were used to determine the level of deuterium incorporation, using the equation shown in **Table 2.15**; the percentage of deuterium incorporation was calculated to be 11.2 ± 4.4%. Similarly, the percentages of deuterium incorporation into isocyalexin A (**104**) and isalexin (**102**) (positive mode) were calculated to be 7.2 ± 2.9% and 6.5 ± 3.8%, respectively **(Table 2.15)**. The HPLC-ESI-MS analysis of rutalexin (**116**) peak at t_R = 13.5 min (negative mode) indicated two ions as well: $[M- 1]^-$ at *m/z* 231 and $[M - 1 + 4]^-$ at *m/z* 235, not detected in the control samples. Using the equation shown in **Table 2.15**,

the percentage of deuterium incorporation was calculated to be 11.3 ± 1.5%. The HPLC-ESI-MS analysis of spirobrassinin (**101**) peak at t_R = 11.8 min (positive mode) showed two ions: $[M + 1]^+$ at *m/z* 251 and the corresponding $[M + 1 + 4]^+$ at *m/z* 255, not detected in the control samples. Accordingly, the percentage of deuterium incorporation was calculated to be 10.0 ± 4.7%. In similar fashion, the percentage of deuterium incorporations into **78** and **110** were calculated to be 6.0 ± 1.6% and 6.0 ± 0.6% respectively (**Table 2.15**; **Figure 2.18**).

Table 2.15 Metabolites of [4,5,6,7-$^2H_4$]indole (**120a**) in UV-irradiated rutabaga roots

Metabolites isolated [a]	% Incorporation ± Std
[5',6',7'-$^2H_3$]rapalexin A (**103a**)	11.2 ± 4.4% [c]
[5',6',7'-$^2H_3$]isocyalexin A (**104a**)	7.2 ± 2.9%[c]
[5,6,7-$^2H_3$]isalexin (**102a**)	6.5 ± 3.8%[b]
[4',5',6',7'-$^2H_4$]rutalexin (**116a**)	11.3 ± 1.5%[c]
[4',5',6',7'-$^2H_4$]spirobrassinin (**101a)**	10.0 ± 4.7%[b]
[4',5',6',7'-$^2H_4$]cyclobrassinin (**78a**)	6.0 ± 1.6%[b]
[5',6',7'-$^2H_3$]-4'-methoxycyclobrassinin (**110a**)	6.0 ± 0.6%[b]
[4',5',6',7'-$^2H_4$]glucobrassicin (**57a**)	12.7 ± 3.6%[c]
[4',5',6',7'-$^2H_4$]-1'-methoxyglucobrassicin (**69a**)	11.2 ± 2.1%[c]
[5',6',7'-$^2H_3$]-4'-methoxyglucobrassicin (**70a**)	10.3 ± 2.0%[c]

[a] Deuterated compounds are referred to by a number followed by the letter a;
[b] Positive ion mode. Incorporations calculated from HPLC-ESI-MS (peak intensities); % of ^2H incorporation = $\{[M + 1 + n]^+/([M + 1]^+ + [M + 1 + n]^+)\} \times 100$ (n = 3 or 4) ± Std (standard deviation), where n = number of deuterium atoms.
[c] Negative ion mode. % of ^2H incorporation = $\{[M-1 + n]^-/([M-1]^- + [M-1 + n]^-)\} \times 100$ (n = 3 or 4) ± Std (standard deviation), where n = number of deuterium atoms.

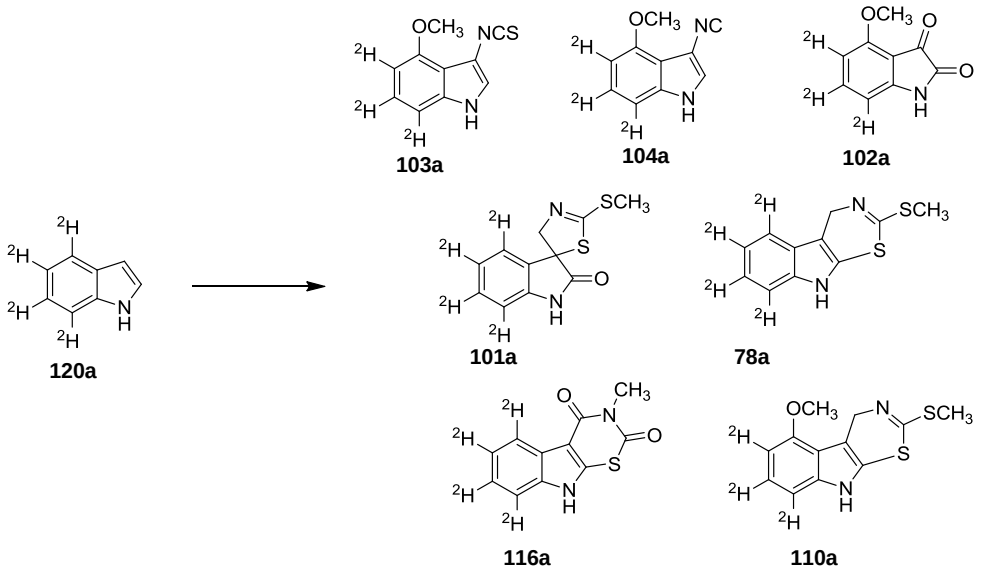

Figure 2.18 Deuterated phytoalexins obtained from feeding of [4,5,6,7-$^2H_4$]indole (**120a**) to UV-irradiated rutabaga root: [5',6',7'-$^2H_3$]rapalexin A (**103a**) (11.2 ± 4.4%), [5',6',7'-$^2H_3$]isocyalexin A (**104a**) (7.2 ± 2.9%), [4',5',6',7'-$^2H_4$]rutalexin (**116a**) (11.3 ± 1.5%), [5,6,7-$^2H_3$]isalexin (**102a**) (6.5 ± 3.8%), [4',5',6',7'-$^2H_4$]spirobrassinin (**101a**) (10.0 ± 4.7%), [4',5',6',7'-$^2H_4$]cyclobrassinin (**78a**) (6.0 ± 1.6%), [5',6',7'-$^2H_3$]-4'-methoxycyclobrassinin (**110a**) (6.0 ± 0.6%).

The incorporation of [4,5,6,7-$^2H_5$]indole (**120a**) into indole glucosinolates (glucobrassicin (**57**), 4'-methoxyglucobrassicin (**70**) and 1'-methoxyglucobrassicin (**69**)) was investigated as described in **Figure 2.15**. The HPLC-ESI-MS analyses of the polar extracts showed the glucobrassicin (**57**) peak at t_R = 5.3 min containing two ions in a negative mode: $[M]^-$ at *m/z* 447 and $[M + 4]^-$ *m/z* 451 that was not detected in the control samples. Peak intensities of the natural abundance and those of deuterated ions were used to determine the level of deuterium incorporation. Accordingly, the percentage of deuterium incorporation into glucobrassicin (**57**) was calculated to be 12.7 ± 3.6%. Similarly, using the equation shown in **Table 2.15**, the percentages of deuterium incorporation into 1'-methoxyglucobrassicin (**69**) and 4'-methoxyglucobrassicin (**70**) were calculated to be 11.2 ± 2.1% and 10.3 ± 2.0%, respectively (**Table 2.15; Figure 2.19**).

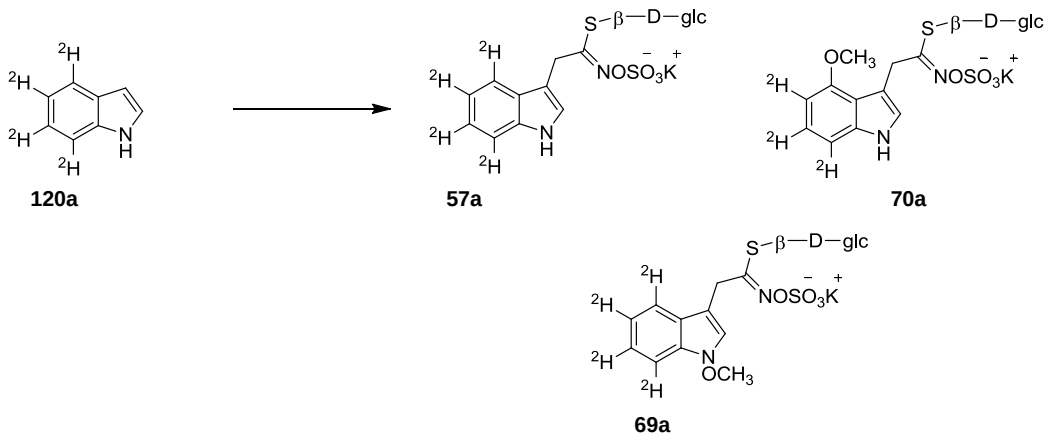

Figure 2.19 Deuterated indole glucosinolates obtained from feeding of [4,5,6,7-$^{2}H_4$]indole (**120a**) to UV-irradiated rutabaga root: [4',5',6',7'-$^{2}H_4$]glucobrassicin (**57a**) (12.7 ± 3.6%), [5',6',7'-$^{2}H_3$]-4'-methoxyglucobrassicin (**70a**) (10.3 ± 2.0%), [4',5',6',7'-$^{2}H_4$]-1'-methoxyglucobrassicin (**69a**) (11.2 ± 2.1%).

Incorporation of [4,5,6,7-$^{2}H_4$]indole (**120a**) into rutabaga phytoalexins and indole glucosinolates was previously reported (Pedras, Okinyo et al., 2009). It showed incorporation levels ranging from 6% to 19%. Compared to the current data, these earlier studies show similar trend and level of incorporations. The minor differences observed are likely due to variations in the amount of metabolites produced.

2.2.2.5.3 Incorporation of *L*-[U-$^{13}C_{11}$,U-$^{15}N_2$]tryptophan (66b)

To establish unambiguously the origin of the carbon and nitrogen atoms of both rapalexin A (**103**) and isocyalexin A (**104**), fully labeled *L*-[$^{13}C_{11}$,$^{15}N_2$]tryptophan (**66b**) was used. An aqueous solution of *L*-[U-$^{13}C_{11}$,U-$^{15}N_2$]tryptophan (500 µL/hole, 5×10^{-4} M) (**66b**) was added to UV-irradiated slices of rutabaga roots and analyzed as described in **Figure 2.15.** The HPLC-ESI-MS analysis of the nonpolar fractions revealed the rapalexin A (**103**) peak at t_R = 22.3 min containing two ions: $[M - 1]^-$ at *m/z* 203 and $[M - 1 + 11]^-$ at *m/z* 214 (resulting from incorporation of *L*-[U-$^{13}C_{11}$,U-$^{15}N_2$]tryptophan (**66b**)) that was not detected in the control samples. Peak intensities of the natural abundance and those of labeled ions were used to determine the ^{13}C and ^{15}N incorporation (% of incorporation =

{[M - 1 + *n*]$^-$/([M - 1]$^-$ + [M - 1 + *n*]$^-$)} × 100 ± standard deviation, where *n* = number of ^{13}C & ^{15}N atoms). Accordingly, the percentage of ^{13}C and ^{15}N incorporation was determined to be 25.9 ± 1.4%. Similarly, using equation shown above, the percentage of ^{13}C and ^{15}N incorporation into isocyalexin A (**104**) was calculated to be 17.0 ± 6.4%. The HPLC-ESI-MS analysis of isalexin (**102**) peak at t_R = 2.0 min (positive mode) indicated two ions: [M + 1]$^+$ at *m/z* 178 and [M + 1 + 9]$^+$ at *m/z* 187, not detected in the control samples. The percentage of ^{13}C and ^{15}N incorporation was calculated as indicated above, 12.1 ± 1.1%. The rutalexin peak (**116)** at t_R = 13.5 min (negative mode) showed two ions: molecular ion [M- 1]$^-$ at *m/z* 231 and [M - 1 + 12]$^-$ *m/z* 243, not detected in the control samples. The percentage of ^{13}C and ^{15}N incorporation was calculated as shown above to be 13.0 ± 0.3%. The spirobrassinin (**101**) peak at t_R = 11.8 min (positive mode) indicated two ions: [M + 1]$^+$ at *m/z* 251 and [M + 1 + 12]$^+$ *m/z* 263, not detected in the control samples. Using the equation shown in **Table 2.16**, the percentage of ^{13}C and ^{15}N incorporation was calculated to be 11.2 ± 0.1%. Using the same equation shown in **Table 2.16**, the percentage of ^{13}C and ^{15}N incorporation into **78** was determined as, 15.5 ± 4.7%. The HPLC-ESI-MS analysis of 4'-methoxyindole-3'-carboxaldehyde (**190**) peak at t_R = 7.5 min (positive mode) indicated two ions: [M + 1]$^+$ at *m/z* 176 and the corresponding [M + 1 + 10]$^+$ *m/z* 186 that was not detected in the control samples. As indicated above, the percentage of ^{13}C and ^{15}N incorporation was calculated, 16.2 ± 0.7%. Likewise, using the equation shown in **Table 2.16**, the percentage of ^{13}C and ^{15}N incorporation into 4'-methoxyindolyl-3'-formamide (**168**) was determined to be 12.2 ± 8.1% (**Table 2.16**; **Figure 2.20**).

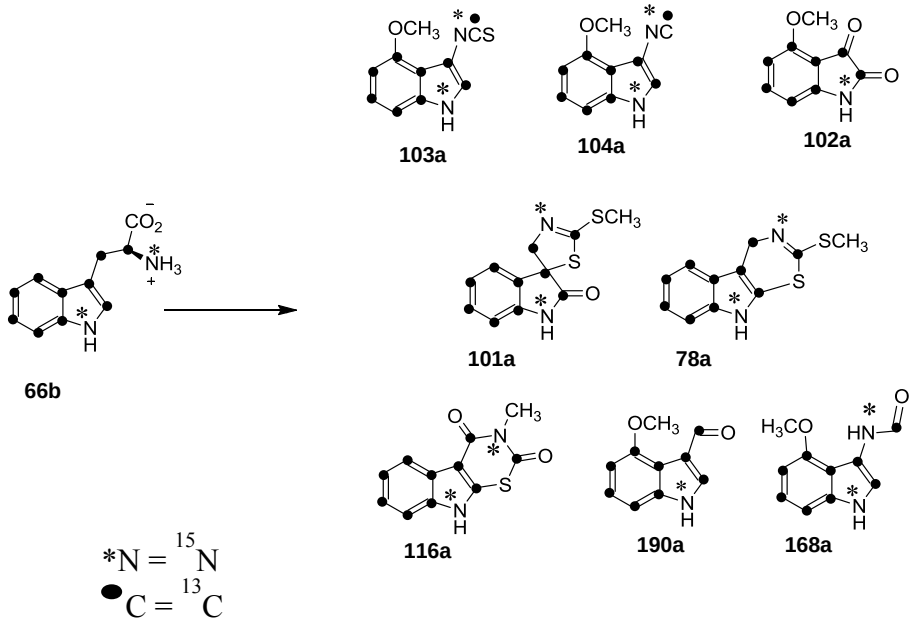

Figure 2.20 ^{13}C and ^{15}N labeled phytoalexins obtained from feeding of *L*-[U-$^{13}C_{11}$,U-$^{15}N_2$]tryptophan (**66b**) to UV-irradiated rutabaga root: [1,2',3',3a',4',5',6',7',7'a-$^{13}C_9$,$^{15}N_2$]rapalexin A (**103a**) (25.9 ± 1.4%), [1,2',3',3a',4',5',6',7',7'a-$^{13}C_9$,$^{15}N_2$]isocyalexin A (**104a**) (17.0 ± 6.4%), [1,2,2',3',3a',4',5',6',7',7'a-$^{13}C_{10}$,$^{15}N_2$]]rutalexin (**116a**) (13.0 ± 0.3%), [2,3,3a,4,5,6,7,7a-$^{13}C_8$,^{15}N]isalexin (**102a**) (12.1 ± 1.1%), [1,2,2',3',3a',4',5',6',7',7'a-$^{13}C_{10}$,$^{15}N_2$]spirobrassinin (**101a**) (11.2 ± 0.1%), [1,2,2',3',3a',4',5',6',7',7'a-$^{13}C_{10}$,$^{15}N_2$]cyclobrassinin (**78a**) (15.5 ± 4.7%), [1,2',3',3a',4',5',6',7',7'a-$^{13}C_9$,^{15}N]-4'-methoxyindole-3'-carboxaldehyde (**190a**) (16.2 ± 0.7%), [1,2',3',3a',4',5',6',7',7'a-$^{13}C_9$,$^{15}N_2$]-4'-methoxyindolyl-3'-formamide (**168a**) 12.2 ± 8.1%.

Table 2.16 Metabolites of *L*-[U-$^{13}C_{11}$,U-$^{15}N_2$]tryptophan (**66b**) in UV-irradiated rutabaga roots.

Metabolites isolated [a]	% Incorporation ± Std
[1,2',3',3a',4',5',6',7',7'a-$^{13}C_9$,$^{15}N_2$]rapalexin A (**103a**)	25.9 ± 1.4% [c]
[1,2',3',3a',4',5',6',7',7'a-$^{13}C_9$,$^{15}N_2$]isocyalexin A (**104a**)	17.0 ± 6.4%[c]
[2,3,3a,4,5,6,7,7a-$^{13}C_8$,^{15}N]isalexin (**102a**)	12.1 ± 1.1%[b]
[1,2,2',3',3a',4',5',6',7',7'a-$^{13}C_{10}$,$^{15}N_2$]]rutalexin (**116a**)	13.0 ± 0.3%[c]
[1,2,2',3',3a',4',5',6',7',7'a-$^{13}C_{10}$,$^{15}N_2$]spirobrassinin (**101a**)	11.2 ± 0.1%[b]
[1,2,2',3',3a',4',5',6',7',7'a-$^{13}C_{10}$,$^{15}N_2$]cyclobrassinin (**78a**)	15.5 ± 4.7%[b]
[1,2',3',3a',4',5',6',7',7'a-$^{13}C_9$,^{15}N]-4'-methoxyindole-3'-carboxaldehyde (**190a**)	16.2 ± 0.7%[b]
[1,2',3',3a',4',5',6',7',7'a-$^{13}C_9$,$^{15}N_2$]-4'-methoxyindolyl-3'-formamide (**168a**)	12.2 ± 8.1%[b]
[1,2,2',3',3a',4',5',6',7',7'a-$^{13}C_{10}$,$^{15}N_2$]glucobrassicin (**57a**)	31.3 ± 0.7%[c]
[1,2,2',3',3a',4',5',6',7',7'a-$^{13}C_{10}$,$^{15}N_2$]-1'-methoxyglucobrassicin (**69a**)	10.0 ± 2.0%[c]
[1,2,2',3',3a',4',5',6',7',7'a-$^{13}C_{10}$,$^{15}N_2$]-4'-methoxyglucobrassicin (**70a**)	10.3 ± 1.5%[c]
L-[U-$^{13}C_{11}$,U-$^{15}N_2$]tryptophan (**66b**)	74.0 ± 3.0%[b]

[a] ^{13}C and ^{15}N labeled compounds are referred to by a number followed by the letter a or b; [b] Positive ion mode. Incorporations calculated from HPLC-ESI-MS (peak intensities); % of $^{13}C^{15}N$ incorporation = $\{[M + 1 + n]^+/([M + 1]^+ + [M + 1 + n]^+)\} \times 100$ (n =9-12) ± Std (standard deviation), where n = number of ^{13}C & ^{15}N atoms.
[c] Negative ion mode. % of $^{13}C^{15}N$ incorporation = $\{[M-1 + n]^-/([M-1]^- + [M-1 + n]^-)\} \times 100$ (n = 9-12) ± Std (standard deviation), where n = number of ^{13}C & ^{15}N atoms.

The incorporation of *L*-[U-$^{13}C_{11}$,U-$^{15}N_2$]tryptophan (**66b**) into indole glucosinolates (glucobrassicin (**57**), 4'-methoxyglucobrassicin (**70**) and 1'-methoxyglucobrassicin (**69**)) was investigated as described in **Figure 2.15**. The HPLC-ESI-MS analyses of the polar extracts showed glucobrassicin (**57**) peak at t_R = 5.3 min containing two ions (negative mode): $[M]^-$ at *m/z* 447 and $[M + 12]^-$ at *m/z* 459 (resulting

from incorporation of *L*-[U-$^{13}C_{11}$,U-$^{15}N_2$]tryptophan (**66b**)) that was not detected in the control samples. Peak intensities of the natural abundance and those of labeled ions were used to determine the level of ^{13}C and ^{15}N incorporation. Using the equation shown in **Table 2.16,** the percentage of ^{13}C and ^{15}N incorporation was calculated to be 31.3 ± 0.7%. Similarly, the percentage of ^{13}C and ^{15}N incorporation into **70** and **69** was calculated to be 10.3 ± 1.5%, and 10.0 ± 2.0% respectively (**Table 2.16**; **Figure 2.21**).

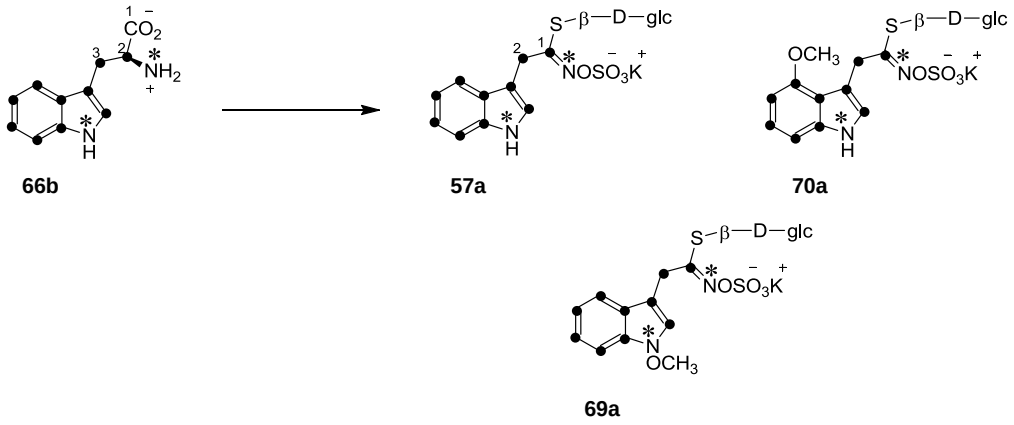

Figure 2.21 ^{13}C and ^{15}N labeled indole glucosinolates obtained from feeding of *L*-[U-$^{13}C_{11}$,U-$^{15}N_2$]tryptophan (**66b**) to UV-irradiated rutabaga root: [1,2,2',3',3a',4',5',6',7',7'a-$^{13}C_{10}$,$^{15}N_2$]glucobrassicin (**57a**) (31.3 ± 0.7), [1,2,2',3',3a',4',5',6',7',7'a-$^{13}C_{10}$,$^{15}N_2$]-4'-methoxyglucobrassicin (**70a**) (10.3 ± 1.5%), [1,2,2',3',3a',4',5',6',7',7'a-$^{13}C_{10}$,$^{15}N_2$]-1'-methoxyglucobrassicin (**69a**) (10.0 ± 2.0%).

The incorporation of *L*-[U-$^{13}C_{11}$,U-$^{15}N_2$]tryptophan (**66b**) into indole glucosinolates (**57, 70** and **69 Figure 2.21)** was viewed as intact incorporation of the side chain without any rearrangement. The side chain carbon atoms, C2 and C3 of the tryptophan (**66**) appeared to be C1 and C2 of the indole glucosinolates. In the case of phytoalexins from the brassinin (**45**) series (**101, 116** and **78**), there is exchange of positions of a carbon and nitrogen on the side chain, which was due to rearrangement of the aglycone (**138**) derived from hydrolysis of indole glucosinolates. Intermediate **138** is transformed to an unstable indolyl-3-methyisothiocyanate (**144**) which can give brassinin (**45**) in the presence of thiomethyl donor (Pedras, Okinyo et al., 2009; Pedras, Yaya et al.,

2011) (**Figure 2.20**). Rapalexin A (**103**) and isocyalexin A (**104**) incorporated a carbon and nitrogen atom of the side chain of tryptophan (**66**), which suggested the rearrangement of the side chain of **66** (**Figure 2.20**). To investigate biosynthetic pathways of metabolites **103**, **104** and **102** and plausible rearrangement sequences, potential biosynthetic intermediates were proposed as per the retro-biosynthetic analysis shown in **Scheme 2.7**.

2.2.2.5.4 Incorporation of [4',5',6',7'-$^{2}H_4$]desulfoglucobrassicin (80a)

Desulfoglucobrassicin (**80**) is the last biosynthetic precursor of glucobrassicin (**57**) (Piotrowski, Schemenewitz et al., 2004). A biosynthetic precursor of desulfoglucobrassicin (**80**), indolyl-3-thiohydroxamic acid (**79**), was proven to be common biosynthetic precursor to both indole glucosinolates and cruciferous phytoalexins (Pedras and Okinyo, 2008). Nevertheless, biosynthetic relationships of desulfoglucobrassicin (**80**) and indole glucosinolates with cruciferous phytoalexins such as rapalexin A (**103**) and isocyalexin A (**104**) have not been established. Therefore, the relationships were investigated using perdeuterated desulfoglucobrassicin (**80a**) and glucobrassicin (**57b**).

An aqueous solution of [4',5',6',7'-$^{2}H_4$]desulfoglucobrassicin (**80a**) (500 µL/hole, 5×10^{-4} M) was added to UV-irradiated slices of rutabaga and analyzed as described in **Figure 2.15**. The nonpolar fractions that contained the rapalexin A (**103**) peak at t_R = 22.3 min revealed two ions (negative mode): $[M - 1]^-$ at *m/z* 203 and $[M - 1 + 3]^-$ at *m/z* 206, not detected in the control samples. Using the equation shown in **Table 2.17**, the percentage of deuterium incorporation was determined to be 4.0 ± 1.7%. Likewise, the percentage of deuterium incorporations into isocyalexin A (**104**) and rutalexin (**116**) were calculated to be 3.0 ± 0.3% and 1.8 ± 0.3%, respectively. The HPLC-ESI-MS analysis of spirobrassinin (**101**) peak at t_R = 11.8 min showed two ions: $[M + 1]^+$ at *m/z* 251 and $[M + 1 + 4]^+$ at *m/z* 255, not detected in the control samples. Using the equation shown in **Table 2.17**, the percentage of deuterium incorporation was measured, 2.0 ± 0.6%. In a similar fashion, the percentage of deuterium incorporation into **78** and **110** were

calculated to be 2.4 ± 0.3% and 3.8 ± 0.8%, respectively. The 4'-methoxyindole-3'-carboxaldehyde (**190**) peak at t_R = 7.5 min (positive mode) indicated two ions as well: $[M + 1]^+$ at *m/z* 176 and $[M + 1 + 3]^+$ *m/z* 179 that was not detected in the control samples. The percentage of deuterium incorporation was calculated to be 2.8 ± 0.8%. Similarly, the percentage of deuterium incorporation into 4'-methoxyindolyl-3'-formamide (**168**) was measured, 2.3 ± 0.9% (**Table 2.17; Figure 2.22**).

Table 2.17 Metabolites of [4',5',6',7'-$^2H_4$]desulfoglucobrassicin (**80a**) in UV-irradiated rutabaga roots.

Metabolites isolated [a]	% Incorporation ± Std
[5',6',7'-$^2H_3$]rapalexin A (**103a**)	4.0 ± 1.7%[c]
[5',6',7'-$^2H_3$]isocyalexin A (**104a**)	3.0 ± 0.3%[c]
[4',5',6',7'-$^2H_4$]spirobrassinin (**101a**)	2.0 ± 0.6%[b]
[4',5',6',7'-$^2H_4$]rutalexin (**116a**)	1.8 ± 0.3%[c]
[4',5',6',7'-$^2H_4$]cyclobrassinin (**78a**)	2.4 ± 0.3%[b]
[5',6',7'-$^2H_3$]-4'-methoxycyclobrassinin (**110a**)	3.8 ± 0.8%[b]
[5',6',7'-$^2H_3$]isalexin (**102a**)	NI[d]
[5',6',7'-$^2H_3$]-4'-methoxyindolyl-3'-formamide (**168a**)	2.3 ± 0.9%[b]
[5',6',7'-$^2H_3$]-4'-methoxyindole-3'-carboxaldehyde (**190a**)	2.8 ± 0.8%[b]
[4',5',6',7'-$^2H_4$]glucobrassicin (**57a**)	10.1 ± 2.0%[c]
[5',6',7'-$^2H_3$]-4'-methoxyglucobrassicin (**70a**)	3.8 ± 2.0%[c]
[4',5',6',7'-$^2H_4$]-1'-methoxyglucobrassicin (**69a**)	2.8 ± 0.5%[c]

[a] Deuterated compounds are referred to by a number followed by the letter a;
[b]Positive ion mode. Incorporations calculated from HPLC-ESI-MS (normalized peak intensities); % of ^2H incorporation = $\{[M + 1 + n]^+/([M + 1]^+ + [M + 1 + n]^+)\} \times 100$ (n = 3 or 4) ± Std (standard deviation), where n = number of deuterium atoms.
[c]Negative ion mode. % of ^2H incorporation = $\{[M-1 + n]^-/([M-1]^- + [M-1 + n]^-)\} \times 100$ (n = 3 or 4) ± Std (standard deviation), where n = number of deuterium atoms.
[d] NI=no incorporation implies ≤0.1% deuterium.

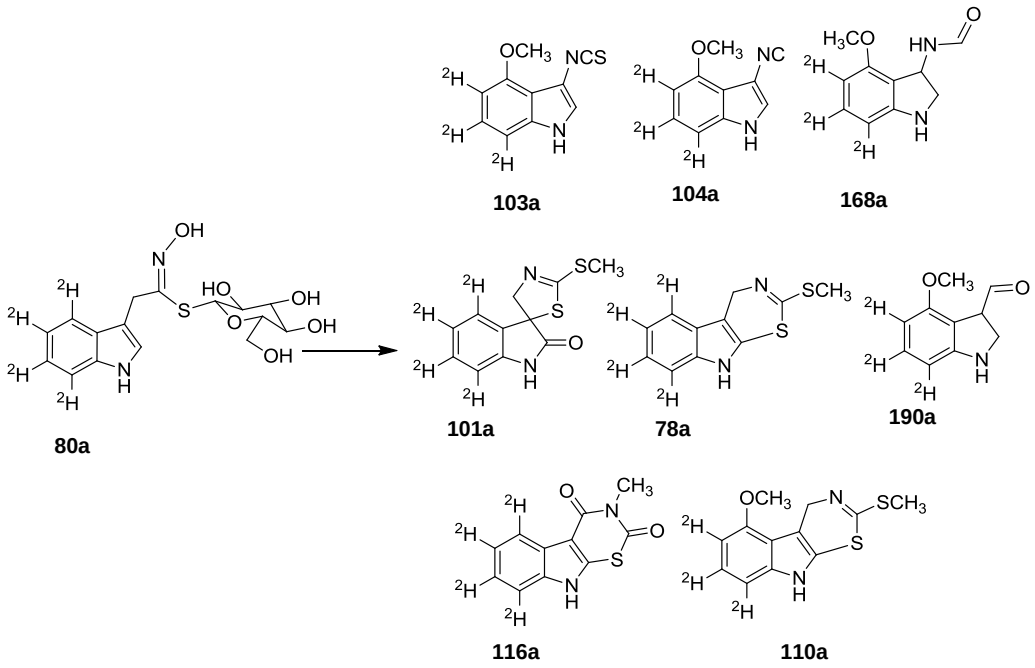

Figure 2.22 Deuterated metabolites obtained from feeding of [4',5',6',7'-$^2H_4$]desulfoglucobrassicin (**80a**) to UV-irradiated rutabaga root: [5',6',7'-$^2H_3$]rapalexin A (**103a**) (4.0 ± 1.7%), [5',6',7'-$^2H_3$]isocyalexin A (**104a**) (3.0 ± 0.3%), [4',5',6',7'-$^2H_4$]rutalexin (**116a**) (1.8 ± 0.3%), [4',5',6',7'-$^2H_4$]spirobrassinin (**101a**) (2.0 ± 0.6%), [4',5',6',7'-$^2H_4$]cyclobrassinin (**78a**) (2.4 ± 0.3%), [5',6',7'-$^2H_3$]-4'-methoxyindole-3'-carboxaldehyde (**190a**) (2.8 ± 0.8%), [5',6',7'-$^2H_3$]-4'-methoxyindolyl-3'-formamide (**168a**) (2.3 ± 0.9%), [5',6',7'-$^2H_3$]-4'-methoxycyclobrassinin (**110a**) (3.8 ± 0.8%).

Similarly, the HPLC-ESI-MS analyses of the polar extracts showed the glucobrassicin (**57**) peak at t_R = 5.3 min containing two ions (negative mode): $[M]^-$ at *m/z* 447 and $[M + 4]^-$ *m/z* 451, the latter of which was not detected in the control samples. Peak intensities of the natural abundance and those of deuterated ions were used to determine the level of incorporation. Thus, the percentage of deuterium incorporation into glucobrassicin (**57**) was calculated, 10.1 ± 2.0%. Likewise, using the equation shown in **Table 2.17**, the percentage of deuterium incorporation into **70** and **69** was calculated to be 3.8 ± 2.0% and 2.8 ± 0.5% respectively (**Table 2.17; Figure 2.23**).

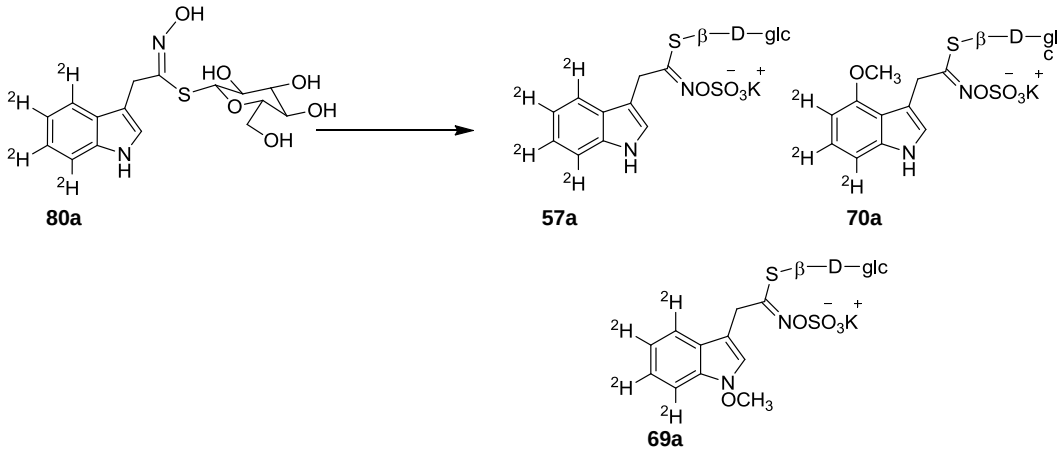

Figure 2.23 Deuterated indole glucosinolates obtained from feeding of [4',5',6',7'-$^2H_4$]desulfoglucobrassicin (**80a**) to UV-irradiated rutabaga root: [4',5',6',7'-$^2H_4$]glucobrassicin (**57a**) (10.1 ± 2.0%), [5',6',7'-$^2H_3$]-4′-methoxyglucobrassicin (**70a**) (3.8 ± 2.0%), [4',5',6',7'-$^2H_4$]-1'-methoxyglucobrassicin (**69a**) (2.8 ± 0.5%).

2.2.2.5.5 Incorporation of [2,2,4',5',6',7'-$^2H_6$]glucobrassicin (57b)

The biosynthetic relationship between indole glucosinolates and cruciferous phytoalexins such as rapalexin A (**103**) and isocyalexin A (**104**) was investigated using perdeuterated glucobrassicin (**57b**). An aqueous solution of [2,2,4',5',6',7'-$^2H_6$]glucobrassicin (**57b**) (500 µL/hole, 5×10^{-4} M) was added to UV-irradiated slices of rutabaga and analyzed as described in **Figure 2.15**. The HPLC-ESI-MS analyses of the nonpolar fractions revealed the rapalexin A (**103**) peak at t_R = 22.3 min containing two ions: $[M - 1]^-$ at *m/z* 203 and $[M - 1 + 3]^-$ at *m/z* 206, not detected in the control samples. Peak intensities of the natural abundance and those of deuterated ions were used to determine the level of incorporation. Using the equation shown in **Table 2.18**, the percentage of deuterium incorporation was calculated to be 3.9 ± 1.1%. Similarly, the percentages of deuterium incorporation into isocyalexin A (**104**) and isalexin (**102,** positive mode) were determined to be 2.4 ± 0.8% and 3.2 ± 1.1%, respectively. The percentage of deuterium incorporation into **168** was also established in a similar fashion, 1.3 ± 0.6% **Table 2.18**. The spirobrassinin (**101**) peak at t_R = 11.8 min (positive mode)

indicated two ions: $[M + 1]^+$ at *m/z* 251 and $[M + 1 + 6]^+$ at *m/z* 257. As indicated in **Table 2.18**, the percentage of deuterium incorporation was calculated, 2.6 ± 0.6%. Similarly, the percentages of deuterium incorporations into **78** and **110** were calculated to be 1.9 ± 0.7% and 3.0 ± 1.2%, respectively (**Table 2.18; Figure 2.24**).

Table 2.18 Metabolites of [2,2,4',5',6',7'-$^2H_6$]glucobrassicin (**57b**) in UV-irradiated rutabaga roots.

Metabolites isolated [a]	% Incorporation ± Std
[5',6',7'-$^2H_3$]rapalexin A (**103a**)	3.9 ± 1.1%[c]
[5',6',7'-$^2H_3$]isocyalexin A (**104a**)	2.4 ± 0.8%[c]
[5,6,7-$^2H_3$]isalexin (**102a**)	3.2 ± 1.1%[b]
[5',6',7'-$^2H_3$]-4'-methoxyindolyl-3'-formamide (**168a**)	1.3 ± 0.6%[b]
[2,2,4',5',6',7'-$^2H_6$]spirobrassinin (**101a**)	2.6 ± 0.6%[b]
[2,2,4',5',6',7'-$^2H_6$]cyclobrassinin (**78a**)	1.9 ± 0.7%[b]
[2,2,5',6',7'-$^2H_5$]-4'-methoxycyclobrassinin (**110a**)	3.0 ± 1.2%[b]
[2,2,4',5',6',7'-$^2H_6$]glucobrassicin (**57a**)	18.8 ± 5.1%[c]
[2,2,5',6',7'-$^2H_5$]-4'-methoxyglucobrassicin (**70a**)	5.0 ± 0.4%[c]
[2,2,4',5',6',7'-$^2H_6$]-1'-methoxyglucobrassicin (**69a**)	1.1 ± 0.2%[c]

[a] Deuterated compounds are referred to by a number followed by the letter a and b;
[b] Negative ion mode. % of ^2H incorporation = $\{[M-1 + n]^-/([M-1]^- + [M-1 + n]^-)\} \times 100$ (n = 3-6) ± Std (standard deviation), where n = number of deuterium atoms.
[c] Positive ion mode. Incorporations calculated from HPLC-ESI-MS (normalized peak intensities); % of ^2H incorporation = $\{[M + 1 + n]^+/([M + 1]^+ + [M + 1 + n]^+)\} \times 100$ (n = 3-6) ± Std (standard deviation), where n = number of deuterium atoms.

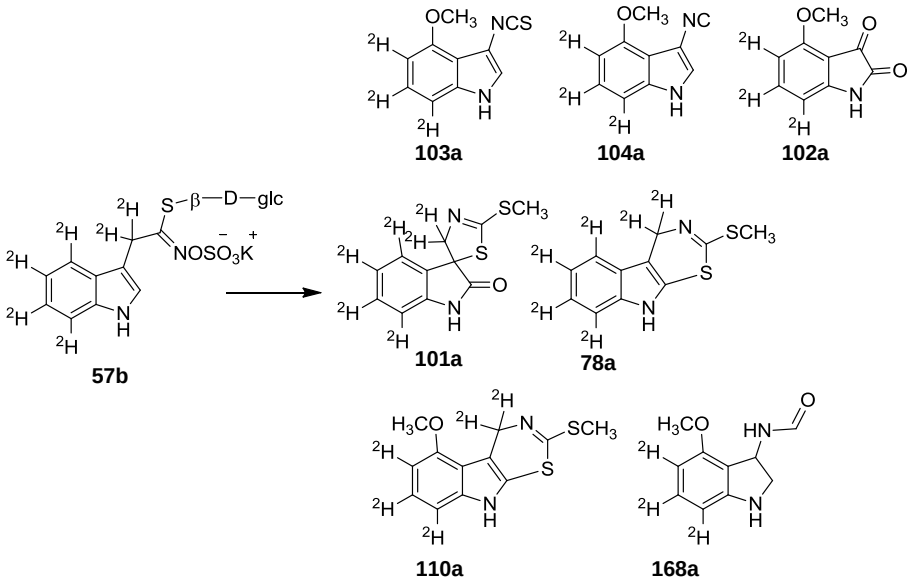

Figure 2.24 Deuterated phytoalexins obtained from feeding of [2,2,4',5',6',7'-$^2H_6$]glucobrassicin (**57a**) to UV-irradiated rutabaga root: [5',6',7'-$^2H_3$]rapalexin A (**103a**) (3.9 ± 1.1%), [5',6',7'-$^2H_3$]isocyalexin A (**104a**) (2.4 ± 0.8%), [2,2,4',5',6',7'-$^2H_6$]spirobrassinin (**101a**) (2.6 ± 0.6%), [2,2,4',5',6',7'-$^2H_6$]cyclobrassinin (**78a**) (1.9 ± 0.7%), [5',6',7'-$^2H_3$]-4'-methoxyindolyl-3'-formamide (**168a**) (1.3 ± 0.6%), [2,2,5',6',7'-$^2H_5$]-4'-methoxycyclobrassinin (**110a**) (3.0 ± 1.2%), [5,6,7-$^2H_3$]isalexin (**102a**) (3.2 ± 1.1%).

Similarly, the HPLC-ESI-MS analyses of the polar extracts showed 4'-methoxy glucobrassicin (**70**) peak at t_R = 6.9 min containing two ions in (negative mode): $[M]^-$ at *m/z* 477 and $[M + 5]^-$ at *m/z* 482, the latter of which was not detected in the control sample. Based on peak intensities, the percentage of deuterium incorporation into **70** was calculated to be 5.0 ± 0.4%. Similarly, the percentage of deuterium incorporation into **69** was determined using the equation shown in **Table 2.18** to be 1.1 ± 0.2% (**Table 2.18**; **Figure 2.25**).

The incorporation of glucobrassicin (**57**) into phytoalexins and indole glucosinolates is consistent with previous results obtained in *T. salsuginea* (Pedras, Yaya et al., 2010). Incorporation into non-methoxylated phytoalexins was proposed to be via brassinin (**45**) while incorporation into 4-methoxylated phytoalexins was via 4'-methoxyglucobrassicin (**70**) (Pedras and Yaya, 2013).

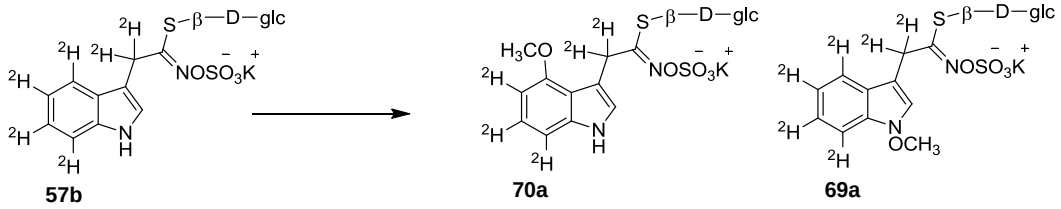

Figure 2.25 Deuterated indole glucosinolates obtained from feeding of [2,2,4',5',6',7'-$^2H_6$]glucobrassicin (**57b**) to UV-irradiated rutabaga root: [2,2,5',6',7'-$^2H_5$]-4'-methoxyglucobrassicin (**70a**) (5.0 ± 0.4%) and [2,2,4',5',6',7'-$^2H_6$]-1'-methoxyglucobrassicin (**69a**) (1.1 ± 0.2%).

2.2.2.5.6 Incorporation of [$^2H_3$CO]-4'-methoxybrassinin (108a)

The biosynthetic relationship between indole glucosinolates and cruciferous phytoalexins investigated in *T. salsuginea* suggested that *T. salsuginea* phytoalexins (wasalexins A (**43**) and B (**109**) and biswasalexins A1 (**131**) and A2 (**132**)) are biosynthesized via 1'-methoxyglucobrassicin (Pedras, Yaya et al., 2010). Based on that finding, investigations of the biosynthetic pathways of 4-methoxyphytoalexins were conducted using 4-methoxylated biosynthetic precursors. First, an aqueous solution of [$^2H_3$CO]-4'-methoxybrassinin (**108a**) (500 µL/hole, 5×10^{-4} M) was added to UV-irradiated slices of rutabaga and analyzed as described in **Figure 2.15**. HPLC-ESI-MS analyses of the nonpolar fractions that contained phytoalexins revealed the 4'-methoxycyclobrassinin (**110**) peak at t_R = 23.4 min (positive mode) containing two ions: $[M + 1]^+$ at *m/z* 265 and $[M + 1 + 3]^+$ at *m/z* 268, not detected in the control samples. Using the equation shown in **Table 2.19,** the percentage of deuterium incorporation was calculated to be 77.0 ± 4.2%. Similarly, the percentage of deuterium incorporation into 4'-methoxydehydrocyclobrassicin (**113**) was calculated to be 72.0 ± 3.5% (**Table 2.19; Figure 2.26**).

Table 2.19 Metabolites of [^2H_3CO]-4'-methoxybrassinin (**108a**) in UV-irradiated rutabaga roots

Metabolites isolated [a]	% Incorporation ± Std
[^2H_3CO]rapalexin A (**103a**)	NI[d]
[^2H_3CO]isocyalexin A (**104a**)	NI[d]
[^2H_3CO]-4'-methoxyindole-3'-formamide (**168a**)	NI[d]
[^nH_n]spirobrassinin (**101a**)	NI[d]
[^nH_n]rutalexin (**116a**)	NI[d]
[^nH_n]cyclobrassinin (**78a**)	NI[d]
[^2H_3CO]-4'-methoxycyclobrassinin (**110a**)	77.0 ± 4.2%[c]
[^2H_3CO]-4'-methoxydehydrocyclobrassinin (**113a**)	72.0 ± 3.5%[c]
[^2H_3CO]-4'-methoxyindole-3'-carboxaldehyde (**190a**)	NI[d]
[^nH_n]glucobrassicin (**57a**)	NI[d]
[^nH_n]-4'-methoxyglucobrassicin (**70a**)	NI[d]
[^nH_n]-1'-methoxyglucobrassicin (**69a**)	NI[d]

[a] Deuterated compounds are referred to by a number followed by the letter **a**.
[b] Negative ion mode. % of ^2H incorporation = $\{[M-1+n]^-/([M-1]^- + [M-1+n]^-)\} \times 100$ ($n = 3$) ± Std (standard deviation), where n = number of deuterium atoms.
[c] Positive ion mode. Incorporations calculated from HPLC-ESI-MS (normalized peak intensities); % of ^2H incorporation = $\{[M+1+n]^+/([M+1]^+ + [M+1+n]^+)\} \times 100$ ($n = 3$) ± Std (standard deviation), where n = number of deuterium atoms.
[d] NI=no incorporation implies ≤0.1% deuterium

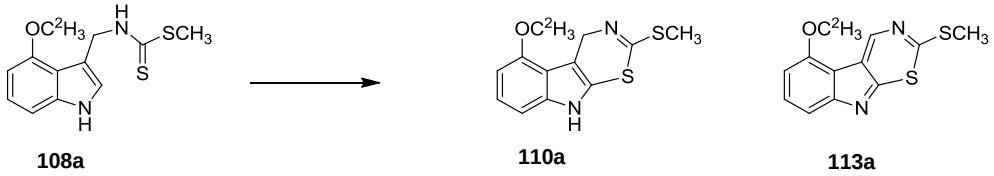

Figure 2.26 Deuterated phytoalexins obtained from feeding of [^2H_3CO]-4'-methoxybrassinin (**108a**) to UV-irradiated rutabaga root: [^2H_3CO]-4'-methoxycyclobrassinin (**110a**) (77.0 ± 4.2%), [^2H_3CO]-4'-methoxydehydrocyclobrassinin (**113a**) (72.0 ± 3.5%).

The HPLC-ESI-MS analysis of the fractions containing 4-methoxy phytoalexins such as rapalexin A (**103**) and isocyalexin A (**104**) did not show incorporation of 4'-methoxybrassinin. Similarly, analysis of polar extracts showed lack of incorporation of 4'-methoxybrassinin (**108**) into indole glucosinolates **57**, **70** and **69** as proposed (**Table 2.19**). High level incorporation into **110** and **113** suggests 4'-methoxybrassinin (**108**) is a close precursor of the metabolites. Lack of incorporation into **103** and **104** suggests biosynthesis of these metabolites may follow a different route downstream of 4'-methoxyglucobrassicin (**70**).

2.2.2.5.7 Incorporation of (*R*,*S*)-[$^2H_3$CO,5',6',7'-$^2H_3$]-4'-methoxyindolyl-3'-glycine (**107b**)

An aqueous solution of (*R*,*S*)-[$^2H_3$CO,5',6',7'-$^2H_3$]-4'-methoxyindolyl-3'-glycine (**107b**) (500 µL/hole, 5×10^{-4} M) was added to UV-irradiated slices of rutabaga and analyzed as described above (**Figure 2.15**). The HPLC-ESI-MS analyses of the nonpolar fractions showed the rapalexin A (**103**) peak at t_R = 22.3 min containing two ions: [M - 1]$^-$ at *m/z* 203 and [M - 1 + 6]$^-$ at *m/z* 209 (resulting from incorporation of (*R*,*S*)-[$^2H_3$CO,5',6',7'-$^2H_3$]-4'-methoxyindolyl-3'-glycine (**107b**)) that was not detected in the control samples. Peak intensities of the natural abundance and those of deuterated ions were used to determine the level of deuterium incorporation. Using the equation shown in **Table 2.20**, the percentage of deuterium incorporation was determined to be 4.2 ± 0.7%. In similar fashion, the percentage of deuterium incorporation into isocyalexin A (**104)** and isalexin (**102,** positive mode) were calculated to be 12.8 ± 3.4% and 5.0 ± 2.6%, respectively. Similarly, the percentage of deuterium incorporation into 4'-methoxyindole-3'-carboxaldehyde (**190a**) was calculated to be 66.0 ± 2.0%. Similar results were obtained from feeding of tri-deuterated amino acid **(***R*,*S*)-[$^2H_3$CO]-4'-methoxyindolyl-3'-glycine (**107a**) (**Table 2.21)**. No deuterium incorporation was detected into indole glucosinolates **57**, **70** and **69** (**Table 2.20** and **2.21; Figure 2.27)**.

Table 2.20 Metabolites of (*R*,*S*)-[$^2H_3$CO,5',6',7'-$^2H_3$]-4'-methoxyindolyl-3'-glycine (**107b**) in UV-irradiated rutabaga roots.

Metabolites detected (**#a**)[a]	% Incorporation ± Std
[$^2H_3$CO,5',6',7'-$^2H_3$]rapalexin A (**103a**)	4.2 ± 0.7%[b]
[$^2H_3$CO,5',6',7'-$^2H_3$]isocyalexin A (**104a**)	12.8 ± 3.4%[b]
[$^2H_3$CO,5,6,7-$^2H_3$]isalexin (**102a**)	5.0 ± 2.6%[c]
[^2H_n]cyclobrassinin (**78a**)	NI[d]
[^2H_n]spirobrassinin (**101a**)	NI[d]
[^2H_n]rutalexin (**116a**)	NI[d]
[$^2H_3$CO,5',6',7'-$^2H_3$]-4'-methoxyindolyl-3'-glycine (**107b**)	100[c]
[$^2H_3$CO,5',6',7'-$^2H_3$]-4'-methoxyindole-3'-carboxaldehyde oxime (**171a**)	ND[d]
[$^2H_3$CO,5',6',7'-$^2H_3$]-4'-methoxyindole-3'-carbonitrile **(205a**)	ND[d]
[$^2H_3$CO,5',6',7'-$^2H_3$]-4'-methoxyindole-3'-carboxaldehyde (**190a**)	66.0 ± 2.0%[c]
[$^2H_3$CO,5',6',7'-$^2H_3$]desulfoglucorapassicin (**172a**)	ND[d]
[^2H_n]glucobrassicin (**57a**)	NI[d]
[^2H_n]-4'-methoxyglucobrassicin (**70a**)	NI[d]
[^2H_n]-1'-methoxyglucobrassicin (**69a**)	NI[d]

[a] Deuterated compounds are referred to by a number followed by the letter a or b.
[b] Negative ion mode. Incorporations calculated from HPLC-ESI-MS (normalized peak intensities); % of ^2H incorporation = $\{[M-1+n]^-/([M-1]^- + [M-1+n]^-)\} \times 100$ (n = 6) ± Std (standard deviation), where n = number of deuterium atoms.
[c] Positive ion mode. Incorporations calculated from HPLC-ESI-MS (normalized peak intensities); % of ^2H incorporation = $\{[M+1+n]^+/([M+1]^+ + [M+1+n]^+)\} \times 100$ (n = 6) ± Std (standard deviation), where n = number of deuterium atoms.
[d] NI=no incorporation implies ≤0.1% deuterium; ND=not detected.

Table 2.21 Metabolites of (*R*,*S*)-[^2H_3CO]-4'-methoxyindolyl-3'-glycine (**107a**) in UV–irradiated rutabaga roots.

Metabolites detected (**#a**)[a]	% Incorporation ± Std
[^2H_3CO]rapalexin A (**103a**)	6.1 ± 2.4[b]
[^2H_3CO]isocyalexin A (**104a**)	2.3 ± 0.7[b]
[^2H_3CO]isalexin (**102a**)	17.3 ± 8.3[c]
[^2H_3CO]-4'-methoxyindolyl-3'-glycine (**107b**)	100[c]
[^2H_3CO]-4'-methoxyindole-3'-carboxaldehyde (**190a**)	83.7 ± 5.0[c]

[a] Deuterated compounds are referred to by a number followed by the letter a.
[b] Negative ion mode. Incorporations calculated from HPLC-ESI-MS (normalized peak intensities); % of ^2H incorporation = $\{[M-1+n]^-/([M-1]^- + [M-1+n]^-)\} \times 100$ (n = 3) ± Std (standard deviation), where n = number of deuterium atoms.
[c] Positive ion mode. Incorporations calculated from HPLC-ESI-MS (normalized peak intensities); % of ^2H incorporation = $\{[M+1+n]^+/([M+1]^+ + [M+1+n]^+)\} \times 100$ (n = 3) ± Std (standard deviation), where n = number of deuterium atoms.
[d] NI=no incorporation implies ≤0.1% deuterium; ND=not detected.

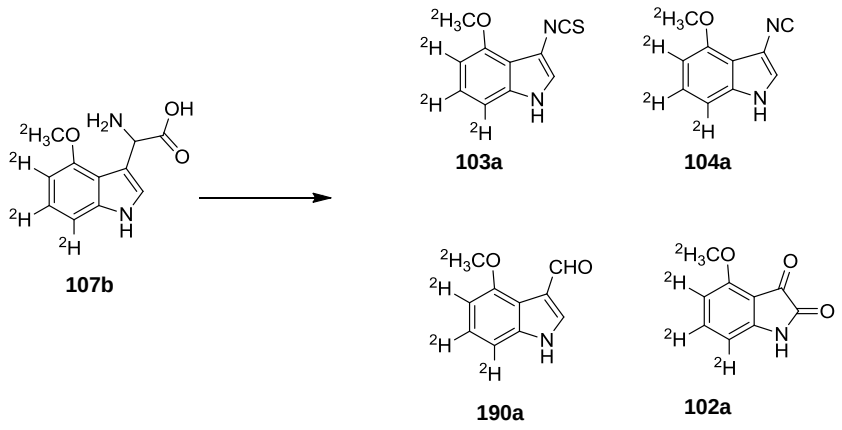

Figure 2.27 Deuterated phytoalexins obtained from feeding of (*R*,*S*)-[^2H_3CO,5',6',7'-$^2H_3$]-4'-methoxyindolyl-3'-glycine (**107b**) to UV-irradiated rutabaga root: [^2H_3CO,5',6',7'-$^2H_3$]rapalexin A (**103a**) (4.2 ± 0.7%), [^2H_3CO,5',6',7'-$^2H_3$]isocyalexin A (**104a**) (12.8 ± 3.4%), [^2H_3CO,5,6,7-$^2H_3$]isalexin (**102a**) (5.0 ± 2.6%), [^2H_3CO,5',6',7'-$^2H_3$]-4'-methoxyindole-3'-carboxaldehyde (**190a**) (66.0 ± 2.0%).

The incorporation 4'-methoxyindolyl-3'-glycine (**107**) into 4-methoxy phytoalexins **104**, **103** and **102** suggested that **107** is likely a biosynthetic intermediate between 4'-methoxyglucobrassicin (**70**) and the phytoalexins **104**, **103** and **102**. 4'-Methoxyindolyl-3'-glycine **(107)** is likely derived from 4'-methoxyglucobrassicin (**70**) via a Neber type rearrangement via azirine intermediate similar to the base-catalyzed chemical hydrolysis of benzylglucosinolate to phenyl glycine (Pedras and Yaya, 2013). The next proposed intermediate was **171** (**Scheme 2.7**), which can be obtained from **107** via *N*-oxidative decarboxylation of **107**. This transformation was proposed to be similar to the transformation of tryptophan (**66**) to indolyl-3'-acetaldoxime (**122**).

2.2.2.5.8 [$^2H_3$CO,5',6',7'-$^2H_3$]-4'-methoxyindolyl-3'-carboxaldehyde oxime (171b)

An aqueous solution of [$^2H_3$CO,5',6',7'-$^2H_3$]-4'-methoxyindolyl-3'-carboxaldehyde oxime (**171b**) (500 µL/hole, 5×10^{-4} M) was added to UV-irradiated slices of rutabaga and analyzed as described above (**Figure 2.15**). The HPLC-ESI-MS analyses of the nonpolar fractions that contained phytoalexins showed the rapalexin A (**103**) peak at t_R = 22.3 min containing two ions: $[M - 1]^-$ at *m/z* 203 and $[M - 1 + 6]^-$ at *m/z* 209, the latter of which was not detected in the control samples. Peak intensities of the natural abundance and those of deuterated ions were used to determine the level of deuterium incorporation. Accordingly, the percentage of deuterium incorporation was calculated to be 3.4 ± 2.5%. Similarly, using the equation in **Table 2.22**, the percentage of deuterium incorporation into isocyalexin A (**104**) and isalexin (**102**) were determined to be 9.0 ± 6.0% and 2.5 ± 0.6%, respectively. Likewise, the percentage of deuterium incorporation into 4'-methoxyindole-3'-carboxaldehyde (**190a**) was calculated to be 52.0 ± 1.0% (**Tables 2.22)**. The HPLC-ESI-MS analyses of the nonpolar fractions also showed [$^2H_3$CO,5',6',7'-$^2H_3$]-4'-methoxyindole-3'-carbonitrile **(205a**) peak at t_R = 9.7 min containing two ions: $[M - 1]^+$ at *m/z* 171 and $[M - 1 + 6]^-$ at *m/z* 177. The percentage of deuterium incorporation was calculated to be 69.0 ± 2.7%. Identical results were obtained from feeding of [$^2H_3$CO]-4'-methoxyindolyl-3'-carboxaldehyde oxime (**171a**) (**Table 2.23)**. No deuterium

incorporations were detected into indole glucosinolates **57**, **70** and **69** (**Tables 2.22** and **2.23; Figure 2.28)**.

Table 2.22 Metabolites of [$^2H_3$CO,5',6',7'-$^2H_3$]-4'-methoxyindolyl-3'-carboxaldehyde oxime (**171b**) in UV-irradiated rutabaga roots.

Metabolites detected (**#a**)[a]	% Incorporation ± Std
[$^2H_3$CO,5',6',7'-$^2H_3$]rapalexin A (**103a**)	3.4 ± 2.5%[b]
[$^2H_3$CO,5',6',7'-$^2H_3$]isocyalexin A (**104a**)	9.0 ± 6.0%[b]
[$^2H_3$CO,5,6,7-$^2H_3$]isalexin (**102a**)	2.5 ± 0.6%[c]
[^2H_n]cyclobrassinin (**78a**)	NI[d]
[^2H_n]spirobrassinin (**101a**)	NI[d]
[^2H_n]rutalexin (**116a**)	NI[d]
[$^2H_3$CO,5',6',7'-$^2H_3$]-4'-methoxyindole-3'-carboxaldehyde oxime (**171b**)	100
[$^2H_3$CO,5',6',7'-$^2H_3$]-4'-methoxyindole-3'-carbonitrile **(205a**)	69.0 ± 2.7%[b]
[$^2H_3$CO,5',6',7'-$^2H_3$]-4'-methoxyindole-3'-carboxaldehyde (**190a**)	52.0 ± 1.0% [c]
[$^2H_3$CO,5',6',7'-$^2H_3$]desulfoglucorapassicin (**172a**)	ND[d]
[^2H_n]glucobrassicin (**57a**)	NI[d]
[^2H_n]-4'-methoxyglucobrassicin (**70a**)	NI[d]
[^2H_n]-1'-methoxyglucobrassicin (**69a**)	NI[d]

[a] Deuterated compounds are referred to by a number followed by the letter a or b.
[b] Negative ion mode. Incorporations calculated from HPLC-ESI-MS (normalized peak intensities); % of ^2H incorporation = $\{[M-1+n]^-/([M-1]^- + [M-1+n]^-)\} \times 100$ (n = 6) ± Std (standard deviation), where n = number of deuterium atoms.
[c] Positive ion mode. Incorporations calculated from HPLC-ESI-MS (normalized peak intensities); % of ^2H incorporation = $\{[M+1+n]^+/([M+1]^+ + [M+1+n]^+)\} \times 100$ (n = 6) ± Std (standard deviation), where n = number of deuterium atoms.
[d] NI=no incorporation implies ≤0.1% deuterium; ND=not detected.

Table 2.23 Metabolites of [^2H_3CO]-4'-methoxyindolyl-3'-carboxaldehyde oxime (**171a**) in UV-irradiated rutabaga roots.

Metabolites detected (**#a**)[a]	% Incorporation ± Std
[^2H_3CO]rapalexin A (**103a**)	5.8 ± 2.7[b]
[^2H_3CO]isocyalexin A (**104a**)	3.0 ± 0.2[b]
[^2H_3CO]isalexin (**102a**)	3.1 ± 1.0[c]
[^2H_3CO]-4'-methoxyindole-3'-carboxaldehyde oxime (**171a**)	100
[^2H_3CO]-4'-methoxyindole-3'-carbonitrile **(205a**)	69.0 ± 2.7[b]
[^2H_3CO]-4'-methoxyindole-3'-carboxaldehyde (**190a**)	73.3 ± 2.5 [c]

[a] Deuterated compounds are referred to by a number followed by the letter a.
[b] Negative ion mode. Incorporations calculated from HPLC-ESI-MS (normalized peak intensities); % of ^2H incorporation = $\{[M-1+n]^-/([M-1]^- + [M-1+n]^-)\} \times 100$ (n = 3) ± Std (standard deviation), where n = number of deuterium atoms.
[c] Positive ion mode. Incorporations calculated from HPLC-ESI-MS (normalized peak intensities); % of ^2H incorporation = $\{[M+1+n]^+/([M+1]^+ + [M+1+n]^+)\} \times 100$ (n = 3) ± Std (standard deviation), where n = number of deuterium atoms.
[d] NI=no incorporation implies ≤0.1% deuterium; ND=not detected.

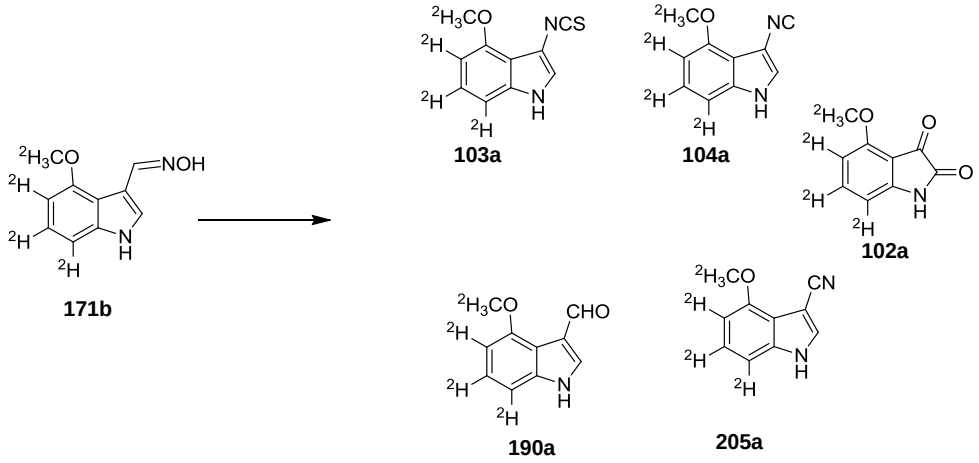

Figure 2.28 Deuterated phytoalexins obtained from feeding of [^2H_3CO,5',6',7'-$^2H_3$]-4'-methoxyindolyl-3'-carboxaldehyde oxime (**171b**) to UV-irradiated rutabaga root: [^2H_3CO,5',6',7'-$^2H_3$]rapalexin A (**103a**) (3.4 ± 2.5%), [^2H_3CO,5',6',7'-$^2H_3$]isocyalexin A (**104a**) (9.0 ± 6.0%), [^2H_3CO,5,6,7-$^2H_3$]isalexin (**102a**) (2.5 ± 0.6%), [^2H_3CO,5',6',7'-$^2H_3$]-4'-methoxyindole-3'-carboxaldehyde (**190a**) (52.0 ± 1.0%), [^2H_3CO,5',6',7'-$^2H_3$]-4'-methoxyindole-3'-carbonitrile **(205a**) (69.0 ± 2.7%).

4'-Methoxyindolyl-3'-carboxaldehyde oxime (**171**) was proposed to be biosynthesized from 4'-methoxyindolyl-3'-glycine (**107**) via oxidative decarboxylation (**Scheme 2.7**) similar to the biosynthesis of indolyl-3'-acetaldoxime (**122**) from tryptophan (**66**). Incorporation of **171** into **102**, **103** and **104** is in agreement with the proposed pathway (**Scheme 2.7**). Transformation of **171** to rapalexin A (**103**) isocyalexin A (**104**) and isalexin (**102**) is likely through the glucosinolate **118** intermediate that can give rapalexin A (**103**) via hydrolysis, followed by Lossen type rearrangement (Pedras and Yaya, 2013). Isocyalexin A (**104**) is likely formed through desulfurization of rapalexin A (**103**) (Pedras and Yaya, 2013). Another possibility is likely via sulfation of compound **171** followed by Beckmann type rearrangement. Isalexin (**102**) is possibly derived from rapalexin A (**103**) through oxidation reaction.

2.2.2.5.9 Incorporation of [$^2H_3$CO,5',6',7'-$^2H_3$]desulfoglucorapassicin (172b)

An aqueous solution of [$^2H_3$CO,5',6',7'-$^2H_3$]desulfoglucorapassicin (**172b**) (500 µL/hole, 5×10^{-4} M) was added to UV-irradiated slices of rutabaga and analyzed as described above (**Figure 2.15**). The HPLC-ESI-MS analyses of the nonpolar fractions that contained phytoalexins showed the rapalexin A (**103**) peak at t_R = 22.3 min containing two ions: $[M - 1]^-$ at *m/z* 203 and $[M - 1 + 6]^-$ at *m/z* 209 (resulting from incorporation of [$^2H_3$CO,5',6',7'-$^2H_3$]desulfoglucorapassicin (**172b**)) that was not detected in the control samples. Peak intensities of the natural abundance and those of deuterated ions were used to determine the level of deuterium incorporation as described above. Accordingly, the percentage of deuterium incorporation was calculated to be 6.2 ± 4.2%. Similarly, the percentages of deuterium incorporation into isalexin (**102**) and 4'-methoxyindole-3'-carbonitrile **(205**) were calculated to be 7.1 ± 2.9% and 93.0 ± 1.0% respectively. Identical results were obtained from feeding of [$^2H_3$CO]desulfoglucorapassicin (**172a**) (**Table 2.25**). No deuterium incorporation was detected into indole glucosinolates **57**, **70** and **69** (**Tables 2.24** and **2.25; Figure 2.29**).

Table 2.24 Metabolites of [$^2H_3$CO,5',6',7'-$^2H_3$]desulfoglucorapassicin (**172b**) in UV-irradiated rutabaga roots.

Metabolites detected (**#a**)[a]	% Incorporation ± Std
[$^2H_3$CO,5',6',7'-$^2H_3$]rapalexin A (**103a**)	6.2 ± 4.2%[b]
[$^2H_3$CO,5',6',7'-$^2H_3$]isocyalexin A (**104a**)	NI[d]
[$^2H_3$CO,5,6,7-$^2H_3$]isalexin (**102a**)	7.1 ± 2.9%[c]
[^2H_n]cyclobrassinin (**78a**)	NI[d]
[^2H_n]spirobrassinin (**101a**)	NI[d]
[^2H_n]rutalexin (**116a**)	NI[d]
[$^2H_3$CO,5',6',7'-$^2H_3$]-4'-methoxyindolyl-3'-glycine (**107a**)	ND[d]
[$^2H_3$CO,5',6',7'-$^2H_3$]-4'-methoxyindole-3'-carboxaldehyde oxime (**171a**)	ND[d]
[$^2H_3$CO,5',6',7'-$^2H_3$]-4'-methoxyindole-3'-carbonitrile **(205a**)	93.0 ± 1.0%[b]
[$^2H_3$CO,5',6',7'-$^2H_3$]-4'-methoxyindole-3'-carboxaldehyde (**190a**)	ND[d]
[$^2H_3$CO,5',6',7'-$^2H_3$]desulfoglucorapassicin (**172b**)	100
[^2H_n]glucobrassicin (**57a**)	NI[d]
[^2H_n]-4'-methoxyglucobrassicin (**70a**)	NI[d]
[^2H_n]-1'-methoxyglucobrassicin (**69a**)	NI[d]

[a] Deuterated compounds are referred to by a number followed by the letter a or b.
[b] Negative ion mode. Incorporations calculated from HPLC-ESI-MS (normalized peak intensities); % of ^2H incorporation = $\{[M-1+n]^-/([M-1]^- + [M-1+n]^-)\} \times 100$ (n = 6) ± Std (standard deviation), where n = number of deuterium atoms.
[c] Positive ion mode. Incorporations calculated from HPLC-ESI-MS (normalized peak intensities); % of ^2H incorporation = $\{[M+1+n]^+/([M+1]^+ + [M+1+n]^+)\} \times 100$ (n = 6) ± Std (standard deviation), where n = number of deuterium atoms.
[d] NI=no incorporation implies ≤0.1% deuterium; ND=not detected.

Table 2.25 Metabolites of [^2H_3CO]desulfoglucorapassicin (**172a**) in UV-irradiated rutabaga roots.

Metabolites detected (**#a**)[a]	% Incorporation ± Std
[^2H_3CO]rapalexin A (**103a**)	25.3 ± 8.4[b]
[^2H_3CO]isalexin (**102a**)	6.7 ± 0.4[c]
[^2H_3CO]-4'-methoxyindole-3'-carbonitrile **(205a**)	87.7.0 ± 1.5[b]
[^2H_3CO]desulfoglucorapassicin (**172b**)	100

[a] Deuterated compounds are referred to by a number followed by the letter **a**.
[b] Negative ion mode. Incorporations calculated from HPLC-ESI-MS (normalized peak intensities); % of ^2H incorporation = $\{[M-1+n]^-/([M-1]^- + [M-1+n]^-)\} \times 100$ (n = 3) ± Std (standard deviation), where n = number of deuterium atoms.
[c] Positive ion mode. Incorporations calculated from HPLC-ESI-MS (normalized peak intensities); % of ^2H incorporation = $\{[M+1+n]^+/([M+1]^+ + [M+1+n]^+)\} \times 100$ (n = 3) ± Std (standard deviation), where n = number of deuterium atoms.
[d] NI=no incorporation implies ≤0.1% deuterium; ND=not detected.

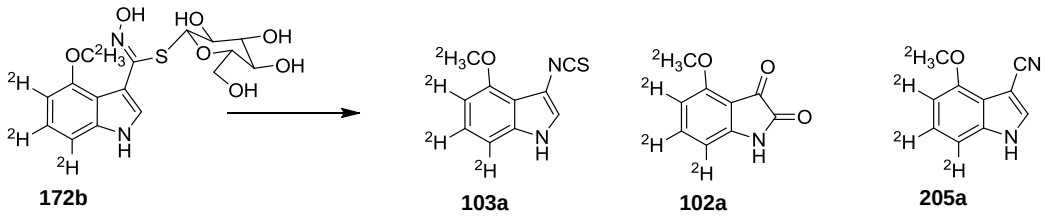

Figure 2.29 Deuterated metabolites obtained from feeding of [^2H_3CO,5',6',7'-$^2H_3$]desulfoglucorapassicin (**172b**) to UV-irradiated rutabaga root: [^2H_3CO,5',6',7'-$^2H_3$]rapalexin A (**103a**) (6.2 ± 4.2%), [^2H_3CO,5,6,7-$^2H_3$]isalexin (**102a**) (7.1 ± 2.9%), [^2H_3CO,5',6',7'-$^2H_3$]-4'-methoxyindole-3'-carbonitrile **(205a**) (93.0 ± 1.0%).

Transformation of **172** to **103** was proposed to occur through enzymatic hydrolysis followed by Lossen type rearrangement, similar to proposed transformation of **69** to **165** (Pedras, Okinyo et al., 2009; Pedras, Yaya et al., 2010) (**Scheme 2.5**). The lack of incorporation of **172** into isocyalexin A (**104**) suggested that the biosynthetic pathways towards **103** and **104** split at the oxime (**171**) stage (both **171** and **107** were incorporated into **104)**. Biosynthesis of **103** requires additional intermediate **118** that may be biosynthesized from **172** (Pedras and Yaya, 2013) (**Scheme 2.7**)**.**

2.2.2.5.10 Incorporation of [^2H_3CO]rapalexin A (103a)

The structural closeness between rapalexin A **(103**) and isocyalexin A **(104**) suggested rapalexin A was a biosynthetic precursor of **104.** It was assumed that desulfurization on the side chain of **103** would give isocyalexin A **104**. In order to prove this hypothesis, a feeding experiment was conducted using labeled **103**. An aqueous solution of [^2H_3CO]rapalexin A **(103a**) (500 µL/hole, 5×10^{-4} M) was added to UV-irradiated slices of rutabaga and analyzed as described in **Figure 2.15**. The HPLC-ESI-MS analyses of the nonpolar extracts that contained phytoalexins revealed the isocyalexin A (**104**) peak at t_R = 12.3 min containing $[M - 1]^-$ at *m/z* 171. However, no ion $[M - 1 + 3]^-$ at *m/z* 174 was detected. This suggests that biosynthetic route of **104** is not through rapalexin A (**103**). In contrast, the isalexin (**102**) peak at t_R = 2.0 min showed two ions: $[M + 1]^+$ at *m/z* 178 and $[M + 1 + 3]^-$ at *m/z* 181, the latter of which was not detected in the control sample. Peak intensities were measured and the percentage of deuterium incorporation was calculated as described above to be 60.0 ± 8.0% (**Figure 2.30**). This transformation is due to oxidation of rapalexin A (**103**) at C-2 and C-3.

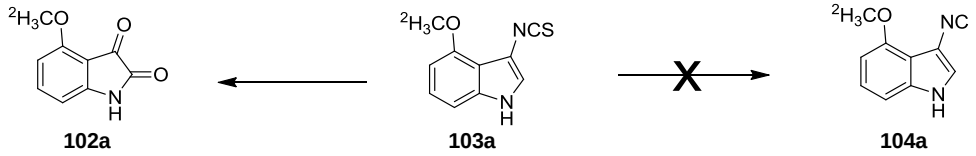

102a **103a** **104a**

Figure 2.30 Deuterated phytoalexin obtained from feeding of [^2H_3CO]rapalexin A **(103a**) to UV-irradiated rutabaga root: [^2H_3CO]isalexin (**102a**) (60.0 ± 8.0%).

2.2.2.5.11 Feeding of [4',5',6',7'-$^2H_4$]indole desulfoglucosinolate (186a), [4',5',6',7'-$^2H_4$]indolyl-3'-glycine (185a), [^2H_3CO]-4'-methoxyindolyl-3'-acetonitrile (135a), [^2H_3CO]-4'-methoxyindole-3'-carboxaldehyde (190a), [4',5',6',7'-$^2H_4$]indole-3'-carboxaldehyde oxime (176a), [^2H_3CO]-4-methoxyindole (149a)

Biosynthetic intermediates of rapalexin A **(103**), isocyalexin A **(104**) and isalexin **(102**) were confirmed using the labeled compounds [4',5',6',7'-$^2H_4$]indole desulfoglucosinolate (**186a**), [4',5',6',7'-$^2H_4$]indolyl-3'-glycine (**185a**), [^2H_3CO]-4'-methoxyindolyl-3'-acetonitrile (**135a**), [^2H_3CO]-4'-methoxyindole-3'-carboxaldehyde

(**190a**), [4',5',6',7'-$^{2}H_4$]indole-3'-carboxaldehyde oxime (**176a**) and [$^{2}H_3CO$]-4-methoxyindole (**149a**) (**Figure 2.31**). As it has been described in **Figure 2.15**, an aqueous solution of each precursor (500 µL/hole, 5×10^{-4} M) was added to UV-irradiated slices of rutabagas and analyzed. HPLC-ESI-MS analyses of the non-polar and polar extracts revealed no deuterium incorporation into the phytoalexins. These results suggest that biosynthetic enzymes downstream of 4'-methoxyglucobrassicin (**70**) are selective.

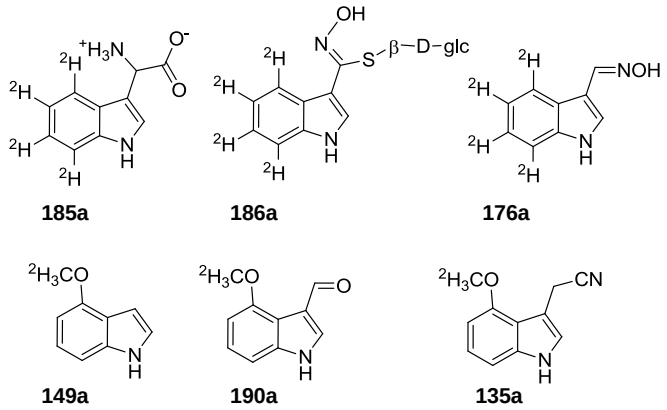

Figure 2.31 Labeled compounds for biosynthetic study.

2.2.2.6 Conclusion

Biosynthetic intermediates of novel cruciferous phytoalexins isolated from rutabaga were established using labeled (^{2}H, ^{13}C, ^{15}N) synthetic and commercially available precursors. The incorporation of *L*-[2',4',5',6',7'-$^{2}H_5$]tryptophan (**66a**) into rutabaga phytoalexins (spirobrassinin (**101**), cyclobrassinin (**78**), rutalexin (**116**), rapalexin A (**103**), isocyalexin A (**104**) and isalexin (**102**) as well as indole glucosinolates, glucobrassicin (**57**), 4'-methoxyglucobrassicin (**70**) and 1'-methoxy glucobrassicin (**69**) show that the indolyl moiety of these metabolites derives from *L*-tryptophan (**66**) (Pedras, Yaya et al., 2011) (**Scheme 2.14**).

Intact incorporation of [2,2,4',5',6',7'-$^{2}H_6$]glucobrassicin (**57b**) into spirobrassinin (**101**), cyclobrassinin (**78**), rutalexin (**116**) shows the biosynthetic relationship between indole glucosinolates and cruciferous phytoalexins (Pedras and Yaya, 2013; Pedras, Yaya

et al., 2010). The same transformation was confirmed using salt cress leaves, in which phytoalexins and indole glucosinolates incorporated glucobrassicin (**57**). The first step is oxidations and subsequent methylations of glucobrassicin (**57**) into 1'- and 4' methoxyglucobrassicins (**69** and **70**), which are precursors for 1 and 4-methoxy phytoalexins respectively (Pedras and Yaya, 2013; Pedras, Yaya et al., 2010). Glucobrassicins (**57, 70, 69**) are hydrolyzed by myrosinase to give unstable intermediates aglycones, which rearrange into the corresponding indolyl-3'-methylisothiocyanates via Lossen type rearrangement and then can be thiomethylated in the presence of thiomethyl donor (*S*-adenosyl methionine) to give the corresponding brassinins (**45**, **108** and **105**) (Pedras and Yaya, 2013; Pedras, Yaya et al., 2010).

The origin of side chain carbon and nitrogen atoms of cruciferous phytoalexins rapalexin A (**103**) and isocyalexin A (**103**) was established by administering [$^{13}C_{11}$,$^{15}N_2$]tryptophan (**66b**) to rutabaga roots. Side chain carbon and nitrogen atoms were proven to be derived from **66b**. 4-Methoxylated phytoalexins were shown to be derived from **57** via **70**. 4'-Methoxybrassinin (**108**) was incorporated into **110** and **113** but not into **103** or **104** suggesting the presence of two distinct pathways for the biosynthesis of 4-methoxyphytoalexins (Pedras and Yaya, 2013). The novel amino acid **107**, oxime **171** and desulfoglucosinolate **172** were identified as biosynthetic precursors for rapalexin A (**103**) and isalexin (**102**) while isocyalexin A incorporated only **107** and **171** (Pedras and Yaya, 2013) (**Scheme 2.14**)**.**

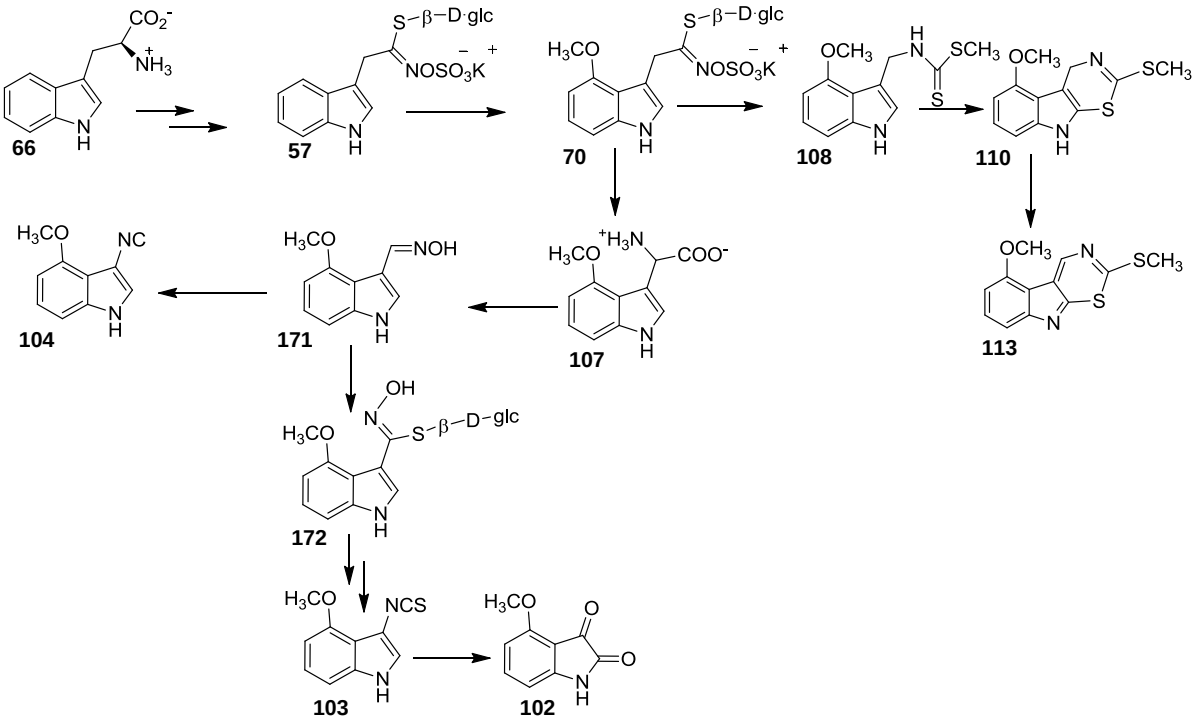

Scheme 2.14 Biosynthetic pathways of metabolites of rutabaga (Pedras and Yaya, 2013).

2.3 General conclusion and future direction

Considering the number of cruciferous species (ca. 3700), it is surprising that only a limited number have been investigated for the production of phytoalexins. Since most wild species have not been investigated, *B. tournefortii*, *C. abyssinica*, *D. tenuifolia* and *D. tenuisiliqua* were screened for the production of elicited metabolites. Arvelexin (**135**) was detected in all species and was the only phytoalexin detected in *D. tenuifolia.* In *D. tenuisiliqua,* arvelexin (**135**) was produced together with another elicited metabolite, 1',4'-dimethoxyindolyl-3'-acetonitrile (tenualexin) (**148**). **148** is reported here for the first time as a phytoalexin. It showed antifungal activity against *A. brassicicola*, *L. maculans*, *R. solani* and *S. sclerotiorum,* strongly inhibiting their mycelial growth. The inhibition effect was stronger compared to 1'-methoxyindolyl-3'-acetonitrile (**67**) and 4'-methoxyindolyl-3'-acetonitrile (**135**), suggesting that dimethoxysubstitution is important

for antifungal inhibition. Indolyl-3'-acetonitrile (**67**) is derived from glucobrassicin (**57**), while 4'-methoxyglucobrassicin (**70**) is a precursor of 4'-methoxyindolyl-3'-acetonitrile (**135**). By analogy, 1',4'-dimethoxyglucobrassicin is proposed to be the biosynthetic precursor of (**148**). The similarity in the metabolic profiles of wild crucifers (*C. abyssinica* and *B. tournefortii*) and cultivated species indicates that they may share common biosynthetic intermediates. As crucifers produce a mixture of phytoalexins, whose composition and amounts depend on the type of stress (Pedras and Yaya, 2010; Pedras, Yaya et al., 2011; Pedras, Zheng et al., 2007b), it is worthy to investigate different plant tissues using different elicitation techniques. Absence of additional phytoalexins in, for example, elicited leaves of *D. tenuifolia* suggests the need to try different elicitation strategies, including UV-light and other heavy metal salt solutions. Especially wild crucifers are likely to produce new metabolites, as most of them are not yet investigated.

The incorporation of *L*-tryptophan (**66**) into phytoalexins wasalexin A (**43)**, wasalexin B (**109**), biswasalexin A1 (**131**), biswasalexin A2 (**132**), isalexin (**102**), rapalexin A (**103**), isocyalexin A (**104**), 4'-methoxycyclobrassinin (**110**), 4'-methoxydehydrocyclobrassinin (**113**) spirobrassinin (**101**), rutalexin (**116**), cyclobrassinin (**78**) and indole glucosinolates glucobrassicin (**57**), 1'-methoxyglucobrassicin (**69**) and 4'-methoxyglucobrassicin (**70**) is consistent with previous work (Pedras, Yaya et al., 2011; Pedras, Zheng et al., 2007b), showing that *L*-tryptophan is the primary building block. Particularly, intact incorporation of fully labelled *L*-tryptophan (**66b**) into cruciferous phytoalexins and indole glucosinolates confirmed the origin of the side chain carbon and nitrogen atoms (Pedras and Yaya, 2013). Two carbon and nitrogen atoms in indole glucosinolate functional group are derived from tryptophan (**66**) (Pedras and Yaya, 2013). Phytoalexins side chains are likely formed from the rearrangement of the indole glucosinolate functional group. Intact incorporation of hexadeuterated glucobrassicin (**57**) into cruciferous phytoalexins indicated that it is are intermediates in the biosynthesis of phytoalexins (Pedras and Yaya, 2013; Pedras, Yaya et al., 2010).

Incorporation of [$^{2}H_3$CS,4',5',6',7'-$^{2}H_4$]-1'-methoxybrassinin (**105a**) into wasalexins A (**43)** and B (**109**), biswasalexins A1 (**131**) and A2 (**132**) suggested that **105**

is a close biosynthetic precursor that upon successive oxidations and thiomethylation gives **43** and **109** (Pedras, Yaya et al., 2010). 1'-Methoxyglucobrassicin (**69**) was proposed to be a biosynthetic intermediate located between glucobrassicin (**57)** and 1'-methoxybrassinin (**105)**. The first step in the metabolism of 1'-methoxyglucobrassicin (**69**) into 1'-methoxybrassinin (**105**) is a deglucosylation likely catalyzed by a hydrolase enzyme to give unstable aglycone (**138**). This intermediate spontaneously rearranges into the corresponding 1'-methoxyindolyl-3'-methylisothiocyanate (**165**) which, in the presence of thiomethyl donor (*S*-adenosyl methionine), could give rise to 1'-methoxybrassinin (**105**) (Pedras, Yaya et al., 2010) (**Scheme 2.15**). Absence of incorporation of [4',5',6',7'-$^{2}H_4$]brassinin (**45a**) into **43, 109, 131** and **132** was consistent with a methoxylation of glucobrassicin (**57**) before functional group modifications (Pedras, Yaya et al., 2010). Nevertheless, detection of metabolites **157, 158, 159** and metabolic products **101, 155, 156** deriving from brassinin (**45**) suggests enzymes can take brassinin (**45**) and metabolize it similarly to 1'-methoxybrassinin (**105**) (Pedras, Yaya et al., 2010). Stages at which oxidations could occur were probed by administering 1'-methoxy-2'-methyl brassinin (**160**). Interestingly, no metabolic products were detected, which suggested the importance of H-2 of indole for oxidation of the ring and the side chain (Pedras, Yaya et al., 2010). *L*-methionine was found to be methyl source for the phytoalexins and indole glucosinolates (Pedras, Yaya et al., 2010).

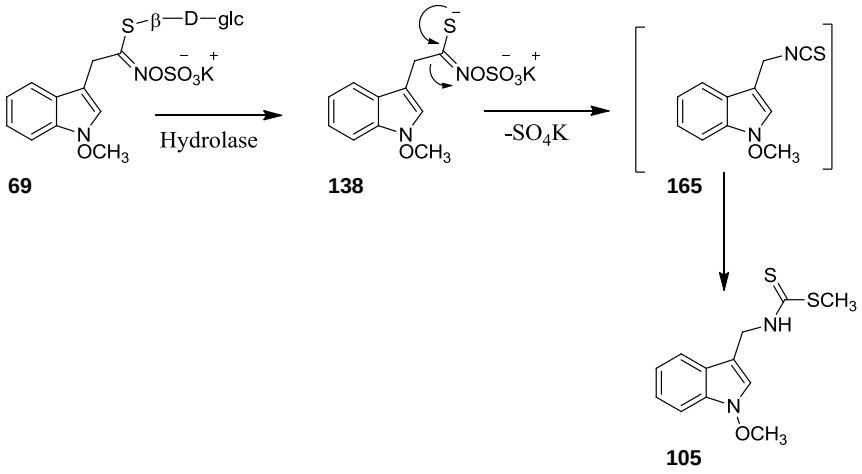

Scheme 2.15 Metabolism of 1'-methoxyglucobrassicin (**69**) to 1'-methoxybrassinin (**105**)

4'-Methoxybrassinin (**108**) was incorporated into 4'-methoxycyclobrassinin (**110**) and 4'-methoxydehydrocyclobrassinin (**113**), but not into rapalexin A (**103**) or isocyalexin A (**104),** suggesting the presence of two distinct pathways in the biosynthesis of 4-methoxyphytoalexins (Pedras and Yaya, 2013). Therefore, 4-methoxyphytoalexins were categorized into two groups, the brassinin (**45**) series and rapalexin A (**103**) series. The brassinin series 4-methoxyphytoalexins includes 4'-methoxycyclobrassinin (**110**) and 4'-methoxydehydrocyclobrassinin (**113**), in which the side chain nitrogen is connected to the indole ring via a carbon linker. The rapalexin A (**103**) series are those in which side chain nitrogen or oxygen is directly connected to the indole ring (rapalexin A (**103**), isocyalexin A (**104**) and isalexin (**102**)). Incorporation of **57** into **110** and **113** occurs likely via **70**. Hydrolysis of **70** is followed by Lossen type rearrangement to give unstable 4'-methoxyindolyl-3'-isothiocyanate (**Scheme 2.15**), which converts to 4'-methoxybrassinin (**108**) in the presence of the thiomethyl donor (*S*-adenosyl methionine) (Pedras and Yaya, 2013). In the case of the rapalexin A (**103**) series, compound **70** likely follows a different route that gives 4'-methoxyindolyl-3'-glycine (**107**). 4'-Methoxyindolyl-3'-glycine **(107)** is possibly derived from 4'-methoxyglucobrassicin (**70**) through Neber type rearrangement via an azirine intermediate similar to the base-catalyzed chemical hydrolysis of benzylglucosinolate to phenylglycine (Pedras and Yaya, 2013). This was confirmed by the incorporation of **107** into **104**, **103** and **102**. 4'-Methoxyindole-3'-carboxaldehyde oxime (**171**) was also incorporated into **104**, **103** and **102,** which could be another intermediate likely formed from **107** via *N*-oxidation followed by decarboxylation (Pedras and Yaya, 2013). Desulfoglucorapassicin (**172**) a proposed biosynthetic precursor of rapalexin A (**103**) was incorporated into **103** and **102,** but not into **104** suggesting splitting of the biosynthetic pathway, probably at the oxime (**171**) stage (Pedras and Yaya, 2013). *In vivo*, **172** is likely to derive from **171** via sulphur transfer from GSH followed by glucosilation (Pedras and Yaya, 2013), similar to glucosinolate biosynthetic pathways (Sønderby, Geu-Flores et al., 2010). Incorporation of rapalexin A (**103**) into **102** shows the biosynthetic link between **102** and **103** (Pedras and Yaya, 2012).

The biosynthetic route established in this thesis is indicated below (**Scheme 2.16**). *L*-tryptophan (**66**) is transformed to glucobrassicin (**57**) which oxidized at N-1 and C-4 to give 1'-methoxyglucobrassicin (**69**) and 4'-methoxyglucobrassicin (**70**), respectively. Glucosinolates **57**, **69** and **70** are first hydrolyzed to give unstable aglycon intermediates, which subjected to rearrangements and thiomethylation to give brassinins (**45**, **105** and **108),** respectively (Pedras and Yaya, 2013; Pedras, Yaya et al., 2010). 1'-methoxybrassinin **105** is further oxidized and methylated to give wasalexin A (**43)** and wasalexin B (**109)** (Pedras, Yaya et al., 2010). Metabolite **43** is transformed to biswasalexins A1 (**131)** and A2 (**132)** via dimerization (Pedras, Yaya et al., 2010; Pedras, Zheng et al., 2009). 4'-Methoxybrassinin (**108**) is a biosynthetic precursor for 4'-methoxycyclobrassinin (**110**) and 4'-methoxydehydrocyclobrassinin (**113**) (Pedras and Yaya, 2013). Rapalexin A (**103**), isocyalexin A (**104**) and isalexin (**102**) are derived from 4'-methoxyindolyl-3-glycine (**107**) (Pedras and Yaya, 2013). Compound **107** gives 4'-methoxyindole-3'-carboxaldehyde oxime (**171**) that metabolized to give isocyalexin A (**104**) via sulfation followed by Beckmann-type rearrangement (Pedras and Yaya, 2012; 2013). Compound **171** can also be metabolized to give desulfoglucorapassicin (**172**) which is a likely precursor of glucorapassicin (**118**), whose synthesis was not accomplished (Pedras and Yaya, 2013). *In vivo* hydrolysis of **118** followed by Lossen type rearrangement would give rapalexin A (**103**) that can be oxidized to isalexin A (**102**) (Pedras and Yaya, 2013).

Even though the major part of the biosynthetic route of cruciferous phytoalexins has been established, there are still a few questions that need to be addressed;

1. In the biosynthesis of rapalexin A (**103**), one of the proposed biosynthetic precursors is glucorapassicin (**118**), whose synthesis was not accomplished. A synthetic methodology needs to be devised so that its stability under different experimental conditions can be studied and it can then be used as a substrate for enzyme isolation.

2. Otherwise, major questions are related to the biosynthetic enzymes involved in biosynthesis of most cruciferous phytoalexins (except camalexin), and the enzymes need to be characterized and genes need to be cloned.

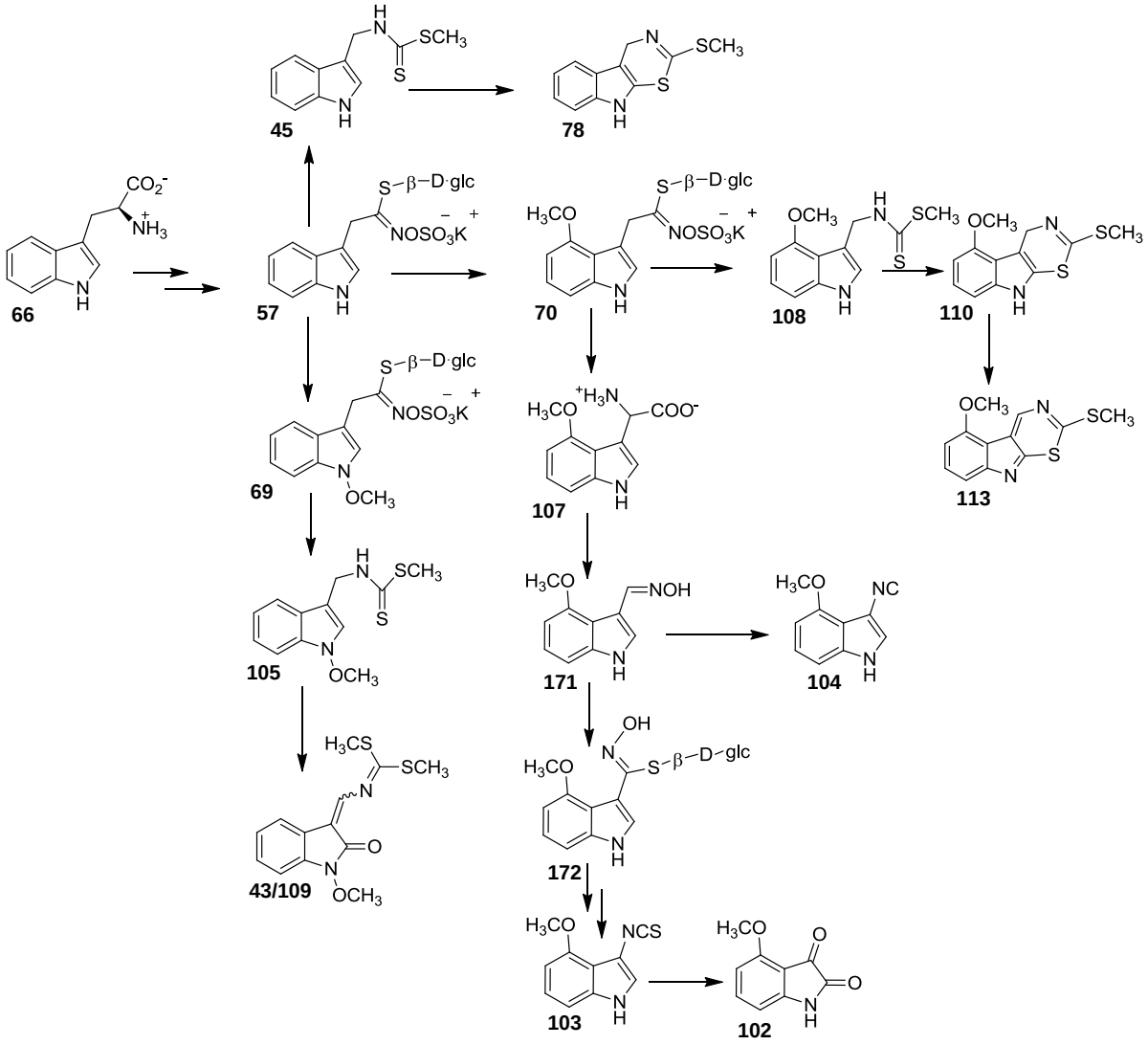

Scheme 2.16 Biosynthetic pathways of metabolites of salt cress and rutabaga (Pedras and Yaya, 2013; Pedras, Yaya et al., 2011; Pedras, Yaya et al., 2010).

3 EXPERIMENTAL

3.1 General

All chemicals were purchased from Sigma-Aldrich Canada Ltd., Oakville, ON, or Alfa Aesar 26 Parkridge Rd, Ward Hill, USA, except for isotope-labeled compounds that were purchased from Cambridge Isotope Laboratories Inc., Andover, MA, and C/D/N Isotopes Inc., Pointe-Claire, Quebec. All solvents were HPLC grade and used as such, except for THF and Et_2O (dried over sodium), CH_2Cl_2 (dried over CaH_2), MeOH (dried over CaO) and DMF (dried over molecular sieves).

Flash column chromatography (FCC) was carried out using silica gel, grade 60, 230-400 μm. Organic extracts were dried over Na_2SO_4 and the solvents were removed using a rotary evaporator.

Analytical TLC was performed on pre-coated silica gel TLC plates (Merck, Kieselgel 60 F_{254}, 5 × 2 cm × 0.2 mm layer thickness) aluminum sheets. The compounds were eluted with suitable solvent systems, then visualized under UV light (254/366 nm), and by dipping the plates in a 5% (w/v) aqueous phosphomolybdic acid solution containing 1% (w/v) cerium(IV) sulfate and 4% (v/v) H_2SO_4, followed by heating at 260 ^oC.

PTLC was performed on pre-coated silica gel, (Merck, Kieselgel 60 F_{254}, 20 × 20 cm × 0.25 mm thickness). The compounds were eluted with suitable solvent systems, then visualized under UV light (254/366 nm).

NMR spectra were recorded on Bruker Avance 500 MHz spectrometers. For ^1H NMR (500 MHz) and ^{13}C NMR (125.8 MHz) spectra, the chemical shifts (δ) are reported in parts per million (ppm) relative to TMS. The δ values are referenced to $CHCl_3$ in $CDCl_3$ at 7.27 ppm CH_3CN in CD_3CN at 1.94 ppm, CH_3OH in CD_3OD at 3.31 or CH_2Cl_2 in CD_2Cl_2 at 5.31. Multiplicities are indicated by the following symbols: s = singlet, d = doublet, dd = doublet of doublets, m = multiplet and br = broad. Spin coupling constants

(*J* values) are reported to the nearest 0.5 Hz. For ^{13}C NMR (125.8 MHz) the δ values are referenced to $CDCl_3$ (77.23 ppm), CD_3CN (118.69 ppm), CD_3OD (49.15 ppm) or CD_2Cl_2 (53.80).

Fourier transform infrared (FT-IR) data were acquired on a Bio-Rad FTS-40 spectrometer and spectra were measured by the diffuse reflectance method on samples dispersed in KBr.

HPLC analysis was carried out with either Agilent 1100 series or Hewlett Packard HPLC systems equipped with quaternary pump, auto sampler, diode array detector (DAD, wavelength range 190-600 nm), and degasser. Method A (phytoalexins and non-polar metabolites) used a Zorbax Eclipse XDB-C18 column (5 µm particle size silica, 150 × 4.6 mm I.D.), equipped with an in-line filter, with the mobile phase H_2O-CH_3OH from 50:50 to 0:100, linear gradient for 25 min, and a flow rate of 0.75 ml/min or H_2O-CH_3CN (75:25 to 25:75 in 35 min, to 0:100 in 5 min) and a flow rate of 1 mL/min; Method B (indolyl glucosinolates and other polar metabolites) used a Zorbax SB-C18 column (3.5 µm particle size silica, 100 × 3.0 mm I.D.), equipped with an in-line filter, with the mobile phase H_2O (with 0.1% TFA) - CH_3OH (with 0.1% TFA) from 85:15 to 70:30 in 25 min, to 50:50 in 5 min, to 40:60 in 5 min and a flow rate of 0.40 ml/min or H_2O-CH_3CN (100:0 to 25:75 in 35 min, to 0:100 in 5 min) and a flow rate of 1 mL/min. Samples were dissolved in CH_3OH or CH_3CN for Method A, and in H_2O-CH_3OH (1:1) for Method B.

HPLC-ESI-MS analysis was carried out with an Agilent 1100 series HPLC system equipped with an auto sampler, binary pump, degasser, and a diode array detector connected directly to a mass detector (Agilent G2440A MSD-Trap-XCT ion trap mass spectrometer) with an electrospray ionization (ESI) source. Chromatographic separations were carried out at room temperature using an Eclipse XDB-C-18 column (5 μm particle size silica, 150 × 4.6 mm I.D.). The mobile phase consisted of a linear gradient of: Method A, in H_2O (with 0.2% HCO_2H) - CH_3CN (with 0.2% HCO_2H) from 75:25 to 25:75 in 35 min, to 0:100 in 5 min and a flow rate of 1.0 ml/min; Method B, H_2O (with 0.2% HCO_2H) - CH_3CN (with 0.2% HCO_2H) from 90:10 to 50:50 in 25 min and a flow rate of 1.0 ml/min. Data acquisition was carried out in positive and negative polarity

modes in a single LC run, and data processing carried out with Agilent Chemstation Software. Samples were dissolved in CH_3CN for Method A, and in methanol-water (50:50) for Method B.

HPLC-ESI-HRMS was performed on an Agilent HPLC 1100 series directly connected to QSTAR XL Systems Mass Spectrometer (Hybrid Quadrupole-TOF LC/MS/MS) with turbo spray ESI source. Chromatographic separation was carried out at room temperature using a Hypersil ODS C-18 column (5 μm particle size silica, 200 × 2.1 mm I.D.) or a Hypersil ODS C-18 column (5 μm particle size silica, 100 × 2.1 mm I.D.). The mobile phase consisted of a linear gradient of; Method A: 0.1% formic acid in water and 0.1% formic acid in acetonitrile (75:25 to 25:75 in 35 min, to 0:100 in 5 min) and a flow rate of 0.25 mL/min; Method B: 0.1% formic acid in water and 0.1% formic acid in acetonitrile (97:3 to 50:50 in 25 min, to 97:3 in 10 min) and a flow rate of 0.25 mL/min. Data acquisition was carried out in either positive or negative polarity mode per LC run. Data processing was carried out by Analyst QS Software. Samples were dissolved in acetonitrile for Method A and in methanol-water (50:50) for Method B. Data were presented as measured and calculated values.

MS [high resolution (HR), electron ionization (EI)] were obtained on a VG 70 SE mass spectrometer employing a solids probe. Data were presented as measured and calculated values.

Specific rotation ($[\alpha]_D$ was determined at ambient temperature on a DigiPol 781 automatic polarimeter by using a 1 mL, 10 cm cell at the concentration of c = g/100 mL. The unit of $[\alpha]_D$ is deg dm^{-1} cm^3 g^{-1}.

3.1.1 Plant materials and growth conditions

Thellungiella salsuginea ecotype Shandong was obtained from TAIR (envelope labeled as *Thellungiella halophila*). Seeds were sown in a perlite and nutrient free LG-3 soil (Sun Gro Horticulture Canada) in a Petri dish and incubated at 4 °C. After 10 days, the Petri dishes containing seeds were transferred to a growth chamber at 16 h of light/8 h

of dark, 23 °C day/ 16 °C night, light intensity of 150 $\mu Em^{-2}s^{-1}$, and with ambient humidity. After seven days, the seedlings were transferred into soil in small pots (50 pots/tray), and kept under the same conditions. Seeds of sand rocket (*Brassica tournefortii*), Abyssinian mustard (*Crambe abyssinica*), *Diplotaxis tenuisiliqua* and *Diplotaxis tenuifolia* were obtained from Plant Gene Resources, AAFC, Saskatoon, Canada. The seeds were sown in a commercial potting soil mixture, and plants were grown in a growth chamber under controlled environmental conditions for 3-4 weeks. Rutabaga roots were purchased from Sobeys or Safeway Saskatoon, Sk.

3.2 Analysis of antifungal secondary metabolites from wild crucifers

3.2.1 Time-course analysis

Plants (*B. tournefortii, C. abyssinica, D. tenuisiliqua* and *D. tenuifolia)* 2 to 4 weeks old were sprayed with $CuCl_2$ (2-10 mM) solution to the point of run-off and incubated in a growth chamber. Leaves from elicited and control plants were harvested at 24, 72 and 120 h, separately frozen in liquid nitrogen, crushed and extracted with methanol (2 x 20 ml) on a shaker for 1 h. Methanol extracts were filtered and concentrated under reduced pressure. The residue was washed with dichloromethane (6 ml) and concentrated. The dichloromethane extract was dissolved in acetonitrile (200 µl) and analyzed by HPLC-DAD and HPLC-ESI-MS. The residue was dissolved in methanol-water (1:1, 1 mL) and analyzed by HPLC-DAD and HPLC-ESI-MS. Known induced compounds were identified by comparing their UV spectra and retention times with that of authentic samples.

3.2.2 TLC biodetection

A solution of potato dextrose broth (PDB) with double strength was prepared by autoclaving a suspension of PDB (4.8 g) in H_2O (100 mL), and spores of *Cladosporium*

cucumerinum were added to make a concentration of 1×10^6 spores/mL. Bioassays were conducted following previously established method (Pedras and Sorensen, 1998). Samples were spotted on 2 × 20 cm TLC plates which were developed using solvent system, EtOAc-hexane (60:40). The developed plates were air dried (60 min), were sprayed with the spore suspension, and incubated under high humidity in the dark for 36 h. Control plates were also prepared similarly but without spotting leaf extracts. From these experiments, the antifungal areas appeared white (due to inhibition of spore germination) against a dark gray background due to fungal growth. The white spots were not observed in control plates.

3.2.3 Isolation of secondary metabolites from *Diplotaxis tenuisiliqua*

A large scale experiment was conducted in order to isolate and characterize antifungal metabolites from 3 week old plants of *D. tenuisiliqua*. Plants were elicited with $CuCl_2$ (10 mM) solution, leaves were harvested, weighed (300 g) and crushed in liquid nitrogen. The crushed leaves were divided into two parts and extracted with methanol for overnight. The plant tissue was filtered and the filtrate was concentrated. The crude methanol extract was washed with dichloromethane and concentrated. The polar residue and the dichloromethane extracts were assayed (TLC biodetection) against a fungus, *Cladosporium cucumerinum,* for the analysis of the antifungal activity. Based on the inhibition effect on the fungus, dichloromethane extract was subjected to chromatographic purification using FCC (hexane:EtOAc 80:20 to 0:100 and CH_2Cl_2:MeOH 95:5 v/v). The fractions were analyzed by HPLC-DAD and TLC biodetection. A fraction containing a peak at t_R = 19.7 min and that had shown antifungal activity was further purified by FCC (hexane:EtOAc 90:20 to 70:30). Final purification of the fraction containing the peak at t_R = 19.7 min was carried out using PTLC (hexane:EtOAc 85:15) to yield 1',4'-dimethoxyindolyl-3'-acetonitrile (**148**) 0.8 mg.

3.2.4 Chemical characterization of a metabolite from *Diplotaxis tenuisiliqua*

3.2.4.1 1',4'-Dimethoxyindolyl-3'-acetonitrile (148)

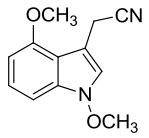

148

HPLC t_R = 19.7 min, method A.

UV (HPLC, H_2O-CH_3CN) λ_{max} (nm): 220, 265, 295.

FTIR (KBr, cm^{-1}) ν_{max}: 2935, 2359, 1502, 1456, 1303, 1260, 1060, 1033.

^1H NMR (500 MHz, $CDCl_3$): δ 7.20 (1H, s), 7.18 (1H, dd, *J* = 8, 8 Hz), 7.03 (1H, d, *J* = 8 Hz), 6.51 (1H, d, *J* = 8 Hz), 4.06 (3H, s), 4.02 (2H, s), 3.92 (3H, s).

^{13}C NMR (125 MHz, $CDCl_3$) δ 154.6, 134.0, 124.3, 120.3, 118.9, 112.8, 101.9, 101.1, 100.2, 66.1, 55.4, 16.1.l.

HREI-MS *m/z* calc. for $C_{12}H_{12}N_2O_2$: 216.0897 $[M]^+$; found 216.0897 (87%), 185.0 (100%), 170.0 (34%).

MS-ESI m/z $[M+1]^+$ 217.0 (100%), 186.0 (20%).

3.3 Syntheses of metabolites

3.3.1 Metabolite of *Diplotaxis tenuisiliqua*

3.3.1.1 1',4'-Dimethoxyindolyl-3'-acetonitrile(148)

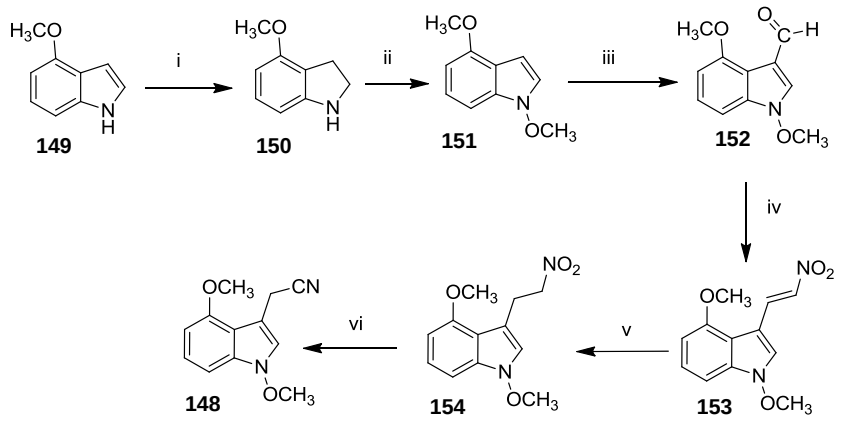

Scheme 3.1 Synthesis of **148**. Reagents and conditions: i) $NaCNBH_3$, AcOH; ii) Na_2WO_4, H_2O_2, K_2CO_3, $(CH_3)_2SO_4$ 41%; iii) $POCl_3$, DMF; iv) CH_3NO_2, NH_4OAc, 105 ^oC; v) $NaBH_4$, THF, MeOH; vi) CS_2, Et_3N , 40 ^oC 77%.

$NaCNBH_3$ (382 mg, 6.06 mmol) was added portion wise over a period of 10 min to a solution of 4-methoxyindole (**149**) (300 mg, 2.04 mmol) in acetic acid (6 mL) and the reaction mixture was stirred at room temperature for 1 hour, diluted with water and basified with NaOH, extracted with ether, and the organic phase was dried and concentrated to yield crude 4-methoxyindoline (**150**) 303 mg in 97% yield (Wang, Gao et al., 2009). $Na_2WO_4.2H_2O$ (126 mg, 0.38 mmol) in water (1 mL) was added to the stirred solution of 4-methoxyindoline (**150**) (333 mg, 2.25 mmol) in MeOH (8 mL) and cooled to -20 ^oC. A solution of H_2O_2 (1.5 mL, 19.6 mmol) in MeOH (2 mL) was added drop wise to the cooled suspension. The reaction mixture was stirred at room temperature for 10 min, K_2CO_3 (2.5 g, 18.11 mmol) and $(CH_3O)_2SO_2$ (341 μL, 3.60 mmol) were added under vigorous stirring (Somei and Kawasaki, 1989). After being stirred for 10 min, the reaction mixture was diluted with water and extracted with ether (40 mL × 3). The

organic extract was dried, concentrated and subjected to FCC (CH_2Cl_2, 100%) to yield 1,4-dimethoxyindole (**151**) (163 mg, 0.92 mmol) in 41% yield.

$POCl_3$ (127 µL, 1.36 mmol) was added drop wise to a solution of 1,4-dimethoxyindole (**151**) (160 mg, 0.91 mmol) in DMF (2 mL) at 0 ^oC. The reaction mixture was stirred for 1 h at room temperature, basified with ammonium hydroxide (28 %), diluted with water and extracted with ether (30 mL × 3). The organic layer was dried, concentrated and subjected to FCC (CH_2Cl_2-MeOH 98:2) to yield 1',4'-dimethoxyindole-3'-carboxaldehyde (**152**) (149 mg, 0.73 mmol) in 81% yield.

NH_4OAc (26 mg, 0.34 mmol) was added to a solution of 1,4-dimethoxyindolyl-3-carboxaldehyde (**152**) (139 mg, 0.68 mmol) in nitromethane (1.5 mL) and refluxed (Canoira, Rodriguez et al., 1989; Somei, Sato et al., 1985) at 105 °C for 90 min. The reaction mixture was allowed to cool, diluted with water, extracted by CH_2Cl_2 and concentrated to yield crude 1,4-dimethoxy-3-nitrovinyl indole (**153**), which was taken to the next step without further purification. $NaBH_4$ (78 mg, 2.04 mmol) was added to a solution of crude 1,4-dimethoxy-3-nitrovinyl indole (**153**) (169 mg, 0.68 mmol) in THF (4 mL) and methanol (500 µL). The reaction mixture was stirred for 3 h at room temperature and excess $NaBH_4$ was destroyed by adding water to the reaction mixture. The reaction mixture was extracted by CH_2Cl_2, concentrated and subjected to FCC (CH_2Cl_2, 100%) to yield 1,4-dimethoxy-3-(2'-nitroethyl) indole (**154**) 65 mg, 0.38 mmol) in 26%.

Et_3N (500 µL, 3.60 mmol) and CS_2 (217 µL, 3.60 mmol) were added to a solution of 1,4-dimethoxy-3-(2'-nitroethyl) indole (**154**) (45 mg, 0.18 mmol) in ACN (4 mL) (Somei, Sato et al., 1985). The reaction mixture was stirred at 40 ºC for 20 h in a sealed reaction vial, excess solvent was evaporated and the residue was diluted with water and extracted by CH_2Cl_2 (3 × 20 mL). The organic layer was dried, concentrated, the crude reaction mixture was purified by FCC (CH_2Cl_2, 100 %) to yield 1',4'-dimethoxyindolyl-3'-acetonitrile (**148**) (30 mg, 0.14 mmol) as a brown oil in 77% (**Scheme 3.1**).

HPLC t_R = 19.7 min, method A.

UV (HPLC, H_2O-CH_3CN) λ_{max} (nm): 220, 265, 295.

FTIR (KBr, cm^{-1}) ν_{max}: 2935, 2359, 1502, 1456, 1303, 1260, 1060, 1033.

^{1}H NMR (500 MHz, $CDCl_3$): δ 7.20 (1H, s), 7.18 (1H, dd, *J* = 8, 8 Hz), 7.03 (1H, d, *J* = 8 Hz), 6.51 (1H, d, *J* = 8 Hz), 4.06 (3H, s), 4.02 (2H, s), 3.92 (3H, s).

^{13}C NMR (125 MHz, $CDCl_3$) δ 154.6, 134.0, 124.3, 120.3, 118.9, 112.8, 101.9, 101.1, 100.2, 66.1, 55.4, 16.1.l.

HREI-MS *m/z* calc. for $C_{12}H_{12}N_2O_2$: 216.0897 $[M]^+$; found 216.0897 (87%), 185.0 (100%), 170.0 (34%).

MS-ESI m/z $[M+1]^+$ 217.0 (100%), 186.0 (20%).

3.3.2 Metabolic products of *Thellungiella salsuginea (*salt cress)

Administration of perdeuterated brassinin to leaves of salt cress resulted in metabolism of brassinin into known as well as new metabolic products. In this section; synthesis of the new metabolic products will be described.

3.3.2.1 Demethoxywasalexins A (157) and B (158)

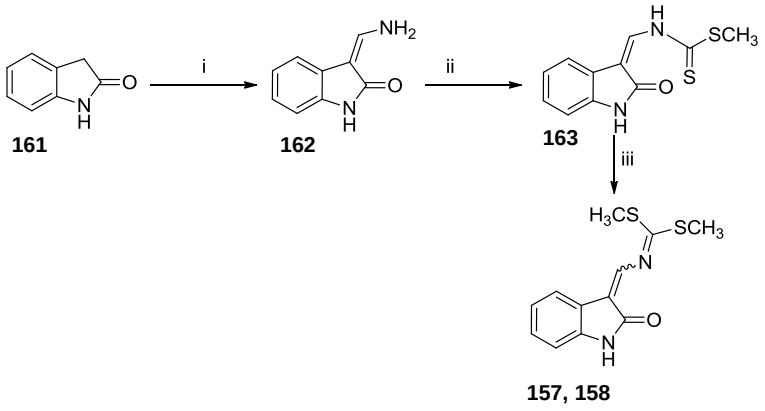

161 162 163 157, 158

Scheme 3.2 Synthesis of **157** and **158**. Reagents and conditions: i) DMF, $POCl_3$, 45 ºC, (aq. NH_3, 28%) 67%; ii) NaH, CS_2, MeI, THF, 0 ºC; iii) pyridine, NEt_3, MeI, CH_2Cl_2 53%.

A solution of 2-oxindole (**161**) (500 mg, 3.80 mmol) in DMF (5 mL) was added to a solution of $POCl_3$ (420 μL, 4.50 mmol) in DMF (1 mL) at 45 ºC (Pedras and Suchy, 2006; Pedras, Yaya et al., 2010; Pedras and Zaharia, 2001). The reaction mixture was stirred at 45 ºC for 30 min and cooled down to 0 °C. Cold aq. NH_3 (28%) was slowly added to the reaction mixture at 0 ^oC and allowed to warm up to room temperature and stirred for 1 h. The mixture was filtered and the filtrate was extracted with EtOAc; the organic layer was dried, concentrated and subjected to FCC (EtOAc/Hexane 1:1) to yield 3-aminomethylene-2-oxindole (**162**) (400 mg, 2.48 mmol) in 67% .

NaH (60% suspension in mineral oil, 10 mg, 0.25 mmol) and CS_2 (30 μL, 0.50 mmol), were added to a stirred solution of 3-aminomethylene-2-oxindole (**162**) (80 mg, 0.50 mmol) in dry THF (1 ml, cooled to 0 °C), and after 10 minutes CH_3I (15 μL, 0.23 mmol) was added (Pedras and Suchy, 2006; Pedras, Yaya et al., 2010). The mixture was stirred for 30 min at 0 °C, diluted with brine (10 ml), extracted (EtOAc) and the combined organic extract was dried and concentrated to yield crude (*E,Z*)-methyl ((2-oxoindolin-3-ylidene)methyl)carbamodithioate (**163**). Pyridine (30 μl, 0.37 mmol) and Et_3N (50 μl, 0.36 mmol) were added to the solution of (*E,Z*)-methyl ((2-oxoindolin-3-ylidene)methyl)carbamodithioate (**163**) (10 mg, 0.04 mmol) in CH_2Cl_2 (3 ml) and the reaction mixture was stirred at 30 °C for 10 min. MeI (8 μl, 0.13 mmol) was added to the reaction mixture and the solution was stirred for 14 h at 30 °C. The reaction mixture was diluted with brine, extracted with EtOAc, and the organic extract was concentrated. After separation of the extract by prep TLC, demethoxywasalexins A (**157**) and B (**158**) (yellow solid, mixture of *E* and *Z* isomers 4:1) was obtained in 53% yield (5 mg, 0.02 mmol) (Pedras, Yaya et al., 2010) (**Scheme 3.2**).

M.P. 207-209 ºC

HPLC t_R = 15.3; 16.2 min, method A.

UV (CH_3CN) λ_{max} (nm): 254, 286, 362.

FTIR (KBr, cm^{-1}) ν_{max}: 3167, 2918, 1695, 1624, 1613, 1466, 1176, 935, 781.

^1H NMR (500 MHz, CD_2Cl_2) 8.00 (1 H, s), 7.88 (1H, s, D_2O exchangeable), 7.86 (1H, d, *J* = 7.5 Hz), 7.18 (1H, dd, *J* = 7.5, 7.5 Hz), 6.99 (1H, dd, *J* = 7.5, 7.5 Hz), 6.86 (1H, d, *J* = 8 Hz), 2.69 (6H, s).

^{13}C NMR (125.8 MHz, CD_2Cl_2) 176.6, 170.8, 140.4, 138.7, 128.7, 125.1, 123.6, 122.3, 119.5, 109.7, 16.2 (2C).

HREI-MS *m/z* calc. for $C_{12}H_{12}N_2OS_2$: 264.0391 $[M]^+$; found 264.0396 (57%), 271.0 (100%), 202.0 (43%), 144.0 (24%).

MS-ESI m/z $[M+1]^+$ 265.0 (100%), 217.0 (64%).

3.3.2.2 Demethoxydihydrowasalexin (159)

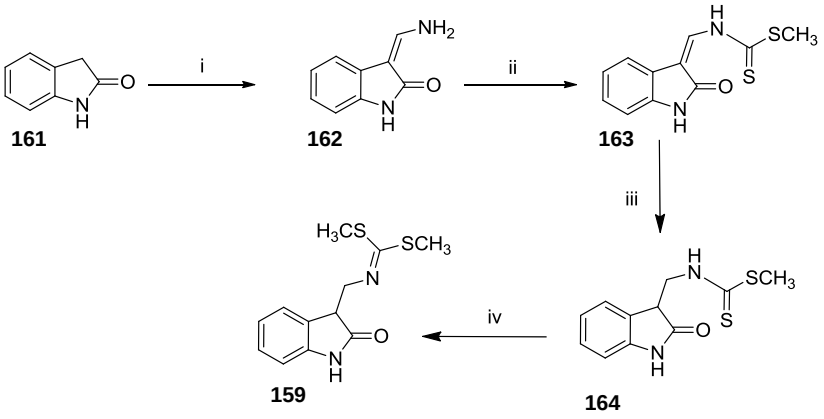

Scheme 3.3 Synthesis of **159**. Reagents and conditions: i) DMF, $POCl_3$, 45 ºC, (aq. NH_3, 28%); ii) NaH, CS_2, MeI, THF, 0 ºC; iii) $NaCNBH_3$, AcOH, 60 ºC, 55%; (iv) K_2CO_3, $(CH_3O)_2SO_2$, acetone, 30 ºC, 58%.

$NaBH_3CN$ (90 mg, 1.42 mmol) was added to a solution of methyl ((2-oxoindolin-3-ylidene)methyl)carbamodithioate (**163**) (18 mg, 0.07 mmol) in AcOH (1.0 ml). The mixture was stirred at 60 °C for 18 h, was diluted with water (3 ml) and the pH of the solution was adjusted to 6 with Na_2CO_3 (sat. solution) and the solution was extracted (EtOAc). The combined organic extract was concentrated and the residue was subjected to FCC (EtOAc-hexane, 3:7) to yield methyl ((2-oxoindolin-3-yl)methyl)carbamodithioate (**164**) (10 mg, 0.04 mmol) in 55%. Dimethylsulfate (4 μl, 0.04 mmol) and K_2CO_3 (6 mg, 0.04 mmol) were added to a solution of methyl ((2-oxoindolin-3-yl)methyl)carbamodithioate (**164**) (8 mg, 0.03 mmol) in acetone (200 μl) and the mixture was stirred at 30 ºC for 20 h. The reaction mixture was concentrated,

then diluted with water (3 ml) and extracted with EtOAc. The combined organic extract was dried, was concentrated and the residue was subjected to FCC (EtO_2) to afford demethoxydihydrowasalexin (**159**) (yellow solid, 5 mg, 0.02 mmol) in 58% (Pedras, Yaya et al., 2010) (**Scheme 3.3**).

M.P. 172-174 ºC

HPLC t_R = 14.8 min, method A.

UV (CH_3CN) λ_{max} (nm): 242.

FTIR (KBr, cm^{-1}) ν_{max}: 3180, 2922, 2851, 1703, 1621, 1574, 1468, 747.

^1H NMR (500 MHz, CD_2Cl_2) 7.95 (1 H, s), 7.29 (1H, d, *J* = 7.5 Hz), 7.20 (1H, dd, *J* = 7.5, 7.5 Hz), 6.99 (1H, dd, *J* = 7.5, 7.5 Hz), 6.86 (1H, d, *J* = 7.5 Hz), 3.98 (1H, dd, *J* = 14, 3 Hz), 3.81-3.74 (2H, m), 2.51 (3H, s), 2.19 (3H, s).

^{13}C NMR (125.8 MHz, CD_2Cl_2) 178.7, 142.6, 129.9, 128.4, 125.2, 122.6, 118.5, 109.6, 53.6, 47.9, 15.2, 14.9.

HREI-MS *m/z* calc. for $C_{12}H_{14}N_2OS_2$: 266.0548; found 266.0542 (6%), 146.0 (100%).

MS-ESI *m/z* $[M+1]^+$ 267 (100%), 219 (47%), 146 (50%).

3.3.3 Metabolites of rutabaga and analogous

In this section synthesis of two new metabolites that were isolated from rutabaga, and their analogues will be described.

3.3.3.1 4'-Methoxyindolyl-3'-formamide (168)

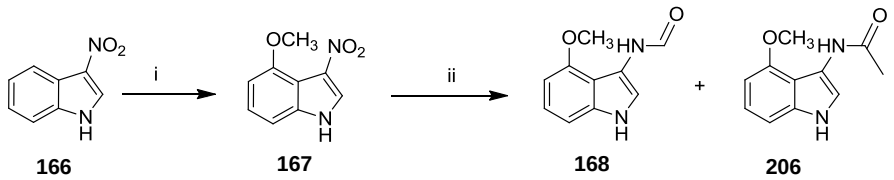

Scheme 3.4 Synthesis of 4'-Methoxyindolyl-3'-formamide **168**. Reagents and conditions: i) TTFA/TFA, I_2/CuI, $NaOCH_3$, 64%; ii) Pd/C-H_2, acetic-formic anhydride, -10 °C, 66%

TTFA (503 mg, 0.93 mmol) was added to a solution of 3-nitroindole (**166**) (100 mg, 0.62 mmol) in TFA (3 mL) and the reaction mixture was stirred for 4 h at 30 °C. The solvent was evaporated under reduced pressure, I_2 (472 mg, 1.86 mmol) and CuI (472 mg, 2.48 mmol) in DMF (4 mL) were added to the reaction mixture and the mixture was stirred for 1 h at 25 °C. $NaOCH_3$ (prepared from Na, 800 mg, 34.80 mmol, in anhydrous MeOH, 5 mL) was added to the reaction mixture and the mixture was refluxed at 110 °C for 1 h. The reaction mixture was neutralized (pH 7, HCl, 1 M), filtered through celite and the solvent was evaporated. The residue was taken in water, extracted with EtOAc, dried, concentrated and the crude product was subjected to FCC (EtOAc-hex, 1:1) to yield 4-methoxy-3-nitroindole (**167**) (77 mg, 0.40 mmol) in 64% yield.

Procedure A: Pd/C (52 mg) was added to a solution of 4-methoxy-3-nitroindole (**167**) (52 mg, 0.27 mmol) in EtOH (1 mL) and reaction mixture was stirred under H_2 at balloon pressure for 5 h. The reaction mixture was cooled to -10 °C, Et_3N (112 µL, 0.81 mmol) and a solution of HCO_2H/Ac_2O (1:0.8, 2 mL) were added and the mixture was further stirred for 1 h, while allowing the temperature to rise to 0 °C. The reaction mixture was diluted with water, extracted with CH_2Cl_2, the organic phase was dried, concentrated and the crude product was subjected to FCC (CH_2Cl_2:MeOH, 98:2) to yield 4'-methoxyindolyl-3'-formamide (**168**) (24 mg, 0.13 mmol) in 47% yield(Pedras and Yaya, 2012).

Procedure B: Pd/C (20 mg) was added to a solution of 4-methoxy-3-nitroindole (**167**) (20 mg, 0.10 mmol) in MeOH (1 mL) and solution of HCO_2H/Ac_2O (1.5:1) (55 µL, 0.62 mmol). The reaction mixture was stirred under H_2 at balloon pressure for 3 h at -10 °C and allowed to warm up to 10 °C for an additional 1 h. The reaction mixture was diluted with water, extracted with CH_2Cl_2, the organic phase was dried, concentrated and the crude product was subjected to FCC (CH_2Cl_2:MeOH, 98:2) to yield 4'-methoxyindolyl-3'-formamide (**168**) (12.6 mg 0.07 mmol) in 66 % yield and 4'-methoxyindolyl-3'-acetamide (**206**) (1.4 mg, 0.007) in 7% yield (Pedras and Yaya, 2012) (**Scheme 3.4**).

HPLC t_R = 5.6 min, method A.

UV (CH_3OH-H_2O, HPLC) λ_{max} (nm): 223, 250, 285.

FTIR (KBr, cm^{-1}) ν_{max}: 3399, 3302, 1661, 1502, 1263, 1085.

^{1}H NMR (500 MHz, CD_3OD) δ 8.25 (1H, s), 7.68 (1H, s), 7.00 (1H, dd, *J* = 8, 8 Hz), 6.91 (1H, d, *J* = 8 Hz), 6.46 (1H, d, *J* = 7.5 Hz), 3.93 (3H, s).

^{13}C NMR (125.8 MHz, CD_3OD) δ 160.5, 155.0, 136.6, 124.1, 115.5, 115.1, 111.3, 106.0, 99.9, 55.7.

HRMS-EI m/z 190.0736 $[M]^+$, calcd. for $C_{10}H_{10}N_2O_2$ 190.0742 (100%), 162.08 (20%), 147.0557 (74%).

HPLC-MS-ESI m/z [M+H]+ 191.2 (40%), 163.2 (100%).

3.3.3.2 Isocyalexin A (104)

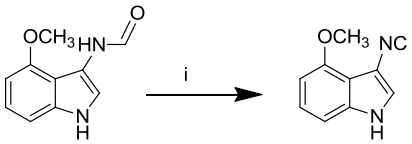

168 **104**

Scheme 3.5 Synthesis of isocyalexin A **104**. Reagents and conditions: i) $POCl_3$, THF, EtN_3, 0 °C; 10% aq Na_2CO_3, 41%.

Freshly distilled $POCl_3$ (22 µL, 0.23 mmol) was added to a stirred solution of 4'-methoxyindole-3'-formamide (**168**) (22 mg, 0.11 mmol) and Et_3N (48 µL, 0.34 mmol) in THF (1 mL) at 0 °C under inert atmosphere. The reaction mixture was stirred for 1 h at 0 °C, was neutralized (10% aq Na_2CO_3) and stirred for 30 min at room temperature. The reaction mixture was diluted with water, extracted with CH_2Cl_2, the organic layer was dried, concentrated, and the crude product was subjected to FCC (CH_2Cl_2 100%) to yield isocyalexin A (**104**) (8 mg, 0.05 mmol) in 41% yield (Pedras and Yaya, 2012) (**Scheme 3.5**).

HPLC t_R= 11.0 min, method A.

UV (CH_3CN-H_2O) λ_{max} (nm): 220, 269.

FTIR (KBr, cm^{-1}) ν_{max}: 3305, 3129, 2964, 2134, 1592, 1514, 1447, 1366, 1336, 1272, 1079.

^{1}H NMR (500 MHz, CD_3OD) δ 7.45 (1H, s), 7.10 (1H, dd, *J* = 8, 8 Hz), 6.97 (1H, d, *J* = 8.5 Hz), 6.58 (1H, d, *J* = 8 Hz), 3.91 (3H, s).

^{13}C NMR (125.8 MHz, CD_3OD) δ 164.1, 154.8, 137.3, 125.5, 124.3, 113.9, 106.4, 103.2 ($J_{C\text{-}3\text{-}N}$ = 15 Hz), 102.1, 56.0.

HREI-MS m/z 172.0633 $(M)^+$, calcd for $C_{10}H_8N_2O$ 172.0632 (100%), 157.04 (69%), 129.05 (69%).

HPLC-MS-ESI m/z $[M-H]^-$, 171.1 (11%), 156.0 (100%).

3.3.3.3 Indolyl-3'-formamide (169)

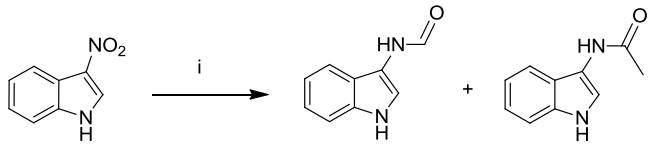

Scheme 3.6 Synthesis of indolyl-3'-formamide **169**. Reagents and conditions: ii) Pd/C-H_2, acetic-formic anhydride, -10 °C, 64%.

Procedure A: Pd/C (50 mg) was added to a solution of 3-nitroindole (**166**) (50 mg, 0.31 mmol) in EtOH (1 mL) and the reaction mixture was stirred under H_2 at balloon pressure for 5 h. The reaction mixture was cooled to -10 °C, Et_3N (129 µL, 0.93 mmol) and HCO_2H/Ac_2O (1:0.8, 2 mL) were added and the reaction mixture was further stirred for 1 h, while temperature was allowed to warm up to 0 °C. The reaction mixture was diluted with water, extracted with CH_2Cl_2, the organic phase was dried, concentrated and the crude product was subjected to FCC (CH_2Cl_2:EtOAC, 8:2) to yield indolyl-3-formamide (**169**) (12.5 mg, 0.08 mmol) in 25% yield and indolyl-3-acetamide (**207**) (5.2 mg, 0.03 mmol) in 9% yield (Pedras and Yaya, 2012).

Procedure B: Pd/C (25 mg) was added to a solution of 3-nitroindole (**166**) (20 mg, 0.12 mmol) in MeOH (1 mL) and HCO_2H/Ac_2O (1.5:1) (100 µL, 1.12 mmol). The reaction mixture was stirred under H_2 balloon pressure for 3 h at -10 °C and allowed to warm up to 10 °C for an additional 1 h. The reaction mixture was diluted with water, extracted by CH_2Cl_2, the organic phase was dried over Na_2SO_4 and concentrated to yield

indolyl-3'-formamide (**169**) (13 mg, 0.08 mmol) in 64% yield and indolyl-3'-acetamide (**207**) 4 mg, (0.02) in 18% yield (Pedras and Yaya, 2012) (**Scheme 3.6**).

HPLC t_R= 4.2 min, method A.

UV (CH_3OH-H_2O, HPLC) λ_{max} (nm): 222, 260.

FTIR (KBr, cm^{-1}) ν_{max} (cm^{-1}): 3263, 3057, 2922, 1665, 1565, 1458, 1385, 1237.

^{1}H NMR (500 MHz, CD_3OD) δ 8.27 (1H, s), 7.69 (1H, s), 7.60 (1H, d, *J* = 8 Hz), 7.32 (1H, d, *J* = 8 Hz), 7.12 (1H, dd, *J* = 8, 7 Hz), 7.02 (1H, dd, *J* = 8, 7 Hz).

^{13}C NMR (125.8 MHz, CD_3OD) δ 160.7, 135.6, 123.2, 122.0, 120.1, 118.1, 117.5, 114.7, 112.5.

HRMS-EI m/z 160.0635 $[M]^+$, calcd. for $C_9H_8N_2O$ 160.0637 (100%), 131.06 (59%), 104.05 (26%).

HPLC-ESI-MS m/z $[M+H]^+$, 161.3 (50%), 134.3 (100%).

3.3.3.4 Indolyl-3-isonitrile (170)

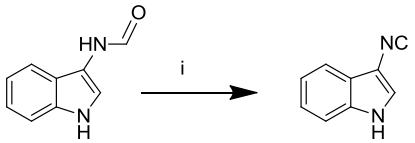

169 **170**

Scheme 3.7 Synthesis of indolyl-3-isonitrile **170**. Reagents and conditions: i) $POCl_3$, THF, EtN_3, 0 °C; 10% aq Na_2CO_3, 54%.

Freshly distilled $POCl_3$ (35 µL, 0.38 mmol) was added to a stirred solution of indolyl-3'-formamide (**169**) (30 mg, 0.19 mmol) and Et_3N (78 µL, 0.56 mmol) in THF (1 mL) at 0 °C under inert atmosphere. The reaction mixture was stirred for 1 h at 0 °C, neutralized (10% aq. Na_2CO_3) and further stirred for 30 min at room temperature. The reaction mixture was diluted with water (5 mL), extracted with CH_2Cl_2, the organic layer was dried, concentrated and the crude product was subjected to FCC (CH_2Cl_2, 100 %) to yield indolyl-3-isonitrile (**170**) (14 mg, 0.10 mmol) in 53% yield (Pedras and Yaya, 2012) (**Scheme 3.7**).

HPLC t_R= 10.3 min, method A.

UV (CH_3OH-H_2O, HPLC) λ_{max} (nm): 240, 279.

FTIR (KBr, cm^{-1}) ν_{max}: 3217, 2144, 1436, 1339, 1241.

^1H NMR (500 MHz, CD_3OD) δ 7.57 (1H, s), 7.55 (1H, d, *J* = 8 Hz), 7.39 (1H, d, *J* = 8 Hz), 7.20 (1H, dd, *J* = 7, 8, Hz), 7.15 (1H, dd, *J* = 7, 8, Hz).

^{13}C NMR (125.8 MHz, CD_3OD) δ 165.3, 135.7, 124.8, 124.6, 124.2, 122.1, 118.2, 113.4, 104.3 (t, 16 Hz, C-3).

HRMS-EI *m/z* 142.0531 $[M]^+$, calcd. for $C_9H_6N_2$ 142.0531 (100%), 115.04 (44%).

HPLC-MS-ESI *m/z* $[M-H]^-$ 141.0 (100%).

3.4 Syntheses of compounds

3.4.1 Synthesis of labeled compounds

3.4.1.1 [4,5,6,7-$^2H_4$]Indole (120a)

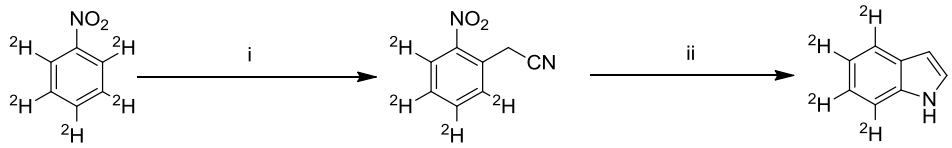

173a **174a** **120a**

Scheme 3.8 Syntheses of **120a**. Reagents and conditions: i) $ClCH_2CN$, NaOH, 49%; ii) Pd/C, AcOH, EtOAc, 68%.

[4,5,6,7-$^2H_4$]indole (**120a**) was synthesized from [2,3,4,5,6,-$^2H_5$]nitrobenzene (**173a**) by modifying a procedure reported by Pedras and Okinyo (Pedras and Okinyo, 2006c). A solution of [2,3,4,5,6,-$^2H_5$]nitrobenzene (**173a**) (4.0 mL, 39.00 mmol) and chloroacetonitrile (246 μL, 3.90 mmol) in DMSO (3.9 mL) was added drop wise over 30 min to a thoroughly stirred suspension of NaOH (1.56 g, 39.00 mmol) in DMSO (4 mL) at room temperature (Makosza and Winiarski, 1984). After 1 hour, the reaction mixture was quenched with ice-cold HCl (35 mL, 1 M), was diluted with H_2O (20 mL), and was extracted with $CHCl_3$ (50 mL × 3). The combined organic extract was washed with H_2O, dried, concentrated and subjected to FCC (hexane-EtOAc, 5:1) to yield a mixture of

[3,4,5,6-$^2H_4$]-2-nitrophenylacetonitrile and [2,3,5,6-$^2H_4$]-4-nitrophenylacetonitrile (**174**) (in a 10:1 ratio, 49% yield).

10% Pd/C (40 mg) was added to the solution of [3,4,5,6-$^2H_4$]-2-nitrophenylacetonitrile and [2,3,5,6-$^2H_4$]-4-nitrophenylacetonitrile (**174**) (106 mg, 0.64 mmol) in freshly distilled EtOAc (6 mL) and AcOH (177 μL) and the resulting reaction mixture was stirred under H_2 atmosphere (balloon pressure) at rt. After 16 h, the catalyst was filtered off, the filtrate was concentrated, the residue was taken in CH_2Cl_2 (20 mL), was washed with HCl (10 mL × 2, 1M). The organic layer was dried, and concentrated under reduced pressure to yield [4,5,6,7-$^2H_4$]indole (**120a**) (53 mg, 0.44) 69% yield (**Scheme 3.8**).

HPLC-DAD, t_R = 13.9 min, method A.

UV (CH_3CN-H_2O) λ_{max} (nm): 215, 275

^{1}H NMR (500 MHz $CDCl_3$) δ 8.14 (brs, NH), 7.23 (brs, 1H), 6.59 (brs, 1H).

HR-EIMS *m/z* measured 121.08293 calcd for $C_8H_3{}^2H_4N$ 121.008295 (100%), 94.07 (22).

3.4.1.2 [4',5',6',7'-$^2H_4$]Indoledesulfoglucosinolate (186a)

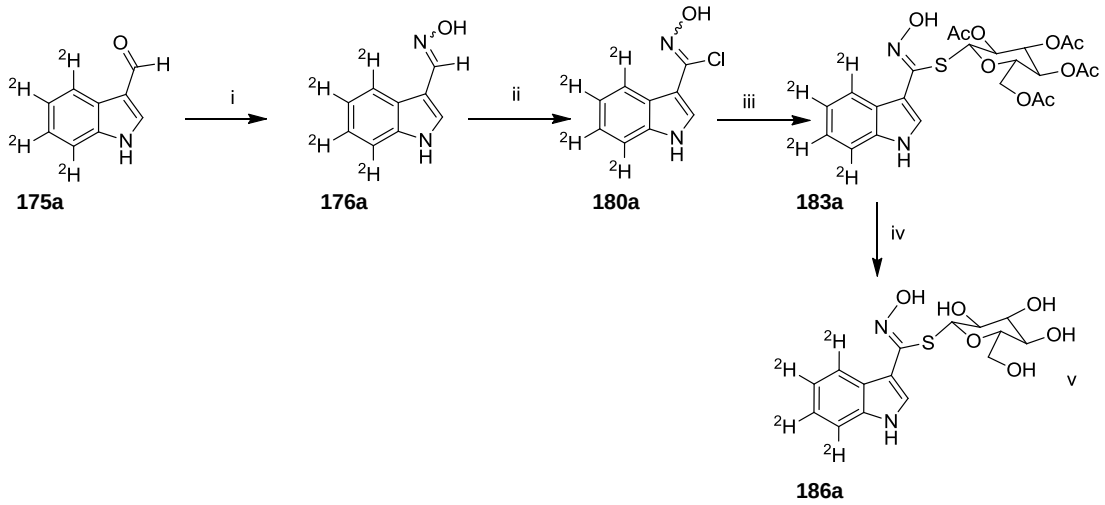

Scheme 3.9 Syntheses of **186a**. Reagents and conditions: i) Na_2CO_3, $NH_2OH.HCl$, 70 °C; ii) NCS, pyridine, CH_2Cl_2; iii) 1-thio-β-D-glucopyranose-2,3,4,6-tetraacetate, NEt_3, 22%; iv) $KOCH_3$, MeOH quant.

To a solution of [4',5',6',7'-$^2H_4$]indole-3'-carboxaldehyde (**175a**) (39 mg, 0.26 mmol) in EtOH (2 mL), a solution of Na_2CO_3 (28 mg, 0.26 mmol) and $NH_2OH.HCl$ (36 mg, 0.52 mmol) in water (1 mL) was added and stirred at 70 °C for 3 h. EtOH was removed, the reaction mixture was diluted with water and extracted with EtOAc. The organic layer was dried and concentrated under reduced pressure to yield [4',5',6',7'-$^2H_4$]indole-3'-carboxaldehyde oxime (**176a**) quantitatively.

NCS (27 mg, 0.20 mmol) was added to a solution of [4',5',6',7'-$^2H_4$]indole-3-carboxaldoxime (**176a**) (28 mg, 0.17 mmol) in pyridine (100 µL) and CH_2Cl_2 (1 mL) at 0 °C. The reaction mixture was stirred for 30 min at rt, 1-thio-β-D-glucopyranose-2,3,4,6-tetraacetate (37 mg, 0.10 mmol) in CH_2Cl_2 (0.2 mL) was added, and then Et_3N (71 µL, 0.51 mmol) and the reaction mixture was stirred for 3 h at rt. The reaction mixture was diluted with water, extracted with CH_2Cl_2, the organic layer was dried and concentrated. The residue was subjected to FCC (EtOAc-Hex, 1:1) to yield [4',5',6',7'-$^2H_4$]indolyl-3'-tetraacetyl glucocarboxythiohydroxamate (**183a**) (20 mg, 0.04 mmol, 22% from oxime).

$KOCH_3$ (75µL, 1 mM) was added to the solution of compound (**183a**) (20 mg, 0.04 mmol) in anhydrous MeOH (1 mL). The reaction mixture was stirred for 30 min and neutralized with acetic acid. The solvent was evaporated, the residue was dissolved in water and freeze dried to yield [4',5',6',7'-$^2H_4$]indole desulfoglucosinolate (**186a**) in quantitative yield **(**22 mg, 0.06 mmol) (**Scheme 3.9**).

HPLC t_R=6.1 min, method B.

UV (CH_3CN-H_2O) λ_{max} (nm): 270.

^{1}H NMR δ (500 MHz, CD_3OD) 7.71 (1H, s), 4.54 (1H, d, *J* = 10 Hz), 3.66 (1H, dd, *J* = 12, 2 Hz), 3.56 (1H, dd, *J* = 12, 5.5 Hz), 3.28-3.15 (2H, m), 3.15 (1H, dd, 9, 9 Hz), 2.77 (1H, m).

HR-ESI-MS *m/z* 397.0769 $[M+K]^+$, calcd for $C_{15}H_{14}{}^2H_4N_2O_6SK$ 397.0768 (28%), 224.11 (100%).

ESI-MS *m/z:* $[M+1]^+$ 197.1 (100%), 359.1 (96%).

3.4.1.3 Indoledesulfoglucosinolate (186)

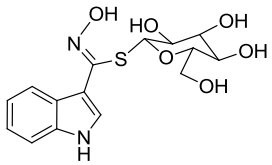

186

Indoledesulfoglucosinolate (**186**) was first synthesized by Rollin's group (Brochard, Joseph et al., 1994) as a standard for HPLC analysis of natural glucosinolates. A solution of $NH_2OH.HCl$ (95 mg. 1.37 mmol) and Na_2CO_3 (73 mg, 0.69 mmol) in water (1 ml) was added to a solution of indole-3'-carboxaldehyde (**175**) (100mg, 0.69 mmol) in EtOH (3 ml) and stirring at 70 ºC for 3 h. Excess EtOH was removed, the reaction mixture was diluted with water, extracted with EtOAc, the organic extract was dried and concentrated to yield indole-3'-carboxaldehyde oxime (**176**) (110 mg, 0.69 mmol) in quantitative yield.

NCS (20 mg, 0.15 mmol) was added to a solution of indole-3'-carboxaldehyde oxime (**176**) (20 mg, 0.13 mmol) in pyridine (100µL) and CH_2Cl_2 (1 mL) at 0 °C. The reaction mixture was stirred at rt for 30 min and then 1-thio-β-D-glucopyrasos-2,3,4,6-tetraacetate (29 mg, 0.08 mmol) in CH_2Cl_2 (0.2 mL) and Et_3N (54 µL) were added and stirred for 3 h. The reaction mixture was diluted with water (5 mL), extracted with CH_2Cl_2, dried, and concentrated. The residue was subjected to FCC (EtOAc:Hexane, 1:1) to yield indolyl-3'-tetraacetylgluco carboxythiohydroxamate (**183**) (32 mg, 0.06 mmol) in 47% from oxime.

$KOCH_3$ (75µL, 1mM) was added to a solution of indolyl-3-tetraacetylgluco carboxythiohydroxamate (**183**) (30 mg, 0.06 mmol) in anhydrous methanol (1 mL). The reaction mixture was stirred for 30 min and neutralized with acetic acid. The solvent was evaporated under reduced pressure to yield indole desulfoglucosinolate (**186**) (21 mg, 0.06 mmol) in quantitative yield (Brochard, Joseph et al., 1994).

HPLC t_R=6.1 min, method B.

UV (CH_3CN-H_2O) λ_{max}(nm): 270.

FTIR (KBr, cm^{-1}) ν_{max}: 3270, 2932, 1565, 1413, 1105, 1048, 747.

^{1}H NMR (500 MHz, CD_3OD) δ 7.83 (1H, d, *J*= 8 Hz), 7.70 (1H, s), 7.39 (1H, d, *J* = 8 Hz), 7.15 (1H, dd, *J* = 7, 8 Hz), 7.08 (1H, dd, *J* = 7, 8 Hz), 4.52 (1H, d, *J* = 10 Hz), 3.66 (1H, dd, *J* = 12, 2 Hz), 3.54 (1H, dd, *J* = 12, 5.5 Hz), 3.29-3.25 (2H, m), 3.13 (1H, dd, *J* = 9, 9 Hz), 2.74 (1H, m).

^{13}C NMR δ (125.8 MHz, CD_3OD). 149.3, 137.9, 128.7, 127.6, 123.4, 121.6, 121.3, 112.6, 110.4, 86.1, 82.0, 79.6, 74.4, 71.1, 62.5.

HR-ESI-MS *m/z* 393.0572 $[M+K]^+$, calcd for $C_{15}H_{19}N_2O_6SK$ 393.0517 (16%).

HPLC-ESI-MS *m/z* $[M+1]^+$ 355.1 (96%), 193.1 (100%).

3.4.1.4 (*R,S*)-[4',5',6',7'-$^{2}H_4$]Indolyl-3'-glycine (185a)

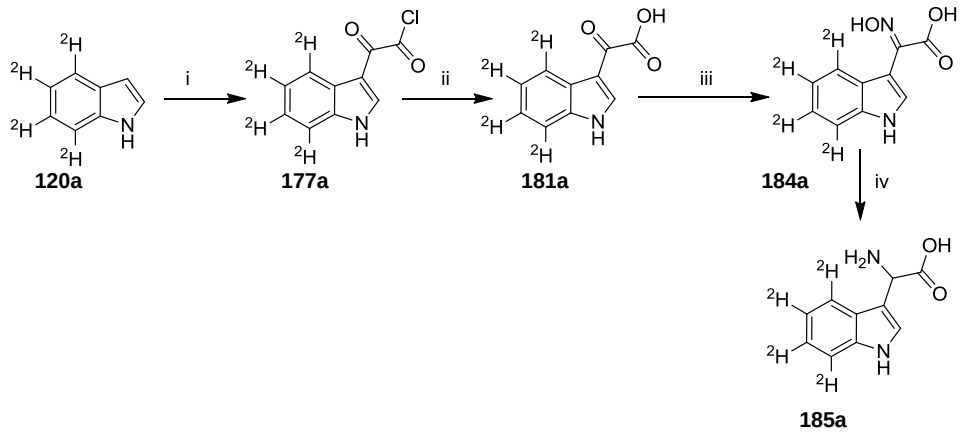

Scheme 3.10 Syntheses of **185a**. Reagents and conditions: i) $C_2O_2Cl_2$, Et_2O ii) NaOH; iii) NaOAc, $NH_2OH.HCl$, 70 °C; iv) $NaBH_4$, $NiCl_2.6H_2O$, 75% over all.

Oxalyl chloride (52 µL, 0.61 mmol) was slowly added to a solution of [4,5,6,7-$^{2}H_4$]indole (**120a**) (60 mg, 0.50 mmol) in anhydrous Et_2O (2 mL) at 0 ºC, and the reaction mixture stirred for 1 h at 0 ºC. The reaction mixture was filtered and residue was washed with ice cold ether and concentrated under reduced pressure to yield crude [4',5',6',7'-$^{2}H_4$]indolyl-3'-oxalylchloride (**177a**) in quantitative yield. NaOH (20%) was slowly added to a suspension of [4',5',6',7'-$^{2}H_4$]indolyl-3'-oxalylchloride (**177a**) (105 mg, 0.50 mmol) in THF to obtain pH 10. The reaction mixture was stirred at room temperature for 30 min, acidified (HCl, 2 M) and further stirred for 30 min. The reaction mixture was

diluted with water, extracted with EtOAc, the organic layer was dried and concentrated to yield [4',5',6',7'-$^2H_4$]indolyl-3'-oxo acid (**181a**) (72 mg, 0.37 mmol, 75% over two steps). A solution of $NH_2OH.HCl$ (108 mg, 1.55 mmol) and NaOAc (211 mg, 1.55 mmol) in water (1 mL) was added to a solution of [4',5',6',7'-$^2H_4$]indolyl-3'-oxo acid (**181a**) (50 mg, 0.26 mmol) in EtOH (2 mL). The reaction mixture was stirred for 3 hours at 70 ºC, EtOH was removed under reduced pressure and the residue was washed with CH_2Cl_2. The residue was diluted with water (10 mL), acidified (HCl, 1 M) and extracted with EtOAc. The organic extract was dried and concentrated to yield crude [4',5',6',7'-$^2H_4$]indolyl-3'-oximino acid (**184a**), which was taken to the next step without further purification. A solution of $NiCl_2.6H_2O$ (61 mg, 0.26 mmol) in EtOH (1 mL) was added to a solution of [4',5',6',7'-$^2H_4$]indolyl-3'-oximino acid (**184a**) (54 mg, 0.26 mmol) in EtOH (3 mL), followed by addition of $NaBH_4$ (30 mg, 0.78 mmol) over 20 min period. The reaction mixture was stirred at rt for 48 h, was acidified with HCl (1 M), the solvent was removed under reduced pressure, the residue was extracted with MeOH and the extract was concentrated to yield [4',5',6',7'-$^2H_4$]indolyl-3'-glycine (**185a**) (50 mg, 0.26 mmol) quantitatively (**Scheme 3.10**).

HPLC t_R=6.9 min, method B.

UV (CH_3CN-H_2O) λ_{max} (nm): 220, 275.

^{1}H NMR (500 MHz, CD_3OD) δ 7.58 (1H, s), 5.50 (1H, s).

HR-ESI-MS *m/z* 178.0796 $[M\text{-}NH_2]^+$, calcd for $C_{10}H_4{}^2H_4NO_2$ 178.0800 (100%).

HPLC-ESI-MS *m/z:* $[M\text{-}H]^-$ 193.1 (100%).

3.4.1.5 (*R,S*)-Indolyl-3'-glycine (185)

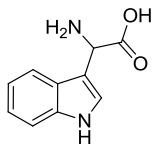

185

The first synthesis of indolyl-3'-glycine was reported by Drost and Wileland, (Droste and Wileland, 1987). Oxalylchloride (450 µL, 5.31 mmol) was slowly added to a

solution of indole (**120**) (500 mg, 4.27 mmol) in anhydrous diethyl ether (8 mL) at 0 °C. The reaction mixture was stirred for 1 h at 0 °C, solid was filtered off, washed with ice cold ether and concentrated under reduced pressure to yield crude indolyl-3'-oxalylchloride (**177**) (730 mg, 3.52 mmol) in 84% yield (Garg, Sarpong et al., 2002). NaOH (20 %) was slowly added to the suspension of indolyl-3'-oxalylchloride (**177**) (300 mg, 1.44 mmol) in THF to attain pH 10. The reaction mixture was stirred at room temperature for 30 min, was acidified by HCl (2 M) and further stirred for 30 min, diluted with water and extracted with EtOAc. The organic layer was dried and concentrated to yield indolyl-3'-oxo acid (**181**) as yellowish solid in (266 mg, 1.41 mmol) in 98% yield.

A solution of $NH_2OH.HCl$ (221 mg. 3.17 mmol) and NaOAc (430 mg, 3.17 mmol) in water (2 ml) was added to a solution of indolyl-3-oxo acid (**181**) (100 mg, 0.53 mmol) in EtOH (4 ml). The reaction mixture was stirred for 2 hours at 60 ºC, EtOH was removed under reduced pressure and the residue was washed with CH_2Cl_2. The residue was diluted in water (10 mL), acidified (HCl, 1 M) and extracted by EtOAc. The organic extract was dried, and concentrated to afford oximino acid (**184**) (99 mg, 0.48 mmol) in 91 % yield.

$NiCl_2.6H_2O$ (24 mg, 0.10 mmol) in EtOH (0.5 mL) was added to a solution of indolyl-3'-oximino acid (**184**) (20 mg, 0.10 mmol) in EtOH (1.5 mL) followed by addition of $NaBH_4$ (11 mg, 0.29 mmol) over a 15 min period. The reaction mixture was stirred at rt for 48 h, acidified (HCl, 1 M) and the solvent was removed. The residue was extracted with MeOH and the extract was concentrated to yield indolyl-3'-glycine (**185**) (23 mg, 0.12 mmol) quantitatively (Droste and Wileland, 1987).

HPLC t_R=6.9 min, method B.

UV (CH_3CN-H_2O) λ_{max}(nm): 220, 275.

FTIR (KBr, cm^{-1}) ν_{max}: 3389, 3000, 1737, 1488, 1454, 1426, 1193, 1105, 753.

^{1}H NMR (500 MHz, D_2O) δ 7.68 (1H, d, *J* = 8 Hz), 7.59 (1H, s), 7.57 (1H, d, *J* = 8.5 Hz), 7.31 (1H, dd, *J* = 8, 8 Hz), 7.23 (1H, dd, *J* = 8, 8 Hz), 5.51 (1H, s).

^{13}C NMR (125.8 MHz, D_2O) δ 171.7, 136.2, 127.0, 124.4, 122.7, 120.4, 117.9, 112.4, 105.0, 49.7.

HR-ESI-MS *m/z* 174.0556 $[M\text{-}NH_2]^+$, calcd for $C_{10}H_8NO_2$ 174.0555 (100%).

HPLC-ESI-MS *m/z* $[M-H]^-$ 189.1 (100%), 146.2 (16%).

3.4.1.6 [4',5',6',7'-$^2H_4$]Desulfoglucobrassicin (80a)

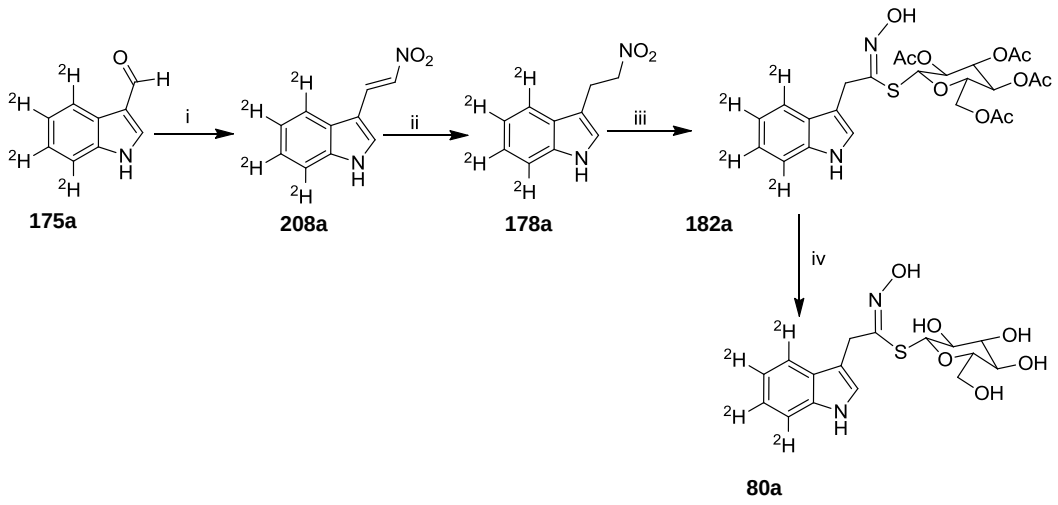

Scheme 3.11 Syntheses of **80a.** Reagents and conditions: i) CH_3NO_2, NH_4OAc; ii) $NaBH_4$, THF, MeOH 38%; iii) $NaOCH_3$, MeOH; $SOCl_2$, DME,-40 °C; 1-thio-β-D-glucopyranose-2,3,4,6-tetraacetate, Et_3N, CH_2Cl_2, Et_2O, 33%; iv) $KOCH_3$, MeOH.

NH_4OAc (13 mg, 0.16 mmol) was added to a solution of [4',5',6',7'-$^2H_4$]indole-3'-carboxaldehyde (**175a**) (48 mg, 0.32 mmol) in nitromethane (1 mL) and refluxed at 105 °C for 90 min. The reaction mixture was diluted with water, extracted by CH_2Cl_2 and concentrated to yield crude [4,5,6,7-$^2H_4$]-3-nitrovinylindole (**208a**), which was taken to the next step without further purification. $NaBH_4$ (38 mg, 0.96 mmol) was added to a solution of crude [4,5,6,7-$^2H_4$]-3-nitrovinylindole (**208a**) (62 mg, 0.32 mmol) in THF (2 mL) and MeOH (200 µL). The reaction mixture was stirred for 3 h at rt and excess $NaBH_4$ was destroyed by adding ice-cold water to the reaction mixture. The reaction mixture was extracted with CH_2Cl_2, the solvent was removed and the residue was subjected to FCC (100% CH_2Cl_2) to yield [4,5,6,7-$^2H_4$]-3-(2'-nitroethyl)indole (**178a**) (23 mg, 0.12 mmol, 38 % over two steps).

$NaOCH_3$ (23 mg/mL, 1mL) was added to a solution of [4,5,6,7-$^2H_4$]-3-(2'-nitroethyl)indole (**178a**) (23 mg, 0.12 mmol) in MeOH (1 mL), the reaction mixture was

stirred for 30 min at rt and the solvent was removed. The residue was suspended in DME (1 mL) at -40 °C, thionyl chloride (35 µL, 0.29 mmol) in DME (0.5 mL) was added drop wise and the reaction mixture was stirred for 1 h at -40 °C. The solvent was removed, the residue was diluted with water, extracted with CH_2Cl_2 and concentrated to yield the corresponding crude oximoyl chloride, which was taken to the next step without further purification. A solution of 1-thio-β-D-glucopyranose tetraacetate (22 mg, 0.09 mmol) in anhydrous CH_2Cl_2 (1 mL) and Et_3N (50 µL, 0.36 mmol) in Et_2O (1 mL) were successively added with stirring to a solution of crude oximoyl chloride in Et_2O-CH_2Cl_2 (2:1, 3 mL) at rt. After 3 h, the reaction mixture was diluted with water, extracted with CH_2Cl_2 and concentrated. The residue was subjected to FCC (CH_2Cl_2-MeOH, 98:2) to yield [4',5',6',7'-$^2H_4$]tetraacetyldesulfoglucobrassicin (**182a**) (22 mg, 0.04 mmol, 33%).

Freshly prepared $KOCH_3$ (1 mM, 75 µL) was added to a solution of [4',5',6',7'-$^2H_4$]tetraacetyldesulfoglucobrassicin (**182a**) (22 mg, 0.04 mmol) in anhydrous MeOH (1 mL) at rt under inert atmosphere, and the mixture was stirred for 30 min. The reaction mixture was neutralized with acetic acid and concentrated. The residue was dissolved in water and freeze-dried to yield [4',5',6',7'-$^2H_4$]desulfoglucobrassicin (**80a**) (23 mg, 0.06 mmol) quantitatively (**Scheme 3.11**).

HPLC t_R=11.9 min, method B.

UV (CH_3CN-H_2O) λ_{max} (nm): 222, 280.

^{1}H NMR δ (500 MHz, CD_3OD) δ 7.11 (1H, s), 4.68 (1H, d, *J* = 10 Hz), 4.23 (1H, d, *J* = 16 Hz), 3.92 (1H, dd, *J* = 16, 1 Hz), 3.78 (1H, dd, *J* = 12, 2 Hz), 3.59 (1H, dd, *J* = 12, 6 Hz), 3.22 (1H, dd, *J* = 9.5, 9.5 Hz), 3.13 (1H, dd, *J* = 9.9.5, 9 Hz), 3.06-3.03 (2H, m).

HR-EI-MS *m/z* 160.0931 $[M-(S\text{-}glc)\text{-}OH]^+$, calcd for $C_{10}H_4{}^2H_4N_2$ 160.0938 (74%), 134.09 (100%).

HPLC-ESI-MS *m/z* $[M+1]^+$ 373.1 (41%), 211.1 (100%).

3.4.1.7 Desulfoglucobrassicin (80)

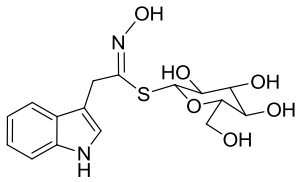

80

Desulfoglucobrassicin was synthesized following previously published procedure (Viaud and Rollin, 1990). NH_4OAc (266 mg, 3.40 mmol) was added to a solution of indole-3-carboxaldehyde (**175**) (1 g, 6.90 mmol) in nitromethane (6 mL) and refluxed at 105 °C for 90 min. The reaction mixture was diluted with water, extracted with CH_2Cl_2 and concentrated to give crude 3-nitrovinylindole (**208**), which was taken to the next step without further purification. $NaBH_4$ (830 mg, 21.58 mmol) was added portion by portion to the solution of 3-nitrovinylindole (**208**) (1.27 g, 6.90 mmol) in THF (35 mL) and methanol (5 mL). The reaction was stirred at rt for 3 h, excess $NaBH_4$ was destroyed by adding water, the reaction mixture was extracted with CH_2Cl_2, concentrated and the crude was subjected to FCC (CH_2Cl_2, 100%) to give 3-(2'-nitroethyl)indole (**178**) (540 mg, 2.84 mmol) in 41 %, over two steps.

$NaOCH_3$ (23 mg/mL, 1 mL) was added to the solution of 3-(2'-nitroethyl)indole (**178**) (50 mg, 0.26 mmol) in anhydrous methanol (1 mL). The reaction mixture was stirred at rt for 30 min and solvent was evaporated. The residue was suspended in DME (1 mL) at -40 ° C, thionyl chloride (50 µL, 0.65 mmol) in DME (1.5 mL) was added drop wise and the reaction mixture was stirred at -40 °C for 1 h. Excess solvent was evaporated, residue was diluted with water and extracted with CH_2Cl_2 and concentrated. Crude oximoyl chloride was taken to the next step without further purification. Solution of 1-thio-β-D-2,3,4,6-glucopyranose tetraacetate (48 mg, 0.13 mmol) in anhydrous CH_2Cl_2 (1 mL) and Et_3N (108 µL, 0.78) in Et_2O (1 mL) were added successively to the solution of crude oximoyl chloride in anhydrous (Et_2O: CH_2Cl_2 2:1, 3 mL) at rt. After 3 h, the reaction mixture was diluted with water, extracted with CH_2Cl_2, concentrated and

the crude was subjected FCC (CH_2Cl_2:MeOH 98:2) to yield tetraacetyl desulfoglucobrassicin (**182**) (60 mg, 0.11 mmol) in 43%..

Freshly prepared $KOCH_3$ (1 mM, 75 µL) was added to a solution of tetraacetyl desulfoglucobrassicin (15 mg, 0.03 mmol) in anhydrous MeOH (1 mL) under inert atmosphere at rt and stirred for 30 min. The reaction mixture was neutralized by acetic acid and concentrated. The residue was diluted with water and freeze dried to give desulfoglucobrassicin (**80**) (15 mg, 0.04 mmol) in quantitative yield (Robertson and Botting, 1999; Viaud and Rollin, 1990).

$[\alpha]_{D=}$ -44.5 (c 0.13, MeOH)

HPLC t_R=11.9 min, method B.

UV (CH_3CN-H_2O) λ_{max}(nm): 222, 280.

FTIR (KBr, cm-1) ν_{max}: 3389, 2889, 1456, 1422, 1340, 1048, 745.

^{1}H NMR (500 MHz, CD_3OD) δ 7.64 (1H, d, *J* = 8.0 Hz), 7.33 (1H, d, *J* = 8 Hz), 7.13 (1H, s), 7.09 (1H, dd, *J* = 8, 7.5 Hz), 7.01 (1H, dd, *J* = 7.5, 7.5 Hz), 4.68 (1H, d, *J* = 10 Hz), 4.25 (1H, d, *J* = 16 Hz), 3.94 (1H, d, *J* = 16 Hz), 3.80 (1H, d, *J* = 12 Hz), 3.59 (1H, m), 3.23 (1H, dd, *J* = 9.5, 9 Hz), 3.14 (1H, dd, *J* = 9, 9 Hz), 3.09-3.03 (2H, m).

^{13}C NMR (125.8 MHz, CD_3OD) δ 154,3, 138.2, 128.3, 124.1, 122.7, 120.0, 119.7, 112.4, 111.7, 83.0, 82.1, 79.5, 74.6, 71.3, 62.8, 30.4.

HR-EI-MS *m/z* 156.0685 $[M\text{-}(S\text{-}glc)\text{-}OH]^+$, calcd for $C_{10}H_8N_2$ 156.0687 (72%), 130.06 (100%). HPLC-ESI-MS *m/z* $[M+1]^+$ 368.9 (42%). 207.0 (100%), 174.0 (27%), 130.0 (40%)

3.4.1.8 [^2H_3CO]-4-Methoxyindole (149a)

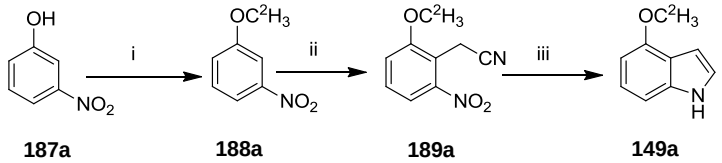

187a **188a** **189a** **149a**

Scheme 3.12 Synthesis of 4-methoxyindole (**149a)**. Reagents and conditions: i) NaH, ^2H_3CI, THF, 65°C; ii) 4-chlorophenoxyacetonitrile, *t*-BuOK, DMF,-20°C, 26%; (iii) 10% Pd/C, H_2, MeOH, AcOH 81%.

A solution of 3-nitrophenol (**187)** (100 mg, 0.72 mmol) in THF (1 mL) was added to a suspension of NaH (24 mg, 1.00 mmol) in THF (2 mL). The reaction mixture was stirred at room temperature for 10 min, ^2H_3CI (90 μL, 1.42 mmol) was added and the reaction mixture was stirred at 65 ºC for 5 hours. The reaction mixture was diluted with water, extracted with CH_2Cl_2, the organic layer was dried and concentrated to yield crude [^2H_3CO]-3-methoxynitrobenzene (**188a)** (112 mg, 0.73 mmol) in quantitative yield. A solution of [^2H_3CO]-3-methoxynitrobenzene (**188a)** (110 mg, 0.70 mmol) and 4-chlorophenyl acetonitrile (127 mg, 0.75 mmol) in DMF (2 mL) was slowly added to a suspension of *t*-BuOK (300 mg, 2.67 mmol) in DMF (1.5 mL) at -20 ºC. The reaction mixture was stirred at -20 ºC for 2 h, quenched with ice cold HCl (1 M) and extracted with EtOAc. The organic extract was washed with NaOH (2 M), dried and concentrated. The crude reaction mixture was subjected to FCC (EtOAc-Hex 1:3) to yield ([^2H_3CO]-6-methoxy-2-nitrophenyl) acetonitrile (**189a)** (37 mg, 0.19 mmol, 26%).

Palladium on carbon (10% Pd/C, 10 mg) was added to the solution of ([^2H_3CO]-6-methoxy-2-nitrophenyl) acetonitrile (50 mg, 0.25 mmol) in MeOH (2.5 mL) and AcOH (244 μL) and the resulting reaction mixture was stirred under H_2 atmosphere (balloon pressure) at rt. After 12 h, the catalyst was filtered off, and the filtrate was concentrated under reduced pressure. The residue was suspended in sat. $NaHCO_3$ (5 mL) and extracted with CH_2Cl_2. The organic layer was washed with water, dried and concentrated under reduced pressure to yield [^2H_3CO]-4-methoxyindole (**149a)** (30 mg, 0.20 mmol, 81%) (Mąkosza, Danikiewicz et al., 1988; Robertson and Botting, 1999) (**Scheme 3.12**).

HPLC t_R=12.5 min, method A.

UV (CH_3CN-H_2O) λ_{max} (nm): 220, 263.

^{1}H NMR (500 MHz, CD_3Cl) δ 8.16 (1H, brs), 7.13 (1H, dd, *J* = 7.5, 8 Hz), 7.13 (1H, s), 7.03 (1H, d, *J* = 8 Hz) 6.67 (1H, brs), 6.53 (1H, d, *J* = 7.5 Hz).

HR-EI-MS *m/z* 150.0872 (M^+), calcd for $C_9H_6{}^2H_3NO$ 150.0872 (100%), 132.04 (73%) 104.04 (36%).

HPLC-ESI-MS *m/z:* $[M+H]^+$ 151.1 (100%), 133.0 (44%).

3.4.1.9 [^2H_3CO]-4'-Methoxyindole-3'-carboxaldehyde (190a)

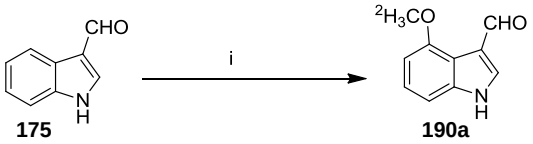

Scheme 3.13 Syntheses of **190a**. Reagents and conditions: i) TTFA, TFA; I_2, CuI; $NaOCD_3$, 78%

[^2H_3CO]-4'-Methoxyindole-3'-carboxaldehyde was synthesized from indole-3'-carboxaldehyde through a reaction route that involves thalliation and iodination (Somei, Yamada et al., 1984). A solution of TTFA (280 mg, 0.51 mmol) in TFA (2 mL) was added to indole-3'-carboxaldehyde (**175)** (50 mg, 0.34 mmol). The mixture was stirred for 3 h at 30 ºC and the solvent was removed under reduced pressure. Iodine (260 mg, 1.02 mmol), CuI (260 mg, 1.36 mmol) and DMF (2 mL) were added to the reaction mixture and the mixture was stirred for 1 h at 25 ºC. $NaOCD_3$ (prepared from Na 400 mg, 17.40 mmol in CD_3OD, 3 mL) was added and the reaction mixture was further stirred at 110 ºC for 1 h. The reaction mixture was cooled, neutralized (HCl, 1 M), filtered through celite, the filtrate was diluted with water and extracted with EtOAc. The organic layer was dried, concentrated and the crude product was subjected to FCC (EtOAc-Hex, 3:7) to yield [^2H_3CO]-4'-methoxyindole-3'-carboxaldehyde (**190a)** (47 mg, 0.26 mmol, 78%). The corresponding non-deuterated compound **190** was prepared similarly but using non-deuterated materials (Somei, Iwasa et al., 1986; Somei, Yamada et al., 1984) (**Scheme 3.13**).

Compound 26. M.P. 146-148 ºC

HPLC t_R=7.3 min, method A.

UV (CH_3CN-H_2O) λ_{max}(nm): 210, 250, 325.

FTIR (KBr, cm^{-1}) ν_{max}: 3194, 1718, 1644, 1624, 1512, 1383, 1271, 1100, 781.

^{1}H NMR (500 MHz, CD_3CN) δ 10.41 (1H, s), 10.2 (1H, brs), 7.90 (1H, s), 7.19 (1H, dd, *J* = 8, 8 Hz), 7.14 (1H, d, *J* = 8 Hz), 6.75 (1H, d, *J* = 7.5 Hz), 3.95 (3H, s).

^{13}C NMR (125.8 MHz, CD_3CN) δ 188.2, 155.4, 139.1, 129.8, 125.0, 119.9, 116.9, 106.6, 103.4, 56.1

HR-EI-MS *m/z* 175.0629 (M^+), calcd for $C_{10}H_9NO_2$ 175.0633 (100%), 160.04 (28%), 144.04 (26%) 129.06 (43%).

HPLC-ESI-MS *m/z* $[M-H]^-$ 173.9 (100%), 158.9 (98%).

Compound 26a. HPLC t_R=7.3 min, method A.

UV (CH_3CN-H_2O) λ_{max} (nm): 210, 250, 325.

^{1}H NMR (500 MHz, CD_3Cl) δ 10.51 (1H, s), 8.95 (1H, brs), 7.93 (1H, d, *J* = 3 Hz), 7.22 (1H, dd, *J* = 8, 8 Hz), 7.09 (1H, d, *J* = 8 Hz), 6.72 (1H, d, *J* = 7.5 Hz).

HR-EI-MS *m/z* 178.0819 (M^+), calcd for $C_{10}H_6{}^2H_3NO_2$ 178.0821 (100%), 145.05 (21%) 131.07 (32%).

HPLC-ESI-MS *m/z*: $[M-H]^-$ 176.9 (92%), 158.9 (100%).

3.4.1.10 [^2H_3CO]-4'-Methoxyindolyl-3'-acetonitrile (135a) (arvelexin)

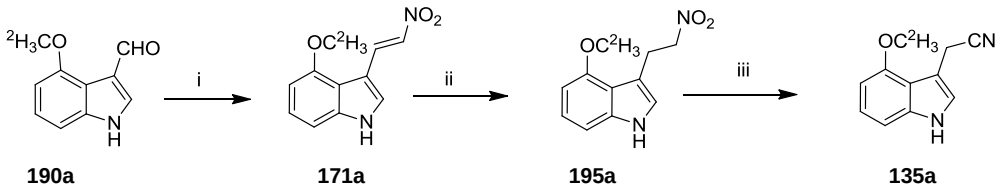

190a **171a** **195a** **135a**

Scheme 3.14 Syntheses of **135a**. Reagents and conditions: i) CH_3NO_2, NH_4OAc; ii) $NaBH_4$, THF, 38%; iii) CS_2, Et_3N, 62%

Synthesis of arvelexin was first reported by Pedras and co-workers, (Pedras, Chumala et al., 2003). A solution of TTFA (280 mg, 0.51 mmol) in TFA (2 mL) was

added to indole-3'-carboxaldehyde (**175a)** (50 mg, 0.34 mmol). The mixture was stirred for 3 h at 30 ºC. Solvent was removed under reduced pressure. Iodine (260 mg, 1.02 mmol), CuI (260 mg, 1.36 mmol) and DMF (2 mL) were added and stirred for 1 h at 25 °C. $NaOCD_3$ (prepared from Na 400 mg, 17.40 mmol in CD_3OD 3 mL) was added and the reaction mixture was further stirred at 110 ºC for 1 h. The reaction mixture was cooled, neutralized (HCl, 1 M), filtered through celite and the filtrate was diluted with water and extracted with EtOAc. The organic layer was dried, concentrated and the crude product was subjected to FCC (EtOAc-Hex, 3:7) to afford [^2H_3CO]-4'-methoxyindole-3'-carboxaldehyde (**190a)** (47 mg, 0.26 mmol, 79%) (Somei, Iwasa et al., 1986; Somei, Yamada et al., 1984).

NH_4OAc (14 mg, 0.18 mmol) was added to a solution of [^2H_3CO]-4'-methoxyindole-3'-carboxaldehyde (**190a)** (65 mg, 0.36 mmol) in nitromethane (1 mL) and refluxed at 105 °C for 90 min. The reaction mixture was allowed to cool, diluted with water, extracted with CH_2Cl_2 and concentrated to yield crude [^2H_3CO]-4-methoxy-3-nitrovinylindole (**192a)**, which was taken to the next step without further purification. $NaBH_4$ (42 mg, 1.11 mmol) was added to a solution of crude [^2H_3CO]-4-methoxy-3-nitrovinylindole (**192a)** (79 mg, 0.36 mmol) in THF (3 mL) and MeOH (300 µL). The reaction mixture was stirred for 3 h at rt, after which excess $NaBH_4$ was destroyed by adding ice-cold water to the reaction mixture. The reaction mixture was extracted with CH_2Cl_2, concentrated and subjected to FCC (CH_2Cl_2, 100%) to yield [^2H_3CO]-4-methoxy-3-(2'-nitroethyl)indole (**195a)** (27 mg, 0.12 mmol, 34%) (Robertson and Botting, 1999).

Et_3N (324 µL, 2.34 mmol) and CS_2 (72 µL, 1.20 mmol) were added to a solution of [^2H_3CO]-4-methoxy-3-(2'-nitroethyl)indole (**195a)** (26 mg, 0.12 mmol) in acetonitrile (1.5 mL) and the reaction mixture was stirred at 40 ºC for 20 h. The solvent was removed, the residue was diluted with water (10 mL) and extracted with CH_2Cl_2. The organic layer was dried, concentrated and the residue was subjected to FCC (CH_2Cl_2, 100%) to yield [^2H_3CO]-4'-methoxyindolyl-3'-acetonitrile (**135a)** (14 mg, 0.07 mmol, 62 %) (**Scheme 3.14**).

HPLC t_R=13.7 min, method A.

UV (CH_3CN-H_2O) λ_{max} (nm): 220, 260.

^{1}H NMR (500 MHz, CD_3Cl) δ 8.16 (1H, brs), 7.13 (1H, dd, *J* = 8, 8 Hz), 7.10 (1H, s), 6.98 (1H, d, *J* = 8 Hz), 6.51 (1H, d, *J* = 8 Hz), 4.06 (2H, s).

HR-EI-MS *m/z* 189.0977 $[M]^+$, calcd for $C_{11}H_7{}^2H_3N_2O$ 189.0981 (100%), 171.05 (92%).

HPLC-ESI-MS *m/z:* $[M+H]^+$ 190.2 (100%), 163.2 (48%), 150.3 (89%).

3.4.1.11 [$^2H_3$CO]-4'-Methoxybrassinin (108a)

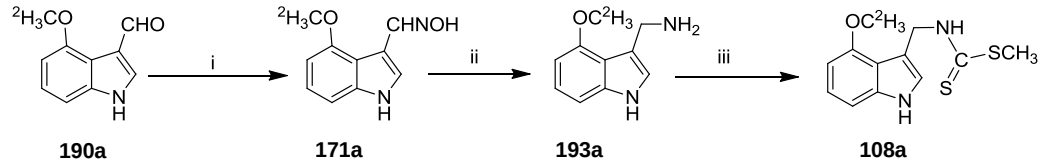

190a **171a** **193a** **108a**

Scheme 3.15 Syntheses of **108a**. Reagents and conditions: i) $NH_2OH.HCl$, Na_2CO_3, 70 ºC; iii) $NaBH_4$, $NiCl_2.6H_2O$, 54%; iv) CS_2, Et_3N, MeI, 77%.

A solution of $NH_2OH.HCl$ (78 mg. 1.12 mmol) and Na_2CO_3 (60 mg, 0.56 mmol) in water (1 ml) was added to a solution of [$^2H_3$CO]-4'-methoxyindole-3'-carboxaldehyde (**190a**) (100 mg, 0.56 mmol) in EtOH (2 mL). The reaction mixture was stirred at 70 ºC for 3 h, EtOH was removed under reduced pressure and the residue was diluted in water and extracted with EtOAc. The organic extract was dried and concentrated to yield [$^2H_3$CO]-4'-methoxyindole-3'-carboxaldehyde oxime (**171a**) (107 mg, 0.56 mmol) in a quantitative yield.

$NaBH_4$ (65 mg, 1.65 mmol) was added, portion by portion, to a solution of [$^2H_3$CO]-4'-methoxyindole-3'-carboxaldehyde oxime (**171a**) (107 mg, 0.56 mmol) and $NiCl_2.6H_2O$ (132 mg, 0.55 mmol) in EtOH (10 mL) at 0 °C. The reaction mixture was stirred for 1 h at room temperature, was concentrated to 1/3 of its original volume, was basified with aq. NH_3 (28%) (10 mL) and then extracted with EtOAc. The organic phase was dried, concentrated and subjected to FCC (CH_2Cl_2:MeOH:NH_4OH (80:20:1)) to afford ([$^2H_3$CO]-4'-methoxy-3'-indolyl) methanamine (**193a**) (53 mg, 0.29 mmol) in 54% yield.

CS_2 (22 µL, 0.35 mmol) was added to a solution of ([^2H_3CO]-4'-methoxy-3'-indolyl) methanamine (**193a**) (53 mg, 0.29 mmol) and Et_3N (82 µL, 0.59 mmol) in pyridine (0.5 ml) and CH_2Cl_2 (1 mL) and stirred for 20 min at 0 ºC. MeI (22 µL, 0.35 mmol) was added to the reaction mixture, stirred further for 1 h at rt, the reaction mixture was diluted with H_2O, extracted with CH_2Cl_2 and the organic extract was dried and concentrated. The residue was subjected to FCC (CH_2Cl_2 100 %) to afford [^2H_3CO]-4'-methoxybrassinin (**108a**) (60 mg, 0.22 mmol) in 77 % (Yamada, Kobayashi et al., 1993) (**Scheme 3.15**).

HPLC t_R = 20.3 min, method A.

UV (CH_3CN-H_2O) λmax (nm): 220, 265.

FTIR (KBr, cm^{-1}) νmax: 3395, 2935, 2834, 1505, 1359, 1255, 1079, 920, 732.

^1H NMR δ (500 MHz, $CDCCl_3$) 8.15 (1H, s), 7.96 (1H, s), 7.14 (1H, dd, *J* = 8, 8 Hz), 7.10 (1H, s), 7.01 (1H, d, *J* = 8 Hz), 6.57 (1H, d, *J* = 8 Hz) 5.13 (2H, d, *J* = 5.5 Hz), 2.63 (3H, s).

^{13}C NMR δ (125.8 MHz, $CDCCl_3$). 179.3, 153.4, 138.0, 123.3, 122.7, 116.7, 110.6, 105.1, 99.9, 43.6, 17.8.

HREI-MS m/z 269.0738 (M^+), calcd. for $C_{10}H_{11}{}^2H_3N_2OS_2$ 269.0738 (89), 254.05 (27), 195.0686 (28), 163.09 (100), 130.06 (31)

MS-ESI m/z $[M+1]^+$ 325 (100%), 163 (51%)

3.4.1.12 4'-Methoxybrassinin (108)

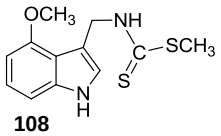

108

Synthesis of 4'-methoxybrassinin was first reported by Somei and co-workers (Yamada, Kobayashi et al., 1993). A solution of $NH_2OH.HCl$ (79 mg. 1.14 mmol) and Na_2CO_3 (60 mg, 0.57 mmol) in water (1 mL) was added to a solution of 4'-methoxyindole-3'-carboxaldehyde (**190**) (100 mg, 0.57 mmol) in EtOH (2 mL). The reaction mixture was stirred for 3 h at 70 ºC, EtOH was removed under reduced pressure

and residue was diluted in water (10 mL) and extracted with EtOAc. The organic extract was dried and concentrated to yield 4'-methoxyindole-3'-carboxaldehyde oxime (**171**) in quantitative yield. $NaBH_4$ (65 mg, 1.71 mmol) was added, portion by portion, to a solution of **171** (108 mg, 0.57 mmol) and $NiCl_2.6H_2O$ (136 mg, 0.57 mmol) in EtOH (10 mL) at 0 °C. The reaction mixture was stirred for 1 h at room temperature, was concentrated to 1/3 of its original volume, was basified with aq. NH_3 28% (10 mL) and then extracted with EtOAc. The organic phase was dried, concentrated and subjected to FCC (CH_2Cl_2:MeOH:NH_4OH (80:20:1)) to afford (4'-methoxy-3'-indolyl)methanamine (**193**) (66 mg, 0.38 mmol) in 66% yield.

CS_2 (13 µL, 0.23 mmol) was added to a solution of (4'-methoxy-3'-indolyl) methanamine (**193**) (35 mg, 0.20 mmol) and Et_3N (53 µL, 0.38 mmol) in pyridine (0.5 mL) and CH_2Cl_2 (1 mL) and stirred for 20 min at 0 ºC. MeI (14 µL, 0.23 mmol) was added and stirred further for 1 h at rt. The reaction mixture was diluted with H_2O, extracted with CH_2Cl_2 and the organic extract was dried and concentrated. The residue was subjected to FCC (CH_2Cl_2, 100%) to afford 4'-methoxybrassinin (**108**) (51 mg, 0.20 mmol) in quantitative yield (Yamada, Kobayashi et al., 1993).

HPLC t_R = 20.3 min, method A.

UV (CH_3CN-H_2O) λ_{max} (nm): 220, 265.

FTIR (KBr, cm-1) ν_{max}: 3395, 2935, 2834, 1505, 1359, 1255, 1079, 920, 732.

^{1}H NMR δ (500 MHz, $CDCCl_3$) 8.15 (1H, s), 7.96 (1H, s), 7.14 (1H, dd, *J* = 8, 8 Hz), 7.10 (1H, s), 7.01 (1H, d, *J* = 8 Hz), 6.57 (1H, d, *J* = 8 Hz) 5.13 (2H, d, *J* = 5.5 Hz), 4.01 (3H, s), 2.63 (3H, s).

HREI-MS m/z 266.05492 (M^+), calcd for $C_{12}H_{14}N_2OS_2$ 266.05475 (83%), 251.03 (23%), 192.05 (24%), 160.07 (100%), 130.06 (45%)

HPLC-ESI-MS m/z $[M+1]^+$ 319 (100%), 160 (51%)

3.4.1.13 (*R,S*)-[^2H_3CO]-4'-Methoxyindolyl-3'-glycine (107a)

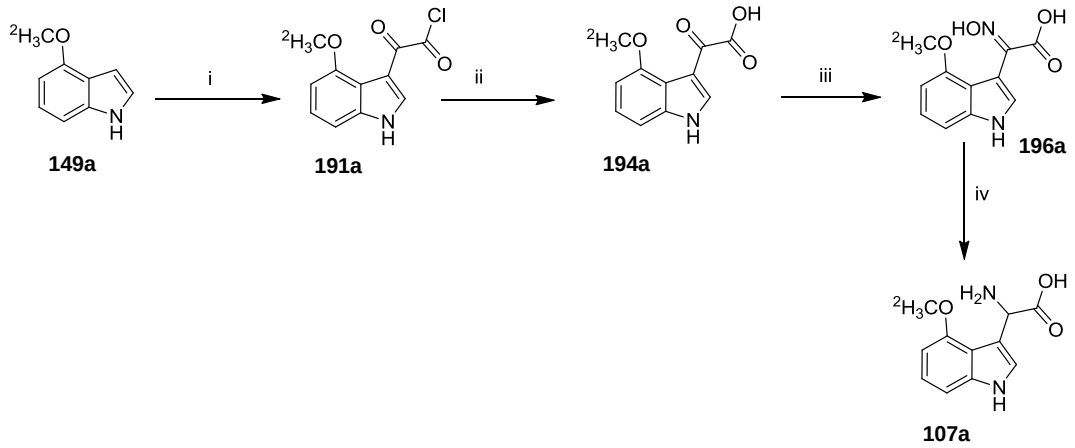

Scheme 3.16 Reagents and conditions: i) $C_2O_2Cl_2$, Et_2O ii) NaOH; iii) Na_2CO_3, $NH_2OH.HCl$, 70 °C; iv) $NaBH_4$, $NiCl_2.6H_2O$, 39% over all.

Oxalylchloride (39 µL, 0.44 mmol) was slowly added to a solution of [^2H_3CO]-4-methoxyindole (**149a**) (54.6 mg, 0.37 mmol) in anhydrous diethyl ether (2 mL) at 0 °C. The reaction mixture was stirred at 0 °C for 1 h, the solvent was removed, the residue was washed with ice cold ether and concentrated to yield crude [^2H_3CO]-4'-methoxyindolyl-3'-oxalylchloride (**191a**) (90 mg, 0.38 mmol). NaOH (20%) was slowly added to the suspension of crude [^2H_3CO]-4'-methoxyindolyl-3'-oxalylchloride (**191a**) (88 mg, 0.37 mmol) in THF (1 mL) to attain pH 10, the reaction mixture was stirred at room temperature for 30 min, acidified (HCl, 1 M) and stirred for 30 more minutes. The reaction mixture was diluted with water, extracted with EtOAc, the organic layer was dried, and concentrated to yield [^2H_3CO]-4'-methoxyindolyl-3'-oxo acid (**194a**) (83 mg, 0.37 mmol) quantitatively.

A solution of $NH_2OH.HCl$ (51 mg. 0.73 mmol) and Na_2CO_3 (39 mg, 0.37 mmol) in water (1 mL) was added to a solution of [^2H_3CO]-4'-methoxyindolyl-3'-oxo acid (**194a**) (82 mg, 0.37 mmol) in EtOH (3 mL). The reaction mixture was stirred at 70 ºC for 3 h, EtOH was removed under reduced pressure and the residue was washed with CH_2Cl_2. The residue was diluted with water (10 mL), acidified with HCl and extracted

with EtOAc. The organic extract was dried and concentrated to yield crude [^2H_3CO]-4'-methoxyindolyl-3'-oximino acid (**196a**) (74 mg, 0.31 mmol) in 84% yield over two steps.

A solution of $NiCl_2.6H_2O$ (63 mg, 0.27 mmol) in EtOH (1 mL) was added to a solution of [^2H_3CO]-4'-methoxyindolyl-3'-oximino acid (**196a**) (64 mg, 0.27 mmol) in ethanol (3 mL) followed by portion wise addition of $NaBH_4$ (30 mg, 0.78 mmol) over a period of 20 min. The reaction mixture was stirred at rt for 48 h, was acidified (HCl, 1 M) and the solvent was removed. The residue was extracted with methanol, was concentrated and subjected to FCC (CH_2Cl_2:MeOH:AcOH 80:20:1) to yield [^2H_3CO]-4'-methoxyindolyl-3'-glycine (**107a**) (28 mg, 0.13 mmol) in 47% (**Scheme 3.16**).

HPLC t_R= 6.8 min, Method B.

UV (CH_3CN-H_2O) λ_{max} (nm): 220, 265

FTIR (KBr, cm^{-1}) ν_{max}: 3181, 2928, 1624, 1504, 1466, 1362, 1246, 1088, 731.

^{1}H NMR (500 MHz, CD_3OD) δ 7.22 (1H, s), 7.07 (1H, dd, *J* = 8, 8 Hz), 7.00 (1H, d, *J* = 8 Hz), 6.56 (1H, d, *J* = 7.5 Hz), 5.12 (1H, s).

^{13}C NMR (125.8 MHz, CD_3OD) δ 173.9, 154.5, 139.9, 125.7, 124.2, 117.4, 109.9, 106.5, 100.9, 55.1.

HPLC-ESI-MS *m/z* $[M-H]^-$ 222.3 (34%), 205.3 (27%), 179.3 (41%), 161.3 (100%).

3.4.1.14 (*R,S*)-[^2H_3CO,5',6',7'-$^2H_3$]-4'-Methoxyindolyl-3'-glycine (107b)

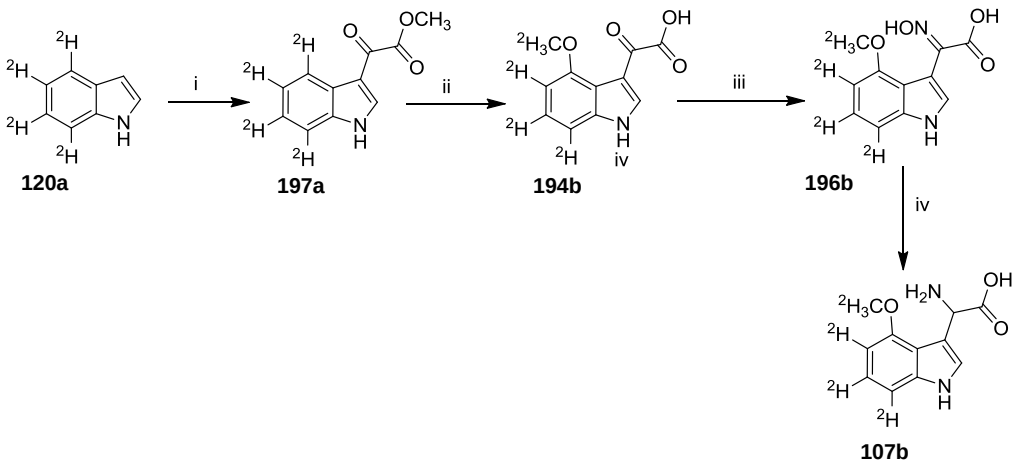

Scheme 3.17 Synthesis of **107b**. Reagents and conditions: i) $C_2O_2Cl_2$, Et_2O; MeOH; ii) TTFA, TFA; I_2, CuI; $NaOCD_3$; iii) $NH_2OH.HCl$, Na_2CO_3, 70 ºC; iv) $NaBH_4$, $NiCl_2.6H_2O$ 37% over all yield.

Oxalyl chloride (52 µL, 0.60 mmol) was slowly added to a solution of [4,5,6,7-$^2H_4$]indole (**120a**) (60 mg, 0.50 mmol) in anhydrous diethyl ether (2 mL) at 0 ºC. The reaction mixture was stirred for 1 h at 0 ºC, was filtered and the residue was washed with ice cold ether and concentrated under reduced pressure to yield crude [4',5',6',7'-$^2H_4$]indolyl-3'-oxalylchloride (**177a**) quantitatively. [4',5',6',7'-$^2H_4$]Indolyl-3'-oxalylchloride (**177a**) (100 mg, 0.48 mmol) was dissolved in MeOH (2 mL) and stirred at rt for 1 h. The solvent was evaporated under reduced pressure to yield methyl[4',5',6',7'-$^2H_4$]indolyl-3'-oxoacetate (197**a**) quantitatively. TTFA (209 mg, 0.38 mmol) was added to a solution of methyl[4',5',6',7'-$^2H_4$]indolyl-3'-oxoacetate (197**a**) (53 mg, 0.26 mmol) in TFA (2 mL) and stirred for 15 h at 60 °C. The solvent was evaporated under reduced pressure, a solution of I_2 (195 mg, 0.77 mmol) and CuI (195 mg, 1.02 mmol) in DMF (2 mL) was added to the reaction mixture and stirred for 1 h at 25 °C. Fresh $NaOCD_3$ (prepared from Na, 400 mg, 17.40 mmol, in anhydrous CD_3OD, 3 mL) was added to the reaction mixture and refluxed at 110 °C for 1 h. The reaction mixture was acidified (HCl, 1 M), filtered through celite and extracted with EtOAc. The organic layer was dried and

concentrated. The crude product was subjected to FCC (CH_2Cl_2-MeOH-AcOH, 80:20:1) to yield [$^2H_3$CO,5',6',7'-$^2H_3$]-4'-methoxyindolyl-3'-oxo acid (**194b**) (0.10 mmol, 22 mg, 37%). A solution of $NH_2OH.HCl$ (13 mg, 0.19 mmol) and Na_2CO_3 (10 mg, 0.09 mmol) in water (1 mL) was added to a solution of [$^2H_3$CO,5',6',7'-$^2H_3$]-4'-methoxyindolyl-3'-oxo acid (**194b**) (21 mg, 0.09 mmol) in EtOH (2 mL). The reaction mixture was stirred for 3 h at 70 ºC, EtOH was removed under reduced pressure and the residue was washed with CH_2Cl_2. The residue was dissolved in water (10 mL), acidified with HCl (1 M) and extracted with EtOAc. The organic extract was dried and concentrated to afford crude [$^2H_3$CO,5',6',7'-$^2H_3$]-4'-methoxyindolyl-3'-oximino acid (**196b**)quantitatively.

$NiCl_2.6H_2O$ (11 mg, 0.05 mmol) in EtOH (0.5 mL) was added to a solution of [$^2H_3$CO,5',6',7'-$^2H_3$]-4'-methoxyindolyl-3'-oximino acid (**196b**) (11 mg, 0.05 mmol) in EtOH (1 mL) followed by addition of $NaBH_4$ (5 mg, 0.13 mmol) over a period of 5 min. The reaction mixture was stirred at rt for 48 h, acidified (HCl, 1 M) and the solvent was removed. The residue was extracted with MeOH and the extract was concentrated to yield [$^2H_3$CO,5',6',7'-$^2H_3$]-4'-methoxyindolyl-3'-glycine (**107b**) quantitatively (**Scheme 3.17**).

HPLC t_R=6.8 min, method B.

UV (CH_3CN-H_2O) λ_{max}(nm): 220, 265.

^{1}H NMR (500 MHz, CD_3OD) δ 7.43 (1H, s), 5.32 (1H, s).

HR-ESI-MS *m/z*: 210.1033 $[M\text{-}NH_2]^+$, calcd. for $C_{11}H_4{}^2H_6NO_3$ 210.1031.

HPLC-ESI-MS *m/z*: $[M\text{-}H]^-$ 224.9 (34%), 207.9 (47%), 180.9 (38%), 162.9 (100).

3.4.1.15 (*R,S*)-4'-Methoxyindolyl-3'-glycine (107)

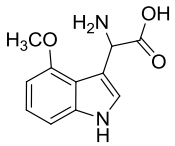

107

Oxalylchloride (32 µL, 0.41 mmol) was slowly added to a solution of 4-methoxyindole (**149**) (50 mg, 0.34 mmol) in anhydrous diethyl ether (2 mL) at 0 °C. The

reaction mixture was stirred for 1 h at 0 °C, solvent was evaporated and the residue was washed with ice cold ether and concentrated under reduced pressure to give crude 4'-methoxyindolyl-3'-oxalylchloride (**191**). NaOH (20 %) was slowly added to a solution of crude 4'-methoxyindolyl-3'-oxalylchloride (**191**) in THF (1 mL) to attain pH 10. The reaction mixture was stirred at room temperature for 30 min and acidified with HCl (2 M) and further stirred for 30 min. The reaction mixture was diluted with water and extracted with EtOAc. The organic layer was dried and concentrated to give 4'-methoxyindolyl-3'-oxo acid (**194**) (crude, 68 mg, 0.31mmol) in 91 % over two steps.

A solution of $NH_2OH.HCl$ (40 mg, 0.58 mmol) and NaOAc (31 mg, 0.29 mmol) in water (1 ml) was added to a solution of 4'-methoxyindolyl-3'-oxo acid (**194**) (64 mg, 0.29 mmol) in EtOH (2 ml). The reaction mixture was stirred for 3 h at 70 ºC, EtOH was removed under reduced pressure and the residue was washed with CH_2Cl_2. The residue was diluted with water (10 mL), acidified (HCl, 1 M) and extracted with EtOAc. The organic extract was dried, and concentrated to afford crude 4'-methoxy indolyl-3'-oximino acid (**196**) (55 mg, 0.24 mmol) in 81%.

A solution of $NiCl_2.6H_2O$ (55 mg, 0.24 mmol) in EtOH (1 mL) was added to a solution of 4'-methoxyindolyl-3'-oximino acid (**196**) (55 mg, 0.24 mmol) in Ethanol (3 mL) followed by portion wise addition of $NaBH_4$ (27 mg, 0.72 mmol) over a period of 20 min. The reaction mixture was stirred at rt for 48 h, was acidified (HCl, 1 M) and the solvent was removed. The residue was washed with CH_2Cl_2, extracted with methanol and concentrated to yield 4'-methoxyindolyl-3'-glycine (**107**) (44 mg, 0.20 mmol) in 83%.

M.P. 222-224 ºC

HPLC t_R= 6.8 min, method B.

UV (CH_3CN-H_2O) λ_{max}(nm): 220, 265.

FTIR (KBr, cm^{-1}) ν_{max} 3181, 2928, 1624, 1504, 1466, 1362, 1246, 1088, 731.

^{1}H NMR (500 MHz, CD_3OD) δ 7.11 (1H, s), 6.97 (1H, dd, *J* = 8, 8 Hz), 6.91 (1H, d, *J* = 8 Hz), 6.46 (1H, d, *J* = 7.5 Hz), 5.03 (1H, s), 3.83 (3H, s).

^{13}C NMR (125.8 MHz, CD_3OD) δ 173.9, 154.5, 139.9, 125.7, 124.2, 117.4, 109.9, 106.6, 100.9, 55.9, 53.9.

HR-ESI-MS *m/z*: $[M+H-NH_2]^+$ 204.0662, calcd for $C_{11}H_{10}NO_3$ 204.0665.

HPLC-ESI-MS *m/z* $[M-H]^-$ 219.2 (41%), 202.2 (24%), 176.2 (29%), 158 .2 (100%).

3.4.1.16 [^2H_3CO,5',6',7'-$^2H_3$]-4'-Methoxyindole-3'-carboxaldehyde oxime (171b)

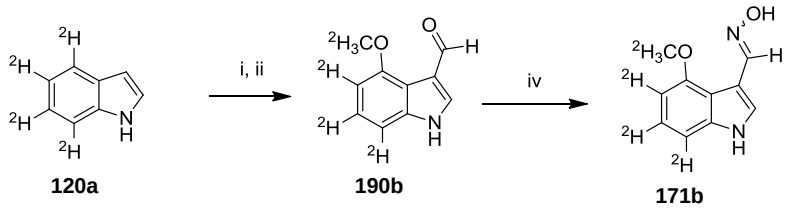

Scheme 3.18 Synthesis of **171b**. Reagents and conditions: i) $POCl_3$, DMF, 95%; ii) TTFA, TFA; I_2, CuI; $NaOCD_3$, 45%; iii) $NH_2OH.HCl$, Na_2CO_3, 70 ºC, 82%;

Freshly distilled $POCl_3$ (96 μL, 1.02 mmol) was added drop wise to a solution of [4,5,6,7-$^2H_4$]indole (**120a**) (83 mg, 0.69 mmol) in anhydrous DMF (1 mL) at 0 ºC. The reaction mixture was stirred for 1 h at rt, basified with aq. NH_3 (28%), diluted with water and extracted with EtOAc. The organic extract was dried and concentrated to yield [4',5',6',7'-$^2H_4$]indole-3'-carboxaldehyde (**175a**) (98 mg, 0.66 mmol, 95%). A solution of TTFA (260 mg, 0.49 mmol) in TFA (2 mL) was added to [4',5',6',7'-$^2H_4$]indole-3'-carboxaldehyde (**175a**) (49 mg, 0.33 mmol), the mixture was stirred 12 h at 30 ºC, and the solvent was removed under reduced pressure. DMF (2 mL), iodine (260 mg, 1.02 mmol) and CuI (260 mg, 1.36 mmol) were added (Somei, Iwasa et al., 1986) to the residue and the reaction mixture was stirred for 2 h at 25 °C. $NaOCD_3$ (prepared from Na 400 mg, 17.40 mmol in CD_3OD 3 mL) was added to the reaction mixture and the mixture was further stirred at 110 °C for 1 h. The reaction mixture was cooled to room temperature, neutralized (HCl, 1 M) and filtered through celite. The filtrate was diluted with water and extracted with EtOAc. The organic layer was dried, concentrated and the crude product was subjected to FCC (EtOAc-Hex, 3:7) to afford [^2H_3CO,5',6',7'-$^2H_3$]-4'-methoxyindole-3'-carboxaldehyde (**190b**) (27 mg, 0.15 mmol, 45%).

A solution of $NH_2OH.HCl$ (15 mg, 0.22 mmol) and Na_2CO_3 (13 mg, 0.12 mmol) in water (1 mL) was added to a solution of [^2H_3CO,5',6',7'-$^2H_3$]-4'-methoxyindole-3'-carboxaldehyde (**190b**) (20 mg, 0.11 mmol) in MeOH (2 mL) at 70 ºC. After 3 h, the solvent was removed, the residue was dissolved in water, extracted with EtOAc, the

organic phase was dried, concentrated and subjected to FCC (CH_2Cl_2-MeOH, 98:2) to yield [^2H_3CO,5',6',7'-$^2H_3$]-4'-methoxyindole-3'-carboxaldehyde oxime (**171b**) (18 mg, 0.09 mmol, 82%) (**Scheme 3.18**). The corresponding non-deuterated compound **171** was prepared similarly but using non-deuterated materials.

Compound 171. M.P. 205-207 ºC

HPLC t_R=7.9 min, method A.

UV (CH_3CN-H_2O) λ_{max}(nm): 220, 240, 295.

FTIR (KBr, cm-1) ν_{max}: 3260, 2932, 1620, 1379, 1267, 1100, 1026.

^{1}H NMR (500 MHz CD_3CN) δ 9.68 (1H, brs), 8.23 (1H, brs), 8.22 (1H, s), 8.21 (1H, d, *J* = 3 Hz), 7.13 (1H, dd, *J* = 8, 8 Hz), 7.08 (1H, d, *J* = 8 Hz), 6.64 (1H, d, *J* = 7.5 Hz), 3.94 (3H, s).

^{13}C NMR (125.8 MHz, CD_3CN) δ 155.5, 146.7, 142.2, 137.7, 131.1, 124.3, 108.0, 106.0, 102.0, 55.9

HR-EI-MS m/z 190.0741 (M^+), calcd for $C_{10}H_{10}N_2O_2$ 190.0742 (32%), 172.06 (100%), 157.04 (65%), 129.05 (72%).

HPLC-ESI-MS m/z $[M+H]^+$ 191.0 (100%), 174.0 (11%).

Compound 171b. HPLC-DAD, t_R=7.9 min, method A.

UV (CH_3CN-H_2O) λ_{max} (nm): 220, 240, 295.

^{1}H NMR (500 MHz CD_3CN) δ 9.68 (1H, br s), 8.23 (1H, s), 8.21 (1H, s).

HR-EI-MS *m/z* 196.1124 (M^+), calcd for $C_{10}H_4{}^2H_6N_2O_2$ 196.1119 (88%), 178.10 (100%), 160.05 (62%), 132.06 (44%).

HPLC-ESI-MS *m/z*: $[M+H]^+$ 197.0 (100%), 180.0 (12%).

3.4.1.17 [^2H_3CO,5',6',7'-$^2H_3$]Desulfoglucorapassicin (172b)

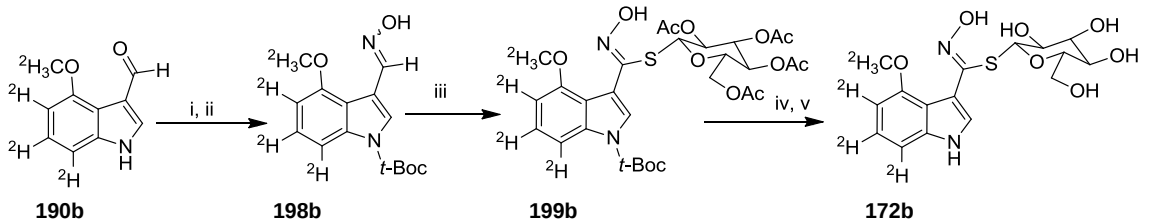

Scheme 3.19 Synthesis of **172b**. Reagents and conditions: i) $(t\text{-Boc})_2O$, DMAP, THF; ii) $NH_2OH.HCl$, Na_2CO_3, 60 ºC, 95%; iii) pyridine, NCS, DCM, 1-thio-β-D-glucopyranose tetraacetate, Et_3N, 52%; iv) D-TFA, CH_2Cl_2, 92%; v) $KOCH_3$, MeOH, quant.

(t-Boc)$_2$O (72 mg, 0.33 mmol) and DMAP (2 mg, 0.02 mmol) were added to a solution of [^2H_3CO,5',6',7'-$^2H_3$]-4'-methoxyindole-3'-carboxaldehyde (**190b**) (40 mg, 0.22 mmol) in THF (3 mL) at 0 ºC. The reaction mixture was stirred at rt for 2 h, was neutralized (HCl, 1M), diluted with water and extracted with CH_2Cl_2. The organic phase was dried and concentrated to yield crude *N*-*t*-Boc[^2H_3CO,5',6',7'-$^2H_3$]-4'-methoxyindole-3'-carboxaldehyde (63 mg, 0.22 mmol). A solution of $NH_2OH.HCl$ (31 mg, 0.44 mmol) and Na_2CO_3 (24 mg, 0.22 mmol) in water (1 mL) was added to a solution of *N*-*t*-Boc[^2H_3CO,5',6',7'-$^2H_3$]-4'-methoxyindole-3'-carboxaldehyde (63 mg, 0.22 mmol) in MeOH (4 mL) at 60 ºC. After 3 h the solvent was removed, the residue was dissolved in water and extracted with CH_2Cl_2. The organic phase was dried, and concentrated to yield crude *N*-*t*-Boc[^2H_3CO,5',6',7'-$^2H_3$]-4'-methoxyindole-3'-carboxaldehyde oxime (**198b**) (65 mg, 0.21 mmol) 95%. NCS (16 mg, 0.12 mmol) was added to a solution of *N*-*t*-Boc[^2H_3CO,5',6',7'-$^2H_3$]-4'-methoxyindole-3'-carboxaldehyde oxime (**198b**) (35 mg, 0.12 mmol) in CH_2Cl_2 (1 mL) and pyridine (100 µL) at 0 ºC and the reaction mixture was stirred for 30 min at rt. 1-Thio-β-D-glucopyranose-2,3,4,6-tetraacetate (26 mg, 0.06 mmol) in CH_2Cl_2 (200 µL) and Et_3N (50 µL, 0.36 mmol) were added to the reaction mixture and the mixture was stirred for 3 h at rt. The reaction mixture was diluted with water, extracted with CH_2Cl_2, the organic layer was dried, concentrated and the residue was subjected to FCC (EtOAc-Hexane, 1:1) to yield *N*-*t*-Boc[^2H_3CO,5',6',7'-

$^2H_3$]desulfoglucorapassicin tetraacetate (**199b**) (41 mg, 0.06 mmol, 52%). *N-t*-Boc[$^2H_3$CO,5',6',7'-$^2H_3$]desulfoglucorapassicin tetraacetate (**199b**) (41 mg, 0.06 mmol) was dissolved in CH_2Cl_2 (3.7 mL) and D-TFA (750 µL) and stirred at rt for 3 h. The reaction mixture was diluted with water and extracted with CH_2Cl_2. The organic layer was dried, concentrated and subjected to FCC (EtOAc-Hexane, 1:1) to yield [$^2H_3$CO,5',6',7'-$^2H_3$]desulfoglucorapassicin tetraacetate (31 mg, 0.06, 92%). Freshly prepared $KOCH_3$ (1 mM, 75 µL) was added to the solution of [$^2H_3$CO,5',6',7'-$^2H_3$]desulfoglucorapassicin tetraacetate (31 mg, 0.06 mmol) in anhydrous MeOH (1 mL) and stirred at rt for 30 min. The reaction mixture was neutralized with acetic acid and the solvent was evaporated under reduced pressure to yield [$^2H_3$CO,5',6',7'-$^2H_3$]desulfoglucorapassicin (**172b**) quantitatively (**Scheme 3.19**).

HPLC t_R=9.3 min, method B.

UV (CH_3CN-H_2O) λ_{max} (nm): 220, 270.

^{1}H NMR (500 MHz, CD_3OD) δ 7.28 (1H, s) 4.20 (1H, d, *J* = 10 Hz), 3.43-3.23 (4H, m) 2.98 (1H, dd, *J* = 9, 9 Hz), 2.24-2.21 (1H, m).

HR-MS-ESI *m/z* 429.1009 $[M+K]^+$, calcd for $C_{16}H_{14}{}^2H_6N_2O_7SK$ 429.1004 (100%), 391.1440 $[M+1]^+$ (82%), 229.0 (17%), 201 (36%).

HPLC-ESI-MS *m/z* $[M+H]^+$ 391.0 (100%), 229.0 (38%).

3.4.1.18 [$^2H_3$CO]Desulfoglucorapassicin(172a)

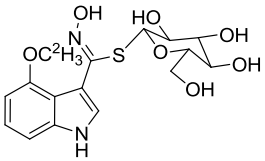

172a

(*t*-Boc)$_2$O (23 mg, 0.19 mmol) and DMAP (2 mg, 0.02 mmol) were added to a solution of [$^2H_3$CO]-4'-methoxyindole-3'-carboxaldehyde (**190a**) (23 mg, 0.13 mmol) in THF (1 mL) at 0 ºC. The reaction mixture was stirred at rt for 2 h, neutralized with HCl (1M), diluted with water and extracted with CH_2Cl_2. The organic phase was dried, and

concentrated to give *N*-*t*-Boc[^2H_3CO]-4'-methoxyindole-3'-carboxaldehyde (37 mg, 0.13 mmol) quantitatively.

$NH_2OH.HCl$ (19 mg, 0.27 mmol) and Na_2CO_3 (14 mg, 0.13 mmol) in water (1 mL) was added to a solution of *N*-*t*-Boc[^2H_3CO]-4'-methoxyindole-3'-carboxaldehyde (37 mg, 0.13 mmol) in methanol (3 mL) at 60 ºC and stirred for 3 hr. Excess solvent was evaporated, the residue was diluted with water and extracted with CH_2Cl_2. The organic phase was dried, concentrated and subjected to FCC (CH_2Cl_2:MeOH 98:2) to yield *N*-*t*-Boc[^2H_3CO]-4'-methoxyindole-3'-carboxaldehyde oxime (**198a**) (36 mg, 0.12 mmol) in 95%.

NCS (9 mg, 0.07 mmol) was added, portion by portion, to a solution of *N*-*t*-Boc[^2H_3CO]-4'-methoxyindole-3'-carboxaldehyde oxime (**198a**) (19 mg, 0.07 mmol) in CH_2Cl_2 (500 µL) and pyridine (50 µL) at 0 ºC and stirred at rt for 30 min. 1-Thio-β-D-glucopyrasos-2,3,4,6- tetraacetate (15 mg, 0.04 mmol) in CH_2Cl_2 (200 µL) and Et_3N (29 µL, 0.21 mmol) were added to the reaction mixture and stirred at rt for 3 h. The reaction mixture was diluted with water, extracted with CH_2Cl_2, the organic layer was dried, concentrated and subjected to FCC (EtOAc:Hexane 1:1) to yield *N*-*t*-Boc[^2H_3CO]desulfoglucorapassicin tetraacetate (**199a**) (24.2 mg, 0.04 mmol) in 52 %.

N-*t*-Boc[^2H_3CO]desulfoglucorapassicin tetraacetate (**199a**) (45 mg, 0.07 mmol) was dissolved in CH_2Cl_2 (1 mL) and TFA (200 µL) and stirred at rt for 3 h. The reaction mixture was diluted with water, extracted with CH_2Cl_2, the organic layer was dried, concentrated and subjected to FCC (EtOAc:Hexane 1:1) to yield [^2H_3CO]desulfoglucorapassicin tetraacetate (26 mg, 0.05 mmol) in 67%. Freshly prepared $KOCH_3$ (1 mM, 75 µL) was added to the solution of [^2H_3CO]desulfoglucorapassicin tetraacetate (26 mg, 0.05 mmol) in anhydrous MeOH (1 mL) and stirred at rt for 30 min. The reaction mixture was neutralized with acetic acid and the solvent was evaporated to yield [^2H_3CO]desulfoglucorapassicin (**172a**) (20 mg, 0.05 mmol) in quantitative yield.

HPLC t_R= 9.3 min, Method B.

UV (CH_3CN-H_2O) λ_{max} (nm): 220, 270.

FTIR (KBr, cm^{-1}) ν_{max}: 3160, 1687, 2926, 1667, 1405, 1263, 1085.

^{1}H NMR (500 MHz, CD_3OD) δ 7.32 (1H, s), 7.08 (1H, dd, *J* = 8, 8 Hz), 7.01 (1H, d, *J* = 8 Hz), 6.55 (1H, d, *J* = 7.5 Hz), 4.20 (1H, d, *J* = 10 Hz), 3.45-3.23 (4H, m), 2.98 (1H, dd, *J* = 9, 9 Hz), 2.24-2.21 (1H, m).

^{13}C NMR (125.8 MHz, CD_3OD) δ 155.7, 151.7, 137.4, 125.4, 122.8, 117.1, 106.2, 104.6, 100.4, 83.7, 80.0 78.2, 72.2, 69.2, 60.4.

HPLC-ESI-MS *m/z* $[M+H]^+$ 388 (100%), 226 (38%).

3.4.1.19 Desulfoglucorapassicin(172)

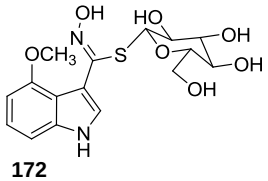

172

(*t*-Boc)$_2$O (95, 0.44 mmol) and DMAP (2 mg, 0.02 mmol) were added to a solution of 4'-methoxyindole-3'-carboxaldehyde (**190**) (50 mg, 0.29 mmol) in THF (2 mL) at 0 ºC. The reaction mixture was stirred for 3 h at rt, neutralized by HCl (1 M), diluted with water and extracted with CH_2Cl_2. The organic phase was dried, and concentrated to give *N*-*t*-Boc-4'-methoxyindole-3'-carboxaldehyde (99 mg, 0.35 mmol) in quantitative yield.

$NH_2OH.HCl$ (12 mg, 0.17 mmol) and Na_2CO_3 (9 mg, 0.08 mmol) in water (1 mL) was added to a solution of *N*-*t*-Boc-4'-methoxyindole-3'-carboxaldehyde (23 mg, 0.08 mmol) in methanol (2 mL) at 60 ºC and stirred for 3 h. Excess solvent was evaporated, the residue was diluted in water and extracted with CH_2Cl_2. The organic phase was dried, concentrated and subjected to FCC (CH_2Cl_2:MeOH 98:2) to yield *N*-*t*-Boc-4'-methoxyindole-3'-carboxaldehyde oxime (**198**) (22 mg, 0.07 mmol) in 93% yield.

NCS (7.2 mg, 0.05 mmol) was added, portion by portion, to a solution of *N*-*t*-Boc-4'-methoxyindole-3'-carboxaldoxime (**198**) (15.8 mg, 0.05 mmol) in CH_2Cl_2 (400 µL) at 0 ºC and stirred at rt for 30 min. 1-Thio-β-D-glucopyranos-2,3,4,6-tetraacetate (12 mg, 0.03 mmol) in CH_2Cl_2 (200 µL) and Et_3N (23 µL, 0.16 mmol) were added to the reaction mixture and stirred at rt for 3 h. The reaction mixture was diluted with water,

extracted with CH_2Cl_2, the organic layer was dried, concentrated and subjected to FCC (EtOAc:Hexane 1:1) to yield *N*-*t*-Bocdesulfoglucorapassicin tetraacetate (**199**) (19 mg, 0.03 mmol) in 52 % yield.

N-*t*-Bocdesulfoglucorapassicin tetraacetate (**199**) (12 mg, 0.02 mmol) was dissolved in CH_2Cl_2 (1 mL) and TFA (200 µL) and stirred at rt for 3 h. The reaction mixture was diluted with water and extracted with CH_2Cl_2. The organic layer was dried, concentrated and flash chromatographed (EtOAc:Hexane 1:1) to yield desulfoglucorapassicin tetraacetate (7.17 mg, 0.01 mmol) in 71% yield. Freshly prepared $KOCH_3$ (1 mM, 75 µL) was added to the solution of desulfoglucorapassicin tetraacetate (12.6 mg, 0.02 mmol) in anhydrous MeOH (1 mL) and stirred at rt for 30 min. The reaction mixture was neutralized with acetic acid and solvent was evaporated to yield desulfoglucorapassicin (**172**) (10 mg, 0.02 mmol) quantitatively.

HPLC t_R=9.3 min, method B.

UV (CH_3CN-H_2O) λ_{max}(nm): 220, 270.

FTIR (KBr, cm^{-1}) ν_{max}: 3160, 1667, 1405.

^{1}H NMR (500 MHz, CD_3OD) δ 7.32 (1H, s), 7.08 (1H, dd, *J* = 8, 8 Hz), 7.02 (1H, d, *J* = 8 Hz), 6.56 (1H, d, *J* = 7.5 Hz), 4.19 (1H, d, *J* = 10 Hz), 3.87 (3H, s), 3.45-3.23 (4H, m) 2.99 (1H, dd, *J* = 9, 9 Hz), 2.24-2.21 (1H, m).

^{13}C NMR (125.8 MHz, CD_3OD) δ 155.3, 153.2, 139.0, 127.0, 124.3, 118.7, 107.7, 106.2, 102.1, 85.3, 81.6, 79.8, 73.7, 70.7, 61.9, 56.2.

HR-EI-MS *m/z* 423.0632 $[M+K]^+$, calcd for $C_{16}H_{20}N_2O_7SK$ 423.0622 (100%).

HPLC-ESI-MS *m/z* $[M+H]^+$ 385.0 (100%), 223.0 (38%).

3.4.1.20 [^2H_3CO]Rapalexin A (103a)

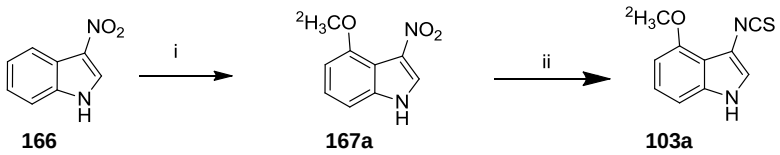

Scheme 3.20 Synthesis of [^2H_3CO]rapalexin A (**103a).** Reagents and conditions: i) TTFA, TFA; I_2, CuI; $NaOCD_3$, 54%; ii) Pd/C, H_2, THF, EtOH; $CSCl_2$, Et_3N, -10 °C, 51% over two steps.

TTFA (252 mg, 0.46 mmol) was added to a solution of 3-nitroindole (**166**) (50 mg, 0.31 mmol) in TFA (3 mL) and the reaction mixture was stirred for 4 h at 30 °C. The solvent was evaporated under reduced pressure, I_2 (236 mg, 0.93 mmol) and CuI (236 mg, 1.24 mmol) in DMF (4 mL) were added to the reaction mixture and the mixture was stirred for 1 h at 25 °C. $NaOCD_3$ (prepared from Na, 400 mg, 17.40 mmol, in D_3COD, 3 mL) was added to the reaction mixture and the mixture was refluxed at 110 °C for 1 h. The reaction mixture was neutralized (pH 7, HCl, 1 M), was filtered through celite and the solvent was evaporated. The residue was taken in water (10 mL), extracted with EtOAc, dried, concentrated and the crude product was subjected to FCC (EtOAc-Hexane, 1:1) to yield [^2H_3OC]-4-methoxy-3-nitroindole (**167a**) (33 mg, 0.17 mmol) in 54% yield.

Pd/C (25 mg) was added to a solution of [^2H_3OC]-4-methoxy-3-nitroindole (**167a**) (25 mg, 0.13 mmol) in THF (1 mL) and EtOH (200 µL) and the reaction mixture was stirred under H_2 at balloon pressure for 5 h. The reaction mixture was cooled to -10 °C, Et_3N (54 µL, 0.39 mmol) and $CSCl_2$ (12 µL, 0.16 mmol) were added and further stirred for 10 min. The reaction mixture was diluted with water, extracted with CH_2Cl_2, the organic phase was dried, concentrated and the crude product was subjected to FCC (CH_2Cl_2, 100%) to yield [^2H_3CO]rapalexin A (**103a**) (14 mg, 0.07) in 51% (Pedras and Yaya, 2012) (**Scheme 3.20**).

HPLC t_R = 16.9 min, method A.

UV (CH_3OH-H_2O, HPLC) λ_{max} (nm): 222, 292.

^{1}H NMR (500 MHz, $CDCl_3$) δ 7.94 (1H, s), 7.27 (1H, s), 7.16 (1H, dd, *J* = 8, 8 Hz), 7.07 (1H, d, *J* = 3 Hz), 6.94 (1H, d, *J* = 8 Hz), 6.56 (1H, d, *J* = 8 Hz).

HRMS-EI *m/z* 207.0544 $[M]^+$, calcd. for $C_{10}H_5{}^2H_3N_2S$ 207.0546 (100%), 189.01 (52%), 161.01 (27%).

HPLC-ESI-MS *m/z* $[M-H]^-$, 206.1 (100%), 188.1 (44%).

3.4.1.21 Rapalexin A (103)

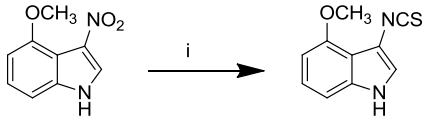

167 **103**

Scheme 3.21 Synthesis of rapalexin A (**103).** Reagents and conditions: i) Pd/C, H_2, THF, EtOH; $CSCl_2$, Et_3N, -10 °C, 59%.

Rapalexin A (**103**) was synthesized from 3-nitroindole (**166**) by modifying the first synthetic route (Pedras, Zheng et al., 2007a). Pd/C (25 mg) was added to a solution of 4-methoxy-3-nitroindole (**167**) (25 mg, 0.13 mmol) in THF (1 mL) and EtOH (200 µL) and the reaction mixture was stirred under H_2 at balloon pressure for 5 h. The reaction mixture was cooled to -10 °C, Et_3N (54 µL, 0.39 mmol) and $CSCl_2$ (12 µL, 0.16 mmol) were added and further stirred for 10 min. The reaction mixture was diluted with water, extracted with CH_2Cl_2, the organic phase was dried over Na_2SO_4 and concentrated. The crude product was subjected to FCC (CH_2Cl_2, 100%) to yield rapalexin A (**103**) (18 mg, 0.09) in 69% (Pedras and Yaya, 2012) (**Scheme 3.21**).

HPLC t_R = 16.9 min, method A

UV (CH_3OH-H_2O, HPLC) λ_{max} (nm): 222, 292.

FTIR (KBr, cm^{-1}) ν_{max}: 3399, 2072, 1592, 1508, 1280, 1100, 1075, 774, 729.

^{1}H NMR (500 MHz, $CDCl_3$) δ 7.94 (1H, s), 7.27 (1H, s), 7.16 (1H, dd, *J* = 8, 8 Hz), 7.07 (1H, d, *J* = 3 Hz), 6.94 (1H, d, *J* = 8 Hz), 6.57 (1H, d, *J* = 8 Hz), 3.98 (3H, s).

HRMS-EI *m/z* 204.03541 $[M]^+$, calcd. for $C_{10}H_8N_2OS$ 204.03573 (100%), 189.01 (53%), 161.01 (28%).

HPLC-ESI-MS *m/z* $[M-H]^-$, 203.1 (100%), 188.1 (44%).

3.4.1.22 [4',5',6',7'-$^2H_4$]Indole-3'-carboxaldehyde oxime (176a)

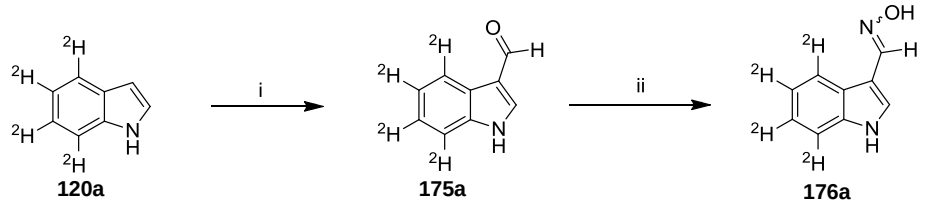

Scheme 3.22 Syntheses of **176a.** Reagents and conditions: i) $POCl_3$, DMF, 95%; ii) Na_2CO_3, $NH_2OH.HCl$, 70 °C, 92%.

Freshly distilled $POCl_3$ (96 μL, 1.02 mmol) was added drop wise to a solution of [4,5,6,7-$^2H_4$]indole (**120a)** (83 mg, 0.69 mmol) in anhydrous DMF (1 mL) at 0 ºC. The reaction mixture was stirred for 1 h at room temperature, basified with aq. NH_3 (28%), diluted with water and extracted with EtOAc. The organic extract was dried over Na_2SO_4 and concentrated to yield [4',5',6',7'-$^2H_4$]indole-3'-carboxaldehyde (**175a)** (98 mg, 0.65 mmol, 95%). A solution of $NH_2OH.HCl$ (70 mg, 1.00 mmol) and Na_2CO_3 (53 mg, 0.50 mmol) in water (1 mL) was added to a solution of [4',5',6',7'-$^2H_4$]indole-3'-carboxaldehyde (**175a)** (75 mg, 0.50 mmol) in EtOH (2 mL) at 70 ºC. After 3 h the solvent was removed, the residue was dissolved in water and extracted with EtOAc. The organic phase was dried, concentrated and subjected to FCC (CH_2Cl_2-MeOH, 98:2) to yield [4',5',6',7'-$^2H_4$]indole-3'-carboxaldehyde oxime (**176a)** (76 mg, 0.46 mmol, 92%) (**Scheme 3.22**).

HPLC-DAD, t_R = 6.3 min, method A.

UV (CH_3CN-H_2O) λ_{max} (nm): 230, 260.

^1H NMR (500 MHz CD_3CN) δ 9.76 (1H, brs), 8.25 (1H, d, *J* = 3 Hz), 7.73 (1H, s).

HR-EI-MS m/z 164.0885 (M^+), calcd for $C_9H_4{}^2H_4N_2O$ 164.0887 (20%), 147.08 (100%), 119.07 (35%).

HPLC-ESI-MS m/z $[M+H]^+$ 165.1 (100%), 148.1 (48%).

3.4.1.23 *N-t*-Bocindole glucosinolate (204)

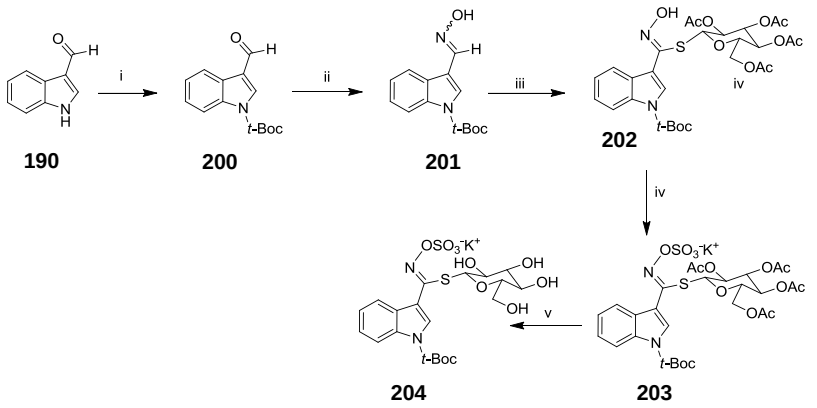

Scheme 3.23 Synthesis of **204**. Reagents and conditions: i) DMAP, $(t\text{-Boc})_2O$, THF quant.; ii) Na_2CO_3, $NH_2OH.HCl$, EtOH, 60 °C, quant; iii) pyridine, NCS, DCM; 1-thio-β-D-glucopyranose tetraacetate, NEt_3, 37%; iv) $ClSO_3H$, pyridine, DCM/ether, 66%; v) $KOCH_3$, MeOH, quantitative.

DMAP (2 mg, 0.02 mmol)) was added to a solution of indole-3'-carboxaldehyde (**175**) (300 mg, 2.06 mmol) and $(t\text{-Boc})_2O$ (541 mg, 2.48 mmol) in dry THF (10 mL) at 0 °C. The reaction mixture was stirred for 2 h at rt, solvent was evaporated under reduced pressure and residue was taken in water and extracted with EtOAc. The organic phase was dried over Na_2SO_4 and concentrated to yield *N-t*-Bocindole-3'-carboxaldehyde (**200**) (506 mg, 2.06 mmol) quantitatively.

To a solution of *N-t*-Bocindole-3'-carboxaldehyde (**200**) (300 mg, 1.22 mmol) in MeOH (10 mL), a solution of Na_2CO_3 (138 mg, 1.30 mmol) and $NH_2OH.HCl$ (181 mg, 2.6 mmol) in water (2 mL) was added and stirred at 60 °C for 2 h. Excess MeOH was evaporated, the reaction mixture was diluted with water and extracted with EtOAc. The organic layer was dried, and concentrated under reduced pressure to yield *N-t*-Bocindole-3'-carboxaldehyde oxime (**201**) (334 mg, 1.30 mmol) quantitatively.

NCS (120 mg, 0.90 mmol) was added to a solution of *N-t*-Bocindole-3'-carboxaldehyde oxime (**201**) (230 mg, 0.90 mmol) in pyridine (100µL) and CH_2Cl_2 (2

mL) at 0 °C. The reaction mixture was stirred for 30 min at the rt and then 1-thio-β-D-glucopyrasos-2,3,4,6-tetraacetate (182 mg, 0.47 mmol) and Et_3N (391 µL, 2.82 mmol) were added and the reaction mixture was stirred for 3 h. The reaction mixture was diluted with water, extracted with CH_2Cl_2, dried, concentrated and the residue was subjected to FCC (EtOAc-Hexane 1:1) to yield *N*-*t*-Bocindolyl-3'-tetraacetylgluco carboxythiohydroxamate (**202**) (205 mg, 0.33 mmol) 37% from oxime (Brochard, Joseph et al., 1994).

To a solution of (**202**) (100 mg, 0.16 mmol) in dry CH_2Cl_2 (500 µL) and dry pyridine (600 µL) at 0 °C, a solution of HSO_3Cl (21 µL, 0.32 mmol) in dry ether (500 µL) was slowly added. The reaction mixture was stirred for 24 h and neutralized with $KHCO_3$ solution (100 mg/mL) to pH 7 and stirred for 1 h. The reaction mixture was diluted with water and extracted by CH_2Cl_2, dried and concentrated. The residue was subjected to FCC (CH_2Cl_2-MeOH 95:5) to yield *N*-*t*-Boctetraacetylindole glucosinolate (**203**) (74 mg, 0.11 mmol) in 67% yield.

$KOCH_3$ (75µL, 1mM) was added to solution of **203** (32 mg, 0.05 mmol) in anhydrous methanol (1mL). The reaction mixture was stirred for 30 min and neutralized with acetic acid. The solvent was evaporated, residue was dissolved in water, extracted by EtOAc and the aqueous layer was freeze dried to yield *N*-*t*-Bocindole glucosinolate (**204**), 31 mg, in quantitative yield (Viaud and Rollin, 1990) (**Scheme 3.23**).

HPLC t_R = 28.2 min, method B

UV (CH_3CN-H_2O) λ_{max} (nm): 220, 285, 295.

FTIR (KBr, cm^{-1}) ν_{max}: 3396, 2982, 2925, 1738, 1559, 1451, 1373, 1240, 1062, 766.

^{1}H NMR δ (500 MHz, D_2O) 8.21 (1 H, d, *J* = 8 Hz), 8.18 (1H, d, *J* = 2 Hz), 7.87 (1H, d, *J* = 8 Hz), 7.52 (1H, dd, *J* = 8, 8 Hz), 7.45 (1H, dd, *J* = 8, 8 Hz), 4.58 (1H, d, *J* = 10 Hz), 3.55-3.37 (5H, m), 3.26 (1H, dd, *J* = 9, 9 Hz), 2.7 (1H, m).

^{13}C NMR δ (125.8 MHz, D_2O) 170.7, 150.7, 145.2, 136.8, 129.6, 129.1, 126.6, 124.6, 122.3, 116.6, 83.1, 76.5, 74.4, 71.5, 69.1, 62.7, 28.7.

HPLC-ESI-MS m/z $[M]^-$ 533.1 (100).

3.5 Administration of precursors to *Thellungiella salsuginea* (salt cress)

Four-week-old potted plants were irradiated with a 30 W (UV λ_{max} 254 nm) lamp for 60 min in a laminar flow cabinet. After UV-irradiation, plants were allowed to stand in flow cabinet under fluorescent light for 3 h, and then were uprooted, the leaves were cut at the base of the petiole and were immediately immersed in tubes containing an aqueous solution of the precursor (4 ml, 5×10^{-4} M dissolved in H_2O or H_2O-CH_3OH-Tween 80, 90:10:0.1, v/v). On average, leaves of two plants were used per precursor, experiments were conducted in triplicate and repeated at least twice for each precursor. Following the uptake of each precursor solution (ca. 12 h), the tubes were filled with H_2O and leaves were further incubated for 48 h under continuous fluorescent light. The leaves were frozen in liq. nitrogen, extracted with methanol (20 ml), the methanol extract was filtered off, and was concentrated to dryness. The methanolic residue was extracted with CH_2Cl_2, the CH_2Cl_2 fraction was concentrated under reduced pressure, and the residue was dissolved in acetonitrile (500 µl) to yield the non-polar fraction containing mostly phytoalexins for HPLC-DAD and HPLC-ESI-MS analysis. The insoluble residue was dissolved in MeOH-H_2O (1:1, 1 mL)) and was filtered to yield the polar fraction for HPLC-DAD and HPLC-ESI-MS analysis.

3.6 Administration of precursors to *Brassica napus* (rutabaga)

3.6.1 Extraction of phytoalexins

Rutabaga tubers were cut horizontally in 10-15 mm thick discs and cylindrical holes (16 mm in diameter) were made on one surface of the discs with a cork-borer (Pedras et al., 2004). The discs were kept in tightly sealed plastic boxes and incubated at 21-23 °C in darkness. After 24 h, the discs were UV-irradiated on the surface with holes for 1.5 h, and were incubated for further 24 h. Precursors (5×10^{-4} M) dissolved in H_2O, H_2O-CH_3OH (90:10 v/v) or H_2O-CH_3OH-Tween 80 (90:10:0.1 v/v) were pipetted into

each hole (500 µL per hole) and the discs were further incubated at 21-23 °C in dark. Following adsorption of precursor solution, holes were filled with water. 48 h later the aqueous solution in the holes was harvested and was extracted with EtOAc (20 ml x 2). The combined organic extract was dried over Na_2SO_4 and solvent was removed under reduced pressure. The residue obtained was dissolved in CH_3CN (200 µl) and was analyzed by HPLC-DAD, HPLC-ESI-MS, and HPLC-HRMS-ESI. Control experiments were similarly prepared by incubating rutabaga root tubers with non-labeled precursors or with carrier solution only.

3.6.2 Extraction of glucosinolates

Tissue around the holes was cut, soaked in CH_3OH, ground inside a mortar and extracted with CH_3OH. Extraction was carried out overnight on a shaker, after which the tissue was filtered off and the filtrate was concentrated under reduced pressure. The crude extract was dissolved in H_2O-CH_3OH (1:1) and analyzed by HPLC-DAD, HPLC-ESI-MS, and HR-ESI-MS.

3.7 Antifungal bioassays

Leptosphaeria maculans, *Rhizoctonia solani* AG 2-1, *Sclerotinia sclerotiorum*, *Alternaria brassicicola* were obtained from AAFC, Saskatoon, Canada. Solid cultures were initiated with spores of *A. brassicicola* and *L. maculans*, *sclerotia* of *S. sclerotiorum*, and mycelia of *R. solani* were grown on potato dextrose agar (PDA) plates at 23 ± 2 ºC, under constant light and mycelial plugs cut from the edge of actively growing cultures used to initiate bioassay cultures, as follows.

Solutions of each compound in DMSO were used to prepare sterile assay plates (6 wells per plate, 36 mm diameter, 2 ml per well) in PDA media (5.0×10^{-4} M, 2.0×10^{-4} M, 1.0×10^{-4} M). Control plates contained 1% DMSO in PDA. Plates containing test

solutions and the control solution were inoculated with mycelia plugs (4 mm diameter) placed upside down on the center of each plate, the plates were sealed with parafilm, and incubated at 23 ± 2 ºC under constant light for 24 h for *S. sclerotiorum*, 72 h for *R. solani*, 120 h for *L. maculans* (isolates BJ-125 and Laird-2) and *A. brassicicola*. The radial growth of mycelia was measured and compared with control plates containing only DMSO. Each experiment was conducted in triplicate and repeated three times.

4 REFERENCES

Abbaoui, B., Riedl, K. M., Ralston, R. A., Thomas-Ahner, J. M., Schwartz, S. J., Clinton, S. K., Mortazavi, A., 2012. Inhibition of bladder cancer by broccoli isothiocyanates sulforaphane and erucin: characterization, metabolism, and interconversion. Molecular Nutrition and Food Research 56, 1675-1687.

Agerbirk, N., Olsen, C. E., 2012. Glucosinolate structures in evolution. Phytochemistry 77, 16-45.

Agerbirk, N., Petersen, B. L., Olsen, C. E., Halkier, B. A., Nielsen, J. K., 2001. 1,4-Dimethoxyglucobrassicin in *Barbarea* and 4-hydroxyglucobrassicin in *Arabidopsis* and *Brassica*. Journal of Agricultural and Food Chemistry 49, 1502-1507.

Ahuja, I., Kissen, R., Bones, A. M., 2012. Phytoalexins in defense against pathogens. Trends in Plant Science 17, 73-90.

Andersson, D., Chakrabarty, R., Bejai, S., Zhang, J. M., Rask, L., Meijer, J., 2009. Myrosinases from root and leaves of *Arabidopsis thaliana* have different catalytic properties. Phytochemistry 70, 1345-1354.

Angelova, S., Buchheim, M., Frowitter, D., Schierhorn, A., Roos, W., 2010. Overproduction of alkaloid phytoalexins in california poppy cells is associated with the co-expression of biosynthetic and stress-protective enzymes. Molecular Plant 3, 927-939.

Arman, M., 2011. LC-ESI-MS characterisation of phytoalexins induced in chickpea and pea tissues in response to a biotic elicitor of *Hypnea musciformis* (red algae). Natural Product Research 25, 1352-1360.

Bahekar, R. H., Jain, M. R., Goel, A., Patel, D. N., Prajapati, V. M., Gupta, A. A., Jadav, P. A., Patel, P. R., 2007. Design, synthesis, and biological evaluation of substituted-N-(thieno[2,3-b]pyridin-3-yl)-guanidines, N-(1H-pyrrolo[2,3-b]pyridin-3-yl)-guanidines, and N-(1H-indol-3-yl)-guanidines. Bioorganic and Medicinal Chemistry 15, 3248-3265.

Bailey, J. A., Mansfield, J. W., 1982. In Phytoalexins. New York: John Wiley, 319-323.

Bais, H. P., Weir, T. L., Perry, L. G., Gilroy, S., Vivanco, J. M., 2006. The role of root exudates in rhizosphere interactions with plants and other organisms. Annual Review of Plant Biology 57, 233-266.

Bak, S., Feyereisen, R., 2001. The involvement of two P450 enzymes, CYP83B1 and CYP83A1, in auxin homeostasis and glucosinolate biosynthesis. Plant Physiology 127, 108-118.

Bak, S., Olsen, C. E., Halkier, B. A., Møller, B. L., 2000. Transgenic tobacco and *Arabidopsis* plants expressing the two multifunctional *sorghum* cytochrome P450 enzymes, CYP79A1 and CYP71E1, Are cyanogenic and accumulate metabolites derived from intermediates in dhurrin biosynthesis. Plant Physiology 123, 1437-1448.

Bak, S., Paquette, S., Morant, M., Morant, A., Saito, S., Bjarnholt, N., Zagrobelny, M., Jørgensen, K., Osmani, S., Simonsen, H., Pérez, R., Van Heeswijck, T., Jørgensen, B., Møller, B., 2006. Cyanogenic glycosides: a case study for evolution and application of cytochromes P450. Phytochemistry Reviews 5, 309-329.

Barile, E., Bonanomi, G., Antignani, V., Zolfaghari, B., Sajjadi, S. E., Scala, F., Lanzotti, V., 2007. Saponins from *Allium minutiflorum* with antifungal activity. Phytochemistry 68, 596-603.

Bellostas, N., Bjergegaard, C., Jensen, S. K., Sørensen, H., Sørensen, J. C., Sørensen, S., 2007. Nutritional value of cruciferous oilseed crops in relation to profile of accumulated biomolecules with especial regard to glucosinolates transformation products. Organic eprints (12th International Rapeseed Congress), 1-6.

Bellostas, N., Petersen, I. L., Sørensen, J. C., Sørensen, H., 2008. A fast and gentle method for the isolation of myrosinase complexes from Brassicaceous seeds. Journal of Biochemical and Biophysical Methods 70, 918-925.

Bellostas, N., Sørensen, J. C., Sørensen, H., 2006. Micellar electrokinetic capillary chromatography-synchronous monitoring of substrate and products in the myrosinase catalysed hydrolysis of glucosinolates. Journal of Chromatography A 1130, 246-252.

Benedict, A. L., Mountney, A., Hurtado, A., Bryan, K. E., Schnaar, R. L., Dinkova-Kostova, A. T., Talalay, P., 2012. Neuroprotective effects of sulforaphane after contusive spinal cord injury. Journal of Neurotrauma 29, 2576-2586.

Bennett, R. N., Wallsgrove, R. M., 1994. Secondary metabolites in plant defence mechanisms. New Phytologist, 617-633.

Bernardi, R., Finiguerra, M. G., Rossi, A. A., Palmieri, S., 2003. Isolation and biochemical characterization of a basic myrosinase from ripe *Crambe abyssinica* Seeds, highly specific for epi-progoitrin. Journal of Agricultural and Food Chemistry 51, 2737-2744.

Bjorkman, R., Janson, J. C., 1972. Studies on myrosinases I. Purification and characterization of a myrosinase from white mustard seed *Sinapis alba* L. Biochimica et Biophysica Acta 276, 508-518.

Björkman, R., Lönnerdal, B., 1973. Studies on myrosinases III. Enzymatic properties of myrosinases from *Sinapis alba* and *Brassica napus* seeds. Biochimica et Biophysica Acta (BBA) - Enzymology 327, 121-131.

Bones, A., Iversen, T. H., 1985. Myrosin cells and myrosinase. Israel Journal of Botany 34, 351-376.

Bones, A., Slupphaug, G., 1989. Purification, characterization and partial amino acid sequencing of β-thioglucosidase from *Brassica napus* L. Journal of Plant Physiology 134, 722-729.

Bones, A. M., 1990. Distribution of β-thioglucosidase activity in intact plants, cell and tissue culture and regenerant plants of *Brassica napus* L. Journal of Experimental Botany 41, 737-744.

Bones, A. M., Rossiter, J. T., 1996. The myrosinase-glucosinolate system, its organisation and biochemistry. Physiologia Plantarum 97, 194-208.

Bones, A. M., Rossiter, J. T., 2006. The enzymic and chemically induced decomposition of glucosinolates. Phytochemistry 67, 1053-1067.

Bor, M., Ozkur, O., Ozdemir, F., Turkan, I., 2009. Identification and characterization of the glucosinolate-myrosinase system in caper (*Capparis ovata* Desf.). Plant Molecular Biology Reporter 27, 518-525.

Borgen, B. H., Thangstad, O. P., Ahuja, I., Rossiter, J. T., Bones, A. M., 2010. Removing the mustard oil bomb from seeds: transgenic ablation of myrosin cells in oilseed rape (*Brassica napus*) produces MINELESS seeds. Journal of Experimental Botany 61, 1683-1697.

Boutsalis, P., Karotam, J., Powles, S. B., 1999. Molecular basis of resistance to acetolactate synthase-inhibiting herbicides in *Sisymbrium orientale* and *Brassica tournefortii*. Pesticide Science 55, 507-516.

Bowyer, P., Clarke, B. R., Lunness, P., Daniels, M. J., Osbourn, A. E., 1995. Host range of a plant pathogenic fungus determined by a saponin detoxifying enzyme. Science 267, 371-374.

Bridges, M., Jones, A. M. E., Bones, A. M., Hodgson, C., Cole, R. J., Bartlet, E., Wallsgrove, R. M., Karapapa, V. K., Watts, N., Rossiter, J. T., 2002. Spatial organization of the glucosinolate–myrosinase system in brassica specialist aphids

is similar to that of the host plant. Proceedings of the Royal Society of London. Series B: Biological Sciences 269, 187-191.

Brochard, L., Joseph, B., Viaud, M. C., Rollin, P., 1994. (Z)-Stereospecific addition of glycosylmercaptans on nitrilium betaines - synthesis of 1-S-glucopyranosyl arylthiohydroximates. Synthetic Communications 24, 1403-1414.

Brooks, C. J. W., Watson, D. G., 1985. Phytoalexins. Natural Product Reports 2, 427-459.

Browne, L. M., Conn, K. L., Ayert, W. A., Tewari, J. P., 1991. The camalexins: New phytoalexins produced in the leaves of *camelina sativa* (cruciferae). Tetrahedron 47, 3909-3914.

Canoira, L., Rodriguez, J. G., Subirats, J. B., Escario, J.-A., Jimenez, I., Martinez-Fernandez, A. R., 1989. Synthesis, structure and anti-fungal activity of 3-(2′-nitrovinyl)indoles. European Journal of Medicinal Chemistry 24, 39-42.

Cartea, M. E., Velasco, P., 2008. Glucosinolates in *Brassic*a foods: bioavailability in food and significance for human health. Phytochemistry Reviews 7, 213-229.

Chaieb, I., 2010. Saponins as insecticides. Tunisian Journal of Plant Protection 5, 39-50.

Chen, C. Y., Séguin-Swartz, G., 1999. Reaction of wild crucifers to *Leptosphaeria maculans*, the causal agent of blackleg of crucifers. Canadian Journal of Plant Pathology 21, 361-367.

Chen, S., Glawischnig, E., Jørgensen, K., Naur, P., Jørgensen, B., Olsen, C.-E., Hansen, C. H., Rasmussen, H. M., Pickett, J. A., Halkier, B. A., 2003. CYP79F1 and CYP79F2 have distinct functions in the biosynthesis of aliphatic glucosinolates in Arabidopsis. The Plant Journal 33, 923-937.

Chisholm, M. D., Wetter, L. R., 1964. Biosynthesis of mustard oil glucosides: iv. The administration of methionine-^{14}C and related compounds to horseradish. Canadian Journal of Biochemistry 42, 1033-1040.

Conn, K. L., Tewari, J. P., Dahiya, J. S., 1988. Resistance to *Alternaria brassicae* and phytoalexin-elicitation in rapeseed and other crucifers. Plant Science 56, 21-25.

Cromack, H. T. H., 1998. The effect of sowing date on the growth and production of *Lunaria annua* in Southern England. Industrial Crops and Products 7, 217-221.

De Geyter, E., Lambert, E., Geelen, D., Smagghe, G., 2007. Novel advances with plant saponins as natural insecticides to control pest insects. Pest Technology 1, 96-105.

De Vos, M., Kriksunov, K. L., Jander, G., 2008. Indole-3-acetonitrile production from indole glucosinolates deters oviposition by *pieris rapae*. Plant Physiology 146, 916-926.

Dewick, P. M., 1998. The biosynthesis of shikimate metabolites. Natural Product Reports 15, 17-58.

Dewick, P. M., 2006. *Medicinal natural products, a biosynthetic approach*. London: John Wiley and Sons.

Droste, H., Wileland, T., 1987. Hexahydropyrroloindole Versuche zur Synthese von 2-Indolylthioethern. Liebigs Annalen der Chemie 1987, 901-910.

Durham, P. L., Poulton, J. E., 1989. Effect of castanospermine and related polyhydroxyalkaloids on purified myrosinase from *Lepidium sativum* Seedlings. Plant Physiology 90, 48-52.

Eriksson, S., Andreasson, E., Ekbom, B., Graner, G., Pontoppidan, B., Taipalensuu, J., Zhang, J. M., Rask, L., Meijer, J., 2002. Complex formation of myrosinase isoenzymes in oilseed rape seeds are dependent on the presence of myrosinase-binding proteins. Plant Physiology 129, 1592-1599.

Eriksson, S., Ek, B., Xue, J. P., Rask, L., Meijer, J., 2001. Identification and characterization of soluble and insoluble myrosinase isoenzymes in different organs of *Sinapis alba*. Physiologia Plantarum 111, 353-364.

Francis, G., Kerem, Z., Makkar, H. P. S., Becker, K., 2002. The biological action of saponins in animal systems. British Journal of Nutrition 88, 587-605.

Garg, N. K., Sarpong, R., Stoltz, B. M., 2002. The first total synthesis of dragmacidin D. Journal of the American Chemical Society 124, 13179-13184.

Geshi, N., Andreasson, E., Meijer, J., Rask, L., Brandt, A., 1998. Co-localization of myrosinase- and myrosinase-binding proteins in grains of myrosin cells in cotyledon of *Brassica napus* seedlings. Plant Physiology and Biochemistry 36, 583-590.

Geu-Flores, F., Møldrup, M. E., Böttcher, C., Olsen, C. E., Scheel, D., Halkier, B. A., 2011. Cytosolic γ-glutamyl peptidases process glutathione conjugates in the biosynthesis of glucosinolates and camalexin in *Arabidopsis*. The Plant Cell 23, 2456-2469.

Geu-Flores, F., Olsen, C. E., Halkier, B. A., 2009. Towards engineering glucosinolates into non-cruciferous plants. Planta 229, 261-270.

Glawischnig, E., Hansen, B. G., Olsen, C. E., Halkier, B. A., 2004. Camalexin is synthesized from indole-3-acetaldoxime, a key branching point between primary and secondary metabolism in *Arabidopsis*. Proceedings of the National Academy of Sciences of the United States of America 101, 8245-8250.

Glinwood, R., Pettersson, J., Ahmed, E., Ninkovic, V., Birkett, M., Pickett, J. A., 2003. Change in acceptability of barley plants to aphids after exposure to allelochemicals from couch-grass (*Elytrigia repens*). Journal of Chemical Ecology 29, 261-274.

Gong, Q., Li, P., Ma, S., Indu, R. S., Bohnert, H. J., 2005. Salinity stress adaptation competence in the extremophile *Thellungiella halophila* in comparison with its relative *Arabidopsis thaliana*. The Plant Journal: For Cell And Molecular Biology 44, 826-839.

Graser, G., Schneider, B., Oldham, N. J., Gershenzon, J., 2000. The methionine chain elongation pathway in the biosynthesis of glucosinolates in *Eruca sativa* (Brassicaceae). Archives of Biochemistry and Biophysics 378, 411-419.

Grayer, R. J., Harborne, J. B., 1994. A survey of antifungal compounds from higher plants, 1982–1993. Phytochemistry 37, 19-42.

Griffiths, D. W., Birch, A. N. E., Hillman, J. R., 1998. Antinutritional compounds in the Brassicaceae: Analysis, biosynthesis, chemistry and dietary effects. Journal of Horticultural Science and Biotechnology 73, 1-18.

Grubb, C. D., Zipp, B. J., Ludwig-Müller, J., Masuno, M. N., Molinski, T. F., Abel, S., 2004. *Arabidopsis* glucosyltransferase UGT74B1 functions in glucosinolate biosynthesis and auxin homeostasis. The Plant Journal 40, 893-908.

Gupta, S. K., 2009. *Biology and breeding of crucifers*. New York: CRC Press.

Hain, R., Reif, H.-J., Krause, E., Langebartels, R., Kindl, H., Vornam, B., Wiese, W., Schmelzer, E., Schreier, P. H., Stocker, R. H., Stenzel, K., 1993. Disease resistance results from foreign phytoalexin expression in a novel plant. Nature 361, 153-156.

Halkier, B. A., Gershenzon, J., 2006. Biology and biochemistry of glucosinolates. Annual Review of Plant Biology 57, 303-333.

Hammerschmidt, R., 1999. Phytoalexins: what have we learned after 60 years? Annual Review of Phytopathology 37, 285-306.

Hansen, B. G., Kliebenstein, D. J., Halkier, B. A., 2007. Identification of a flavin-monooxygenase as the S-oxygenating enzyme in aliphatic glucosinolate biosynthesis in *Arabidopsis*. The Plant Journal 50, 902-910.

Hansen, C. H., Du, L., Naur, P., Olsen, C. E., Axelsen, K. B., Hick, A. J., Pickett, J. A., Halkier, B. A., 2001. CYP83B1 is the oxime-metabolizing enzyme in the glucosinolate pathway in *Arabidopsis*. Journal of Biological Chemistry 276, 24790-24796.

Hara, M., Eto, H., Kuboi, T., 2001. Tissue printing for myrosinase activity in roots of turnip and Japanese radish and horseradish: a technique for localizing myrosinases. Plant Science 160, 425-431.

Härtel, F. V., Brandt, A., 2002. Characterization of a *Brassica napus* myrosinase expressed and secreted by *Pichia pastoris*. Protein Expression and Purification 24, 221-226.

Hartmann, T., 2004. Plant-derived secondary metabolites as defensive chemicals in herbivorous insects: a case study in chemical ecology. Planta 219, 1-4.

Hartmann, T., 2007. From waste products to ecochemicals: Fifty years research of plant secondary metabolism. Phytochemistry 68, 2831-2846.

Hartmann, T., Ober, D., 2000. Biosynthesis and metabolism of pyrrolizidine alkaloids in plants and specialized insect herbivores. In Biosynthesis. Springer Berlin Heidelberg, 207-243. (Topics in Current Chemistry; vol. 209.)

Hartmann, T., Theuring, C., Beuerle, T., Bernays, E. A., Singer, M. S., 2005. Acquisition, transformation and maintenance of plant pyrrolizidine alkaloids by the polyphagous arctiid *Grammia geneura*. Insect Biochemistry and Molecular Biology 35, 1083-1099.

Helmlinger, J., Rausch, T., Hilgenberg, W., 1985. Metabolism of ^{14}C-indole-3-acetaldoxime by hypocotyls of Chinese cabbage. Phytochemistry 24, 2497-2502.

Hopkins, R. J., Van Dam, N. M., Van Loon, J. J. A., 2009. Role of glucosinolates in insect-plant relationships and multitrophic interactions. In Annual Review of Entomology. Palo Alto: Annual Reviews, 57-83. (54.)

Inan, G., Zhang, Q., Li, P., Wang, Z., Cao, Z., Zhang, H., Zhang, C., Quist, T. M., Goodwin, S. M., Zhu, J., Shi, H., Damsz, B., Charbaji, T., Gong, Q., Ma, S., Fredricksen, M., Galbraith, D. W., Jenks, M. A., Rhodes, D., Hasegawa, P. M., Bohnert, H. J., Joly, R. J., Bressan, R. A., Zhu, J.-K., 2004. Salt Cress. A halophyte and cryophyte *Arabidopsis* relative model system and its applicability to molecular genetic analyses of growth and development of extremophiles. Plant Physiology 135, 1718-1737.

Iriti, M., Faoro, F., 2009. Chemical diversity and defence metabolism: how plants cope with pathogens and ozone pollution. International Journal of Molecular Sciences 10, 3371-3399.

Iversen, T. H., Baggerud, C., 1980. Myrosinase activity in differentiated and undifferentiated plants of Brassicaceae. Zeitschrift für Pflanzenphysiologie 97, 399-407.

Jimenez, L. D., Ayer, W. A., Tewari, J. P., 1997. Phytoalexins produced in the leaves of *Capsella bursa-pastoris* (shepherd's purse). Phytoprotection. 78, 99-103.

Jørgensen, K., Morant, A. V., Morant, M., Jensen, N. B., Olsen, C. E., Kannangara, R., Motawia, M. S., Møller, B. L., Bak, S., 2011. Biosynthesis of the cyanogenic glucosides linamarin and lotaustralin in cassava: isolation, biochemical characterization, and expression pattern of CYP71E7, the oxime-metabolizing cytochrome p450 enzyme. Plant Physiology 155, 282-292.

Kai, K., Mizutani, M., Kawamura, N., Yamamoto, R., Tamai, M., Yamaguchi, H., Sakata, K., Shimizu, B., 2008. Scopoletin is biosynthesized via ortho-hydroxylation of feruloyl CoA by a 2-oxoglutarate-dependent dioxygenase in *Arabidopsis thaliana*. Plant Journal 55, 989-999.

Kissen, R., Bones, A. M., 2009. Nitrile-specifier proteins involved in glucosinolate hydrolysis in *Arabidopsis thaliana*. Journal of Biological Chemistry 284, 12057-12070.

Kissen, R., Rossiter, J. T., Bones, A. M., 2009. The 'mustard oil bomb': not so easy to assemble?! Localization, expression and distribution of the components of the myrosinase enzyme system. Phytochemistry Reviews 8, 69-86.

Kliebenstein, D. J., Kroymann, J., Brown, P., Figuth, A., Pedersen, D., Gershenzon, J., Mitchell-Olds, T., 2001. Genetic control of natural variation in *Arabidopsis* glucosinolate accumulation. Plant Physiology 126, 811-825.

Kliebenstein, D. J., Lambrix, V. M., Reichelt, M., Gershenzon, J., Mitchell-Olds, T., 2001. Gene duplication in the diversification of secondary metabolism: tandem 2-oxoglutarate–dependent dioxygenases control glucosinolate biosynthesis in *Arabidopsis*. The Plant Cell 13, 681-693.

Kuc, J., 1995. Phytoalexins, stress metabolism, and disease resistance in plants. Annual Review of Phytopathology 33, 275-297.

Kurosaki, F., Nishi, A., 1983. Isolation and antimicrobial activity of the phytoalexin 6-methoxymellein from cultured carrot cells. Phytochemistry 22, 669-672.

Kurt, Ş., Güneş, U., Soylu, E. M., 2011. *In vitro* and *in vivo* antifungal activity of synthetic pure isothiocyanates against *Sclerotinia sclerotiorum*. Pest Management Science 67, 869-875.

Kutacek, M., Kefeli, V., 1970. Biogenesis of indole compounds from *D*-tryptophan and *L*-tryptophan in segments of etiolated seedlings of cabbage, maize and pea. Biologia Plantarum 12, 145-158.

Kutacek, M., Kralova, M., 1972. Biosynthesis of the glucobrassicin aglycone from ^{14}C and ^{15}N labelled *L*-tryptophan precursors. Biologia Plantarum 14, 279-285.

Kutacek, M., Prochazka, Z., Grunberger, D., 1960. Biogenesis of ascorbigen, 3-indolylacetonitrile and indole-3-carboxylic acid from (*D,L*)-tryptophan-3-^{14}C in *brassica oleracea* L. Nature 187, 61-62.

Kutacek, M., Prochazka, Z., Veres, K., 1962. Biogenesis of glucobrassicin, the *in vitro* precursor of ascorbigen. Nature 194, 393-394.

Li, J., Hansen, B. G., Ober, J. A., Kliebenstein, D. J., Halkier, B. A., 2008. Subclade of flavin-monooxygenases involved in aliphatic glucosinolate biosynthesis. Plant Physiology 148, 1721-1733.

Li, X., Kushad, M. M., 2005. Purification and characterization of myrosinase from horseradish (*Armoracia rusticana*) roots. Plant Physiology and Biochemistry 43, 503-511.

Li, Y., Karagöz, G. E., Seo, Y. H., Zhang, T., Jiang, Y., Yu, Y., Duarte, A. M. S., Schwartz, S. J., Boelens, R., Carroll, K., Rüdiger, S. G. D., Sun, D., 2012. Sulforaphane inhibits pancreatic cancer through disrupting Hsp90–p50Cdc37 complex and direct interactions with amino acids residues of Hsp90. The Journal of Nutritional Biochemistry 23, 1617-1626.

Literakova, P., Lochman, J., Zdrahal, Z., Prokop, Z., Mikes, V., Kasparovsky, T., 2010. Determination of capsidiol in tobacco cells culture by HPLC. Journal of Chromatographic Science 48, 436-440.

Lonnerda, B., Janson, J. C., 1973. Studies on myrosinases II. Purification and characterization of a myrosinase from rapeseed *Brassica napus* L. Biochimica Et Biophysica Acta 315, 421-429.

Lyon, G. D., 1972. Occurrence of rishitin and phytuberin in potato tubers inoculated with *Erwinia carotovora* var. atroseptica. Physiological Plant Pathology 2, 411-416.

Macel, M., Bruinsma, M., Dijkstra, S. M., Ooijendijk, T., Niemeyer, H. M., Klinkhamer, P. L., 2005. Differences in effects of pyrrolizidine alkaloids on five generalist insect herbivore species. Journal of Chemical Ecology 31, 1493-1508.

Mahadevan, S., Stowe, B. B., 1972. An intermediate in the synthesis of glucobrassicins from 3-indoleacetaldoxime by Woad Leaves. Plant Physiology 50, 43-50.

Mąkosza, M., Danikiewicz, W., Wojciechowski, K., 1988. Reactions of organic anions, 147. Simple and general synthesis of hydroxy- and methoxyindoles via vicarious nucleophilic substitution of hydrogen. Liebigs Annalen der Chemie 1988, 203-208.

Makosza, M., Winiarski, J., 1984. Vicarious substitution of hydrogen with carbanions of dithioacetals. The Journal of Organic Chemistry 49, 5272-5274.

Matich, A. J., Mckenzie, M. J., Lill, R. E., Brummell, D. A., Mcghie, T. K., Chen, R. K. Y., Rowan, D. D., 2012. Selenoglucosinolates and their metabolites produced in *Brassica* spp. fertilised with sodium selenate. Phytochemistry 75, 140-152.

Melchini, A., Traka, M. H., 2010. Biological profile of erucin: a new promising anticancer agent from cruciferous vegetables. Toxins 2, 593-612.

Mikkelsen, M. D., Hansen, C. H., Wittstock, U., Halkier, B. A., 2000. Cytochrome P450 CYP79B2 from *Arabidopsis* catalyzes the conversion of tryptophan to indole-3-acetaldoxime, a precursor of indole glucosinolates and indole-3-acetic acid. Journal of Biological Chemistry 275, 33712-33717.

Mikkelsen, M. D., Olsen, C. E., Halkier, B. A., 2010. Production of the cancer-preventive glucoraphanin in tobacco. Molecular Plant 3, 751-759.

Monde, K., Takasugi, M., 1991. Biosynthesis of cruciferous phytoalexins: the involvement of a molecular rearrangement in the biosynthesis of brassinin. Journal of Chemical Society Chemical Communications, 1582-1583.

Monde, K., Tamura, K., Takasugi, M., 1995. No involvement of methoxybrassinin in the biosynthesis of cyclobrassinin. Phytochemistry 39, 587-589.

Morant, A. V., Jørgensen, K., Jørgensen, B., Dam, W., Olsen, C. E., Møller, B., Bak, S., 2007. Lessons learned from metabolic engineering of cyanogenic glucosides. Metabolomics 3, 383-398.

Müller, C., Boevé, J. L., Brakefield, P. M., 2002. Host plant derived feeding deterrence towards ants in the turnip sawfly *Athalia rosae*. Entomologia experimentalis et applicata 104, 153-157.

Muller, K. O., Borger, H., 1941. Experimental studies on the *Phytophthora* resistance of the Potato, together with a contribution to the problem of 'acquired resistance' in the plant kingdom. Arbeiten aus der Biologischen Reichsanstalt fur Land-und Forstwirtschaft. Berlin. 23, 189-231.

Mustakas, G. C., Kirk, L. D., Griffin, E. L., Jr., Booth, A. N., 1976. *Crambe* seed processing: Removal of glucosinolates by water extraction. Journal of the American Oil Chemists Society 53, 12-16.

Nafisi, M., Goregaoker, S., Botanga, C. J., Glawischnig, E., Olsen, C. E., Halkier, B. A., Glazebrook, J., 2007. *Arabidopsis* cytochrome P450 monooxygenase 71A13 catalyzes the conversion of indole-3-acetaldoxime in camalexin synthesis. The Plant Cell 19, 2039-2052.

Narberhaus, I., Zintgraf, V., Dobler, S., 2005. Pyrrolizidine alkaloids on three trophic levels – evidence for toxic and deterrent effects on phytophages and predators. Chemoecology 15, 121-125.

Naur, P., Petersen, B. L., Mikkelsen, M. D., Bak, S., Rasmussen, H. M., Olsen, C. E., Halkier, B. A., 2003. CYP83A1 and CYP83B1, two nonredundant cytochrome P450 enzymes metabolizing oximes in the biosynthesis of glucosinolates in *Arabidopsis*. Plant Physiology 133, 63-72.

Osbourn, A. E., 1996. Preformed antimicrobial compounds and plant defense against fungal attack. The Plant Cell 8, 1821-1831.

Osbourn, A. E., Clarke, B. R., Lunness, P., Scott, P. R., Daniels, M. J., 1994. An oat species lacking avenacin is susceptible to infection by *Gaeumannomyces graminis* var. *tritici*. Physiological and Molecular Plant Pathology 45, 457-467.

Otomo, K., Kanno, Y., Motegi, A., Kenmoku, H., Yamane, H., Mitsuhashi, W., Oikawa, H., Toshima, H., Itoh, H., Matsuoka, M., 2004. Diterpene cyclases responsible for the biosynthesis of phytoalexins, momilactones A, B, and oryzalexins AF in rice. Bioscience, biotechnology, and biochemistry 68, 2001-2006.

Pang, Q., Chen, S., Li, L., Yan, X., 2009. Characterization of glucosinolate-myrosinase system in developing salt cress *Thellungiella halophila*. Physiologia Plantarum 136, 1-9.

Papadopoulou, K., Melton, R. E., Leggett, M., Daniels, M. J., Osbourn, A. E., 1999. Compromised disease resistance in saponin-deficient plants. Proceedings of the National Academy of Sciences 96, 12923-12928.

Paulose, B., Kandasamy, S., Dhankher, O. P., 2010. Expression profiling of *Crambe abyssinica* under arsenate stress identifies genes and gene networks involved in arsenic metabolism and detoxification. BMC Plant Biology 10, 1471-2229.

Pedras, M. S. C., 2008. The chemical ecology of crucifers and their fungal pathogens: Boosting plant defenses and inhibiting pathogen invasion. The Chemical Record 8, 109-115.

Pedras, M. S. C., Adio, A. M., 2008. Phytoalexins and phytoanticipins from the wild crucifers *Thellungiella halophila* and *Arabidopsis thaliana*: Rapalexin A, wasalexins and camalexin. Phytochemistry 69, 889-893.

Pedras, M. S. C., Chumala, P. B., Suchy, M., 2003. Phytoalexins from *Thlaspi arvense*, a wild crucifer resistant to virulent *Leptosphaeria maculans*: structures, syntheses and antifungal activity. Phytochemistry 64, 949-956.

Pedras, M. S. C., Hossain, S., 2011. Interaction of cruciferous phytoanticipins with plant fungal pathogens: Indole glucosinolates are not metabolized but the corresponding desulfo-derivatives and nitriles are. Phytochemistry 72, 2308-2316.

Pedras, M. S. C., Jha, M., 2005. Concise Syntheses of the Cruciferous Phytoalexins Brassilexin, Sinalexin, Wasalexins, and Analogues: Expanding the Scope of the Vilsmeier Formylation. The Journal of Organic Chemistry 70, 1828-1834.

Pedras, M. S. C., Loukaci, A., Okanga, F. I., 1998. The cruciferous phytoalexins brassinin and cyclobrassinin are intermediates in the biosynthesis of brassilexin. Bioorganic and Medicinal Chemistry Letters 8, 3037-3038.

Pedras, M. S. C., Montaut, S., 2004. The biosynthesis of crucifer phytoalexins: unprecedented incorporation of a 1-methoxyindolyl precursor. Chemical Communications, 452-453.

Pedras, M. S. C., Montaut, S., Suchy, M., 2004. Phytoalexins from the crucifer rutabaga: Structures, syntheses, biosyntheses, and antifungal activity. Journal of Organic Chemistry 69, 4471-4476.

Pedras, M. S. C., Okinyo, D. P. O., 2006a. En route to erucalexin: a unique rearrangement in the crucifer phytoalexin biosynthetic pathway. Chemical Communications, 1848-1850.

Pedras, M. S. C., Okinyo, D. P. O., 2006b. Studies on the biosynthesis of phytoalexins from the wild crucifer *Erucastrum gallicum*. Canadian Journal of Plant Pathology 28, 334-334.

Pedras, M. S. C., Okinyo, D. P. O., 2006c. Syntheses of perdeuterated indoles and derivatives as probes for the biosyntheses of crucifer phytoalexins. Journal of Labelled Compounds and Radiopharmaceuticals 49, 33-45.

Pedras, M. S. C., Okinyo, D. P. O., 2008. Remarkable incorporation of the first sulfur containing indole derivative: another piece in the biosynthetic puzzle of crucifer phytoalexins. Organic and Biomolecular Chemistry 6, 51-54.

Pedras, M. S. C., Okinyo, D. P. O., Thoms, K., Adio, A. M., 2009. The biosynthetic pathway of crucifer phytoalexins and phytoanticipins: De novo incorporation of deuterated tryptophans and quasi-natural compounds. Phytochemistry 70, 1129-1138.

Pedras, M. S. C., Sarma-Mamillapalle, V. K., 2012. The cruciferous phytoalexins rapalexin A, brussalexin A and erucalexin: chemistry and metabolism in *Leptosphaeria maculans*. Bioorganic and Medicinal Chemistry 20, 3991-3996.

Pedras, M. S. C., Sorensen, J. L., 1998. Phytoalexin accumulation and antifungal compounds from the crucifer wasabi. Phytochemistry 49, 1959-1965.

Pedras, M. S. C., Sorensen, J. L., Okanga, F. I., Zaharia, I. L., 1999. Wasalexins A and B, new phytoalexins from *Wasabi*: isolation, synthesis, and antifungal activity. Bioorganic and Medicinal Chemistry Letters 9, 3015-3020.

Pedras, M. S. C., Suchy, M., 2006. Metabolism of the crucifer phytoalexins wasalexin A and B in the plant pathogenic fungus *Leptosphaeria maculans*. Organic and Biomolecular Chemistry 4, 3526-3535.

Pedras, M. S. C., Suchy, M., Ahiahonu, P. W. K., 2006. Unprecedented chemical structure and biomimetic synthesis of erucalexin, a phytoalexin from the wild crucifer *Erucastrum gallicum*. Organic and Biomolecular Chemistry 4, 691-701.

Pedras, M. S. C., Yaya, E. E., 2010. Phytoalexins from Brassicaceae: News from the front. Phytochemistry 71, 1191-1197.

Pedras, M. S. C., Yaya, E. E., 2012. The first isocyanide of plant origin expands functional group diversity in cruciferous phytoalexins: synthesis, structure and bioactivity of isocyalexin A. Organic and Biomolecular Chemistry 10, 3613-3616.

Pedras, M. S. C., Yaya, E. E., 2013. Dissecting metabolic puzzles through isotope feeding: a novel amino acid in the biosynthetic pathway of the cruciferous phytoalexins rapalexin A and isocyalexin A. Organic and Biomolecular Chemistry 11, 1149-1166.

Pedras, M. S. C., Yaya, E. E., Glawischnig, E., 2011. The phytoalexins from cultivated and wild crucifers: chemistry and biology. Natural Product Reports 28, 1381-1405.

Pedras, M. S. C., Yaya, E. E., Hossain, S., 2010. Unveiling the phytoalexin biosynthetic puzzle in salt cress: unprecedented incorporation of glucobrassicin into wasalexins A and B. Organic and Biomolecular Chemistry 8, 5150-5158.

Pedras, M. S. C., Zaharia, I. L., 2001. Unprecedented vilsmeier formylation: Expedient syntheses of the cruciferous phytoalexins sinalexin and brassilexin and discovery of a new heteroaromatic ring system. Organic Letters 3, 1213-1216.

Pedras, M. S. C., Zheng, Q.-A., 2010. Metabolic responses of *Thellungiella halophila*/salsuginea to biotic and abiotic stresses: Metabolite profiles and quantitative analyses. Phytochemistry 71, 581-589.

Pedras, M. S. C., Zheng, Q. A., Gadagi, R. S., 2007a. The first naturally occurring aromatic isothiocyanates, rapalexins A and B, are cruciferous phytoalexins. Chemical Communications 4, 368-370.

Pedras, M. S. C., Zheng, Q. A., Sarma-Mamillapalle, V. K., 2007b. The phytoalexins from Brassicaceae: Structure, biological activity, synthesis and biosynthesis. Natural Product Communications 2, 319-330.

Pedras, M. S. C., Zheng, Q. A., Schatte, G., Adio, A. M., 2009. Photochemical dimerization of wasalexins in UV-irradiated *Thellungiella halophila* and in vitro generates unique cruciferous phytoalexins. Phytochemistry 70, 2010-2016.

PeñAs, E., Frias, J., MartíNez-Villaluenga, C., Vidal-Valverde, C., 2011. Bioactive compounds, myrosinase activity, and antioxidant capacity of white cabbages grown in different locations of Spain. Journal of Agricultural and Food Chemistry 59, 3772-3779.

Peters, R. J., 2006. Uncovering the complex metabolic network underlying diterpenoid phytoalexin biosynthesis in rice and other cereal crop plants. Phytochemistry 67, 2307-2317.

Peterson, C. J., Cossé, A., Coats, J. R., 2000. Insecticidal components in the meal of *Crambe abyssinica*. Journal of Agricultural and Urban Entomology 17, 27-36.

Pignone, D., Martínez-Laborde, J. B., 2011. Diplotaxis. In Wild crop relatives: Genomic and breeding resources. Springer Berlin Heidelberg, 137-147.

Piotrowski, M., Schemenewitz, A., Lopukhina, A., Müller, A., Janowitz, T., Weiler, E. W., Oecking, C., 2004. Desulfoglucosinolate sulfotransferases from *Arabidopsis thaliana* catalyzing the final step in biosynthesis of the glucosinolate core structure. Journal of Biological Chemistry 279, 50717-50725.

Prakash, S., 1974. Haploid meiosis and origin of *Brassica tournefortii* Gouan. Euphytica 23, 591-595.

Quintana, N., Weir, T. L., Du, J., Broeckling, C. D., Rieder, J. P., Stermitz, F. R., Paschke, M. W., Vivanco, J. M., 2008. Phytotoxic polyacetylenes from roots of Russian knapweed (*Acroptilon repens* (L.) DC.). Phytochemistry 69, 2572-2578.

Ratzka, A., Vogel, H., Kliebenstein, D. J., Mitchell-Olds, T., Kroymann, J., 2002. Disarming the mustard oil bomb. Proceedings of the National Academy of Sciences 99, 11223-11228.

Rausch, T., Butcher, D. N., Hilgenberg, W., 1983. Indole-3-methylglucosinolate biosynthesis and metabolism in clubroot diseased plants. Physiologia Plantarum 58, 93-100.

Robertson, A. B., Botting, N. P., 1999. Synthesis of deuterium labelled desulfoglucosinolates as internal standards for LC-MS analysis. Tetrahedron 55, 13269-13284.

Rouxel, T., Kollmann, A., Boulidard, L., Mithen, R., 1991. Abiotic elicitation of indole phytoalexins and resistance to *Leptosphaeria maculans* within Brassiceae. Planta 184, 271-278.

Sarwar, M. G., 2007. Chemical investigation of phytoalexins and phytoanticipins: isolation, synthesis and antifungal activity. MSc. Thesis (U of Saskatchewan).

Scherrer, A. M., Motti, R., Weckerle, C. S., 2005. Traditional plant use in the areas of Monte Vesole and Ascea, Cilento National Park (Campania, Southern Italy). Journal of Ethnopharmacology 97, 129-143.

Schranz, M. E., Lysak, M. A., Mitchell-Olds, T., 2006. The ABC's of comparative genomics in the Brassicaceae: building blocks of crucifer genomes. Trends in Plant Science 11, 535-542.

Schraudolf, H., 1966. Metabolism of indole derivatives in *Sinapis alba* L. Synthesis and reactions of *L*-tryptophan in etiolated hypocotyl segments following the application of indole-2-^{14}C. Phytochemistry 5, 83-90.

Schraudolf, S. H., Bergmann, F., 1965. Metabolism of indole derivatives in *Sinapis alba*. II. Investigation of the biogenesis and metabolism of indole glucosinolates with the aid of ring-labeled tryptophan-^{14}C and sulfate-(^{35}S). Planta 67, 75-95.

Schumacher, H. M., Gundlach, H., Fiedler, F., Zenk, M. H., 1987. Elicitation of benzophenanthridine alkaloid synthesis in *Eschscholtzia* cell cultures. Plant Cell Reports 6, 410-413.

Serif, G. S., Schmotzer, L. A., 1968. Biosynthesis of the aglycones of plant thioglucosides—I: Precursor studies of the aglycone of progoitrin. Phytochemistry 7, 1151-1157.

Shikita, M., Fahey, J. W., Golden, T. R., Holtzclaw, W. D., Talalay, P., 1999. An unusual case of 'uncompetitive activation' by ascorbic acid: purification and kinetic properties of a myrosinase from *Raphanus sativus* seedlings. Biochemical Journal 341, 725-732.

Sibbesen, O., Koch, B., Halkier, B. A., Møller, B. L., 1994. Isolation of the heme-thiolate enzyme cytochrome P450TYR, which catalyzes the committed step in the biosynthesis of the cyanogenic glucoside dhurrin in *Sorghum bicolor* (L.) Moench. Proceedings of the National Academy of Sciences 91, 9740-9744.

Simões, K., Du, J., Kretzschmar, F. S., Broeckling, C. D., Stermitz, F. S., Vivanco, J. M., Braga, M. R., 2008. Phytotoxic catechin leached by seeds of the tropical weed *Sesbania virgata*. Journal of Chemical Ecology 34, 681-687.

Smith, C. J., 1996. Accumulation of phytoalexins: defence mechanism and stimulus response system. New Phytologist 132, 1-45.

Sobolev, V. S., Neff, S. A., Gloer, J. B., 2008. New Stilbenoids from peanut (*Arachis hypogaea*) seeds challenged by an *Aspergillus caelatus* strain. Journal of Agricultural and Food Chemistry 57, 62-68.

Somei, M., Iwasa, E., Yamada, F., 1986. A practical and short access to 4-hydroxy-3-indolecarboxaldehyde and its application for the synthesis of pindolol analog. Heterocycles 24, 3065-3069.

Somei, M., Kawasaki, T., 1989. A new and simple synthesis of 1-hydroxyindole derivatives. Heterocycles 29, 1251-1254.

Somei, M., Sato, H., Komura, N., Kaneko, C., 1985. The chemistry of indoles. Part XXV. Synthetic study for 1-methoxyindoles and 1-methoxy-2-oxindoles. Heterocycles 23, 1101-1106.

Somei, M., Yamada, F., Kunimoto, M., Kaneko, C., 1984. A practical one pot synthesis of 4-alkoxy-3-formylindoles. Hetrocycles 22, 797-801.

Sønderby, I. E., Geu-Flores, F., Halkier, B. A., 2010. Biosynthesis of glucosinolates - gene discovery and beyond. Trends in Plant Science 15, 283-290.

Stanjek, V., Piel, J., Boland, W., 1999. Biosynthesis of furanocoumarins: mevalonate-independent prenylation of umbelliferone in *Apium graveolens* (Apiaceae). Phytochemistry 50, 1141-1146.

Steinsiek, J. W., Oliver, L. R., Collins, F. C., 1982. Allelopathic potential of wheat (*Triticum aestivum*) straw on selected weed species. Weed Science 30, 495-497.

Storck, M., Sacristan, M., 1995. The role of phytoalexins in the seedling resistance to *Leptosphaeria maculans* in some crucifers. Zeitschrift fuer Naturforschung. Section C 50, 15-20.

Stotz, H. U., Sawada, Y., Shimada, Y., Hirai, M. Y., Sasaki, E., Krischke, M., Brown, P. D., Saito, K., Kamiya, Y., 2011. Role of camalexin, indole glucosinolates, and side chain modification of glucosinolate-derived isothiocyanates in defense of *Arabidopsis* against *Sclerotinia sclerotiorum*. The Plant Journal 67, 81-93.

Su, T., Xu, J., Li, Y., Lei, L., Zhao, L., Yang, H. Z., Feng, J., Liu, G., Ren, D., 2011. Glutathione-indole-3-acetonitrile is required for camalexin biosynthesis in *Arabidopsis thaliana*. The Plant Cell 23, 364-380.

Szakiel, A., Pączkowski, C., Henry, M., 2011. Influence of environmental biotic factors on the content of saponins in plants. Phytochemistry Reviews 10, 493-502.

Takasugi, M., Katsui, N., Shirata, A., 1986. Isolation of 3 novel sulfur-containing phytoalexins from the Chinese-cabbage *Brassica-campestris* L Ssp *Pekinensis* (Cruciferae). Journal of the Chemical Society-Chemical Communications, 1077-1078.

Takasugi, M., Kawashima, S., Katsui, N., Shirata, A., 1987. Studies on Stress Metabolites: 5. Two polyacetylenic phytoalexins from *Arctium lappa*. Phytochemistry 26, 2957-2958.

Tattersall, D. B., Bak, S., Jones, P. R., Olsen, C. E., Nielsen, J. K., Hansen, M. L., Hoj, P. B., Moller, B. L., 2001. Resistance to an herbivore through engineered cyanogenic glucoside synthesis. Science 293, 1826-1828.

Thangstad, O., Winge, P., Husebye, H., Bones, A., 1993. The myrosinase (thioglucoside glucohydrolase) gene family in Brassicaceae. Plant Molecular Biology 23, 511-524.

Tsuji, J., Jackson, E. P., Gage, D. A., Hammerschmidt, R., Somerville, S. C., 1992. Phytoalexin accumulation in *Arabidopsis thaliana* during the hypersensitive reaction to *Pseudomonas syringae* pv *syringae*. Plant Physiology 98, 1304-1309.

Tsuzuki, J. K., Svidzinski, T. I. E., Shinobu, C. S., Silva, L. F. A., Rodrigues-Filho, E., Cortez, D. a. G., Ferreira, I. C. P., 2007. Antifungal activity of the extracts and saponins from *Sapindus saponaria* L. Anais da Academia Brasileira de Ciências 79, 577-583.

Underhil, E. W., 1967. Biosynthesis of mustard oil glucosides - conversion of phenylacetaldehyde oxime and 3-phenylpropionaldehyde oxime to glucotropaeolin and gluconasturtiin. European Journal of Biochemistry 2, 61-63.

Underhil, E. W., Wetter, L. R., 1969. Biosynthesis of mustard oil glucosides - sodium phenylacetothiohydroximate and desulfobenzylglucosinolate precursors of benzylglucosinolate in *Tropaeolum majus* L. Plant Physiology 44, 584-590.

Vanetten, H. D., Mansfield, J. W., Bailey, J. A., Farmer, E. E., 1994. 2 Classes of plant antibiotics - phytoalexins versus phytoanticipins. Plant Cell 6, 1191-1192.

Vaughn, S. F., Berhow, M. A., 1998. 1-Cyano-2-hydroxy-3-butene, A phytotoxin from *Crambe abyssinica* seedmeal. Journal of Chemical Ecology 24, 1117-1126.

Verpoorte, R., Memelink, J., 2002. Engineering secondary metabolite production in plants. Current Opinion in Biotechnology 13, 181-187.

Viaud, M. C., Rollin, P., 1990. First synthesis of an indole glucosinolate. Tetrahedron Letters 31, 1417-1418.

Vlieger, L., Brakefield, P. M., Müller, C., 2004. Effectiveness of the defence mechanism of the turnip sawfly, *Athalia rosae* (Hymenoptera: Tenthredinidae), against predation by lizards. Bulletin of Entomological Research 94, 283-289.

Wang, X., Gao, Y., Xu, Y. M., Li, L., Zhang, Z., Liu, J., 2009. Efficient preparation of photolabile agent MNI-glu by regioselective nitration of 4-methoxyindoline derivative. Synthetic Communications 39, 4030-4038.

Warwick, S., Gugel, R., 2003. Genetic variation in the *Crambe abyssinica* - *C. hispanica* - *C. glabrata* complex. Genetic Resources and Crop Evolution 50, 291-305.

Weir, T. L., Park, S.-W., Vivanco, J. M., 2004. Biochemical and physiological mechanisms mediated by allelochemicals. Current Opinion in Plant Biology 7, 472-479.

Weir, T. L., Vivanco, J. M., 2008. Allelopathy: full circle from phytotoxicity to mechanisms of resistance. Allelopathy in Sustainable Agriculture and Forestry, 105-117.

Williams, D. J., Critchley, C., Pun, S., Chaliha, M., O'hare, T. J., 2009. Differing mechanisms of simple nitrile formation on glucosinolate degradation in *Lepidium sativum* and *Nasturtium officinale* seeds. Phytochemistry 70, 1401-1409.

Wittstock, U., Agerbirk, N., Stauber, E. J., Olsen, C. E., Hippler, M., Mitchell-Olds, T., Gershenzon, J., Vogel, H., 2004. Successful herbivore attack due to metabolic diversion of a plant chemical defense. Proceedings of the National Academy of Sciences of the United States of America 101, 4859-4864.

Wittstock, U., Halkier, B. A., 2000. Cytochrome P450 CYP79A2 from *Arabidopsis thaliana* L. catalyzes the conversion of *L*-phenylalanine to phenylacetaldoxime in the biosynthesis of benzylglucosinolate. Journal of Biological Chemistry 275, 14659-14666.

Wu, H.-J., Zhang, Z., Wang, J.-Y., Oh, D.-H., Dassanayake, M., Liu, B. Y., Huang, Q., Sun, H., Xia, R., Wu, Y., Wang, Y., Yang, Z. B., Liu, Y., Zhang, W., Zhang, H., Chu, J., Yan, C., Fang, S., Zhang, J. M., Wang, Y., Zhang, F., Wang, G., Lee, S. Y., Cheeseman, J. M., Yang, B., Li, B., Min, J., Yang, L., Wang, J., Chu, C., Chen, S. I., Bohnert, H. J., Zhu, J., Wang, X., Xie, Q., 2012. Insights into salt tolerance from the genome of *Thellungiella salsuginea*. Proceedings of the National Academy of Sciences 109, 12219-12224.

Wu, H., Haig, T., Pratley, J., Lemerle, D., An, M., 2000. Allelochemicals in wheat (*Triticum aestivum L.*): variation of phenolic acids in root tissues. Journal of Agricultural and Food Chemistry 48, 5321-5325.

Wu, H., Haig, T., Pratley, J., Lemerle, D., An, M., 2002. Biochemical basis for wheat seedling allelopathy on the suppression of annual ryegrass (*Lolium rigidum*). Journal of Agricultural and Food Chemistry 50, 4567-4571.

Wu, H., Pratley, J., Lemerle, D., Haig, T., 2001. Allelopathy in wheat (*Triticum aestivum*). Annals of Applied Biology 139, 1-9.

Yamada, F., Kobayashi, K., Shimizu, A., Aoki, N., M., S., 1993. A Synthesis method of indole-3-methanamine and/or gramine from indole-3-carboxaldehyde, and its application for the synthesis of brassinin, its 4-substituted analogs, and 1,3,4,5-tetrahydropyrrolo[4,3,2-de]quinoline. Hetrocycles 36, 2783-2804.

Yang, C. R., Zhang, Y., Jacob, M. R., Khan, S. I., Zhang, Y. J., Li, X. C., 2006. Antifungal activity of C-27 steroidal saponins. Antimicrob Agents Chemother 50, 1710-1714.

Yang, G. F., Wang, D.-F., Dong, Z., Wang, Q., Wang-P., You, M., 2012. Characterization of a myrosinase cDNA from *Brassica parachinensis* and its defense role against *Plutella xylostella* after suppression. Insect Science 19, 461-471.

Zagrobelny, M., Bak, S., Rasmussen, A. V., Jørgensen, B., Naumann, C. M., Lindberg, M. B., 2004. Cyanogenic glucosides and plant–insect interactions. Phytochemistry 65, 293-306.

Zagrobelny, M., Møller, B. L., 2011. Cyanogenic glucosides in the biological warfare between plants and insects: The Burnet moth-birds foot trefoil model system. Phytochemistry 72, 1585-1592.

Zhang, J. M., Pontoppidan, B., Xue, J. P., Rask, L., Meijer, J., 2002. The third myrosinase gene TGG3 in *Arabidopsis thaliana* is a pseudogene specifically expressed in stamen and petal. Physiologia Plantarum 115, 25-34.

Zhou, C., Tokuhisa, J. G., Bevan, D. R., Esen, A., 2012. Properties of β-thioglucoside hydrolases (TGG1 and TGG2) from leaves of *Arabidopsis thaliana*. Plant Science 191, 82-92.

Zook, M., Leege, L., Jacobson, D., Hammerschmidt, R., 1998. Camalexin accumulation in *Arabis lyrata*. Phytochemistry 49, 2287-2289.